

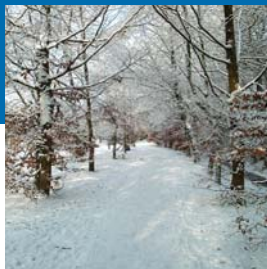


ALTERRA

WAGENINGEN UR

Reference Manual SWAP version 3.0.3

J.G. Kroes and J.C. van Dam (eds)



Alterra-rapport 773, ISSN 1566-7197

Reference Manual SWAP version 3.0.3

J.G. Kroes¹ and J.C. van Dam² (eds)

¹ *Alterra*

² *Wageningen University, department of Water Resources*

Alterra-report 773

Alterra, Green World Research, Wageningen, 2003

ABSTRACT

Kroes, J.G. and J.C. van Dam (eds), 2003. *Reference Manual SWAP version 3.0.3*. Wageningen, Alterra, Green World Research.. Alterra-report 773. Reference Manual SWAP version 3.0.3.doc. 211 pp. 39 figs.; 6 tables; 17 appendices.

SWAP simulates vertical transport of water, solutes and heat in variably saturated, cultivated soils. The program has been developed by Alterra and Wageningen University, and is designed to simulate transport processes at field scale level and during whole growing seasons. This manual describes the theoretical background and modeling concepts that were used for soil water flow, solute transport, heat flow, evapotranspiration, crop growth, multi-level drainage and interaction between field water balance and surface water management. An overview is given of model use, input requirements and output tables

Keywords: agrohydrology, drainage, evapotranspiration, irrigation, salinization, simulation model, soil water, surface water management.

ISSN 1566-7197

This report can be ordered by paying € 27,- into bank account number 36 70 54 612 in the name of Alterra, Wageningen, the Netherlands, with reference to Alterra-Report 773, Reference Manual SWAP version 3.0.3. This amount is inclusive of VAT and postage.

© 2003 Alterra, Green World Research,
P.O. Box 47, NL-6700 AA Wageningen (The Netherlands).
Phone: +31 317 474700; fax: +31 317 419000; e-mail: postkamer@alterra.wag-ur.nl

No part of this publication may be reproduced or published in any form or by any means, or stored in a data base or retrieval system, without the written permission of Alterra.

Alterra assumes no liability for any losses resulting from the use of this document.

Project 230427-report 773

Contents

| | |
|---|----|
| Preface | 13 |
| Summary..... | 15 |
| 1 Introduction..... | 19 |
| 1.1 System description | 19 |
| 1.2 Reading guide | 21 |
| 2 Soil water flow..... | 23 |
| 2.1 Basic equations | 23 |
| 2.2 Numerical solution of soil water flow equation | 23 |
| 2.2.1 Numerical discretization in the soil profile | 24 |
| 2.2.2 Top boundary condition | 27 |
| 2.2.3 Actual soil evaporation | 29 |
| 2.2.4 Other boundary condition | 31 |
| 2.3 Soil hydraulic functions | 31 |
| 2.4 Sink term: actual plant transpiration | 33 |
| 2.5 Frost conditions | 35 |
| 3 Atmosphere – Plant and Soil interaction | 37 |
| 3.1 Rainfall and snowfall | 37 |
| 3.2 The snowpack | 37 |
| 3.3 Interception of rainfall | 39 |
| 3.3.1 Agricultural crops | 39 |
| 3.3.2 Forests | 40 |
| 3.4 Potential evapotranspiration | 41 |
| 3.4.1 Penman-Monteith equation | 42 |
| 3.4.1.1 Radiation term | 43 |
| 3.4.1.2 Aerodynamic term | 44 |
| 3.4.1.3 Fluxes above homogeneous surfaces | 46 |
| 3.4.2 Reference evapotranspiration and crop factors | 47 |
| 3.4.3 Partitioning of potential evapotranspiration | 49 |
| 3.4.3.1 Use of leaf area index | 49 |
| 3.4.3.2 Use of soil cover fraction | 50 |
| 4 Soil water - surface water interaction | 51 |

| | | |
|---------|---|-----|
| 4.1 | Surface flow | 51 |
| 4.1.1 | Surface runoff and inundation | 52 |
| 4.1.2 | Surface runoff | 52 |
| 4.2 | Drainage and infiltration | 52 |
| 4.2.1 | Linear or tabular relation | 53 |
| 4.2.2 | Drainage equations of Hooghoudt and Ernst | 53 |
| 4.2.3 | Basic drainage | 57 |
| 4.2.4 | Interflow | 58 |
| 4.2.5 | Extended drainage | 58 |
| 4.2.5.1 | Surface water balance | 60 |
| 4.2.5.2 | Drainage resistance (subregional approach) | 61 |
| 4.2.5.3 | Multi level drainage | 64 |
| 4.2.5.4 | Procedure for surface water level as input | 66 |
| 4.2.5.5 | Procedure for surface water level as output | 66 |
| 4.2.5.6 | Implementation aspects | 69 |
| 4.3 | Residence time approach | 72 |
| 4.3.1 | Introduction | 72 |
| 4.3.2 | The horizontal groundwater flux | 73 |
| 4.3.3 | Maximum depth of a discharge layer | 77 |
| 4.3.4 | Concentrations of solute in drainage water | 80 |
| 4.3.5 | Discussion | 82 |
| 5 | Soil water – groundwater interaction..... | 85 |
| 5.1 | Introduction | 85 |
| 5.2 | Field scale | 86 |
| 5.3 | Regional scale | 87 |
| 6 | Soil heterogeneity | 91 |
| 6.1 | Introduction | 91 |
| 6.2 | Hysteresis | 91 |
| 6.3 | Scaling of soil hydraulic properties | 94 |
| 6.3.1 | Introduction | 94 |
| 6.3.2 | Similar media scaling | 95 |
| 6.4 | Mobile/immobile flow | 96 |
| 6.4.1 | Introduction | 96 |
| 6.4.2 | Water flow | 97 |
| 6.5 | Macropore flow | 99 |
| 6.5.1 | Introduction | 99 |
| 6.5.2 | Simple macropore flow | 100 |
| 6.5.2.1 | Introduction | 100 |
| 6.5.2.2 | Shrinkage characteristic | 101 |

| | | |
|---------|---|-----|
| 6.5.2.3 | Water flow concept | 103 |
| 6.5.3 | Advanced macropore flow | 106 |
| 6.5.3.1 | Introduction | 106 |
| 6.5.3.2 | Macropore geometry | 106 |
| 6.5.3.3 | Water flow | 108 |
| 6.5.3.4 | Parameterisation of model input | 112 |
| 6.5.3.5 | Output for solute transport models | 112 |
| 7 | Crop growth | 115 |
| 7.1 | Introduction | 115 |
| 7.2 | Simple crop module | 115 |
| 7.3 | Detailed crop module | 117 |
| 7.3.1 | Phenological development stage | 117 |
| 7.3.2 | Radiation fluxes above the canopy | 119 |
| 7.3.3 | Radiation profiles within the canopy | 120 |
| 7.3.4 | Instantaneous assimilation rates per leaf layer | 121 |
| 7.3.5 | Daily gross assimilation rate of the canopy | 122 |
| 7.3.6 | Maintenance respiration | 123 |
| 7.3.7 | Dry matter partitioning and growth respiration | 124 |
| 7.3.8 | Senescence | 126 |
| 7.3.9 | Net growth | 127 |
| 7.3.10 | Root growth | 128 |
| 8 | Solute transport | 131 |
| 8.1 | Introduction | 131 |
| 8.2 | Basic equations | 132 |
| 8.2.1 | Transport processes | 132 |
| 8.2.2 | Continuity and transport equation | 133 |
| 8.3 | Boundary conditions | 135 |
| 8.4 | Mobile/immobile solute transport | 137 |
| 8.5 | Crack solute transport | 138 |
| 8.6 | Residence time in the saturated zone | 139 |
| 9 | Soil temperature | 141 |
| 9.1 | Introduction | 141 |
| 9.2 | Temperature conductance equation | 141 |
| 9.3 | Analytical solution (sinus wave) | 142 |
| 9.4 | Numerical solution | 142 |
| 10 | Management aspects | 145 |

| | | |
|----------|---|-----|
| 10.1 | Introduction | 145 |
| 10.2 | Sprinkling and surface irrigation | 145 |
| 10.2.1 | Irrigation scheduling options | 146 |
| 10.2.2 | Timing criteria | 146 |
| 10.2.2.1 | Allowable daily stress | 146 |
| 10.2.2.2 | Allowable depletion of readily available water in the root zone | 146 |
| 10.2.2.3 | Allowable depletion of totally available water in the root zone | 146 |
| 10.2.2.4 | Allowable depletion amount of water in the root zone | 147 |
| 10.2.2.5 | Critical pressure head or moisture content at sensor depth | 147 |
| 10.2.3 | Application depth criteria | 147 |
| 10.2.3.1 | Back to Field Capacity (+/- specified amount) | 147 |
| 10.2.3.2 | Fixed irrigation depth | 147 |
| 10.3 | Design of field drainage | 147 |
| 10.4 | Land use | 148 |
| 10.5 | Surface water management | 148 |
| 11 | Program operation..... | 149 |
| 11.1 | Program input | 149 |
| 11.2 | Program execution | 150 |
| 11.3 | Program output | 150 |
| | References..... | 153 |

| | |
|---|----|
| Figure 1 Schematized overview of the modelled system..... | 19 |
| Figure 2 Flowchart of the main fluxes between the sub systems | 20 |
| Figure 3 Spatial and temporal discretization used to solve Richards' equation..... | 25 |
| Figure 4 Procedure to select head (h_{sur}) or flux (q_{sur}) top boundary condition. The variables are explained in the text | 27 |
| Figure 5 Reduction coefficient for root water uptake, α_{rw} , as function of soil water pressure head h and potential transpiration rate T_p (after Feddes et al., 1978)..... | 34 |
| Figure 6 Reduction coefficient for root water uptake, α_{rs} , as function of soil water electrical conductivity EC (after Maas and Hoffman, 1977)..... | 34 |
| Figure 7 Partly frozen soil profile | 36 |
| Figure 8 The water fluxes to and from the snow layer | 38 |
| Figure 9 Interception for agricultural crops (Von Hoyningen-Hüne, 1983; Braden, 1985) and forests (Gash, 1979; 1985) | 40 |
| Figure 10 Partitioning of evapotranspiration over crop and soil | 49 |
| Figure 11 The water fluxes on the soil surface..... | 51 |
| Figure 12 Five field drainage situations considered in SWAP (after Ritzema, 1994).... | 54 |
| Figure 13 Schematized surface water system. The primary water course functions separately from the others, but it does interact with the SWAP soil column by the drainage or infiltration flux..... | 59 |
| Figure 14 Linear relationships between drainage ($q_{drain} > 0$) and infiltration ($q_{drain} < 0$) flux and mean groundwater level ϕ_{avg} | 63 |
| Figure 15 Cross-section of multi-level drainage, involving a third-order system of ditches and a fourth-order system of pipe drains | 64 |
| Figure 16 Cross section of multi-level drainage. The main part of the flow resistance is assumed to be located near the drains and ditches, which results in a horizontal groundwater table | 65 |
| Figure 17 Discharge q_{drain} as function of mean phreatic surface ϕ_{avg} in the Beltrum area (Massop and de Wit, 1994) | 70 |
| Figure 18 Illustration of regional drainage concept. The resistance mainly consists of radial and entrance resistance near the drainage devices..... | 73 |
| Figure 19 Schematization of regional groundwater flow to drains of three different orders | 74 |
| Figure 20 Schematization of regional groundwater flow to drains of three orders when either $q_{d,1}L_1 - q_{d,2}L_2 < 0$ or $q_{d,2}L_2 - q_{d,3}L_3 < 0$ | 75 |
| Figure 21 Discharge layer thickness D_i as function of cumulative transmissivity kD_i in a heterogeneous soil profile | 76 |
| Figure 22 Flow field to a drain with half circular shaped stream lines..... | 77 |
| Figure 23 Stream line pattern in a groundwater system of infinite thickness | 79 |
| Figure 24 (a) Streamlines and isochrones of a soil profile with complete drains and (b) schematization of the flow pattern by a cascade of perfectly mixed reservoirs | 81 |
| Figure 25 Step response of outflow concentrations per soil layer (numbered lines) and step response of the averaged concentration which enters the drains (circles)..... | 82 |
| Figure 26 Pseudo two-dimensional Cauchy lower boundary conditions, in case of drainage to ditches and seepage from a deep aquifer..... | 88 |

| | |
|--|-----|
| Figure 27 Water retention function with hysteresis, showing the main wetting, main drying and scanning curves | 91 |
| Figure 28 (A) Linear scaling of the main drying water retention curve in order to derive a drying scanning curve; (B) Linear scaling of the main wetting water retention curve in order to derive a drying wetting curve. | 93 |
| Figure 29 Characteristic lengths λ_i in geometrically similar media (Miller and Miller, 1956)..... | 95 |
| Figure 30 Schematization of mobile and immobile regions for flow and transport in water repellent soils | 98 |
| Figure 31 Void ratio e as function of moisture ratio v , showing four stages of a typical shrinkage characteristic (after Bronswijk, 1988)..... | 100 |
| Figure 33 Concept of water flow in a cracked clay soil as applied in the simple macropore concept. The variables are explained in the text. | 103 |
| Figure 34 Schematic representation of the 2 domains: 1) main bypass flow domain (left part): transporting water and solutes deeper into profile and rapid drainage, 2) internal catchment (right part) domain: infiltration of trapped water into unsaturated matrix at different depths. The figure on the left gives a graphical representation of the two domains..... | 107 |
| Figure 35 The decline of the number of internal catchment macropores is described by a power law function with power m . $m = 1$ represents a linear decline, while $m < 1$ represents a shallow system and $m > 1$ a deep system. ‘ S_{Zah} ’ in the figure is similar to ‘ R_{Zah} ’ in the list of Model input in 6.4.3.4..... | 107 |
| Figure 36 Partition between static and dynamic macropore volume: white area represents static and grey area dynamic macropore volume. Dark colour is the soil matrix. | 108 |
| Figure 37 Schematic representation of the soil profile with the soil matrix, divided in 20 model compartments, and macropores and the various water fluxes ($m d^{-1}$) within the soil profile: I is infiltration rate into the soil matrix, I_{mp1} is part of total crack infiltration caused by rainfall intensity exceeding the maximum infiltration rate of the soil matrix, I_{mp2} is part of total crack infiltration caused by rain falling directly into the cracks, E is actual evapotranspiration, q_i is Darcy flux between two nodal points, q_b is bottom boundary flux, q_{intfl} is interflow over layer of low permeability into macropores, q_{cd} is drainage flux via cracks, q_{ul} is lateral infiltration out of macropores into unsaturated matrix, q_{sl} is lateral infiltration out of macropores into saturated matrix. | 109 |
| Figure 38 Schematization of the crop growth processes incorporated in WOFOST | 117 |

| | |
|--|-----|
| Appendix 1 Measurement methods to determine soil hydraulic functions..... | 165 |
| Appendix 2 Parameters of soil hydraulic functions: Staring series (Wösten et al., 2001) | 167 |
| Appendix 3 Critical pressure head values for root water extraction (Taylor and Ashcroft, 1972)..... | 169 |
| Appendix 4 Salt tolerance data (Maas, 1990) ^(a) | 170 |
| Appendix 5 Shrinkage characteristic data (Bronswijk and Vermeer, 1990) | 171 |
| Appendix 6 Summary of input data..... | 172 |
| Appendix 7 Example main input file .SWP | 173 |
| Appendix 8 Example weather input file .YYY..... | 181 |
| Appendix 9 Example simple crop input file .CRP..... | 182 |
| Appendix 10 Example detailed crop input file .CRP..... | 185 |
| Appendix 11 Example lateral drainage input file .DRA | 189 |
| Appendix 12 Summary of output data | 194 |
| Appendix 13 Example short water and solute balance output file *.bal | 195 |
| Appendix 14 Example extended water balance output file *.blc | 196 |
| Appendix 15 Description of the output files *.afo and *.aun..... | 197 |
| Appendix 16 Description of the output files *.bfo and *.bun | 199 |
| Appendix 17 Ranges of values of input parameters | 203 |

Preface

SWAP (Soil-Water-Atmosphere-Plant) is the successor of the agrohydrological model SWATR (Feddes et al., 1978) and some of its numerous derivatives. Earlier versions were published as SWATR(E) by Feddes et al. (1978), Belmans et al. (1983) and Wesseling et al. (1991), as SWACROP by Kabat et al. (1992) and as SWAP93 by Van den Broek et al. (1994). The latest version was published as SWAP2.0 by Van Dam et al. (1997) and Kroes et al. (2001). Main differences between the current version SWAP 3.0 and the previous version are:

- Source code was restructured (input, output, timing, error handling)
- Snow and frost options were implemented
- MacroPore flow was extended
- Extended options for interaction with water quality models
- Extended options for bottom boundary conditions
- Interception according to Gash has been added
- Runon is facilitated for sloping areas

All reports, together with the SWAP program and examples, are available through the SWAP-development group and the Internet (www.alterra.nl/models/swap or www.swap.alterra.nl).

The general reference to the SWAP model is Van Dam (2000).

Summary

Water movement in top soils determines the rate of plant transpiration, soil evaporation, runoff and recharge to the groundwater. In this way unsaturated soil water flow is a key factor in the hydrological and energy cycle. Due to the high solubility of water, soil water transports large amounts of solutes, ranging from nutrients to all kind of contaminations. Therefore an accurate description of unsaturated soil water movement is essential to derive proper management conditions for vegetation growth and environmental protection in agricultural and natural systems. Chapter 1 provides an overview of the modelled top system and a reading guide.

In chapter 2 the basic equations for soil water flow are discussed. SWAP employs the Richards' equation, which allows the use of soil hydraulic data bases. The strong physical base of Richards' equation is important for generalization of field experiments and for analysis of all kind of scenario's. A versatile numerical solution of the non-linear Richards' equation is described, along with an automatic procedure for the top boundary which accommodates rapidly changing field conditions. Physical and empirical methods to determine actual soil evaporation are considered. The soil hydraulic functions are described by the analytical expressions of Van Genuchten and Mualem. One of the most important outputs of agrohydrological models is the amount of water and salt stress for crops and vegetation. Therefore the concepts employed for water and salt stress are discussed. The chapter ends with the conditions used during frost periods.

In chapter 3 we consider the interactions between atmosphere, plants and soils. First snow accumulation and –melt are discussed. Next we describe options to calculate interception of agricultural crops and forests. Potential evapotranspiration is calculated with the Penman-Monteith equation, using the method recommended by Allen et al. (1998). SWAP allows direct use of the Penman-Monteith equation, in which case crop specific values of minimum resistance, leaf area index, albedo and crop height are required, or the Penman-Monteith method as applied to reference grass in combination with crop coefficients. Also reference evapotranspiration can be specified as input, which accommodates alternative evapotranspiration formulas. During the growing season SWAP will calculate potential evapotranspiration rates of wet canopies, dry canopies and wet bare soils. These fluxes, in combination with either leaf area index or crop cover, allow the calculation of potential transpiration and potential evaporation. The reduction to actual transpiration and evaporation fluxes has been described in chapter 2.

The interaction of soil water and surface water is subject of chapter 4. This interaction may consist of surface flow (runoff, runoff and inundation) and subsurface flow (drainage or infiltration). The runoff and runoff options allow the calculation of a sequence of soil profiles along a slope with runoff. Drainage and infiltration can be calculated with linear or tabular relations between groundwater level and drainage/infiltration flux, or with analytical equations of Hooghoudt and Ernst. For regional analysis the drainage to 5 different levels can be simulated. The highest level can be used to mimic interflow, which is characterised by relatively short residence times. The extended drainage option allows the evaluation of different surface water management options. SWAP will calculate surface water levels from all incoming and outgoing fluxes. As function of time, the user may specify target levels for surface water, the maximum groundwater level, the maximum soil water pressure head and

the minimum air volume. SWAP will determine the highest surface water levels which meet the specified targets. The final part of chapter 4 explains the method used to determine residence times in case of heterogeneous soils and drainage to different levels. Proper residence times and distribution of drainage fluxes to different levels is useful for nutrient and pesticide leaching studies.

In chapter 5 the interaction of soil water and groundwater is described. SWAP allows the use of time dependent pressure heads, soil water fluxes or the relation between both. The interaction may include fluxes from deep aquifers, relative to the conditions simulated in the phreatic aquifer. The interactions between soil water and groundwater apply to field and regional level.

In many cases SWAP is used at field scale level, which can be viewed as a natural basic unit of larger regions. Most natural or cultivated fields have one cropping pattern, soil profile, drainage condition and management scheme. This information comes increasingly available in geographical data bases. Geographical information systems can be used to generate input data for field scale models, to run these models for fields with unique boundary conditions and physical properties, and to compile regional results of viable management scenarios. The regional scale is of most interest to water managers and politicians. In order the use SWAP at field scale level, we should consider the natural soil heterogeneity within a field. SWAP has options to accommodate hysteresis in the retention function, spatial variability of soil hydraulic functions, preferential flow in water repellent soils and in soils with macropores. The concepts used for this soil heterogeneity are discussed in Chapter 6. To simulate the effects of hysteresis in the retention function, SWAP may scale main wetting and drying curves to relevant scanning curves. Spatial soil hydraulic variability can be generated according to geometrically similar media with single scale factors for both soil hydraulic functions. Mobile-immobile concepts are employed for water flow in water repellent soils. Macropore flow occurs both in clay and peat soils. SWAP contains a simple and an extensive concept to simulate macropore flow. The extensive macropore concept is still in the testing phase and therefore still under construction.

SWAP contains a simple and a detailed crop module (Chapter 7). In the simple crop model the crop development with time is prescribed. The user should specify leaf area index (or soil cover fraction), crop height and rooting depth as function of development stage. The detailed crop module is based on the crop growth model WOFOST. This model calculates the radiation energy absorbed by the canopy as function of incoming radiation and crop leaf area. Using the absorbed radiation and taking into account photosynthetic leaf characteristics, the potential gross photosynthesis is calculated. The latter is reduced in case of water and/or salinity stress, which yields the actual gross photosynthesis. Part of the carbohydrates (CH_2O) produced are used to provide energy for the maintenance of the existing live biomass. The remaining carbohydrates are converted into structural matter. In this conversion, some of the assimilates are lost as growth respiration. The resulting dry matter is divided among roots, leaves, stems and storage organs, using partitioning factors that are a function of the crop development stage. The fraction partitioned to the leaves determines leaf area development and hence the dynamics of light interception. The dry weights of the plant organs are obtained by integrating their growth rates over time. During the development of the crop, a part of the living biomass dies due to senescence.

Chapter 8 describes the solute transport mechanisms which are included in the model. SWAP simulates the solute processes convection, diffusion and dispersion, non-linear adsorption, first order decomposition and root uptake. This permits the simulation of ordinary pesticide and salt transport, including the effect of salinity on crop growth. In case of detailed pesticide transport or nitrate leaching, daily water fluxes can be generated as input for the pesticide model PEARL or the nutrient model ANIMO. Chapter 8 also describes the solute boundary conditions and the provisions for solute transport in water repellent and macropore soils. In the saturated zone two- or three-dimensional flow patterns exist, depending on the existing hydraulic head gradients. It can be shown that the solute residence time distribution of an aquifer with drainage to drains or ditches is similar to that of a mixed reservoir. Using this similarity, SWAP solves the differential equation for solute amounts in a mixed reservoir, with flux type boundary conditions to the unsaturated zone and the drainage devices. In this way solute transport from the soil surface to the surface water can be calculated.

The heat flow equation (chapter 9) is solved either analytically or numerically. The analytical solution assumes uniform and constant thermal conductivity and soil heat capacity. At the soil surface a sinusoidal temperature wave is assumed. In case of the numerical solution, the thermal conductivity and soil heat capacity are calculated from the soil texture and the volume fractions of water and air as described by De Vries (1975). At the soil surface the daily average temperature is used as boundary condition.

In chapter 10 various water management aspects are discussed. SWAP can be used to optimize timing and amount of sprinkling or surface irrigation. Also the effects of different drainage designs in relation to long term water and salinity stress can be evaluated. SWAP may simulate water and solute balances for different land use options. Also SWAP may generate optimal surface water levels depending on the actual situation, desired groundwater levels, and expected weather conditions.

Finally chapter 11 discusses program operation. A summary and description of input files is given. Example input files are listed in Appendices 7-11. The program execution and error handling are shortly described. The chapter ends with an overview of the output files. Appendix 12 lists in detail the variables that are printed in each output file.

1 Introduction

J.G. Kroes

Knowledge of water and solute movement in the variably saturated soil near the earth surface is essential to understand man's impact on the environment. Top soils show the largest concentration of biological activity on earth. Water movement in the upper soil determines the rate of plant transpiration, soil evaporation, runoff and recharge to the groundwater. In this way unsaturated soil water flow is a key factor in the hydrological cycle. Due to the high solubility of water, soil water transports large amounts of solutes, ranging from nutrients to all kind of contaminations. Therefore an accurate description of unsaturated soil water movement is essential to derive proper management conditions for vegetation growth and environmental protection in agricultural and natural systems.

1.1 System description

The core of the SWAP model exists of implementations of mathematical descriptions of soil water flow, solute transport and soil temperatures, with special emphasis on soil heterogeneity. A schematized overview of the modelled system is given in Figure 1.

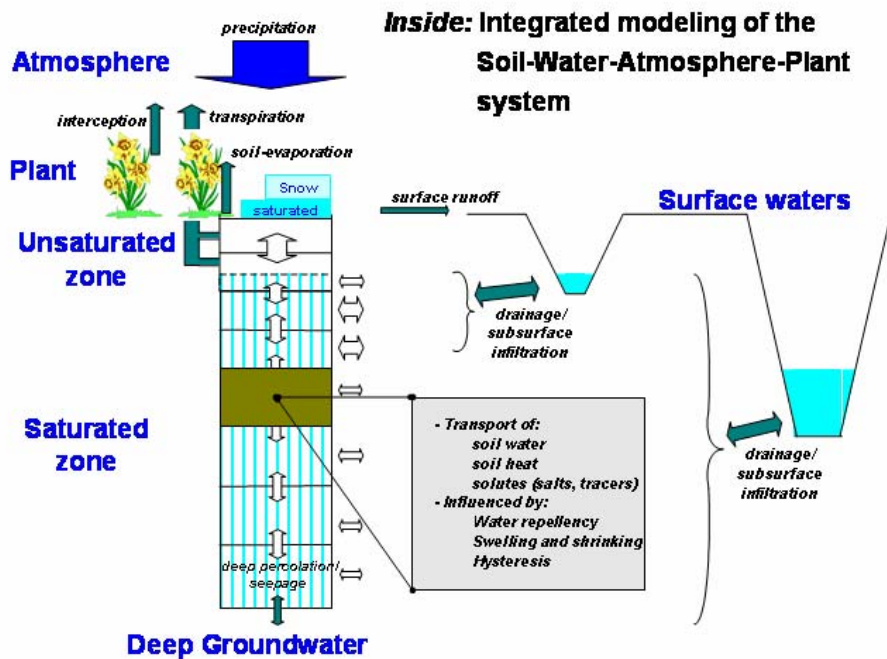


Figure 1 Schematized overview of the modelled system

For the modelled system as a whole a general water balance may be constructed for a flexible time interval (days – years):

$$\text{Storage change} = \text{Supply} - \text{Discharge}$$

where:

- *Storage change* over a certain time interval occurs in: soil, snow pack, superficial ponding layer, and soil cracks;
- *Supply* terms during a certain time interval are: precipitation, irrigation, surface runoff, inundation from surface water, infiltration from 5 different surface water systems, upward seepage across the lower boundary of the system;
- *Discharge* terms during a certain time interval are: surface runoff, drainage to 5 different surface water systems, downward leaching across the lower boundary of the system and evaporation by intercepted rainfall, soil, ponding layer, and crop.

Interactions are described between the sub systems soil (unsaturated and saturated), atmosphere, plant, groundwater and surface water. A flow chart of the main water flows to and from the modelled sub systems is given in Figure 2.

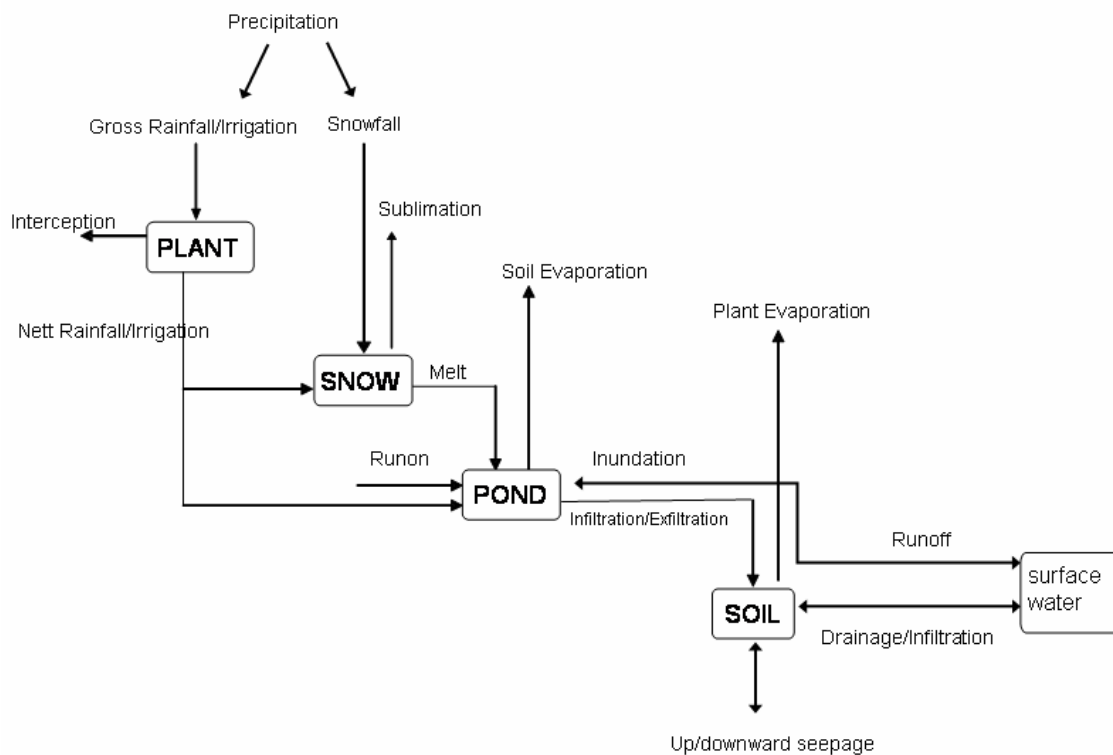


Figure 2 Flowchart of the main fluxes between the sub systems

1.2 Reading guide

This reference manual describes the modelling concepts implemented in SWAP version 3. After a system description in chapter 1, the core of the model is explained in a chapter about soil water flow (chapter 2). Next follow chapters on interactions with the atmosphere, surface water and groundwater: top, lateral and bottom boundary, respectively chapters 3, 4, and 5. In the following chapters an explanation is given of the modelled processes on soil heterogeneity, crop growth, solute transport and soil temperatures. Examples of application in water management are given in chapter 10. This manual ends with a chapter on program operating.

The annexes contain information on values for input parameters, such as soil hydraulic functions, critical pressure head values of the root water extraction term and salt tolerance data. Furthermore the annexes contain printed versions of input and output files that belong to an example which is distributed with the model.

2 Soil water flow

J.C. van Dam, R.A. Feddes

2.1 Basic equations

Spatial differences of the soil water potential induce soil water movement. Darcy's equation is commonly used to quantify these soil water fluxes. For one-dimensional vertical flow, Darcy's equation can be written as:

$$q = -K(h) \frac{\partial(h+z)}{\partial z} \quad (2.1)$$

where q is soil water flux density (positive upward) (cm d^{-1}), K is hydraulic conductivity (cm d^{-1}), h is soil water pressure head (cm) and z is the vertical coordinate (cm), taken positively upward.

Water balance considerations of an infinitely small soil volume result in the continuity equation for soil water:

$$\frac{\partial \theta}{\partial t} = -\frac{\partial q}{\partial z} - S_a(h) \quad (2.2)$$

where θ is volumetric water content ($\text{cm}^3 \text{cm}^{-3}$), t is time (d) and S_a is soil water extraction rate by plant roots ($\text{cm}^3 \text{cm}^{-3} \text{d}^{-1}$).

Combination of Eqs. (2.1) and (2.2) provides the general water flow equation in variably saturated soils, known as the Richards' equation:

$$\frac{\partial \theta}{\partial t} = C(h) \frac{\partial h}{\partial t} = \frac{\partial \left[K(h) \left(\frac{\partial h}{\partial z} + 1 \right) \right]}{\partial z} - S_a(h) \quad (2.3)$$

where C is the water capacity ($\partial\theta/\partial h$) (cm^{-1}).

Richards' equation has a clear physical basis at a scale where the soil can be considered to be a continuum of soil, air and water. SWAP solves Eq. (2.3) numerically, subject to specified initial and boundary conditions and with known relations between θ , h and K . These relationships can be measured directly in the soil, determined in the laboratory, or might be obtained from basic soil data as discussed in Par. 3.2. SWAP applies Richards' equation integrally for the unsaturated-saturated zone, including possible transient and perched groundwater levels.

2.2 Numerical solution of soil water flow equation

Accurate numerical solution of Richards' partial differential equation is not easy due to its hyperbolic nature, the strong non-linearity of the soil hydraulic functions and the rapid

changing boundary conditions near the soil surface. In the past calculated soil water fluxes could be significantly affected by the structure of the numerical scheme, the applied time and space discretizations, and the procedure for the top boundary condition (Van Genuchten, 1982; Milly, 1985; Celia et al., 1990; Warrick, 1991; Zaidel and Russo, 1992). In SWAP a numerical scheme has been chosen which solves the one-dimensional Richards' equation with an accurate mass balance and which converges rapidly. This scheme in combination with the top boundary procedure has been shown to handle rapid soil water movement during infiltration in dry soils accurately. At the same time the scheme is fast, calculating periods of 40-70 years in a few minutes (Van Dam and Feddes, 2000).

2.2.1 Numerical discretization in the soil profile

A common method to solve Richards' equation has been the implicit, backward, finite difference scheme with explicit linearization as described by Haverkamp et al. (1977) and Belmans et al. (1983). Three adaptations to this scheme were made to arrive at the numerical scheme currently applied in SWAP. The first adaptation concerns the handling of the differential water capacity C . The old scheme was limited to the unsaturated zone only. The saturated zone and fluctuations of the groundwater table had to be modelled separately (Belmans et al., 1983). The new numerical scheme enables us to solve the flow equation in the unsaturated and saturated zone simultaneously. In order to do so, in the numerical discretization of Richards' equation, the C -term only occurs as numerator, not as denominator (see Eq. (2.3)).

The second adaptation concerns the numerical evaluation of the C -term. Because of the high non-linearity of C , averaging during a time step results in serious mass balance errors when simulating highly transient conditions. A simple but effective adaptation was suggested by Milly (1985) and further analysed by Celia et al. (1990). Instead of applying during a *time* step

$$\theta_i^{j+1} - \theta_i^j = C_i^{j+1/2} (h_i^{j+1} - h_i^j) \quad (2.4)$$

where $C_i^{j+1/2}$ denotes the average water capacity during the time step, subscript i is the node number (increasing downward) and superscript j is the time level, they applied at each *iteration* step:

$$\theta_i^{j+1} - \theta_i^j = C_i^{j+1,p-1} (h_i^{j+1,p} - h_i^{j+1,p-1}) + \theta_i^{j+1,p-1} - \theta_i^j \quad (2.5)$$

where superscript p is the iteration level and $C_i^{j+1,p-1}$ is the water capacity evaluated at the h value of the last iteration. At convergence $(h_i^{j+1,p} - h_i^{j+1,p-1})$ will be small, which eliminates effectively remaining inaccuracies in the evaluation of C .

The third adaptation concerns the averaging of K between the nodes. Haverkamp and Vauclin (1979), Belmans et al. (1983) and Hornung and Messing (1983) proposed to use the geometric mean. In their simulations the geometric mean increased the accuracy of calculated fluxes and caused the fluxes to be less sensitive to changes in nodal distance. However, the geometric mean has serious disadvantages too (Warrick, 1991). When simulating infiltration in dry soils or high evaporation from wet soils, the geometric mean severely underestimates the water fluxes. Other researchers proposed to use the harmonic mean of K or various kind of weighted averages (Ross, 1990; Warrick, 1991; Zaidel and Russo, 1992; Desbarats, 1995). Van Dam and Feddes (2000) show that, although arithmetic

averages at larger nodal distances overestimate the soil water fluxes in case of infiltration and evaporation events, at nodal distances in the order of 1 cm arithmetic averages are more close to the theoretically correct solution than geometric averages. Also they show that the remaining inaccuracy between calculated and theoretically correct fluxes, is relatively small compared to effects of soil spatial variability and hysteresis. Therefore SWAP applies arithmetic averages of K , which is in line with commonly applied finite element models (Kool and Van Genuchten, 1991; Šimůnek et al., 1992).

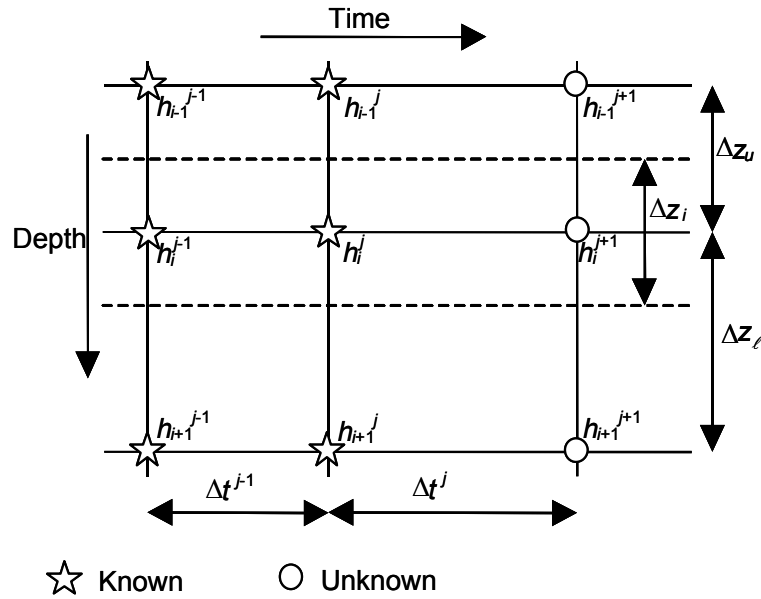


Figure 3 Spatial and temporal discretization used to solve Richards' equation

The implicit, backward, finite difference scheme of Eq. (2.3) with explicit linearization, including the three adaptations, yields the following discretization of Richards' equation:

$$C_i^{j+1,p-1} (h_i^{j+1,p} - h_i^{j+1,p-1}) + (\theta_i^{j+1,p-1} - \theta_i^j) = \frac{\Delta t^j}{\Delta z_i} \left[K_{i-1/2}^j \left(\frac{h_{i-1}^{j+1,p} - h_i^{j+1,p}}{\Delta z_u} \right) + K_{i-1/2}^j - K_{i+1/2}^j \left(\frac{h_i^{j+1,p} - h_{i+1}^{j+1,p}}{\Delta z_\ell} \right) - K_{i+1/2}^j \right] - \Delta t^j S_i^j \quad (2.6)$$

where $\Delta t^j = t^{j+1} - t^j$, $\Delta z_u = z_{i-1} - z_i$, $\Delta z_\ell = z_i - z_{i+1}$ and Δz_i is compartment thickness. Figure 3 shows the symbols in the space-time domain. K and S are evaluated at the old time level j (explicit linearization), which can be shown to give a good approximation at the time steps used. This numerical scheme applies both to the saturated and unsaturated zone. Starting in the saturated zone, the groundwater table is simply found at $h = 0$. Also perched water tables may occur above dense layers in the soil profile. Calculations show that in order to simulate infiltration and evaporation accurately, near the soil surface the nodal distance should be in the order of centimetres. For this reason the nodal distance in SWAP is made variable. Application of Eq. (2.6) to each node, subject to the prevailing boundary conditions, results in a tri-diagonal system of equations which can be solved efficiently (Press et al., 1989).

In the past the pressure head difference $|h_i^{j+1,p} - h_i^{j+1,p-1}|$ in the iterative solution of Eq. (2.6) has been used as convergence criterium. Instead Huang et al. (1996) proposed to use the water content difference $|\theta_i^{j+1,p} - \theta_i^{j+1,p-1}|$. The advantage of a criterium based on θ is that it is automatically more sensitive in pressure head ranges with a large differential soil water capacity, $C=(d\theta/dh)$, while it allows less iterations at low h -values where θ hardly changes. Huang et al. (1996) show the higher efficiency of the θ -criterium for a large number of infiltration problems. Moreover the θ -criterium was found to be more robust when the soil hydraulic characteristics were extremely non-linear. Therefore in SWAP the main convergence criterium in the unsaturated zone is based on the water content difference $|\theta_i^{j+1,p} - \theta_i^{j+1,p-1}|$. In saturated or near-saturated compartments the θ -criterium is insensitive, therefore SWAP uses in addition a maximum of the pressure head difference $|h_i^{j+1,p} - h_i^{j+1,p-1}|$.

The optimal time step should minimize the computational effort of a simulation while the numerical solution still meets the convergence criteria mentioned above. The number of iterations needed to reach convergence, N_{it} , can effectively be used for this purpose (Kool and Van Genuchten, 1991). In SWAP the following criteria are applied:

$N_{it} < 2$: multiply time step with a factor 1.25
 $2 \leq N_{it} \leq 4$: keep time step the same
 $N_{it} > 4$: divide time step by a factor 1.25

In the SWAP input file a minimum and a maximum time step, Δt_{min} and Δt_{max} (d), are defined. For the initial time step, SWAP will take $\Delta t = \sqrt{\Delta t_{min}\Delta t_{max}}$. Depending on N_{it} , the time step will be decreased, maintained or increased for the following timesteps. If during an iteration N_{it} exceeds 6, SWAP will divide Δt by a factor 3, and start iterating again. The timestep is always confined to the range $\Delta t_{min} \leq \Delta t \leq \Delta t_{max}$. Exceptions to above procedure occur, when the upper boundary flux changes from evaporation to intensive rainfall ($> 1.0 \text{ cm d}^{-1}$), in which case Δt is reset to Δt_{min} , and at the end of a day, in which case Δt is set equal to the remaining time in the day.

In some application it is known that large fluctuations in the groundwater level do not occur. An input parameter (GWLCONV) may be used to influence the convergence process and prevent large fluctuations in groundwater levels. However, when the model is applied under frost conditions, this input parameters can best be set to a high value (e.g. 500 cm) because groundwater levels in frozen soils (permafrost) are inaccurate and should not be used to influence the iteration scheme.

For some applications the accuracy of the water balance requires critical values. For this purpose the absolute deviation in the water balance is determined during each timestep and the iteration process continues until a given critical values is achieved. This critical value (CritDevMasBalDt) is input to the model.

| <i>Model input</i> | | | |
|--|-----------------|--|----------------|
| <i>Variable</i> | <i>Code</i> | <i>Description</i> | <i>Default</i> |
| Δt_{\min} | DTMIN | minimum time step (d) | 10^{-5} |
| Δt_{\max} | DTMAX | maximum time step (d) | 0.2 |
| $ \theta_i^{j+1} - \theta_i^j _{\max}$ | THETOL | maximum difference in water content between iterations (-) | 0.001 |
| | GWLCONV | maximum difference of gwl between iterations (cm) | 100.0 |
| | CritDevMasBalDt | Critical deviation in water balance of each timestep(cm) | 0.01 |
| | MSTEPS | maximum number of time steps during a day (-) | 10^5 |

2.2.2 Top boundary condition

Appropriate criteria for the procedure with respect to the top boundary condition are important for accurate simulation of rapidly changing soil water fluxes near the soil surface. This is for instance the case with infiltration/runoff events during intensive rain showers or when the soil occasionally gets flooded in areas with shallow groundwater tables.

At moderate weather and soil wetness conditions the soil top boundary condition will be flux-controlled. In either very wet or very dry conditions the prevailing water pressure head at the soil surface starts to govern the boundary condition. Figure 4 shows the applied procedure in SWAP to select between flux- and pressure head controlled top boundary. A prescribed flux at the soil surface is denoted as q_{sur} (cm d^{-1}), and a prescribed pressure head as h_{sur} (cm). Soil water fluxes are defined positive when they are directed upward.

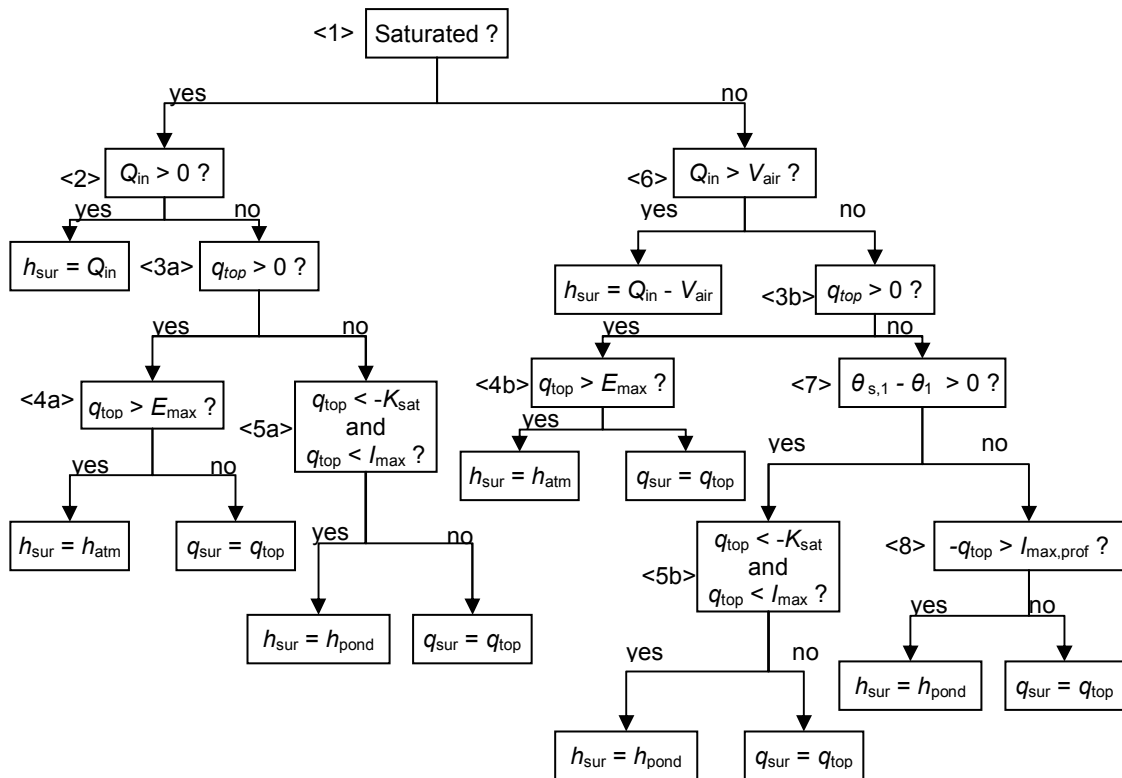


Figure 4 Procedure to select head (h_{sur}) or flux (q_{sur}) top boundary condition. The variables are explained in the text

In Figure 4 criterium <1> refers to whether the soil is saturated. If so, criterium <2> determines whether the soil is still saturated at the next time level t^{j+1} or becomes unsaturated. The inflow Q_{in} (cm) is defined as:

$$\begin{aligned} Q_{in} &= (q_{bot} - q_{top} - q_{root} - q_{drain}) \Delta t^j & \text{if } q_{top} > I_{max} \\ Q_{in} &= (q_{bot} - I_{max} - q_{root} - q_{drain}) \Delta t^j & \text{if } q_{top} < I_{max} \end{aligned} \quad (2.7)$$

where q_{bot} is the flux at the soil profile bottom (cm d⁻¹), q_{top} the potential flux at the soil surface (cm d⁻¹), q_{drain} the flux to drains or ditches (cm d⁻¹) and I_{max} is the maximum infiltration rate (cm d⁻¹). The potential flux at the soil surface q_{top} follows from:

$$q_{top} = q_{eva} - q_{prec} - q_{irrig} - q_{melt} - q_{runon} - \frac{h_{pond}}{\Delta t^j} \quad \text{with } q_{top} \geq I_{max} \quad (2.8)$$

where q_{eva} is the actual soil evaporation (cm d⁻¹), q_{prec} is the precipitation at the soil surface (cm d⁻¹), q_{irrig} is the irrigation at the soil surface (cm d⁻¹), q_{melt} is the melt water flux from the snowpack (cm d⁻¹) (paragraph 3.2), q_{runon} is the runoff (cm d⁻¹) (paragraph 4.1.2) and h_{pond} is the height of water ponding on the soil surface (cm).

Criterium <3> determines whether the soil becomes or remains unsaturated. If the soil becomes unsaturated, criterium <3a>, a distinction is made between evaporation and infiltration. In case of evaporation, criterium <4>, the maximum flux is limited to the maximum flux according to Darcy, E_{max} (cm d⁻¹):

$$E_{max} = K_{\frac{1}{2}} \left(\frac{h_{atm} - h_1^{j+1,p-1} - z_1}{z_1} \right) \quad (2.9)$$

with h_{atm} (cm) the soil water pressure head in equilibrium with the prevailing air relative humidity:

$$h_{atm} \approx -2.75 \cdot 10^5 \text{ cm} \quad (2.10)$$

In the case of infiltration (criterium <5>) a head-controlled condition applies if the potential flux q_{top} exceeds the maximum infiltration rate I_{max} and the saturated hydraulic conductivity K_{sat} . I_{max} (cm d⁻¹) is calculated as:

$$I_{max} = K_{\frac{1}{2}} \left(\frac{h_{pond} - h_1^{j+1,p-1} - z_1}{z_1} \right) \quad (2.11)$$

The average hydraulic conductivity ($K_{\frac{1}{2}}$) is calculated with the saturated hydraulic conductivity and, in the case of a frozen soil, a correction factor for the soil temperature (Eq.(2.28) and (2.29)).

When the soil is unsaturated, criterium <6> determines if the soil will be saturated at the next time level t^{j+1} (head is prescribed) or if the soil remains unsaturated. The symbol V_{air} (cm) denotes the pore volume in the soil profile being filled with air at time level t^j (see also

Eq. (2.30). If the soil remains unsaturated, criterium <3b>, a distinction is made between evaporation, criterium <4b>, and infiltration.

In case of infiltration, criterium <7>, the difference between the saturated and actual water content determines if the infiltration capacity of the soil is sufficient for the infiltration flux. During the iteration, when no convergence is reached, it might be possible that the actual water content is higher than the saturated water content. For criterium <8> the maximum infiltration capacity of the soil profile ($I_{\max, \text{prof}}$) is calculated:

$$I_{\max, \text{prof}} = \frac{-q_{\text{top}} \sum_{i=1}^m z_i}{\sum_{i=1}^m K_i + \sum_{i=1}^m z_i} \quad (2.12)$$

where m is the number of soil compartments with a total V_{air} smaller than Q_{in} , z_i is the depth of soil compartment i and K_i is the conductivity of soil compartment i .

During the iterative procedure of calculating $h_i^{j+1, p}$ from the tri-diagonal system of equations (Par. 2.2.1), the top boundary condition is updated at each iteration p . Therefore the runoff and depth of the ponding layer are also recalculated as described in paragraph 4.1

2.2.3 Actual soil evaporation

In the case of a wet soil, soil evaporation is determined by the atmospheric demand and equals potential soil evaporation rate E_p . When the soil becomes drier, the soil hydraulic conductivity decreases, which may reduce E_p to a lower actual evaporation rate, E_a (cm d^{-1}). In SWAP the maximum evaporation rate which the top soil may deliver, E_{\max} (cm d^{-1}), is calculated according to Darcy's law (see also Eq. (2.9)):

$$E_{\max} = K_{1/2} \left(\frac{h_{\text{atm}} - h_1 - z_1}{z_1} \right) \quad (2.13)$$

where $K_{1/2}$ is the average hydraulic conductivity (cm d^{-1}) between the soil surface and the first node, h_{atm} is the soil water pressure head (cm) in equilibrium with the air relative humidity, h_1 is the soil water pressure head (cm) of the first node, and z_1 is the soil depth (cm) at the first node. Equation (2.13) excludes water flow due to thermal differences in the top soil and due to vapour flow, as on daily basis the concerned flow amounts are probably negligible compared to isothermal, liquid water flow (Koorevaar et al., 1983; Ten Berge, 1986; Jury et al., 1991). Note that the value of E_{\max} in Eq. (2.13) depends on the thickness of the top soil compartments. Increase of compartment thickness, generally results in smaller values for E_{\max} due to smaller hydraulic head gradients. For accurate simulations at extreme hydrological conditions, the thickness of the top compartments should not be more than 1 cm (see Par. 2.2.1).

There is one serious limitation of the E_{\max} procedure as described above. E_{\max} is governed by the soil hydraulic functions $\theta(h)$ and $K(\theta)$. Still it is not clear to which extent the soil hydraulic functions, that usually represent a top layer of a few decimeters, are valid for the top few centimeter of a soil, which are subject to splashing rain, dry crust formation, root

extension and various cultivation practices. Therefore also empirical evaporation functions may be used, which require calibration of their parameters for the local climate, soil, cultivation and drainage situation. SWAP has the option to choose the empirical evaporation functions of Black (1969) or Boesten and Stroosnijder (1986).

Black calculated the cumulative actual evaporation during a drying cycle, ΣE_a (cm) as:

$$\sum E_a = \beta_1 t_{\text{dry}}^{1/2} \quad (2.14)$$

where β_1 is a soil specific parameter ($\text{cm d}^{-0.5}$), characterizing the evaporation process and t_{dry} is the time (d) after a significant amount of rainfall, P_{min} . SWAP resets t_{dry} to zero if the net precipitation P_{net} exceeds P_{min} .

| <i>Model input</i> | | | |
|--------------------|-------------|--|----------------|
| <i>Variable</i> | <i>Code</i> | <i>Description</i> | <i>Default</i> |
| β_1 | COFRED | soil evaporation coefficient of Black ($\text{cm d}^{-1/2}$) | 0.35 |
| P_{min} | RSIGNI | Minimum amount of rainfall for reset Black time (cm d^{-1}) | 0.5 |

The Black parameter β_1 has been shown to be affected by E_p itself. In order to avoid this effect, Boesten and Stroosnijder (1986) proposed to use the sum of potential evaporation, ΣE_p (cm), as time variable:

$$\begin{aligned} \sum E_a &= \sum E_p & \text{for } \sum E_p &\leq \beta_2^2 \\ \sum E_a &= \beta_2 \left(\sum E_p \right)^{1/2} & \text{for } \sum E_p &> \beta_2^2 \end{aligned} \quad (2.15)$$

where β_2 is a soil parameter ($\text{cm}^{1/2}$), which should be determined experimentally. The parameter β_2 determines the length of the potential evaporation period, as well as the slope of the ΣE_a versus $(\Sigma E_p)^{1/2}$ relationship in the soil limiting stage.

For days with $P_{\text{net}} < P_{\text{min}}$, Boesten and Stroosnijder suggest the following procedure with respect to updates of ΣE_p . On days with no excess in rainfall ($P_{\text{net}} < E_p$), ΣE_p follows from Eq. (2.15), that is:

$$\left(\sum E_p \right)^j = \left(\sum E_p \right)^{j-1} + \left(E_p - P_{\text{net}} \right)^j \quad (2.16)$$

in which superscript j is the day number. $(\Sigma E_a)^j$ is calculated from $(\Sigma E_p)^j$ with Eq. (2.15) and E_a is calculated with

$$E_a^j = P_{\text{net}}^j + \left(\sum E_a \right)^j - \left(\sum E_a \right)^{j-1} \quad (2.17)$$

On days of excess in rainfall ($P_{\text{net}} > E_p$)

$$E_a^j = E_p^j \quad (2.18)$$

and the excess rainfall is subtracted from ΣE_a

$$\left(\sum E_a \right)^j = \left(\sum E_a \right)^{j-1} - \left(P_{\text{net}} - E_p \right)^j \quad (2.19)$$

Next $(\Sigma E_p)^j$ is calculated from $(\Sigma E_a)^j$ with Eq. (2.15). If the daily rainfall excess is larger than $(\Sigma E_p)^{j-1}$, then both $(\Sigma E_a)^j$ and $(\Sigma E_p)^j$ are set at zero.

| <i>Model input</i> | | | |
|--------------------|-------------|---|----------------|
| <i>Variable</i> | <i>Code</i> | <i>Description</i> | <i>Default</i> |
| β_2 | COFRED | soil evaporation coefficient of Boesten/Stroosn. (cm ^{1/2}) | 0.54 |
| P_{\min} | RSIGNI | Minimum amount of rainfall to reset sum E_p (cm d ⁻¹) | 0.5 |

SWAP will determine E_a by taking the minimum value of E_p , E_{\max} and, if selected by the user, one of the empirical functions. This procedure implicitly assumes that E_{\max} in general overestimates the maximum soil water flow near the soil surface.

2.2.4 Other boundary condition

The following other boundary conditions are taken into account:

- lateral boundary conditions (chapter 4);
- bottom boundary conditions (chapter 5);
- initial conditions.

Lateral and bottom boundary conditions are described elsewhere, respectively in chapters 4 and 5.

Initial conditions are implemented with 2 options:

- a) input of pressure heads for each compartment;
- b) input of a groundwater level. The nodal pressure heads will be calculated assuming hydrostatic equilibrium with the groundwater level, both in the saturated and unsaturated zone.

2.3 Soil hydraulic functions

The relationships between the water content θ , the pressure head h and the hydraulic conductivity K are generally summarized in the retention function $\theta(h)$ and the unsaturated hydraulic conductivity function $K(\theta)$. These soil hydraulic functions need to be specified for each distinct soil layer. An overview of measurement methods is given in Appendix 1.

Although tabular forms of $\theta(h)$ and $K(\theta)$ have been used for many years, currently analytical expressions are generally applied for a number of reasons. Analytical expressions are more convenient as model input and a rapid comparison between horizons is possible by comparing parameter sets. In case of hysteresis (Par. 6.2), scanning curves can be derived by some modification of the analytical function. Also scaling (Par. 6.3), which is used to describe spatial variability of $\theta(h)$ and $K(\theta)$, requires an analytical expression of the reference curve. Another reason is to enable extrapolation of the functions beyond the measured data range. Last but not least, analytical functions allow for calibration and estimation of the soil hydraulic functions by inverse modeling.

Brooks and Corey (1964) proposed an analytical function of $\theta(h)$ which has been widely used for a number of years. Mualem (1976) derived a predictive model of the $K(\theta)$ relation based on the retention function. Van Genuchten (1980) proposed a more flexible $\theta(h)$

function than the Brooks and Corey relation and combined it with Mualem's predictive model to derive $K(\theta)$. The Van Genuchten function has been used in numerous studies, forms the basis of several national and international data-bases (e.g. Carsel and Parrish, 1988; Yates et al., 1992; Leij et al., 1996; Wösten et al., 2001), and is implemented in SWAP.

The analytical $\theta(h)$ function proposed by Van Genuchten (1980) reads:

$$\theta = \theta_{\text{res}} + \frac{\theta_{\text{sat}} - \theta_{\text{res}}}{\left(1 + |\alpha h|^n\right)^m} \quad (2.20)$$

where θ_{sat} is the saturated water content ($\text{cm}^3 \text{cm}^{-3}$), θ_{res} is the residual water content in the very dry range ($\text{cm}^3 \text{cm}^{-3}$) and α (cm^{-1}), n (-) and m (-) are empirical shape factors. Without losing much flexibility, m can be taken equal to :

$$m = 1 - \frac{1}{n} \quad (2.21)$$

Using the above $\theta(h)$ relation and applying the theory on unsaturated hydraulic conductivity by Mualem (1976), the following $K(\theta)$ function results:

$$K = K_{\text{sat}} S_e^\lambda \left[1 - \left(1 - S_e^{\frac{1}{m}} \right)^m \right]^2 \quad (2.22)$$

where K_{sat} is the saturated conductivity (cm d^{-1}), λ is a shape parameter (-) depending on $\partial K / \partial h$, and S_e is the relative saturation defined as:

$$S_e = \frac{\theta - \theta_{\text{res}}}{\theta_{\text{sat}} - \theta_{\text{res}}} \quad (2.23)$$

Van Genuchten et al. (1991) developed the program RETC to estimate the parameter values of this model from measured $\theta(h)$ and $K(\theta)$ data.

| <i>Model input</i> | | | |
|-------------------------------------|-------------|---|----------------|
| <i>Specify for each soil layer:</i> | | | |
| <i>Variable</i> | <i>Code</i> | <i>Description</i> | <i>Default</i> |
| θ_{res} | ORES | residual water content ($\text{cm}^3 \text{cm}^{-3}$) | 0.01 |
| θ_{sat} | OSAT | saturated water content ($\text{cm}^3 \text{cm}^{-3}$) | |
| α | ALFA | shape parameter of main drying curve (cm^{-1}) | |
| n | NPAR | shape parameter of main drying and main wetting curve (-) | |
| K_{sat} | KSAT | saturated hydraulic conductivity (cm d^{-1}) | |
| λ | LEXP | exponent hydraulic conductivity function (-) | 0.5 |

2.4 Sink term: actual plant transpiration

The maximum possible root water extraction rate, integrated over the rooting depth, is equal to the potential transpiration rate, T_p (cm d^{-1}), which is governed by atmospheric conditions (Chapter 3). The potential root water extraction rate at a certain depth, $S_p(z)$ (d^{-1}), may be determined by the root length density, $\ell_{\text{root}}(z)$ (cm cm^{-3}), at this depth as fraction of the integrated root length density (e.g. Bouten, 1992):

$$S_p(z) = \frac{\ell_{\text{root}}(z)}{\int_{-D_{\text{root}}}^0 \ell_{\text{root}}(z) dz} T_p \quad (2.24)$$

where D_{root} is the root layer thickness (cm).

SWAP can handle every distribution of $\ell_{\text{root}}(z)$. In practice this distribution is often not available. Therefore in many applications of SWAP, a uniform root length density distribution is assumed:

$$\frac{\ell_{\text{root}}(z)}{\int_{-D_{\text{root}}}^0 \ell_{\text{root}}(z) dz} = \frac{1}{D_{\text{root}}} \quad (2.25)$$

which leads to a simplified form of Eq. (2.24) (Feddes et al., 1978):

$$S_p(z) = \frac{T_p}{D_{\text{root}}} \quad (2.26)$$

Stresses due to dry or wet conditions and/or high salinity concentrations may reduce $S_p(z)$. The water stress in SWAP is described by the function proposed by Feddes et al. (1978), which is depicted in Figure 6.

Critical pressure head values of this sink term function are given in Appendix 3 (Taylor and Ashcroft, 1972). For salinity stress the response function of Maas and Hoffman (1977) is used (Figure 6), as this function has been calibrated for many crops (Maas, 1990). Appendix 4 lists salt tolerance data for a number of crops. It is still not clear if under the conditions where both stresses apply, the stresses are *additive* or *multiplicative* (Van Genuchten, 1987; Dirksen, 1993; Shalhevet, 1994; Homae, 1999). In order to simplify parameter calibration and data retrieval, we assume in SWAP the water and salinity stress to be multiplicative. This means that the actual root water flux, $S_a(z)$ (d^{-1}), is calculated from:

$$S_a(z) = \alpha_{\text{rw}} \alpha_{\text{rs}} S_p(z) \quad (2.27)$$

where α_{rw} (-) and α_{rs} (-) are the reduction factors due to water and salinity stresses, respectively.

Integration of $S_a(z)$ over the root layer yields the actual transpiration rate T_a (cm d^{-1}).

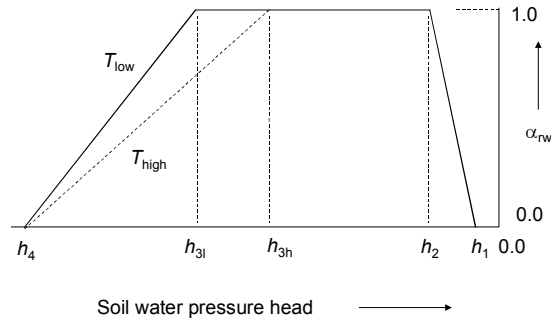


Figure 5 Reduction coefficient for root water uptake, α_{rw} , as function of soil water pressure head h and potential transpiration rate T_p (after Feddes et al., 1978).

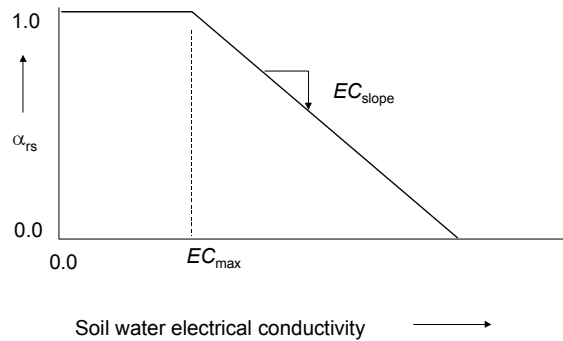


Figure 6 Reduction coefficient for root water uptake, α_{rs} , as function of soil water electrical conductivity EC (after Maas and Hoffman, 1977).

Model input

Specify for each crop:

| <i>Variable Code</i> | <i>Description</i> | <i>Default</i> | |
|----------------------|--------------------|---|-----|
| l_{root} | RDENSITY | root length density as function of root depth | |
| D_{root} | RD | root depth as function of crop development stage (optional) | |
| h_1 | HLIM1 | no water extraction at higher pressure heads (cm) | |
| h_2 | HLIM2U | h below which optimum water uptake starts for top layer (cm) | |
| h_2 | HLIM2L | h below which optimum water uptake starts for sub layer (cm) | |
| h_{3h} | HLIM3H | h below which water uptake reduction starts at high T_{pot} (cm) | |
| h_{3l} | HLIM3L | h below which water uptake reduction starts at low T_{pot} (cm) | |
| h_4 | HLIM4 | Wilting point, no water uptake at lower pressure heads (cm) | |
| T_{high} | ADCRH | Level of high atmospheric demand ($cm\ d^{-1}$) | 0.5 |
| T_{low} | ADCRL | Level of low atmospheric demand ($cm\ d^{-1}$) | 0.1 |
| EC_{max} | ECMAX | EC_{sat} level at which salt stress starts ($dS\ m^{-1}$) | |
| EC_{slope} | ECSLOPE | Decline of root water uptake above EC_{max} ($\% / dS\ m^{-1}$) | |

2.5 Frost conditions

The soil water freezes below a soil temperature of 0 °C. Optionally a frozen soil can be simulated, in which case the following parameters are directly adjusted:

- hydraulic conductivity K :

$$K^*(z) = f_T(z)(K(z) - K_{\min}) + K_{\min} \quad (2.28)$$

where $K^*(z)$ is the adjusted hydraulic conductivity at depth z (cm d⁻¹), K_{\min} is a very small hydraulic conductivity (cm d⁻¹). For K_{\min} a default value is taken of 10⁻¹⁰ cm d⁻¹.

$f_T(z)$ is a correction factor for soil temperature at depth z , which is determined as:

$$\begin{aligned} f_T(z) &= \frac{T(z) - T_2}{T_1 - T_2} && \text{when } T_2 < T(z) < T_1 \\ f_T(z) &= 0 && \text{when } T(z) \leq T_2 \\ f_T(z) &= 1 && \text{when } T(z) \geq T_1 \end{aligned} \quad (2.29)$$

where $T(z)$ is the soil temperature at depth z (°C), T_1 is the soil temperature where reduction of hydraulic conductivity just begins (°C), and T_2 is the soil temperature where reduction of hydraulic conductivity ends (°C). For T_1 and T_2 default values of 0.0 and -1.0 °C are taken.

- Pore volume in the soil V_{air} (cm) for a soil profile that becomes saturated:

$$V_{\text{air}} = \sum_{i=1}^m (\theta_{s,i} - \theta_i) \quad (2.30)$$

where θ_s is the saturated water content (cm cm⁻³), θ is the actual water content (cm cm⁻³), i is the number of the soil compartment and m is the number of soil compartments with a temperature below T_2 starting to count from the top compartment. When a soil compartment is frozen ($T(z) < T_2$) the pore volume of the total soil profile becomes smaller, because only the compartments above this layer are used in the calculation. An example is a soil in spring that is melting (Figure 7). The lower compartments were never frozen and the melting starts at the soil surface. It is possible that the first 4 compartments have melted and only the 5th is frozen. Now the pore volume is only calculated with the first 4 compartments.

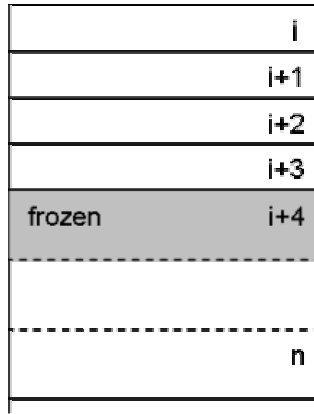


Figure 7 Partly frozen soil profile

- drainage fluxes of all drainage levels:

$$q_{drain,i}(z) = f_T(z) q_{drain,i}(z) \quad (2.31)$$

where $q_{drain,i}(z)$ is the drainage flux at depth z from drainage level i (cm d^{-1})

- bottom flux:

$$q_{bot} = f_T(z) q_{bot} \quad (2.32)$$

where q_{bot} is the flux across the bottom of the modelled soil profile

- actual crop uptake is reduced as:

$$S_a(z) = \alpha_f S_a(z) \quad \text{with} \quad \alpha_f = 0 \quad \text{when} \quad T(z) < 0 \text{ } ^\circ\text{C} \quad (2.33)$$

where α_f is a multiplication factor for soil temperatures (-)

Model input

Variable Code

Description

- SWFROST Switch, in case of frost: stop soil water flow, [Y=1, N=0]

3 Atmosphere – Plant and Soil interaction

J.C. van Dam, M. Groenendijk

3.1 Rainfall and snowfall

Precipitation and irrigation are the main incoming water fluxes. Irrigation will be discussed in chapter 10. For most model applications data of daily rainfall amounts will suffice. In such a case SWAP will distribute the daily rainfall amount equally over the day.

For studies with fast reacting components, e.g. runoff (Par. 4.1) or macro pore flow (Par. 6.5), actual rain intensities are important. In that case extra options are available to specify the mean rain intensity (cm d^{-1}) for each season or to give the duration of rainfall for each day. When the mean rainfall intensities are specified, the period of rainfall during a day is calculated by dividing the total amount of rainfall by the intensity. SWAP will schedule the rainfall at the beginning of a day.

Optionally the precipitation can be subdivided in rain and snowfall. With this option the snowfall accumulates in a snow pack, which will be discussed in Par. 3.2. The subdivision in rain and snow is based on the air temperature. Above $0.5\text{ }^{\circ}\text{C}$ the precipitation is rain and below $0.5\text{ }^{\circ}\text{C}$ the precipitation is snow. It is obvious that for this option the daily air temperatures are necessary.

3.2 The snowpack

In case of snowfall, the water accumulates in a snowpack. The water will be released by snowmelt, during which a large volume of water becomes available for runoff or infiltration into the soil.

To use SWAP for cold regions it is necessary to expand the model with snow and frost conditions. Numerous ways exist to do so, from a delay in precipitation till a complete water and energy balance of the snowpack. The more complex the method, the more data will be needed. The method implemented in SWAP requires just the daily weather data, which are usually available to the model.

With the option to calculate snow accumulation and snowmelt for each day, the water balance of the snowpack on the soil surface will be calculated. This balance consists of several fluxes and a storage change in the snow layer (Figure 8).

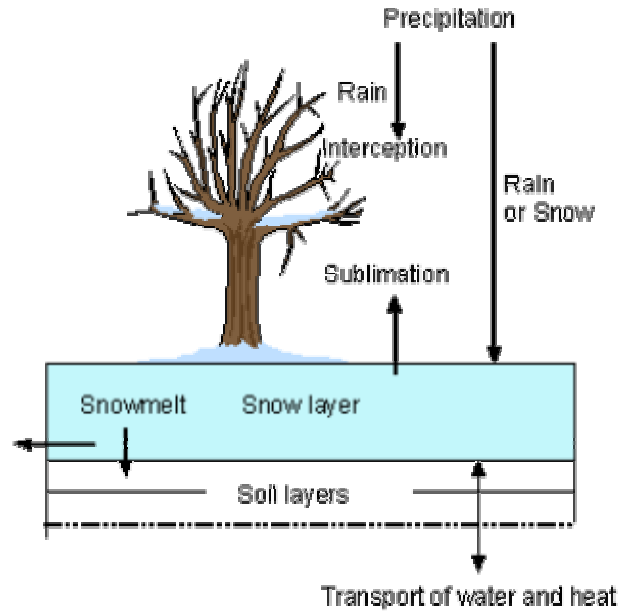


Figure 8 The water fluxes to and from the snow layer

The incoming fluxes are the rain and snowfall. The outgoing fluxes are the snowmelt and sublimation. The snowmelt q_{melt} (cm d^{-1}) is calculated when the air temperature rises above 0°C (Kustas & Rango, 1994) with:

$$q_{\text{melt}} = C (T_{\text{av}} - T_s) \quad (3.1)$$

where C is a constant which can be specified by the user ($\text{d } ^\circ\text{C cm}^{-1}$), T_{av} is the daily average air temperature ($^\circ\text{C}$) and T_s is the temperature of the snow ($^\circ\text{C}$). The assumption is made that the maximum snow temperature is 0°C when the air temperature is above 0°C .

In case of rainfall on the snow pack P_r ($\text{cm}\cdot\text{d}^{-1}$) additional melt will occur due to heat released by splashing raindrops. This amount of snowmelt $q_{\text{melt},r}$ ($\text{cm}\cdot\text{d}^{-1}$) is calculated with (Fernández, 1998; Singh et al., 1997):

$$q_{\text{melt},r} = \frac{P_r \cdot C_m \cdot (T_{\text{av}} - T_s)}{L_m} \quad (3.2)$$

where C_m is the specific heat of water ($4180 \text{ J kg}^{-1} \text{ K}^{-1}$) and L_m is the latent heat of melting (333580 J kg^{-1}). The melt fluxes leave the snow pack as runoff or infiltrate into the soil.

The snow can also evaporate directly into the air, a process called sublimation. The sublimation rate is taken equal to the potential evaporation rate (Par. 3.4). When a snow pack exists, the evapotranspiration from the soil and vegetation is set to zero.

The snow storage (S_{snow}) is calculated as the storage of the previous day plus the precipitation (P_r and P_s) minus the melt (q_{melt} and $q_{\text{melt},r}$) and sublimation (E_s) amounts:

$$S_{\text{snow}}^{t+1} = S_{\text{snow}}^t + (P_r + P_s - q_{\text{melt}} - q_{\text{melt},r} - E_s) \Delta t \quad (3.3)$$

| <i>Model input</i> | | | |
|----------------------|----------|--|----------------|
| <i>Variable Code</i> | | <i>Description</i> | <i>Default</i> |
| S_{snow} | SNOWINCO | initial soil water equivalent (cm) | 0.0 |
| C | SNOWCOEF | snowmelt calibration factor ($\text{d } ^\circ\text{C cm}^{-1}$) | 0.2 |

3.3 Interception of rainfall

For the interception of rainfall two methods are available in SWAP, one for agricultural crops and one for trees and forests.

3.3.1 Agricultural crops

Von Hoyningen-Hüne (1983) and Braden (1985) measured interception of precipitation for various crops. They proposed the following general formula for canopy interception (Figure 9):

$$P_i = a \cdot LAI \left(1 - \frac{1}{1 + \frac{b \cdot P_{\text{gross}}}{a \cdot LAI}} \right) \quad (3.4)$$

where P_i is intercepted precipitation (cm d^{-1}), LAI is leaf area index, P_{gross} is gross precipitation (cm d^{-1}), a is an empirical coefficient (cm d^{-1}) and b is the soil cover fraction ($\approx LAI/3.0$) (-). For increasing precipitation amounts, the amount of intercepted precipitation asymptotically reaches the saturation amount $a LAI$. In principle a must be determined experimentally and should be specified in the input file. In case of ordinary agricultural crops we may, generally, assume $a = 0.25 \text{ cm d}^{-1}$.

In case irrigation water is applied through sprinklers, total intercepted precipitation must be divided into a rain part and an irrigation part, as the solute concentration of both water sources may be different. Observed rainfall P_{gross} minus intercepted rainfall P_i is called net rainfall P_{net} . Likewise, applied irrigation depth I_{gross} minus intercepted irrigation water is called net irrigation depth I_{net} .

The method of Von Hoyningen-Hüne and Braden is based on daily precipitation values, so daily rainfall must be specified in the meteo input file. Additionally, rainfall may be specified in SWAP in smaller time steps. In this case the daily fraction $P_{\text{net}}/P_{\text{gross}}$ is used to correct small time step rainfall for interception losses.

| <i>Model input</i> | | | |
|----------------------|-------|--|----------------|
| <i>Variable Code</i> | | <i>Description</i> | <i>Default</i> |
| P_{gross} | RAIN | gross precipitation as a daily value (mm) | |
| a | COFAB | empirical coefficient Von Hoyningen-Hüne and Braden (cm d^{-1}) | 0.25 |
| LAI | LAI | Leaf Area Index as a function of crop development stage (-) | |

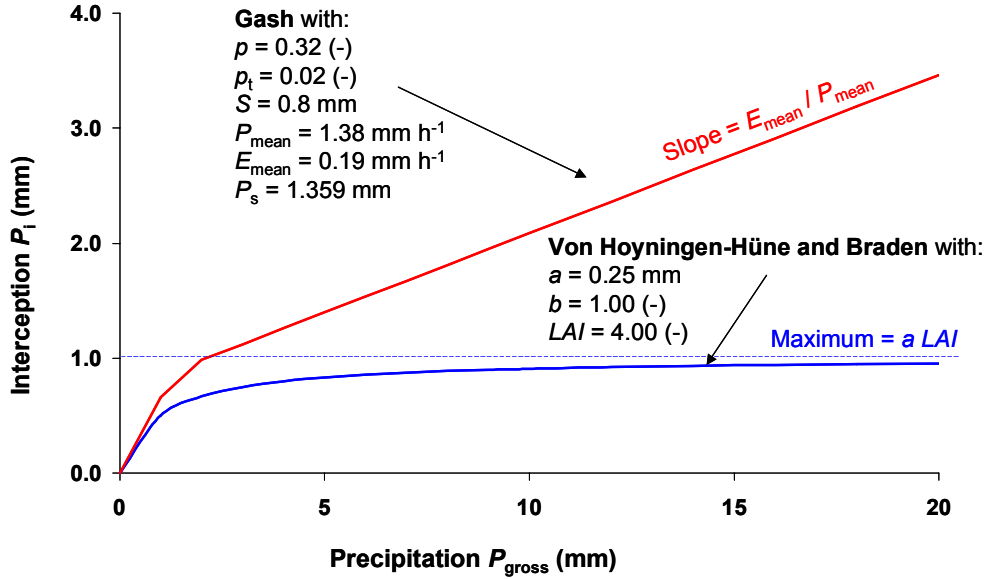


Figure 9 Interception for agricultural crops (Von Hoyningen-Hüne, 1983; Braden, 1985) and forests (Gash, 1979; 1985)

3.3.2 Forests

An important drawback of Eq. (3.4) is that the effect of rain duration and evaporation during the rain event is not explicitly taken into account. In case of interception by trees the effect of evaporation during rainfall can not be neglected. Gash (1979, 1985) formulated a physically based and widely used interception formula for forests. He considered rainfall to occur as a series of discrete events, each comprising a period of wetting up, a period of saturation and a period of drying out after rainfall ceases. The canopy is assumed to have sufficient time to dry out between storms. During wetting up, the increase of intercepted amount is described by:

$$\frac{\partial P_i}{\partial t} = (1 - p - p_t) P_{\text{mean}} - \frac{P_i}{S} E_{\text{mean}} \quad (3.5)$$

where p is a free throughfall coefficient (-), p_t is the proportion of rainfall diverted to stemflow (-), P_{mean} is the mean rainfall rate (mm h⁻¹), E_{mean} is the mean evaporation rate of intercepted water when the canopy is saturated (mm h⁻¹) and S is the maximum storage of intercepted water in the canopy (mm). Integration of Eq. (3.5) yields the amount of rainfall which saturates the canopy, P_s (mm):

$$P_s = -\frac{P_{\text{mean}} S}{E_{\text{mean}}} \ln \left(1 - \frac{E_{\text{mean}}}{P_{\text{mean}} (1 - p - p_t)} \right) \quad \text{with} \quad 1 - \frac{E_{\text{mean}}}{P_{\text{mean}} (1 - p - p_t)} \geq 0 \quad (3.6)$$

For small storms ($P_{\text{gross}} < P_s$) the interception can be calculated from:

$$P_i = (1 - p - p_t) P_{\text{gross}} \quad (3.7)$$

For large storms ($P_{\text{gross}} > P_s$) the interception according to Gash (1979) follows from:

$$P_i = (1 - p - p_t) P_s + \frac{E_{\text{mean}}}{P_{\text{mean}}} (P_{\text{gross}} - P_s) \quad (3.8)$$

Figure 9 shows the relation of Gash for typical values of a pine forest as function of rainfall amounts. The slope $\partial P_i / \partial P_{\text{gross}}$ before saturation of the canopy equals $(1 - p - p_t)$, after saturation of the canopy this slope equals $E_{\text{mean}} / P_{\text{mean}}$.

| <i>Model input</i> | | | |
|--------------------|-------------|---|----------------|
| <i>Variable</i> | <i>Code</i> | <i>Description</i> | <i>Default</i> |
| P_{gross} | RAIN | gross precipitation as a daily value (mm) | |
| S | SCANOPY | storage capacity of the canopy (cm) | |
| p | PFREE | free throughfall coefficient (-) | |
| p_t | PSTEM | stemflow coefficient (-) | |
| P_{mean} | AVPREC | average rainfall intensity (cm d ⁻¹) | |
| E_{mean} | AVEVAP | average evaporation intensity during rainfall from a wet canopy (cm d ⁻¹) | |

3.4 Potential evapotranspiration

Evapotranspiration covers both transpiration of the plants and evaporation of the soil or of water intercepted by vegetation or ponding on the soil surface. In the past, many empirical equations have been derived to calculate potential evapotranspiration which refers to evapotranspiration of cropped soils with an optimum water supply. These empirical equations are valid for the local conditions under which they were derived; they are hardly transferable to other areas. Nowadays, therefore, the focus is mainly on physically-based approaches, which have a wider applicability (Feddes and Lenselink, 1994).

For the process of evapotranspiration, three conditions in the soil-plant-atmosphere continuum must be met (Jensen et al., 1990):

- a) A continuous supply of water;
- b) Energy available to change liquid water into vapour;
- c) A vapour pressure gradient to maintain a flux from the evaporating surface to the atmosphere.

The various methods of determining evapotranspiration are based on one or more of these requirements. For example, the soil water balance approach is based on (a), the energy balance approach on (b), and the combination method (energy balance plus heat and mass transfer) on parts of (b) and (c). Penman (1948) was the first to introduce the combination method. He estimated the evaporation from an open water surface, and then used that as a reference evaporation. Multiplied by a crop factor, this provided an estimate of the potential evapotranspiration from a cropped surface. The combination method requires measured climatic data on temperature, humidity, solar radiation and wind speed. Since the combination method retains a number of empirical relationships, numerous modifications to adjust it to local conditions have been proposed.

Analyzing a range of lysimeter data worldwide, Doorenbos and Pruitt (1977) proposed the FAO Modified Penman method, which has found worldwide application in irrigation and drainage projects. These authors adopted the same two-step approach as Penman to estimate crop water requirements (i.e. estimating a reference evapotranspiration, selecting crop

coefficients per crop and per growth stage, and then multiplying the two to find the crop water requirements, in this way accounting for incomplete soil cover and different surface roughness). They replaced Penman's open water evaporation by the evapotranspiration from a reference crop. The reference crop of Doorenbos and Pruitt was defined as 'an extended surface of a tall green grass cover of uniform height (8 - 15 cm), actively growing, completely shading the ground, and not short of water'. There was evidence, however, that the method sometimes over-predicted the crop water requirements (Allen, 1991).

Using similar physics as Penman (1948), Monteith (1965) derived an equation that describes the evapotranspiration from a dry, extensive, horizontally-uniform vegetated surface, which is optimally supplied with water. This equation is known as the Penman-Monteith equation. Jensen et al. (1990) analyzed the performance of 20 different evapotranspiration formula against lysimeter data for 11 stations around the world under different climatic conditions. The Penman-Monteith formula ranked as the best for all climatic conditions. This equation has become an international standard for calculation of potential evapotranspiration.

Potential and even actual evapotranspiration estimates are possible with the Penman-Monteith equation, through the introduction of canopy and air resistances to water vapour diffusion. This direct, or one-step, approach is increasingly being followed nowadays, especially in research environments. Nevertheless, since accepted canopy and air resistances may not yet be available for many crops, a two-step approach is still recommended under field conditions. The first step is the calculation of the potential evapotranspiration, using the minimum value of the canopy resistance and the actual air resistance. In the second step the actual evapotranspiration is calculated using the root water uptake reduction due to water and/or salinity stress and evaporation reduction (Par. 2.2.3). This two-step approach is followed in SWAP.

3.4.1 Penman-Monteith equation

The original form of the Penman-Monteith equation can be written as (Monteith, 1965, 1981):

$$ET_p = \frac{\frac{\Delta_v}{\lambda_w} (R_n - G) + \frac{p_1 \rho_{air} C_{air}}{\lambda_w} \frac{e_{sat} - e_a}{r_{air}}}{\Delta_v + \gamma_{air} \left(1 + \frac{r_{crop}}{r_{air}} \right)} \quad (3.9)$$

where ET_p is the potential transpiration rate of the canopy (mm d^{-1}), Δ_v is the slope of the vapour pressure curve ($\text{kPa } ^\circ\text{C}^{-1}$), λ_w is the latent heat of vaporization (J kg^{-1}), R_n is the net radiation flux at the canopy surface ($\text{J m}^{-2} \text{d}^{-1}$), G is the soil heat flux ($\text{J m}^{-2} \text{d}^{-1}$), p_1 accounts for unit conversion ($=86400 \text{ s d}^{-1}$), ρ_{air} is the air density (kg m^{-3}), C_{air} is the heat capacity of moist air ($\text{J kg}^{-1} ^\circ\text{C}^{-1}$), e_{sat} is the saturation vapour pressure (kPa), e_a is the actual vapour pressure (kPa), γ_{air} is the psychrometric constant ($\text{kPa } ^\circ\text{C}^{-1}$), r_{crop} is the crop resistance (s m^{-1}) and r_{air} is the aerodynamic resistance (s m^{-1}).

To facilitate analysis of the combination equation, an aerodynamic and radiation term are defined:

$$ET_p = ET_{rad} + ET_{aero} \quad (3.10)$$

where ET_p is potential transpiration rate of crop canopy (cm d^{-1}), ET_{rad} is the radiation term (cm d^{-1}) and ET_{aero} is the aerodynamic term (cm d^{-1}).

The radiation term equals:

$$ET_{rad} = \frac{\Delta_v(R_n - G)}{\lambda_w(\Delta_v + \gamma_{air}^*)} \quad (3.11)$$

where the modified psychrometric constant ($\text{kPa } ^\circ\text{C}^{-1}$) is:

$$\gamma_{air}^* = \gamma_{air} \left(1 + \frac{r_{crop}}{r_{air}} \right) \quad (3.12)$$

The aerodynamic term equals:

$$ET_{aero} = \frac{p_1 \rho_{air} C_{air} (e_{sat} - e_a)}{\lambda_w(\Delta_v + \gamma_{air}^*) r_{air}} \quad (3.13)$$

Many meteorological stations provide mean daily values of air temperature T_{air} ($^\circ\text{C}$), global solar radiation R_s ($\text{J m}^{-2} \text{d}^{-1}$), wind speed u_0 (m s^{-1}) and air humidity e_{act} (kPa). The Food and Agricultural Organisation of the UN has proposed a clearly defined and well established methodology to apply the Penman-Monteith equation using above 4 weather data. (Allen et al., 1998). This methodology is applied in SWAP and is described in Par. 3.4.1.1 and 3.4.1.2.

3.4.1.1 Radiation term

The net radiation R_n ($\text{J m}^{-2} \text{d}^{-1}$) is the difference between incoming and outgoing radiation of both short and long wavelengths. It is the balance between the energy adsorbed, reflected and emitted by the earth's surface:

$$R_n = (1 - \alpha_r) R_s - R_{nl} \quad (3.14)$$

where α_r is the reflection coefficient or albedo (-) and R_{nl} is the net longwave radiation ($\text{J m}^{-2} \text{d}^{-1}$). The albedo is highly variable for different surfaces and for the angle of incidence or slope of the ground surface. It may be as large as 0.95 for freshly fallen snow and as small as 0.05 for a wet bare soil. A green vegetation cover has an albedo of about 0.20-0.25 (De Bruin, 1998). SWAP will assume in case of a crop $\alpha_r = 0.23$, in case of bare soil $\alpha_r = 0.15$.

The earth emits longwave radiation, which increases with temperature and which is adsorbed by the atmosphere or lost into space. The longwave radiation received by the atmosphere increases its temperature and, as a consequence, the atmosphere radiates energy of its own. Part of this radiation finds its way back to the earth's surface. As the outgoing longwave radiation is almost always greater than the incoming longwave radiation, the net longwave radiation R_{nl} represents an energy loss. Allen et al. (1998) recommend the following formula for the net longwave radiation:

$$R_{nl} = \sigma_{sb} \left[\frac{T_{max}^4 + T_{min}^4}{2} \right] \left(0.34 - 0.14 \sqrt{e_{act}} \right) (0.1 + 0.9 N_{rel}) \quad (3.15)$$

where σ_{sb} is the Stefan-Boltzmann constant ($4.903 \cdot 10^{-3} \text{ J K}^{-4} \text{ m}^{-2} \text{ d}^{-1}$), T_{min} and T_{max} are the minimum and maximum absolute temperatures during the day (K), respectively, e_{act} is the actual vapour pressure (kPa), and N_{rel} is the relative sunshine duration. The latter can be derived from the measured global solar radiation R_n and the extraterrestrial radiation R_a ($\text{J m}^{-2} \text{ d}^{-1}$), which is received at the top of the Earth's atmosphere on a horizontal surface:

$$N_{rel} = \frac{R_s}{b R_a} - a \quad (3.16)$$

where a and b are empirical coefficients which depend on the local climate. For international use Allen et al. (1998) recommend $a = 0.25$ and $b = 0.50$.

The extraterrestrial radiation R_a depends on the latitude and the day of the year. R_a is calculated with:

$$R_a = \frac{G_{sc}}{\pi} d_r \left[\omega_s \sin(\varphi) \sin(\delta) + \cos(\varphi) \cos(\delta) \sin(\omega_s) \right] \quad (3.17)$$

where d_r is the inverse relative distance Earth-Sun (-), ω_s is the sunset hour angle (rad), φ is the latitude (rad) and δ is the solar declination (rad). The inverse relative distance Earth-Sun and the solar declination are given by:

$$d_r = 1 + 0.033 \cos\left(\frac{2\pi}{365} J\right) \quad (3.18)$$

$$\delta = 0.409 \sin\left(\frac{2\pi}{365} J - 1.39\right) \quad (3.19)$$

where J is the number of the day in the year (1-365 or 366, starting January 1). The sunset hour angle expresses the day length and is given by:

$$\omega_s = \arccos\left[-\tan(\varphi) \tan(\delta)\right] \quad (3.20)$$

3.4.1.2 Aerodynamic term

Latent heat of vaporization, λ_w (J g^{-1}), depends on the air temperature T_{air} ($^{\circ}\text{C}$) (Harrison, 1963):

$$\lambda_w = 2501 - 2.361 T_{air} \quad (3.21)$$

Saturation vapour pressure, e_{sat} (kPa), also can be calculated from air temperature (Tetens, 1930):

$$e_{sat} = 0.611 \exp\left(\frac{17.27 T_{air}}{T_{air} + 237.3}\right) \quad (3.22)$$

The slope of the vapour pressure curve, Δ_v ($\text{kPa } ^{\circ}\text{C}^{-1}$), is calculated as (Murray, 1967):

$$\Delta_v = \frac{4098 e_{sat}}{(T_{air} + 237.3)^2} \quad (3.23)$$

The psychrometric constant, γ_{air} (kPa °C⁻¹), follows from (Brunt, 1952):

$$\gamma_{air} = 0.00163 \frac{p_{air}}{\lambda_w} \quad (3.24)$$

with p_{air} the atmospheric pressure (kPa) at elevation z_0 (m), which is calculated from (Burman et al., 1987):

$$p_{air} = 101.3 \left(\frac{T_{air,K} - 0.0065 z_0}{T_{air,K}} \right)^{5.256} \quad (3.25)$$

Employing the ideal gas law, the atmospheric density, ρ_a (g cm⁻³), can be shown to depend on p and the virtual temperature T_{vir} (K):

$$\rho_{air} = 3.486 \cdot 10^{-3} \frac{p_{air}}{T_{vir}} \quad (3.26)$$

where the virtual temperature is derived from:

$$T_{vir} = \frac{T_{air,K}}{1 - 0.378 \frac{e_{act}}{p_{air}}} \quad (3.27)$$

The heat capacity of moist air, C_{air} (J g⁻¹ °C⁻¹), follows from:

$$C_{air} = 622 \frac{\gamma_{air} \lambda_w}{p_{air}} \quad (3.28)$$

Aerodynamic resistance

The aerodynamic resistance r_{air} depends on the wind speed profile and the roughness of the canopy and is calculated as (Allen et al., 1998):

$$r_{air} = \frac{\ln \left(\frac{z_m - d}{z_{om}} \right) \cdot \ln \left(\frac{z_h - d}{z_{oh}} \right)}{\kappa_{vk}^2 \cdot u} \quad (3.29)$$

where z_m is height of wind speed measurements (m), z_h is height of temperature and humidity measurements (m), d is zero plane displacement of wind profile (m), z_{om} is roughness parameter for momentum (m) and z_{oh} is roughness parameter for heat and vapour (m), κ_{vk} is von Karman constant = 0.41 (-), u is wind speed measurement at height z_m (m s⁻¹),

The parameters d , z_{om} and z_{oh} are defined as:

$$d = \frac{2}{3} h_{crop} \quad (3.30)$$

$$z_{om} = 0.123 h_{crop} \quad (3.31)$$

$$z_{oh} = 0.1 z_{om} \quad (3.32)$$

with h_{crop} the crop height (cm)

A default height of 2 m is assumed for wind speed measurements (z_m) and height of temperature and humidity measurements (z_h).

Meteorological stations generally provide 24 hour averages of wind speed measurements, according to international standards, at an altitude of 10 meter.

To calculate r_{air} , the average daytime wind (7.00 - 19.00 h) should be used. For ordinary conditions we assume (Smith, 1991) for the average daytime windspeed ($u_{0,day}$):

$$u_{0,day} = 1.33 u_0 \quad (3.33)$$

where u_0 is the measured average wind speed over 24 hours ($m s^{-1}$).

When crop height (h_{crop}) reaches below or above measurement height ($z_{m,meas}$), the wind speed is corrected with the following assumptions:

- a uniform wind pattern at an altitude of 100 meter;
- wind speed measurements are carried out above grassland;
- a logarithmic wind profile is assumed;
- below 2 meter wind speed is assumed to be unchanged with respect to a value at an altitude of 2 meter; applying a logarithmic wind profile at low altitudes is not carried out due to the high variation below 2 meter.

These assumptions result in the following equation for wind speed correction:

$$u = \frac{\ln\left(\frac{z_{act} - d_{act}}{z_{om,act}}\right)}{\ln\left(\frac{z_{100} - d_{act}}{z_{om,act}}\right)} \frac{\ln\left(\frac{z_{100} - d_{grass}}{z_{om,grass}}\right)}{\ln\left(\frac{z_{m,meas} - d_{grass}}{z_{om,grass}}\right)} u_{0,day} \quad (3.34)$$

where: u wind speed at crop height ($m s^{-1}$), z_{act} is the actual crop height with a minimum value of 2 m, d_{act} and d_{grass} are zero plane displacement of actual crop and grass (m), $z_{om,act}$ and $z_{om,grass}$ are roughness parameter for momentum actual crop and grass (m).

3.4.1.3 Fluxes above homogeneous surfaces

SWAP calculates three quantities with the Penman-Monteith equation (eq. (3.9)):

- ET_{w0} ($cm d^{-1}$), potential evapotranspiration rate of a wet canopy, completely covering the soil;
- ET_{p0} ($cm d^{-1}$), potential evapotranspiration rate of a dry canopy, completely covering the soil;

- E_{p0} (cm d⁻¹), potential evaporation rate of a wet, bare soil.

These quantities are obtained by varying the values for crop resistance, crop height and the reflection coefficient. In case of a wet canopy, the crop resistance r_{crop} is set to zero. In case of a dry crop with optimal water supply in the soil, r_{crop} is minimal and varies between 30 s m⁻¹ for arable crop to 150 s m⁻¹ for trees in a forest (Allen et al., 1986, 1989). In case of the bare wet soil, the program takes $r_{\text{crop}} = 0$ and ‘crop height’ $h_{\text{crop}} = 0.1$ cm. Reflection coefficient α_r in case of a (wet or dry) crop equals 0.23, while for a bare soil $\alpha_r = 0.15$ is assumed.

| <i>Model input</i> | | | |
|--|--------------------|--|----|
| <i>Variable Code</i> | <i>Description</i> | <i>Default</i> | |
| L_g | LAT | geographical latitude (degrees, North positive) | |
| z_0 | ALT | altitude above mean sea level (m) | |
| $z_{\text{m, meas}}$ | ALTW | altitude of wind speed measurement above mean soil surface (m) | |
| h_{crop} | CH | crop height as a function of crop development stage (cm) | |
| r_{crop} | RSC | minimum crop resistance (s m ⁻¹) | 70 |
| <i>Daily (average 0-24 hrs) values of:</i> | | | |
| $T_{\text{air, min}}$ | TMIN | minimum air temperature at 2 m height (°C) | |
| $T_{\text{air, max}}$ | TMAX | maximum air temperature at 2 m height (°C) | |
| R_s | RAD | global solar radiation (kJ m ⁻² d ⁻¹) | |
| u_0 | WIND | wind speed at 2 m height (m s ⁻¹) | |
| e_{act} | HUM | air humidity as vapour pressure at 2 m height (kPa) | |

3.4.2 Reference evapotranspiration and crop factors

Application of the Penman-Monteith equation requires daily values of air temperature, net radiation, wind speed and air humidity, which data might not be available. Also in some studies other methods than Penman-Monteith might be needed. For instance in The Netherlands the Makkink equation is widely used (Makkink, 1957; Feddes, 1987). Therefore SWAP allows the use of a reference potential evapotranspiration rate ET_{ref} (cm d⁻¹). In that case ET_{p0} is calculated by:

$$ET_{p0} = k_c ET_{\text{ref}} \quad (3.35)$$

where k_c is the so called crop factor, which depends on the crop type and the method employed to obtain ET_{ref} . The crop factor converts the reference evapotranspiration rate into the potential evapotranspiration rate of a dry canopy that completely covers the soil: k_c is thus taken to be constant from crop emergence up to maturity.

This approach, however, does not allow differentiation between a dry crop and wet crop. Therefore SWAP assumes: $ET_{w0} = ET_{\text{ref}}$. SWAP allows the use of a ‘crop factor’ to translate ET_{ref} into E_{p0} :

$$E_{p0} = k_{\text{soil}} ET_{\text{ref}} \quad (3.36)$$

If this option is not used, SWAP will assume $ET_{p0} = ET_{\text{ref}}$.

The reference evapotranspiration rate can be determined in several ways, such as pan evaporation, the Penman open water evaporation (Penman, 1948), the FAO modified Penman equation (Doorenbos and Pruitt, 1977), the Penman-Monteith equation applied for a reference crop (Allen et al., 1998), Priestly-Taylor (1972), Makkink (Makkink, 1957; Feddes, 1987) or Hargreaves et al. (1985). In order to transform all these reference evapotranspiration rates to the potential transpiration of the considered crop, the crop factors are needed.

| <i>Model input</i> | | | |
|--------------------|-------------|---|----------------|
| <i>Variable</i> | <i>Code</i> | <i>Description</i> | <i>Default</i> |
| k_c | CF | crop factor as function of crop development stage (-) | |
| k_{soil} | CFBS | 'crop factor' for bare soil (-) | 1.0 |

Programs like CROPWAT (Smith, 1992) and CRIWAR (Bos et al., 1996) use crop factors that are a function of the crop development stage. After multiplication with a reference *potential* evapotranspiration rate, a kind of evapotranspiration rate is obtained that is representative for a potentially transpiring crop that is well supplied with water in the root zone and that partly covers the soil. Because the soil has generally a dry top layer, soil evaporation is usually below the potential evaporation rate. Hence, the crop factor combines the effect of an incomplete soil cover and reduced soil evaporation. It enables effective extraction of the potential crop transpiration rate from the reference potential evapotranspiration rate, under the assumption that soil evaporation is constant and relatively small. Significant errors however may be expected when the soil is regularly rewetted and the soil cover fraction is low.

SWAP firstly separates potential plant transpiration rate T_p and potential soil evaporation rate E_p and subsequently calculates the reduction of potential plant transpiration rate and potential soil evaporation rate (Figure 10) according to a physically based approach (Par. 2.2.3). In order to partition potential evapotranspiration rate into potential transpiration rate and potential soil evaporation rate, either the leaf area index, LAI ($m^2 m^{-2}$) or the soil cover fraction, SC (-), both as a function of crop development, are used.

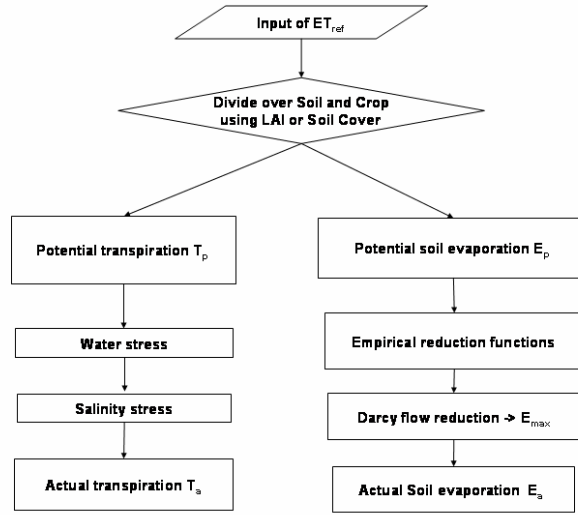


Figure 10 Partitioning of evapotranspiration over crop and soil

3.4.3 Partitioning of potential evapotranspiration

3.4.3.1 Use of leaf area index

The potential evaporation rate of a soil under a standing crop is derived from the Penman Monteith equation by neglecting the aerodynamic term. The aerodynamic term will be small because the wind velocity near the soil surface is relatively small, which makes the aerodynamic resistance r_{air} very large (Ritchie, 1972). Thus, the only source for soil evaporation is net radiation that reaches the soil surface. Assuming that the net radiation inside the canopy decreases according to an exponential function, and that the soil heat flux can be neglected, we can derive (Goudriaan, 1977; Belmans, 1983):

$$E_p = E_{p0} e^{-\kappa_{gr} LAI} \quad (3.37)$$

where κ_{gr} (-) is the extinction coefficient for global solar radiation. Ritchie (1972) and Feddes (1978) used $\kappa_{gr} = 0.39$ for common crops. More recent approaches estimate κ_{gr} as the product of the extinction coefficient for diffuse visible light, κ_{df} (-), which varies with crop type from 0.4 to 1.1, and the extinction coefficient for direct visible light, κ_{dir} (-):

$$\kappa_{gr} = \kappa_{df} \kappa_{dir} \quad (3.38)$$

SWAP assumes that the evaporation rate of the water intercepted by the vegetation is equal to ET_{w0} , independent of the soil cover fraction. Then the fraction of the day that the crop is wet, W_{frac} (-), follows from the ratio of the daily amount of intercepted precipitation P_i (Par. 3.3) and ET_{w0} :

$$W_{frac} = \frac{P_i}{ET_{w0}} \quad \text{with} \quad W_{frac} \leq 1.0 \quad (3.39)$$

During evaporation of intercepted water, the transpiration rate through the leaf stomata is assumed to be negligible. After the canopy has become dry, the transpiration through the leaf stomata starts again at a rate ET_{p0} . SWAP calculates a daily average of the potential

transpiration rate, T_p (cm d^{-1}), taking into account the fraction of the day W_{frac} during which the intercepted water evaporates as well as the potential soil evaporation rate E_p :

$$T_p = (1.0 - W_{\text{frac}}) ET_{p0} - E_p \quad \text{with} \quad T_p \geq 0 \quad (3.40)$$

| <i>Model input</i> | | | |
|-----------------------|------|--|----------------|
| <i>Variable Code</i> | | <i>Description</i> | <i>Default</i> |
| κ_{df} | KDIF | extinction coefficient for diffuse visible light (-) | 0.60 |
| κ_{dir} | KDIR | extinction coefficient for direct visible light (-) | 0.75 |

3.4.3.2 Use of soil cover fraction

As the soil cover is only specified in case of the simple crop growth model, only in that case this option can be used. Taking into account the fraction of the day that the crop is wet (Eq. (3.39)), the potential soil transpiration rate T_p follows straight from:

$$T_p = (1.0 - W_{\text{frac}}) SC ET_{p0} \quad (3.41)$$

The potential soil evaporation rate is calculated as:

$$E_p = (1.0 - SC)(1 - W_{\text{frac}}) E_{p0} \quad (3.42)$$

| <i>Model input</i> | | | |
|----------------------|-----|--|----------------|
| <i>Variable Code</i> | | <i>Description</i> | <i>Default</i> |
| SC | SCF | soil cover as function of crop development stage (-) | |

4 Soil water - surface water interaction

J.C. van Dam, P. Groenendijk, J.G. Kroes, P.E.V. van Walsum

The interaction between soil and surface water system may be described by:

- Surface flow (runoff, runoff and inundation); which is an overland water flow;
- Subsurface flow, or drainage and infiltration; which is a shallow or deep water flow through the soil system.

Different options for this interaction are described in this paragraph.

4.1 Surface flow

Surface flow is regarded as the overland water flow that results in interaction between soil and surface water system. Several water fluxes play a role in this interaction where the so-called ponding reservoir plays a crucial role (Figure 11). This ponding reservoir may be regarded as a thin layer of water on top of the soil surface, which can store water to a certain maximum.

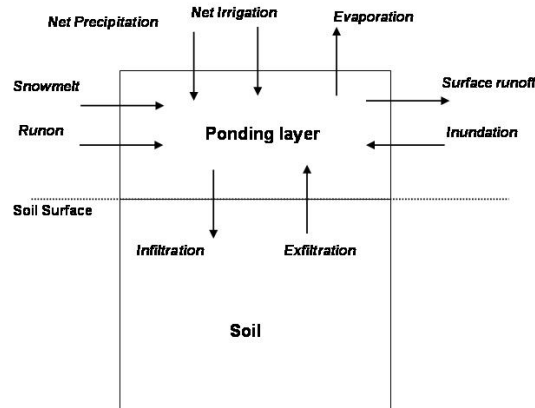


Figure 11 The water fluxes on the soil surface

The water balance of this ponding reservoir is:

$$\Delta_{pond} = P_{net} + I_{net} + q_1 + M + q_{runon} - q_{runoff} - E_{pond} \quad (4.1)$$

where: Δ_{pond} is the storage change of the ponding reservoir (cm d^{-1}), P_{net} is the net precipitation flux (cm d^{-1}), I_{net} is the net irrigation flux (cm d^{-1}), q_1 is the flux between the ponding layer and the 1st model compartment (cm d^{-1} , exfiltration is upward and has a positive value, infiltration is downward and has a negative value), M is snowmelt (cm d^{-1}), q_{runon} is an external runoff flux, e.g. from a neighbouring field (cm d^{-1}), q_{runoff} is discharge to/from the surface water system (cm d^{-1} , as runoff with a positive value, as inundation with a negative value).

4.1.1 Surface runoff and inundation

Surface runoff is simulated when the groundwater level rises above the soil surface or when the infiltration capacity of the soil is not sufficient to infiltrate all the water. In either case the groundwater level will fill the ponding reservoir until a certain threshold ponding level (h_{pond}) is exceeded. When this exceedance occurs, surface runoff as:

$$q_{runoff} = \frac{1}{\gamma_{sill}} (h_{pond} - z_{sill})^{\beta_{sill}} \quad (4.2)$$

where h_{pond} is the ponding depth of water (cm) on the soil surface, z_{sill} the height (cm) of the sill which is equal to the maximum ponding height ($h_{pond,max}$) or to the surface water level, γ_{sill} the runoff/inundation resistance (d) and β_{sill} an exponent (-).

Surface runoff occurs when $h_{pond} > z_{sill}$; inundation occurs when $h_{pond} < z_{sill}$.

The maximum ponding height without surface runoff is determined by the irregularities of the soil surface. As surface runoff is a rapid process, the sill resistance γ_{sill} will typically have values of less than 1 d. For most SWAP applications, realistic dynamic simulation of surface runoff is not required, but only the effect of surface runoff on the soil water balance is relevant. Then a rough estimate of γ_{sill} is sufficient, e.g. $\gamma_{sill} \approx 0.1$ d. When the dynamics of surface runoff are relevant, the values of γ_{sill} and β_{sill} might be derived from experimental data or from a hydraulic model of soil surface flow.

| <i>Model input</i> | | |
|----------------------|---------|--|
| <i>Variable Code</i> | | <i>Description</i> |
| $h_{pond,max}$ | PONDMX | Ponding height (cm) |
| γ_{sill} | RSRO | Runoff/inundation resistance (d) |
| β_{sill} | RSROEXP | Exponent in runoff/inundation relation (-) |

4.1.2 Surface runoff

Surface runoff is supplied to the model as an external source. It originates from an external source (runoff from a neighbouring field) which supplies excess water.

| <i>Model input</i> | | |
|----------------------|-------|--|
| <i>Variable Code</i> | | <i>Description</i> |
| q_{runon} | RUFIL | File with external runoff flux, e.g. from a neighbouring field (cm d ⁻¹) |

4.2 Drainage and infiltration

Lateral field drainage fluxes, q_{drain} (cm d⁻¹) to the drainage system may be defined in different forms. Four methods can be used to calculate q_{drain} :

- Linear or tabular $q_{drain}(\phi_{gw})$ relation (Par. 4.2.1)

- drainage equations of Hooghoudt and Ernst (Par. 4.2.2)
- drainage/infiltration to/from surface water systems (basic drainage, Par. 4.2.3)
- interaction with a simplified surface water system (extended drainage, Par. 4.2.5)

4.2.1 Linear or tabular relation

A linear or tabular relation between groundwater level and drainage flux q_{drain} (cm d⁻¹) may be applied:

$$q_{\text{drain}} = \frac{\phi_{\text{gwl}} - \phi_{\text{drain}}}{\gamma_{\text{drain}}} \quad (4.3)$$

where ϕ_{gwl} is the phreatic groundwater level midway between the drains or ditches (cm), ϕ_{drain} the drain hydraulic head (cm) γ_{drain} the drainage resistance (d). In case of non-linear relations between q_{drain} and ϕ_{gwl} , tabular values of q_{drain} as function of ϕ_{gwl} are input.

| <i>Model input</i> | | |
|---------------------|-------------|--|
| <i>Variable</i> | <i>Code</i> | <i>Description</i> |
| ϕ_{gwl} | GWL | Groundwater level (cm, negative below soil surface) |
| q_{drain} | Qdrain | Drainage flux (cm d ⁻¹) as a function of groundwater level |

4.2.2 Drainage equations of Hooghoudt and Ernst

The drainage equations of Hooghoudt and Ernst allow the evaluation of drainage design. The theory behind these equations is clearly described in Ritzema (1994). Five typical drainage situations are distinguished (Figure 12). For each of which the drainage resistance γ_{drain} can be defined.

| Schematization | Soil profile | Drain position | Theory |
|----------------|---------------------------------------|-------------------------------------|------------------------------------|
| | homogeneous | on top of impervious layer | Hooghoudt Donnan |
| | homogeneous | above impervious layer | Hooghoudt with equivalent depth |
| | two layers | at interface of the two soil layers | Hooghoudt |
| | two layers ($K_{top} < K_{bot}$) | in bottom layer | Ernst |
| | two layers ($K_{top} < K_{bot}$) | in top layer | Ernst |

Figure 12 Five field drainage situations considered in SWAP (after Ritzema, 1994)

Homogeneous profile, drain on top of impervious layer

The drainage resistance is calculated as:

$$\gamma_{\text{drain}} = \frac{L_{\text{drain}}^2}{4K_{\text{hprof}}(\phi_{\text{gwl}} - \phi_{\text{drain}})} + \gamma_{\text{entr}} \quad (4.4)$$

with K_{hprof} the horizontal saturated hydraulic conductivity above the drainage basis (cm d^{-1}), L_{drain} the drain spacing (cm) and γ_{entr} the entrance resistance into the drains and/or ditches (d). The value for γ_{entr} can be obtained, analogous to the resistance value of an aquitard, by dividing the 'thickness' of the channel walls with the permeability. If this permeability does not differ substantially from the conductivity in the surrounding subsoil, the numerical value of the entry resistance will become relatively minor.

Homogeneous profile, drain above impervious layer

This drainage situation has been originally described by Hooghoudt (1940). The drainage resistance follows from:

$$\gamma_{\text{drain}} = \frac{L_{\text{drain}}^2}{8K_{\text{hprof}}D_{\text{eq}} + 4K_{\text{hprof}}(\phi_{\text{gwl}} - \phi_{\text{drain}})} + \gamma_{\text{entr}} \quad (4.5)$$

where D_{eq} is the equivalent depth (cm).

The equivalent depth was introduced by Hooghoudt to incorporate the extra head loss near the drains caused by converging flow lines. We employ in SWAP a numerical solution of Van der Molen and Wesseling (1991) to calculate D_{eq} (Ritzema, 1994). A typical length variable x is used:

$$x = \frac{2\pi(\phi_{\text{drain}} - \tilde{z}_{\text{imp}})}{L_{\text{drain}}} \quad (4.6)$$

If $x < 10^{-6}$, then:

$$D_{eq} = \phi_{\text{drain}} - \tilde{z}_{\text{imp}} \quad (4.7)$$

with z_{imp} the level of the impervious layer. If $10^{-6} < x < 0.5$, then:

$$F(x) = \frac{\pi^2}{4x} + \ln\left(\frac{x}{2\pi}\right) \quad (4.8)$$

and the equivalent depth equals:

$$D_{eq} = \frac{\pi L_{\text{drain}}}{8 \left(\ln\left(\frac{L_{\text{drain}}}{\pi r_{\text{drain}}}\right) + F(x) \right)} \quad (4.9)$$

with r_{drain} the radius of the drain or ditch. If $0.5 < x$, then:

$$F(x) = \sum_{j=1,3,5,\dots}^{\infty} \frac{4e^{-2jx}}{j(1-e^{-2jx})} \quad (4.10)$$

and equivalent depth again follows from Eq. (4.9).

Heterogeneous soil profile, drain at interface between both soil layers

The equivalent depth D_{eq} is calculated with the procedure of Eq. (4.6) to (4.10). The drainage resistance follows from:

$$\gamma_{\text{drain}} = \frac{L_{\text{drain}}^2}{8K_{\text{hbot}}D_{eq} + 4K_{\text{htop}}(\phi_{\text{gwl}} - \phi_{\text{drain}})} + \gamma_{\text{entr}} \quad (4.11)$$

with K_{htop} and K_{hbot} the horizontal saturated hydraulic conductivity (cm d^{-1}) of upper and lower soil layer, respectively.

Heterogeneous soil profile, drain in bottom layer

The drainage resistance is calculated according to Ernst (1956) as:

$$\gamma_{\text{drain}} = \gamma_{\text{ver}} + \gamma_{\text{hor}} + \gamma_{\text{rad}} + \gamma_{\text{entr}} \quad (4.12)$$

where γ_{ver} , γ_{hor} , and γ_{rad} are the vertical, horizontal and radial resistance (d^{-1}), respectively. The vertical resistance is calculated by:

$$\gamma_{\text{ver}} = \frac{\phi_{\text{gwl}} - \tilde{z}_{\text{int}}}{K_{\text{vtop}}} + \frac{\tilde{z}_{\text{int}} - \phi_{\text{drain}}}{K_{\text{vbot}}} \quad (4.13)$$

with z_{int} the level of the transition (cm) between the upper and lower soil layer, and K_{vtop} and K_{vbot} the vertical saturated hydraulic conductivity (cm d^{-1}) of the upper and lower soil layer, respectively. The horizontal resistance is calculated as:

$$\gamma_{hor} = \frac{L_{drain}^2}{8 K_{hbot} D_{bot}} \quad (4.14)$$

with D_{bot} the contributing layer below the drain level (cm), which is calculated as the minimum of $(\phi_{drain} - z_{imp})$ and $1/4 L_{drain}$. The radial resistance is calculated by:

$$\gamma_{rad} = \frac{L_{drain}}{\pi \sqrt{K_{hbot} K_{vbot}}} \ln \left(\frac{D_{bot}}{u_{drain}} \right) \quad (4.15)$$

with u_{drain} the wet perimeter (cm) of the drain.

Heterogeneous soil profile, drain in top layer

Again the approach of Ernst (1956) is applied (Eq. (4.12)). The resistances are calculated as:

$$\gamma_{ver} = \frac{\phi_{gwl} - \phi_{drain}}{K_{vtop}} \quad (4.16)$$

$$\gamma_{hor} = \frac{L_{drain}^2}{8 K_{htop} D_{top} + 8 K_{hbot} D_{bot}} \quad (4.17)$$

$$\gamma_{rad} = \frac{L_{drain}}{\pi \sqrt{K_{htop} K_{vtop}}} \ln \left(g_{drain} \frac{\phi_{drain} - z_{int}}{u_{drain}} \right) \quad (4.18)$$

with D_{top} equal to $(\phi_{drain} - z_{int})$ and g_{drain} is the drain geometry factor, which should be specified in the input. The value of g_{drain} depends on the ratio of the hydraulic conductivity of the bottom (K_{hbot}) and the top (K_{htop}) layer. Using the relaxation method, Ernst (1962) distinguished the following situations:

- $K_{hbot}/K_{htop} < 0.1$: the bottom layer can be considered impervious and the case is reduced to a homogeneous soil profile and $g_{drain} = 1$;
- $0.1 < K_{hbot}/K_{htop} < 50$: g_{drain} depends on the ratios K_{hbot}/K_{htop} and D_{bot}/D_{top} , as given in Table 1.
- $50 < K_{hbot}/K_{htop}$: $g_{drain} = 4$.

Table 1 The geometry factor g_{drain} (-), as obtained by the relaxation method (after Ernst, 1962).

| $K_{\text{hbot}}/K_{\text{htop}}$ | $D_{\text{bot}}/D_{\text{top}}$ | | | | | |
|-----------------------------------|---------------------------------|-----|-----|-----|------|------|
| | 1 | 2 | 4 | 8 | 16 | 32 |
| 1 | 2.0 | 3.0 | 5.0 | 9.0 | 15.0 | 30.0 |
| 2 | 2.4 | 3.2 | 4.6 | 6.2 | 8.0 | 10.0 |
| 3 | 2.6 | 3.3 | 4.5 | 5.5 | 6.8 | 8.0 |
| 5 | 2.8 | 3.5 | 4.4 | 4.8 | 5.6 | 6.2 |
| 10 | 3.2 | 3.6 | 4.2 | 4.5 | 4.8 | 5.0 |
| 20 | 3.6 | 3.7 | 4.0 | 4.2 | 4.4 | 4.6 |
| 50 | 3.8 | 4.0 | 4.0 | 4.0 | 4.2 | 4.6 |

Model input

| <i>Variable</i> | <i>Code</i> | <i>Description</i> |
|--|-------------|--|
| L_{drain} | LM2 | Drain spacing (m) |
| u_{drain} | WETPER | Wet perimeter of the drain (cm) |
| ϕ_{drain} | ZBOTDR | Level of drain bottom (cm) |
| γ_{entr} | ENTRES | Drain entry resistance (d) |
| z_{imp} | BASEGW | Level of impervious layer (cm) |
| K_{htop} | KHTOP | Horizontal hydraulic conductivity top layer (cm d ⁻¹) |
| <i>For a non-homogeneous soil profile:</i> | | |
| K_{hbot} | KHBOT | Horizontal hydraulic conductivity bottom layer (cm d ⁻¹) |
| z_{int} | ZINTF | Level of interface of fine and coarse soil layer (cm) |
| K_{vtop} | KVTOP | Vertical hydraulic conductivity top layer (cm d ⁻¹) |
| K_{vbot} | KVBOT | Vertical hydraulic conductivity bottom layer (cm d ⁻¹) |
| g_{drain} | GEOFAC | Geometry factor of Ernst (-) |

4.2.3 Basic drainage

A simple, basic interaction between groundwater and a maximum of 5 surface water systems may be simulated.

The drainage/infiltration (q_{drain}) to/from each surface water system i is calculated as:

$$q_{\text{drain},i} = \frac{\phi_{\text{gwl}} - \phi_{\text{drain},i}}{\gamma_{\text{drain},i}} \quad (4.19)$$

where $q_{\text{drain},i}$ is the drainage/infiltration (cm d⁻¹) to/from surface water system i , the drainage base $\phi_{\text{drain},i}$ is equal to the surface water level of system i (cm below the soil surface), ϕ_{gwl} is the groundwater level (cm below the soil surface), $\gamma_{\text{drain},i}$ is the drainage or infiltration resistance from system i (d).

| <i>Model input</i> | | |
|---|-------------|--------------------------------------|
| <i>Variable</i> | <i>Code</i> | <i>Description</i> |
| | NRLEVS | Number of drainage levels (-) |
| <i>Specify for each drainage level:</i> | | |
| γ_{drain} | DRARES | Drainage resistance (d) |
| γ_{inf} | INFRES | Infiltration resistance (d) |
| L_{drain} | L | Drain spacing (m) |
| ϕ_{drain} | ZBOTDR | Level of drainage medium bottom (cm) |

4.2.4 Interflow

In some applications one may wish to define one of the systems as an interflow system, which has a rapid discharge with short residence times of the water in the soil system. Interflow should always be assigned to the highest order or level of distinguished drainage systems. This may be applied for either basic or extended drainage options. (paragraphs 4.2.3 and 4.2.5).

The interflow towards surface water systems n is calculated as:

$$q_{\text{drain},n} = A_{\text{interflow}} (\phi_{\text{gwl}} - \phi_{\text{drain},n})^{B_{\text{interflow}}} \quad (4.20)$$

where: $q_{\text{drain},n}$ is the interflow towards surface water system n , $A_{\text{interflow}}$ and $B_{\text{interflow}}$ are respectively coefficient (d^{-1}) and exponent (-) in the relation.

| <i>Model input</i> | | |
|------------------------|-------------|---|
| <i>Variable</i> | <i>Code</i> | <i>Description</i> |
| $A_{\text{interflow}}$ | COFINTFLB | Coefficient for interflow relations (d) |
| $B_{\text{interflow}}$ | EXPINTFLB | Exponent for interflow relation (-) |

4.2.5 Extended drainage

This paragraph describes an extended drainage option, which may be applied when the interaction between groundwater and surface water system can be limited to a single representative groundwater level and a single representative surface water level. The interaction between these two levels is described with extensive options and documented hereafter.

The groundwater-surface water system is described at the scale of a horizontal subregion. Only a single representative groundwater level is simulated, which is 'stretched' over a scale that in reality involves a variety of groundwater levels. In the following, due consideration will be given to the schematization of the surface water system, the simulation of drainage/sub-irrigation fluxes (including surface runoff), and the handling of an open surface water level.

The surface water system is divided into a maximum of five channel orders:

- primary water course (1st order);
- secondary water course(s) (2nd order);
- tertiary water courses (3rd order);
- pipe drains (4th order);

- trenches (5th order).

An example of a surface water system with three channel orders is shown in Figure 13.

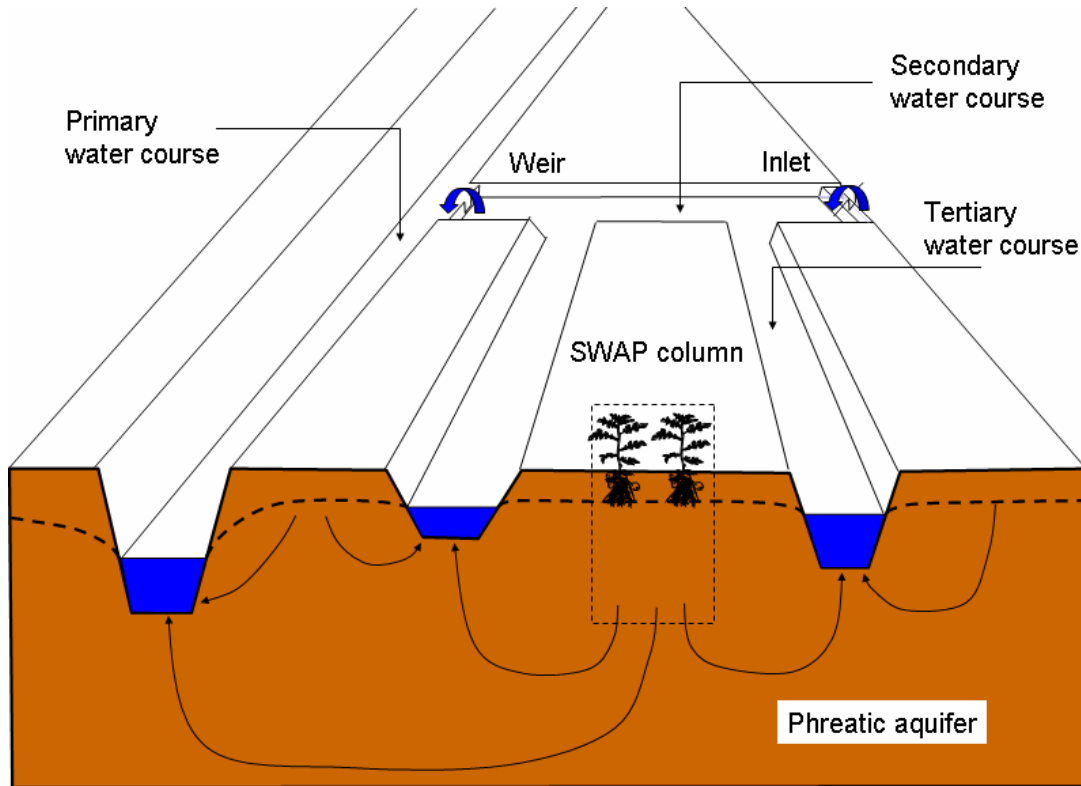


Figure 13 Schematized surface water system. The primary water course functions separately from the others, but it does interact with the SWAP soil column by the drainage or infiltration flux

Each order of channels is defined by its channel bed level, bed width, side-slope, and spacing. For practical cases, the representative spacing L_i (m) is derived by dividing the area of the subregion A_{reg} (m²) by the total length of the i^{th} order channels, l_i (m):

$$L_i = \frac{A_{\text{reg}}}{l_i} \quad (4.21)$$

In the surface water model, we assume that the different channels orders are connected in a dendritic manner. Together they form a surface water 'control unit' with a single outlet and, if present, a single inlet. The surface water level at the outlet is assumed to be omnipresent in the subregion. Friction losses are neglected and thus the slope of the surface water level is assumed to be zero. This means that in all parts of the subregion the surface water level has the same depth below soil surface. Its presence, however, is only locally felt in a water course if it is higher than the channel bed level. If it is lower, the water course is free draining, or remains dry if the groundwater level is below the channel bed.

In most applications, the control unit will include the primary watercourse. It is, however, possible to specify that the primary watercourse, e.g. a large river, functions separately from the rest of the subregional surface water system. In that case it has its own surface water level. This level has to be specified in the input, because it is determined by water balances and flows on a much larger scale than that of the modelled subregion. In the real situation

there may be some interaction between the primary water course and the control unit: for instance a pumping station for removal of drainage water, and/or an inlet for letting in external surface water supply (Figure 13). The hydraulics of such structures are not included in the model.

The channels do not only act as waterways for surface water transport. Depending on the groundwater level and the open surface water level, the channels will also act as either drainage or sub-irrigation media. In the system modelled by SWAP, it is possible that more than one type of surface water channel becomes active simultaneously. For these situations one can best speak of 'multi-level' drainage or sub-irrigation. In the following, we will refer to channels in terms of their 'order' if their role as part of the surface water system is being considered. When considering their drainage characteristics we will refer to them in terms of their 'level'.

When the groundwater level rises above the soil surface, the soil surface also starts to function as a 'drainage medium' generating surface runoff. The storage of water on the soil surface itself, however, is simulated by SWAP as 'ponding' (Par. 4.1).

| <i>Model input</i> | | |
|--------------------------------|-------------|---|
| <i>Variable</i> | <i>Code</i> | <i>Description</i> |
| n | NRSRF | Number of subsurface drainage levels (-) |
| <i>Specify for each level:</i> | | |
| i | LEVEL | Drainage level number (-) |
| - | SWDTYP | Type of drainage medium (open = 0, closed = 1) |
| L | L | Spacing between channels/drains (m) |
| z_{bed} | ZBOTDRE | Altitude of bottom of channel or drain (cm) |
| ϕ_{ang}^{min} | GWLINF | Groundwater level for maximum infiltration (cm) |
| $\gamma_{drain,inp}$ | RDRAIN | Drainage resistance (d) |
| $\gamma_{inf,inp}$ | RINF | Infiltration resistance (d) |
| γ_{entry} | RENRTY | Entry resistance (d) |
| γ_{exit} | REXIT | Exit resistance (d) |
| - | WIDTHR | Bottom width of channel (cm) |
| - | TALUDR | Side-slope of channel (-) |

4.2.5.1 Surface water balance

For the water balance of the subregion as a whole, we assume that the soil profile 'occupies' the whole surface area, even though part of the area is covered by surface water. In other words, the water balance terms of the soil profile that are computed per unit area ($\text{cm}^3 \text{cm}^{-2}$) have the *same numerical value for the subregion as a whole*. This implies that the evapotranspiration of surface water is set equal to the actual evapotranspiration of land surface. For reasons of simplicity evapotranspiration and precipitation are not included in the water balance of surface water. We do, however, compute storage characteristics of the surface water based on the lengths of the water courses and the wetted cross sections. There

is thus a 'duplicate use' of part of the area, introducing some extra storage in the system, which in reality does not exist. The approach followed here is only valid for subregions with a limited area of surface water, certainly not more than 10%.

The surface water balance equation for the control unit is formulated as:

$$V_{\text{sur}}^{j+1} - V_{\text{sur}}^j = (q_{\text{sup}} - q_{\text{dis}} + q_{\text{drain}} + q_{\text{c,drain}} + q_{\text{run}}) \Delta t^j \quad (4.22)$$

where V_{sur} is the regional surface water storage ($\text{cm}^3 \text{ cm}^{-2}$), q_{sup} is the external supply to the control unit ($\text{cm}^3 \text{ cm}^{-2} \text{ d}^{-1}$), q_{dis} is the discharge that leaves the control unit ($\text{cm}^3 \text{ cm}^{-2} \text{ d}^{-1}$), $q_{\text{c,drain}}$ is bypass flow ($\text{cm}^3 \text{ cm}^{-2} \text{ d}^{-1}$) through cracks of a dry clay soil to drains or ditches, q_{run} is the surface runoff/runon ($\text{cm}^3 \text{ cm}^{-2} \text{ d}^{-1}$), Δt is the time increment (d), and superscript j is the time level.

The regional surface water storage V_{sur} ($\text{cm}^3 \text{ cm}^{-2}$) is the sum of the surface water storage in each order of the surface water system:

$$V_{\text{sur}} = \frac{1}{A_{\text{reg}}} \sum_{i=1}^n l_i A_{\text{d},i} \quad (4.23)$$

in which A_{reg} is the total area of the subregion (cm^2), l_i the total length of channels/drains of order i in the subregion (cm), and $A_{\text{d},i}$ is the wetted area of a channel *vertical* cross-section (cm^2). The program calculates $A_{\text{d},i}$ using the surface water level ϕ_{sur} , the channel bed level, the bottom width, and the side-slope. Substitution of Eq. (4.21) in Eq. (4.23) yields the expression:

$$V_{\text{sur}} = \sum_{i=1}^n \frac{A_{\text{d},i}}{L_i} \quad (4.24)$$

Channels of order i only contribute to the storage if $\phi_{\text{sur}} > z_{\text{bed},i}$. The storage in pipe drains is assumed to be zero. Eq. (4.24) is used by the model for computing the storage from the surface water level and vice versa, per time step. Prior to making any dynamic simulations, a table of channel storage as a function of discrete surface water levels is derived.

4.2.5.2 Drainage resistance (subregional approach)

Prior to any calculation of the drainage/sub-irrigation rate, we determine whether the flow situation involves drainage, sub-irrigation, or neither. No drainage or sub-irrigation will occur if both the groundwater level and surface water level are below the drainage base.

Drainage will only occur if the following two conditions are met:

- the groundwater level is higher than the channel bed level;
- the groundwater level is higher than the surface water level.

Sub-irrigation can only occur if the following two conditions are met:

- the surface water level is higher than the channel bed level;
- the surface water level is higher than the groundwater level.

In both cases we take for the drainage base, ϕ_{drain} (cm), either the surface water level, ϕ_{sur} (cm), or the channel bed level, z_{bed} (cm), whichever is higher:

$$\phi_{\text{drain}} = \max(\phi_{\text{sur}}, z_{\text{bed}}) \quad (4.25)$$

The variable ϕ is defined positive upward, with zero at the soil surface.

An example of a single-level drainage case is given in Figure 13. In this example we assume that:

- the considered channel is part of a system involving equidistant and parallel channels, all of the same order;
- the recharge R is evenly distributed and steady-state.

For such situations several drainage formula exist, as described in Par.4.2.2.

The drainage resistance for the subregional approach is defined as:

$$\gamma_{\text{drain}} = \frac{\phi_{\text{avg}} - \phi_{\text{drain}}}{R} \quad (4.26)$$

where ϕ_{avg} is the mean groundwater level of the whole subregion, and ϕ_{drain} the hydraulic head of the drain or ditch (cm), the so-called drainage base.

Note that instead of the maximum groundwater level ϕ_{gw1} midway between the drains or ditches (eq. (4.3)), the mean groundwater level ϕ_{avg} is used. The two definitions of γ_{drain} in eq. (4.3) and (4.26) differ by the so-called shape factor: the shape factor is the ratio between the mean and the maximum groundwater level elevation above the drainage base. The shape factor depends on the vertical, horizontal, radial and entrance resistances of the drainage system (Ernst, 1978). For regional situations, where the 'horizontal' resistance to flow plays an important role, the shape factor is relatively small (≈ 0.7). The smaller the horizontal resistance becomes, the more 'rectangular' the water table: in the most extreme case with all the resistance concentrated in the direct vicinity of the channel, the water table is level, except for the abrupt drop towards the drainage base. In that case the shape factor becomes equal to unity (see Par.4.2.2).

The model calculates drainage using a total drainage resistance:

$$\gamma_{\text{drain}} = \gamma_{\text{drain,inp}} + \frac{L_{\text{drain}}}{u_{\text{drain}}} \gamma_{\text{entry}} \quad (4.27)$$

where: $\gamma_{\text{drain,inp}}$ is input to the model, u_{drain} is the wetted perimeter (cm), γ_{entry} is the entrance resistance (d)

In case of sub-irrigation, the entrance resistance (then denoted as γ_{inf}) can differ from that for drainage (γ_{drain}): it can either be higher or lower, depending on local conditions. A substantial raising of the surface water level can for instance result in infiltration through a 'bio-active' zone (e.g. involving pores of rain worms) which will reduce the entrance resistance. In most situations with sub-irrigation the radial resistance will be higher than with drainage, because the wetted section of the subsoil is less than in the situation with drainage (the groundwater table becomes concave instead of convex). Especially if the conductivity of the subsoil above the drainage base is larger than in the deeper subsoil, the sub-irrigation resistance γ_{inf} will be substantially higher than the drainage resistance γ_{drain} . In view of these various possible practical situations, the model has the option for using sub-irrigation resistances that differ from the ones for drainage (e.g. $\gamma_{\text{inf}} \approx 3/2 \gamma_{\text{drain}}$ in Figure 14).

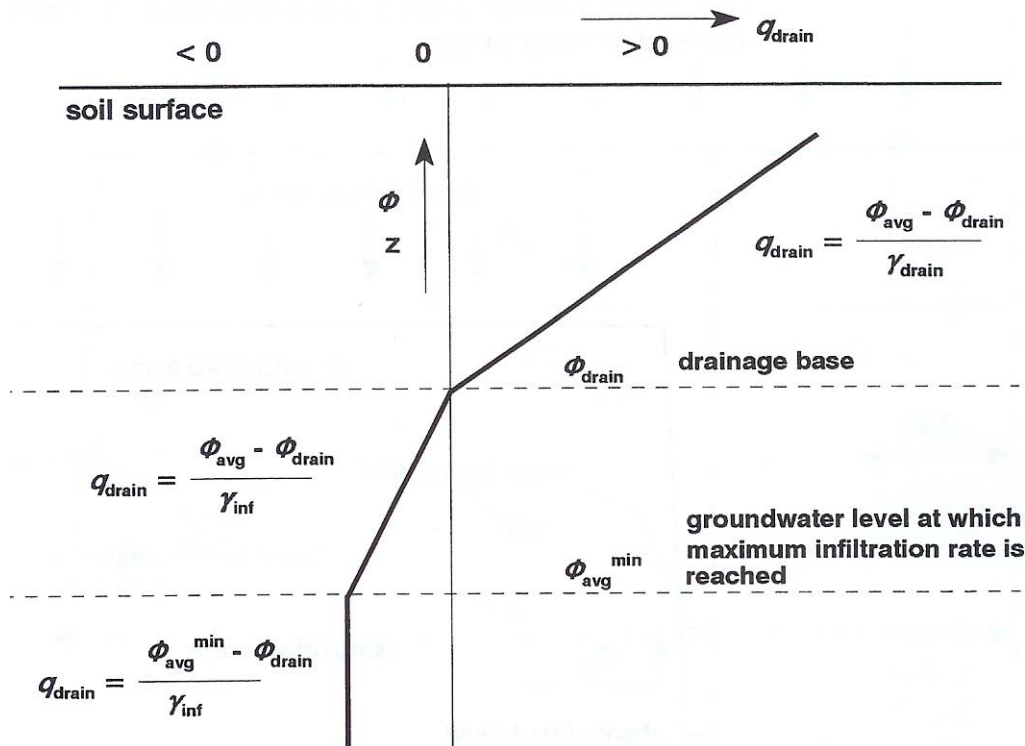


Figure 14 Linear relationships between drainage ($q_{\text{drain}} > 0$) and infiltration ($q_{\text{drain}} < 0$) flux and mean groundwater level ϕ_{avg}

An additional model option is to limit the simulated sub-irrigation rate. Such a limitation is needed because the sub-irrigation rate does not increase forever when the groundwater level drops: asymptotically a maximum rate is reached. This maximum rate is determined by the surface water level, the geometry of the wetted channel cross-section and the permeability of the subsoil. For practical reasons we have not set a limit to the sub-irrigation rate itself (Figure 14). Instead, we have limited the simulated sub-irrigation rate by defining the groundwater level $\phi_{\text{avg}}^{\text{min}}$ at which the maximum sub-irrigation rate is reached. The linearised relationship, given by Eq. (4.26), is not valid at lower groundwater levels.

Because the non-steady groundwater flow is simulated as a sequence of steady-state conditions, we use the linearised relation between q_{drain} and ϕ_{avg} . This approach is only valid if the drainage resistance is concentrated in the direct vicinity of the channel cross-section, i.e. that the radial resistance is far more important than the horizontal resistance. In such cases the shape factor approaches unity. This contrasts with the case of 'perfect' drains where the shape factor varies with time, depending on the sequence of preceding recharges. After a 'storm recharge' the drainage flow to 'perfect' drains is much higher than the flow predicted by the steady-state relationship. In most situations however, the radial resistance is much higher than the horizontal one, and the use of a steady-state relationship for non-steady simulations will not lead to major errors.

4.2.5.3 Multi level drainage

For illustration purposes we consider a multi-level drainage involving third and fourth order systems (Figure 15):

- the third-order drainage system consists of ditches;
- the fourth-order system consists of subsurface drains;
- the ditches and drains are assumed to be equidistant and parallel.

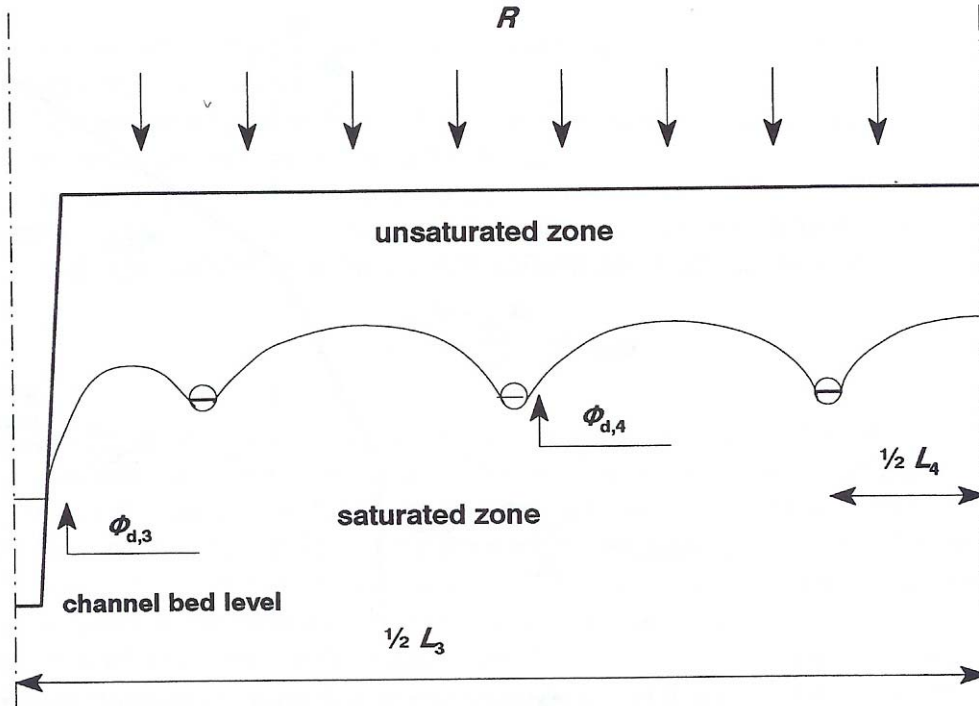


Figure 15 Cross-section of multi-level drainage, involving a third-order system of ditches and a fourth-order system of pipe drains

In this case of two-level drainage we need to quantify the drainage fluxes to both levels of drainage media. We implicitly assume that nearly all of the flow resistance is concentrated in the vicinity of the drainage media (channels and drains). In the most extreme case with only entrance resistance, the water level is horizontal, as shown in Figure 16. In such a case groundwater behaves as a linear reservoir, with outlets at different levels ('tank with holes', see Figure 18). This approach is valid if the main part of the drainage resistance is concentrated near the drains or ditches. For most soils in the Netherlands this seems a reasonable assumption.

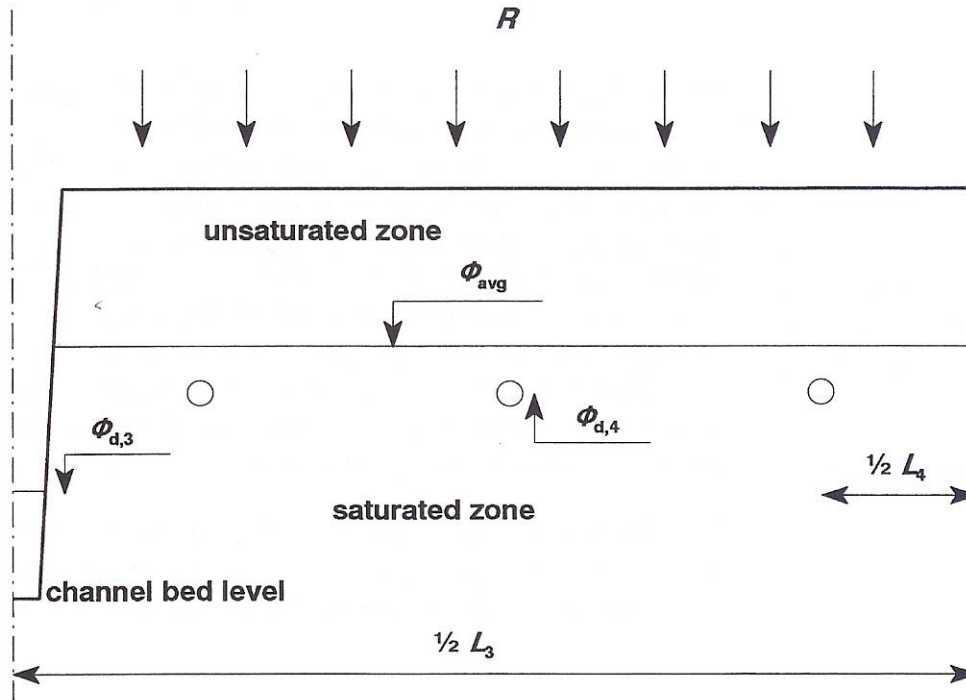


Figure 16 Cross section of multi-level drainage. The main part of the flow resistance is assumed to be located near the drains and ditches, which results in a horizontal groundwater table

Similar to the case of single-level drainage, a drainage level is only 'active' if either the groundwater level or the surface water level is higher than the channel bed level. The drainage base is determined separately for each of the drainage levels, using Eq. (4.25). In computing the total flux to/from surface water, the contributions of the different channel orders are simply added. For the situation with the groundwater level above the highest bed level and with the surface water level below the lowest one, for instance, the total drainage flux is computed with:

$$q_{\text{drain}} = \sum_{i=1}^n \frac{\phi_{\text{avg}} - \phi_{d,i}}{\gamma_{d,i}} \quad (4.28)$$

where the drainage base $\phi_{d,i}$ is in this case equal to the channel bed level, $z_{\text{bed},i}$. If the surface water level becomes higher than the channel bed level $z_{\text{bed},i}$, the latter is replaced by the surface water level.

| <i>Model input</i> | | |
|---------------------------|-------------|--|
| <i>Variable</i> | <i>Code</i> | <i>Description</i> |
| ϕ_{sur}^j | WLP | Water level in primary water course as a function of date (cm) |
| ϕ_{sur}^{j+1} | WLS | Water level in secondary water course as a function of date (cm) |

4.2.5.4 Procedure for surface water level as input

SWAP calculates the net discharge $q_{\text{dis}} - q_{\text{sup}}$ between t^j and t^{j+1} for the given surface water levels ϕ_{sur}^j and ϕ_{sur}^{j+1} at the beginning and end of a time step, using Eq. (4.22) in a rearranged form:

$$q_{\text{dis}} - q_{\text{sup}} = \frac{V_{\text{sur}}^j - V_{\text{sur}}^{j+1}}{\Delta t^j} + q_{\text{drain}} + q_{\text{c,drain}} + q_{\text{run}} \quad (4.29)$$

The terms on the right hand side are known or can be calculated (V_{sur} is a function of the known ϕ_{sur}). If the sum is positive, discharge has taken place and the supply is equal to zero. If the sum is negative, supply has taken place and the discharge is equal to zero.

4.2.5.5 Procedure for surface water level as output

This procedure calculates the surface water level from the surface water balance of a control unit. For each water management period a fixed or an automatic weir can be simulated. The settings of the weirs can be different for each management period, as can be the other input parameters of water management. One of the most important input parameters is the maximum rate at which water can be supplied from an external source (for sub-irrigation). During each time step, SWAP determines:

- the target level;
- whether the target level is reached, and the amount of external supply that is needed (if any);
- the discharge that takes place (if any) and the surface water level at the end of the time step.

In the case of a fixed weir, the target level coincides with the level of the crest (which is fixed during a certain management period, but can be changed from one period to the next). In the case of an automatic weir, the target level is determined by a water management scheme. This scheme gives the desired setting of the target water level $\phi_{\text{sur,tar}}$ in relation to a number of state variables of the system. At present it is possible to relate the target level to:

- the average groundwater level ϕ_{avg} ;
- the soil water pressure head h (cm) at a certain depth in the soil profile;
- total water storage of the unsaturated soil profile V_{uns} (cm).

A high groundwater level will lead to a lower target level, in order to minimize reduction of crop growth due to waterlogging. In nature reserves this criterium does not apply. A soil water pressure head gives a better indication of a threat of waterlogging, than the groundwater level only. The water amount that still can be stored in the soil profile, indicates the buffer capacity in case of heavy rainfall. Maintaining a certain minimum amount of storage, reduces the risk of flooding and subsequent discharge peaks.

Table 2 Example of a water management scheme, with $\phi_{sur,tar}$ the target level for surface water, the criterium $\phi_{avg,max}$ for the mean groundwater level (maximum), the criterium h_{max} for the pressure head (maximum) and $V_{uns,min}$ for the unsaturated volume (minimum). The program selects the highest target level for which all three criteria are met.

| $\phi_{sur,tar}$ (cm) | $\phi_{avg,max}$ (cm) | h_{max} (cm) | $V_{uns,min}$ (cm) |
|-----------------------|-----------------------|----------------|--------------------|
| -180 | 0 | 0 | 0 |
| -160 | -80 | -100 | 1.5 |
| -140 | -90 | -150 | 2.0 |
| -120 | -100 | -200 | 2.5 |
| -100 | -120 | -250 | 3.0 |
| -80 | -130 | -300 | 4.0 |

An example of the water management scheme with target levels and criteria, is shown in Table 2. On the first line the minimum target level is specified. The criteria for this level (zeros) are dummies: the minimum target level is chosen whatever the prevailing conditions. The water management scheme selects the highest level for which all three criteria are met.

The water management scheme also has a *maximum drop rate* parameter, which specifies the maximum rate with which the target level of an automatic weir is allowed to drop (cm d⁻¹). This is needed to avoid situations in which the target level reacts abruptly to the prevailing groundwater level. An abrupt drop can cause instability of channel walls or wastage of water that could have been infiltrated. Such a situation can occur during a period with surface water supply and a rising groundwater level due to infiltrating water: the rising groundwater level can cause a different target level to be chosen for the surface water system.

After having determined the target level, the next step in the procedure is to determine whether it can be reached within the considered time step. If necessary, surface water supply is used to attain the target level. This supply is not allowed to exceed the maximum supply rate $q_{sup,max}$, which is an input parameter. For situations with supply, it is possible to specify a tolerance for the surface water level in relation to the target level. This tolerance, the *allowed dip* of the surface water level, can for instance be 10 cm. Then the model does not activate the water supply as long as the water level remains within this tolerance limit of the target level. An appropriate setting of this parameter can save a substantial amount of water, because quick switches between supply and discharge are avoided.

The final step in the procedure is to determine the discharge that takes place (if any) and the surface water level at the end of the time step. Discharge takes place if no supply is needed for reaching the target level. In that case the supply rate is set to zero. In the case of an automatic weir, the discharge follows simply from the water balance equation in the form given by Eq. (4.29), with q_{sup} set to zero and the storage V_{sur}^{j+1} set equal to the storage for the target level. The discharge q_{dis} is then the only unknown left, and can be solved directly.

In the case of a fixed weir, the discharge can not be determined so easily. For the 'stage-discharge' relationship $q_{dis}(\phi_{sur})$ of a fixed weir, we use:

$$q_{dis} = \alpha (\phi_{sur} - z_{weir})^\beta \quad (4.30)$$

in which z_{weir} is the weir crest level (cm), α is the discharge coefficient ($\text{cm}^{1-\beta} \text{d}^{-1}$), and β is the discharge exponent (-).

In hydraulic literature head-discharge relationships are given in SI-units, i.e. m for length and s for time and the discharge is computed as a volume rate ($\text{m}^3 \text{s}^{-1}$). To facilitate the input for the user we conformed to hydraulic literature. This implies that the user has to specify the weir characteristics that define a relationship of the following form:

$$Q = \alpha_{\text{weir}} H^{\beta_{\text{weir}}} \quad (4.31)$$

where Q is the discharge ($\text{m}^3 \text{s}^{-1}$), $H = \phi_{\text{sur}} - z_{\text{weir}}$ is the head above the crest (m) and α_{weir} is a weir coefficient ($\text{m}^{3-\beta} \text{s}^{-1}$), β_{weir} is a weir exponent (-).

The user has to compute the value of α_{weir} from the various coefficients preceding the upstream head above the crest. For instance, for a broad-crested rectangular weir, α_{weir} is (approximately) given by:

$$\alpha_{\text{weir}} = 1.7b \quad (4.32)$$

where 1,7 is the discharge coefficient of the weir (based on SI-units), b is the width of the weir (m).

To correct for units, the model carries out the following conversion:

$$\alpha = \frac{8.64 * 100^{(1-\beta_{\text{weir}})}}{A_{cu}} \alpha_{\text{weir}} \quad (4.33)$$

where A_{cu} is the size of the control unit (ha).

The model requires input of the size of the control unit (A_{cu}), which in simple cases will be identical to the size of the simulation unit.

Also a table can be used to specify this relationship. The relationship should be specified for all the management periods, *including* those with management using an automatic weir. In situations with increasing discharge, at a certain moment the capacity of the automatic weir will be reached. In such situations the crest is lowered to its lowest possible position, and the water level starts to rise above the target level. This type of situation can only be simulated correctly if the lowest possible crest level has been specified, and the discharge relationship has been defined accordingly.

To determine the discharge of a fixed weir, the stage-discharge relationship has to be substituted in the water balance equation of Eq. (4.22). The (unknown) surface water level ϕ_{sur}^{j+1} influences both V_{sur}^{j+1} and q_{dis} . This equation can not be solved directly because there can be a transition from a no-flow situation at the beginning of the time step to a flow situation at the end of the time step. For this reason an iterative numerical method is used to determine the new surface water level ϕ_{sur}^{j+1} and the discharge (see Par.4.2.5.6).

| <i>Model input</i> | | |
|--|-------------|---|
| <i>Variable</i> | <i>Code</i> | <i>Description</i> |
| ϕ_{sur} | WLACT | Initial surface water level (cm) |
| - | OSSWLM | Criterion for warning about oscillation (cm) |
| <i>For each management period specify:</i> | | |
| - | IMPEND | Date that management ends |
| - | SWMAN | Type of water management (1 = fixed weir crest, 2 = automatic weir) |
| Q_{sup} | WSCAP | Surface water supply capacity (cm d ⁻¹) |
| - | WLDIP | Allowed dip of surface water level, before starting supply (cm) |
| - | INTWL | Length of water-level adjustment period (d) |
| <i>Exponential discharge relation:</i> | | |
| A_u | SOFCU | Size of control unit (ha) |
| <i>Specify for all periods:</i> | | |
| z_{weir} | HBWEIR | Weir crest (cm) |
| α_{weir} | ALPHAW | Alpha-coefficient of discharge formula |
| β_{weir} | BETAW | Beta-coefficient of discharge formula |
| <i>Table discharge relation:</i> | | |
| <i>Specify for all periods:</i> | | |
| - | ITAB | Index per management period (-) |
| ϕ_{sur} | HTAB | Surface water level (cm) |
| Q_{dis} | QTAB | Discharge (cm d ⁻¹) |
| <i>Automatic weir control:</i> | | |
| <i>Specify for all periods:</i> | | |
| - | DROPR | Maximum drop rate of surface water level (cm d ⁻¹) |
| - | HDEPTH | Depth in soil profile for comparing with HCRIT (cm) |
| - | | |
| - | IPHASE | Index per management period (-) |
| $\phi_{\text{sur,tar}}$ | WLSMAN | Surface water level (cm) |
| $\phi_{\text{avg,max}}$ | GWLCRIT | Groundwater level (cm) |
| h_{max} | HCRIT | Critical pressure head, max. value (cm) |
| $V_{\text{uns,min}}$ | VCRIT | Critical unsaturated volume for all surface water levels (cm) |

4.2.5.6 Implementation aspects

Schematization into subregions

A simulation at subregional scale will often not stand on its own. A relatively large study area will be divided into several subregions. The boundaries of the subregion(s) should be chosen in a judicious manner. Ideally a subregion is horizontal, has the same type of soil throughout, has a regularly structured dendritic surface water system, and has a groundwater level that does not vary much in depth (a few decimeters). In practice this will hardly ever be the case. By making the subregions very small, the variation of the groundwater depth will be limited, but the number of defined subregions will increase. Another disadvantage can be that the surface water system becomes divided into units that are smaller than the basic control unit which functions in the field. This makes it hard to translate practical water management strategies into model parameters and vice versa. It may also become difficult to compare measured and simulated water balances with each other, which hampers model calibration. The schematization into subregions is a compromise, affected by these aspects.

Schematisation of the surface water system

SWAP uses at most five distinct 'orders' of channels/drains, with exactly defined channel characteristics per order. In reality, the channel characteristics will not be exactly defined. Variations of channel depths by a few decimeters are quite normal. The classification should not involve more classes than necessary, as more classes require more input data and produce more output data. If this extra data load can not be justified by a significantly better simulation result, the extra data will simply be an extra burden and hamper result interpretation.

Obtaining model input data for the smaller channels is relatively straightforward. Each order of channels can be treated as a separate single-level drainage medium, for which data can be derived using formulae given in Par. 4.2.2. Getting data for the large primary water courses can be more involved, especially if the spacing is at a larger scale than the subregion itself. It will then become less realistic to (for these channels) use the mean groundwater level ϕ_{avg} . Instead, the position of the subregion with respect to two channels of the primary order should be taken into account. If, for instance, the subregion is roughly midway between two such channels, the drainage resistance for the maximum groundwater level ϕ_{gwl} should be used, but only for these large channels, not for the rest of the surface water system. In such a case it is obvious that the surface water level in the primary channel is determined by the water balance on a scale that is much larger than that of the subregion. It is then also appropriate to model the primary channel as being separate from the rest of the surface water system.

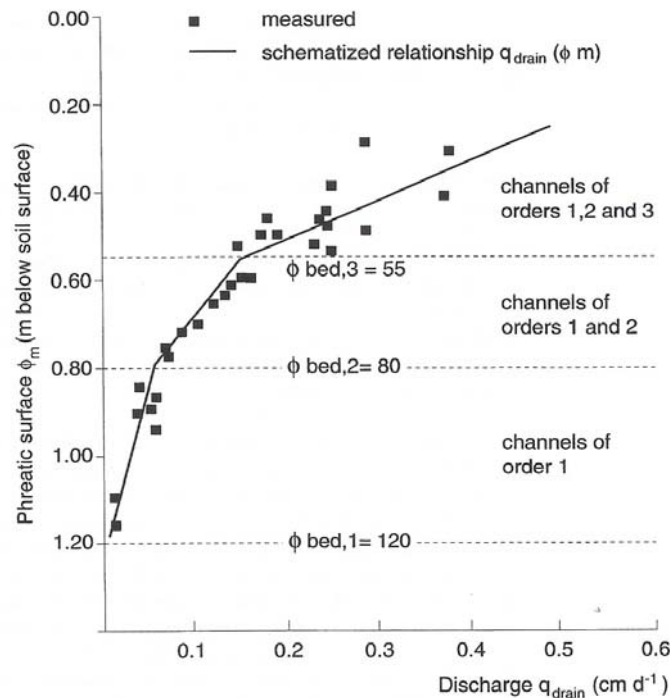


Figure 17 Discharge q_{drain} as function of mean phreatic surface ϕ_{avg} in the Beltrum area (Massop and de Wit, 1994)

An alternative way of making a schematization of the surface water system is by analysis of experimental data. In Figure 17 the results are shown of field measurements by Massop and De Wit (1994) for the Beltrum area. A discharge unit was identified and measurements were made of:

- total surface area;
- discharge at the outlet;
- mean groundwater level.

From Figure 17 one can see that the drainage base of the larger channels is roughly at $z = -120$ cm, as no discharges were measured below that level. The schematized $q_{\text{drain}}(\phi_{\text{avg}})$ -relationship is a piece-wise linear function, with transition points at mean groundwater levels of 80 and 55 cm below soil surface. These transition points correspond to the 'representative' bed levels of the second and third order channels. The drainage resistance of the first order channels can be derived from the transition point at $z = -80$ cm in the following manner:

$$q(-80) = 0.05 = \frac{\phi_{\text{avg}} - \phi_{d,1}}{\gamma_{d,1}} = \frac{-80 + 120}{\gamma_{d,1}} \quad (4.34)$$

which gives $\gamma_{d,1} = 800$ d. The drainage resistance of the second-order channels follows subsequently from:

$$q(-55) = 0.15 = \frac{\phi_{\text{avg}} - \phi_{d,1}}{\gamma_{d,1}} + \frac{\phi_{\text{avg}} - \phi_{d,2}}{\gamma_{d,2}} = \frac{-55 + 120}{800} + \frac{-55 + 80}{\gamma_{d,2}} \quad (4.35)$$

which results in $\gamma_{d,2} = 365$ d. Analogously, the drainage resistance of the third-order channels can be derived: $\gamma_{d,3} = 135$ d.

Numerical schemes

The land surface model, in which the Richards' equation is solved, and the surface water model are coupled by means of an *explicit* numerical scheme. In other words, the surface water level update and the calculation of the drainage fluxes do *not* interact with the calculation of the soil water content and the groundwater level *within a time step*. Thus the drainage fluxes are computed using the groundwater level and the surface water level at the *beginning* of a time step.

The surface runoff (or runon), however, is computed with Eq. (4.2) using more up-to-date information: the ponding height h_{pond} at the *end* of a time step is used. This is made possible by the sequence of calculations in SWAP for situations with total saturation and ponding at the soil surface:

- first the Richard's equation is solved for the soil profile, with prescribed head $h = h_{\text{pond}}$ at the soil surface;
- next the ponding depth h_{pond} is updated from the water balance of the total soil profile, including surface runoff.

Explicit numerical schemes have the disadvantage that the computed levels can become unstable. To reduce the chance of oscillations in the simulated levels, the program reduces the time step automatically as soon as the ponding starts. If the specified 'ponding sill' has been set to zero, however, the first time step with surface runoff may lead to instability,

because the time step is reduced from the second time step after ponding onwards. The user can avoid this instability by specifying a non-zero value for the maximum ponding depth, e.g. of 1 cm.

For computing the surface water level in situations with a fixed weir, an equation has to be solved involving a look-up table (storage as a function of surface water level) and an exponential discharge relationship (discharge of weir as a function of the surface water level). We use an implicit iterative procedure for this, involving the surface water level at the *end* of the time step. This scheme has the advantage of being very stable. The disadvantage is that the computed discharge might deviate from the 'average' discharge during the time step. But since the used time steps are relatively small (<0.2 d), the loss of accuracy is not significant.

It can nevertheless be possible, even without surface runoff, that the simulated surface water and groundwater levels become unstable. SWAP warns the user if large oscillations of surface or *groundwater* levels occur. In such a case the user should reduce the maximum time step. In general, a time step of 1/50 of the smallest drainage resistance should lead to a stable simulation. If, however, the surface water system is highly reactive to drainage flows, an even smaller time step may be required.

4.3 Residence time approach

4.3.1 Introduction

Following the discussion in Par. 4.2, the drain densities of a three level drainage system are defined as:

$$M_1 = \frac{\sum l_1}{A_{\text{reg}}}; \quad M_2 = \frac{\sum l_2}{A_{\text{reg}}}; \quad M_3 = \frac{\sum l_3}{A_{\text{reg}}} \quad (4.36)$$

where A_{reg} (cm²) is the area of the subregion, $\sum l_1$, $\sum l_2$ and $\sum l_3$ are the total lengths (cm) of respectively the first, second and third order drains and M_1 , M_2 , M_3 are the drainage densities (cm⁻¹) of respectively the first order, the second order and the third order drainage system. The drainage fluxes $q_{d,1}$, $q_{d,2}$ and $q_{d,3}$ (cm d⁻¹) are calculated by linearized flux-head relationships (see Eq. 4.26):

$$q_{d,1} = \frac{\phi_{\text{avg}} - \phi_{d,1}}{\gamma_1}; \quad q_{d,2} = \frac{\phi_{\text{avg}} - \phi_{d,2}}{\gamma_2}; \quad q_{d,3} = \frac{\phi_{\text{avg}} - \phi_{d,3}}{\gamma_3} \quad (4.37)$$

where ϕ_{avg} is the regional averaged groundwater level (cm), $\phi_{d,i}$ the drainage hydraulic head (cm) of drainage system order i , and γ_i the drainage resistance (d) of drainage system order i . This drainage concept is schematically illustrated in Figure 18, depicting a linear reservoir model with outlets at different heights.

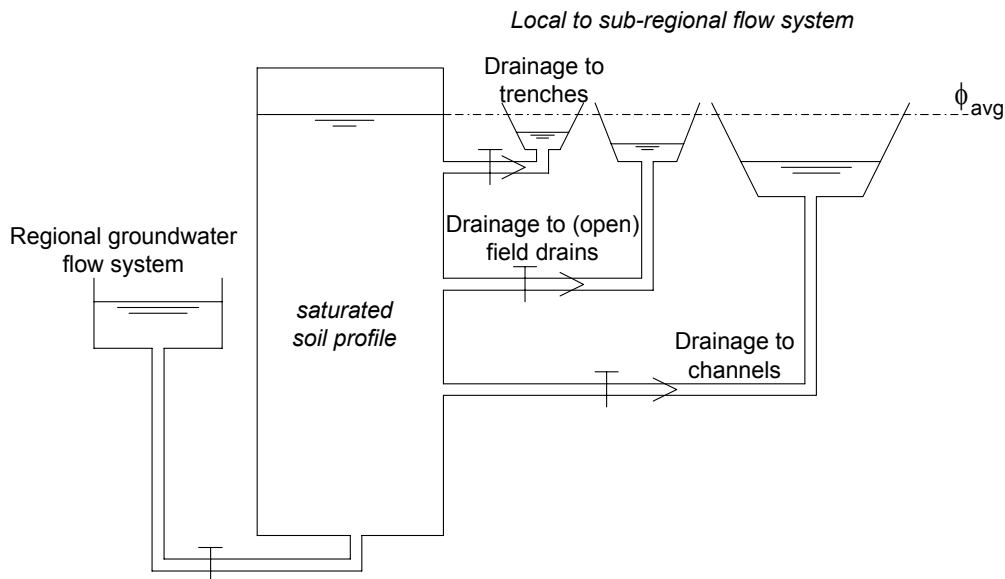


Figure 18 Illustration of regional drainage concept. The resistance mainly consists of radial and entrance resistance near the drainage devices

4.3.2 The horizontal groundwater flux

One-dimensional leaching models generally represent a vertical soil column. Within the unsaturated zone, chemical substances are transported by vertical water flows, whereas in the saturated zone the drainage discharge leaves the vertical column side-ways. For example in the ANIMO model (Rijtema et al., 1997), the distribution of lateral drainage fluxes with depth has been used to simulate the response of the load of chemicals on the surface water system to the inputs in the groundwater system. In this section, the concept for a distribution of lateral drainage fluxes with depth in an one-dimensional hydrological simulation model will be described. The following assumptions are made:

- steady groundwater flow and homogeneous distribution of recharge rates by rainfall;
- the aquifer has a constant thickness.

For convenience, only three levels of drains are considered, although the concept discussed here is valid for a system having any number of drainage levels.

Van Ommen (1986) has shown that for simple single level drainage systems, the travel time distribution is independent from the size and the shape of the recharge area. Under these assumptions, the average concentration of an inert solute in drainage water to a well or a watercourse, can mathematically be described by the linear behaviour of a single reservoir. This behaviour depends only on the groundwater recharge rate, the aquifer thickness and its porosity.

The non-homogeneous distribution of exfiltration points as well as the influence of chemical reactions on the concentration behaviour necessitates to distinguish between the hydraulic and chemical properties of different soil layers. In the drainage model, which describes the drainage discharge to parallel equidistant water courses, the discharge flow of system i , $Q_{d,i}$ is calculated as:

$$Q_{d,i} = L_i q_{d,i} \quad (4.38)$$

where L_i is the spacing of drainage system i . According to the Dupuit-Forcheimer assumption, the head loss due to radial flow and vertical flow can be ignored in the largest part of the flow domain. Following this rule, the ratio between occupied flow volumes V_i can be derived from the proportionality between flow volumes and discharge rates:

$$\frac{V_i}{V_{i-1}} = \frac{Q_{d,i}}{Q_{d,i-1}} \quad (4.39)$$

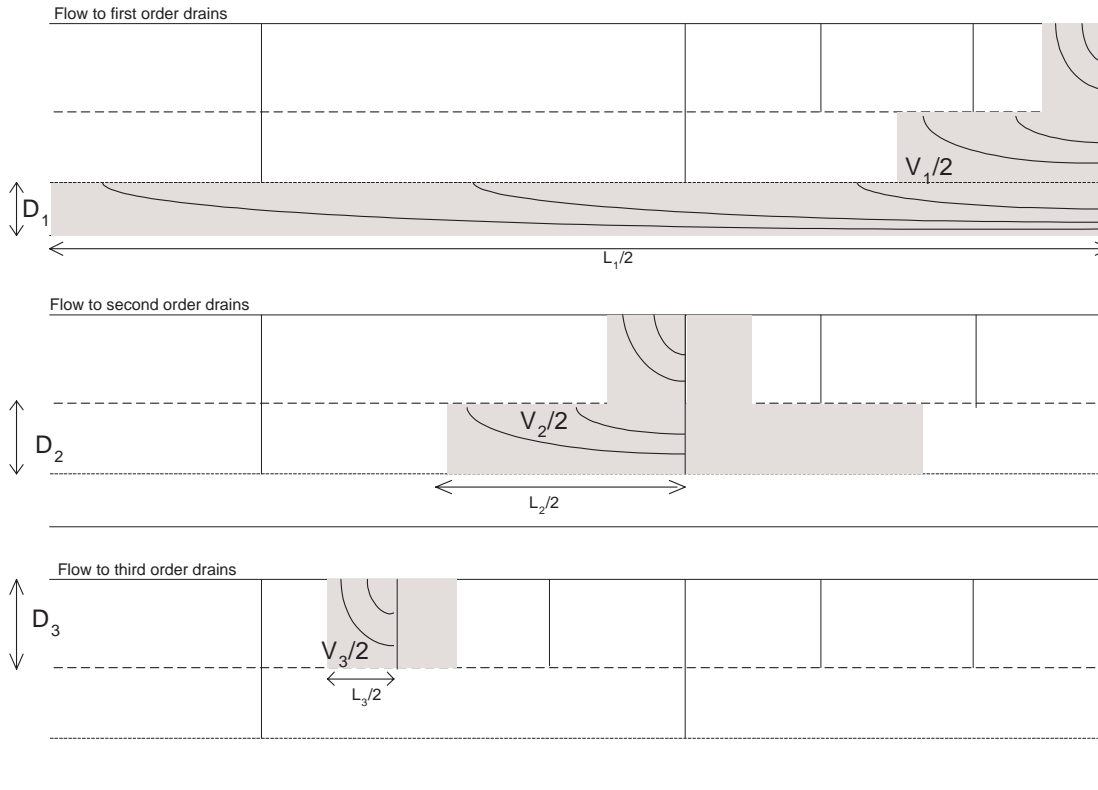


Figure 19 Schematization of regional groundwater flow to drains of three different orders

First order drains act also as field ditches and trenches and next higher drains act partly as third order drains. In the SWAP-model the lumped discharge flux per drainage system is computed from the relation between groundwater elevation and drainage resistance. Figure 19 shows the schematization of the regional groundwater flow, including the occupied flow volumes for the nested drain systems. The volume V_i consists of summed rectangles $L_i D_i$ of superposed drains, where D_i is the thickness (cm) of discharge layer i .

The flow volume V_i assigned to drains of order 1, 2 and 3 is related to drain distances L_i and thickness D_i of discharge layers as follows:

$$V_1 = L_1 D_1 + L_2 D_2 + L_3 D_3 \quad (4.40)$$

$$V_2 = L_2 D_2 + L_3 D_3 \quad (4.41)$$

$$V_3 = L_3 D_3 \quad (4.42)$$

Rewriting Eq. (4.40) to (4.42) and substituting Eq. (4.38) and Eq. (4.39) yields an expression which relates the proportions of the discharge layer to the discharge flow rates:

$$L_1 D_1 : L_2 D_2 : L_3 D_3 = (q_{d,1} L_1 - q_{d,2} L_2) : (q_{d,2} L_2 - q_{d,3} L_3) : (q_{d,3} L_3) \quad (4.43)$$

In theory, the terms $q_{d,1} L_1 - q_{d,2} L_2$ and $q_{d,2} L_2 - q_{d,3} L_3$ can take negative values for specific combinations of $q_{d,1} L_1$, $q_{d,2} L_2$ and $q_{d,3} L_3$. When $q_{d,1} L_1 - q_{d,2} L_2 < 0$ it is assumed that D_1 will be zero and the nesting of superposed flows systems on top of the flow region assigned to drainage class 1 will not occur. Likewise, a separate nested flow region related to a drainage class will not show up when $q_{d,2} L_2 - q_{d,3} L_3 < 0$. These cases are depicted schematically in Figure 20.

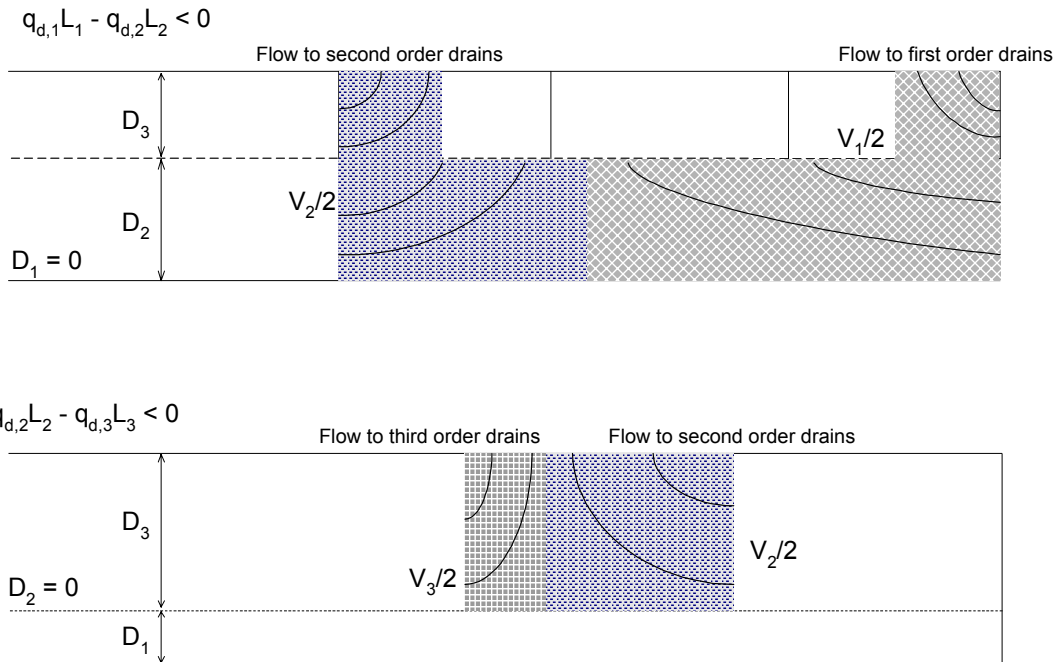


Figure 20 Schematization of regional groundwater flow to drains of three orders when either $q_{d,1}L_1 - q_{d,2}L_2 < 0$ or $q_{d,2}L_2 - q_{d,3}L_3 < 0$

If the soil profile is heterogeneous with respect to horizontal permeabilities, the heterogeneity can be taken into account by substituting transmissivities kD for layer thicknesses in Eq.(4.43):

$$(kD)_1 : (kD)_2 : (kD)_3 = \left(\frac{q_1 L_1 - q_2 L_2}{L_1} \right) : \left(\frac{q_2 L_2 - q_3 L_3}{L_2} \right) : \left(\frac{q_3 L_3}{L_3} \right) \quad (4.44)$$

The thickness of a certain layer can be derived by considering the vertical cumulative transmissivity relation with depth as shown in Figure 21.

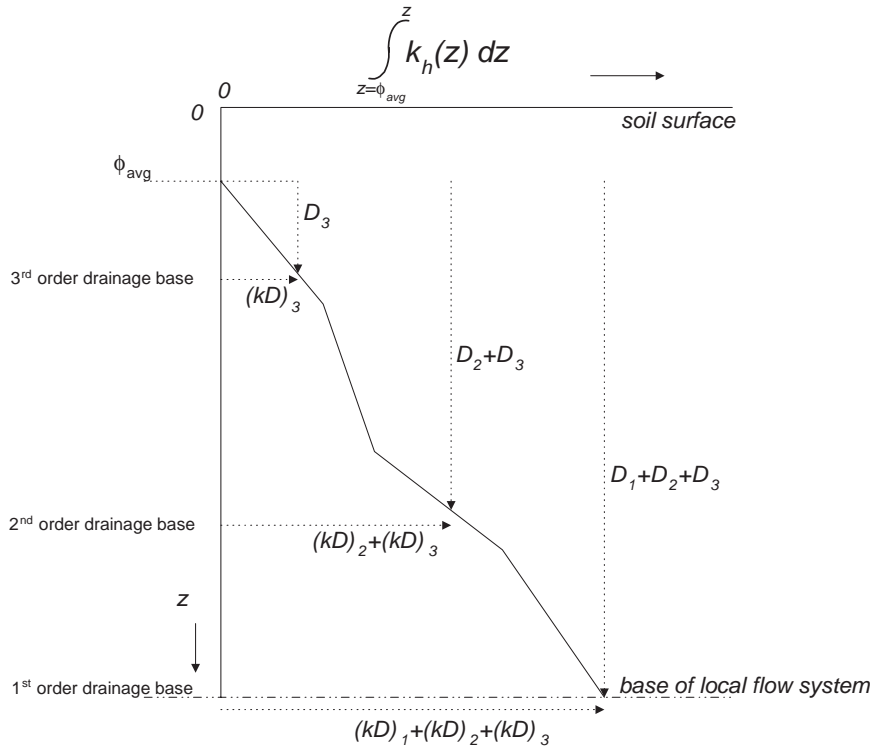


Figure 21 Discharge layer thickness D_i as function of cumulative transmissivity kD_i in a heterogeneous soil profile

The lateral flux relation per unit soil depth shows a uniform distribution. Lateral drainage fluxes $q_{d,k,i}$ to drainage system k for each nodal compartment i of the simulation model are calculated by:

$$q_{d,1,i} = q_{d,1} \frac{k_{h,i} \Delta z_i}{\sum_{i_{z=\phi_{avg}}}^{i_{z=-D_1-D_2-D_3}} k_{h,i} \Delta z_i} \quad \text{for} \quad -D_1 - D_2 - D_3 < z < \phi_{avg} \quad (4.45)$$

$$q_{d,2,i} = q_{d,2} \frac{k_{h,i} \Delta z_i}{\sum_{i_{z=\phi_{avg}}}^{i_{z=-D_2-D_3}} k_{h,i} \Delta z_i} \quad \text{for} \quad -D_2 - D_3 < z < \phi_{avg} \quad (4.46)$$

$$q_{d,3,i} = q_{d,3} \frac{k_{h,i} \Delta z_i}{\sum_{i_{z=\phi_{avg}}}^{i_{z=-D_3}} k_{h,i} \Delta z_i} \quad \text{for} \quad -D_3 < z < \phi_{avg} \quad (4.47)$$

where $k_{h,i}$ is the horizontal conductivity (cm d^{-1}) of compartment i , Δz_i is the thickness (cm) of compartment i , and $i_{z=-D_1-D_2-D_3}$ and $i_{z=\phi_{avg}}$ are resp. the numbers of the bottom compartment and the compartment in which the regional groundwater level is situated. Water quality models such as ANIMO (Rijtema et al., 1997) compute the average concentration of discharge water which flows to a certain order drainage system on the basis of these lateral fluxes. The averaging rules are:

$$\bar{c}_1 = \frac{\sum_{i_z=D_1-D_2-D_3}^{i_z=D_1-D_2-D_3} q_{d,1,i} c_i}{q_{d,1}} \quad (4.48)$$

$$\bar{c}_2 = \frac{\sum_{i_z=D_2-D_3}^{i_z=D_2-D_3} q_{d,2,i} c_i}{q_{d,2}} \quad (4.49)$$

$$\bar{c}_3 = \frac{\sum_{i_z=D_3}^{i_z=D_3} q_{d,3,i} c_i}{q_{d,3}} \quad (4.50)$$

Using these average concentrations computed by a leaching model, the average concentration c_R at the scale of a sub-region is calculated as:

$$\bar{c}_R = \frac{q_{d,1} \bar{c}_1 + q_{d,2} \bar{c}_2 + q_{d,3} \bar{c}_3}{q_{d,1} + q_{d,2} + q_{d,3}} \quad (4.51)$$

4.3.3 Maximum depth of a discharge layer

For the purpose of water quality simulations, the thickness of a model discharge layer has to be limited to a certain depth. In the water quality model, the maximum thickness D of a discharge layer has been set at:

$$D \leq \frac{L}{4} \quad (4.52)$$

This rule of thumb is based on the assumption of a half-circular shape of streamlines in a flow field (Figure 22). The deepest streamline which arrives in the drain, originates from a point at distance $L/2$. It can be seen that following to the circular shape, the horizontal distance $L/2$ corresponds to the length $2D$.

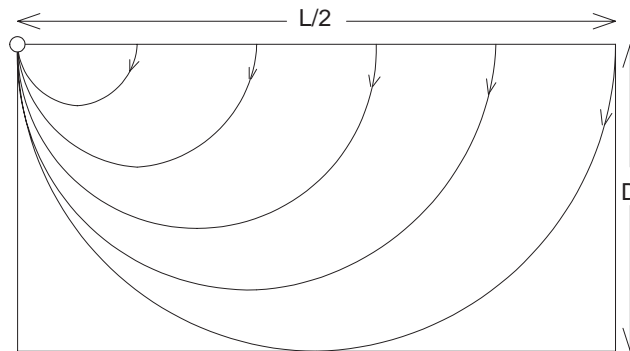


Figure 22 Flow field to a drain with half circular shaped stream lines

Homogeneous anisotropic soil profile

In the saturated zone, the horizontal permeability is often larger than the vertical permeability. General assumptions to deal with the transformation of the anisotropic conditions of a two-dimensional flow field are:

- hydraulic heads and flow rates are the same as in an isotropic situation
- x-coordinate: $x' = x \sqrt{(k_v/k_h)}$
- z-coordinate: $z' = z$
- permeability: $k' = \sqrt{(k_v k_h)}$

where the primes denote the transformed values of an anisotropic condition. Applying these assumptions to the relation between thickness of the discharge layer D and the horizontal drain distance L yields:

$$D' \leq \frac{L'}{4} \quad \Rightarrow \quad D \leq \frac{L}{4} \sqrt{\frac{k_v}{k_h}} \quad (4.53)$$

At first sight, this condition does not agree with the ‘penetration depth’ derived by Zijl and Nawalany (1993) for the estimation of the order of magnitude of the characteristic depth of the flow problem in case of a single layer model. However, these authors consider the wave length of an assumed sinusoidal shaped phreatic head. This assumption does not hold for most of the flow systems where only 1 or 2% of the area shows an upward discharge flux at the phreatic level. Transforming the wave length variable given by Zijl and Nawalany (1993) to the characteristic distance relevant for drainage systems ($L/2$) and taking into account the sinusoidal function can fully explain the difference between Eq. (4.53) and the ‘penetration depth’.

Heterogeneous anisotropic soil profile

For heterogeneous soil profiles, an average value for the anisotropic factor $\sqrt{(k_v/k_h)}$ has to be considered. The average horizontal and vertical conductivity is calculated as:

$$\overline{k_h} = \frac{\sum_{i_z=\phi_{avg}}^{i_z=D_1-D_2-D_3} k_{h,i} \Delta z_i}{\sum_{i_z=\phi_{avg}} \Delta z_i} \quad (4.54)$$

$$\overline{k_v} = \frac{\sum_{i_z=\phi_{avg}}^{i_z=D_1-D_2-D_3} \Delta z_i}{\sum_{i_z=\phi_{avg}} \frac{\Delta z_i}{k_{v,i}}} \quad (4.55)$$

and the maximum depth of the discharge layer bottom:

$$D \leq \frac{L}{4} \sqrt{\frac{\overline{k_v}}{\overline{k_h}}} \quad (4.56)$$

The assumption of cylindrical shaped streamlines is an abstraction of the actual streamline pattern. The condition ($D \leq L/4$) based on this model assumption is most relevant at large D/L ratios. Ernst (1973) provides a mathematical formulation of a streamline pattern in a

saturated soil profile of infinite thickness. Such a hydrological situation can be seen as the most extreme situation for evaluating the influence of the D/L-ratio. In reality, the drainage flow will occupy less space in the saturated groundwater body and the flow paths will be less deep. The streamlines can be described as:

$$\psi(x, z) = \frac{q_0}{\pi} \arctan \left(\frac{e^{\frac{-2\pi L}{L} \sin\left(\frac{2\pi x}{L}\right)} - 1}{e^{\frac{-2\pi L}{L} \cos\left(\frac{2\pi x}{L}\right)} - 1} \right) \quad (4.57)$$

where $\psi(x, z)$ is the stream function and q_0 is the discharge flow rate which originates from the area between $x=0$ en $x=L/2$. The streamline pattern is shown graphically in Figure 23, where the water enters the groundwater body along the line $z=0$ and the water is discharged by a drain at $(0,0)$.

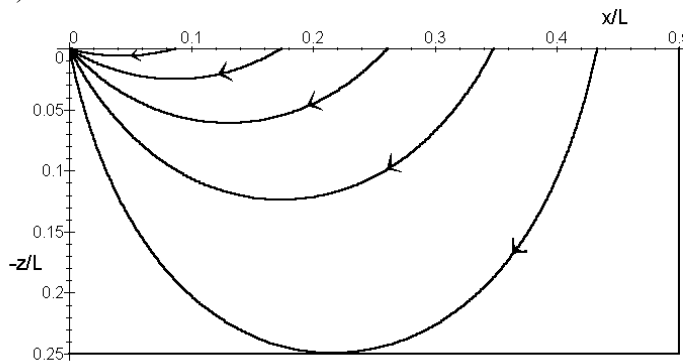


Figure 23 Stream line pattern in a groundwater system of infinite thickness

The majority of the precipitation surplus does not reach the line at depth $-z/D=0.25$. In this soil column, imaginary horizontal planes at $z=-D$ can be considered. The streamline with its deepest point at $-z/D=1$, but not intersecting the line $z=-D$, bounds the stream zone which will never be found below $z=-D$. The following condition holds for the streamline with its tangent-line at $z=-D$:

$$\frac{\partial \psi(x, D)}{\partial x} = 0 \quad (4.58)$$

Evaluation of this expression yields a value for the horizontal coordinate of the point of contact between the streamline and the line $z=-D$. Together with the value $z=-D$, the horizontal distance can be substituted into the general stream function equation. This action yields a flow fraction ψ/q_0 of the total drainage discharge which will never be found below the line $z=-D$. The depth has been transformed to a fraction of the drain distance to summarize all possible relations into one graph.

In a soil profile with infinite thickness, about 87% of the total drain discharge is conveyed above the plane at $z=-L/4$. In a deep soil profile with finite thickness, more than 87% of the total drain discharge will be transported above this plane.

4.3.4 Concentrations of solute in drainage water

The discharge layer approach assumes a uniform function of the lateral flux intensity with depth. Therefore, the vertical flux as a function of depth for a single drainage system can be described by a linear relation:

$$q(z) = \varepsilon \frac{dz}{dt} = \left(1 + \frac{z}{D}\right) q_{\text{drain}} + q_{\text{bot}} \quad (4.59)$$

where ε is the soil porosity (-), q the vertical flux (cm d^{-1}) and q_{bot} the vertical flux across the lower boundary of the soil profile. The relations hold between the phreatic level at $z = \phi_{\text{avg}}$ and the lower boundary at $z = -D$ (m). This equation can be used to derive the residence time T (d) as a function of depth, provided $t = T_0$ at $z = \phi_{\text{avg}}$:

$$T = T_0 + \frac{\varepsilon D}{q_{\text{drain}}} \ln \left(\frac{q(\phi_{\text{avg}})}{q(z)} \right) \quad (4.60)$$

Streamlines can be described mathematically by a stream function. For a two-dimensional transect between parallel drains, assuming a zero flux at the bottom of the aquifer and a negligible radial flow in the vicinity of the drains, the stream function $\psi(x,z)$ can be given as a function of depth z and distance x relative to the origin at the bottom of the aquifer, as depicted in Figure 24:

$$\psi(x,z) = -\frac{R}{D} x(D+z) \quad (4.61)$$

where R is the net recharge and D is the thickness of the homogeneous layer.

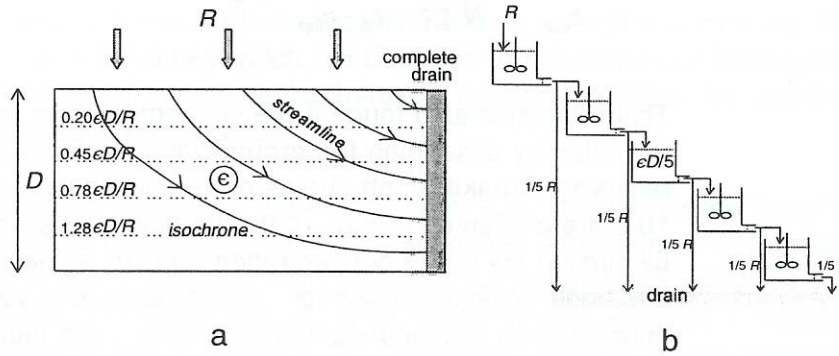


Figure 24 (a) Streamlines and isochrones of a soil profile with complete drains and (b) schematization of the flow pattern by a cascade of perfectly mixed reservoirs

Construction of isochrones for solute displacement after uniform infiltration at the phreatic level yields horizontal lines, because the vertical fluxes do not depend on the horizontal distance relative to the origin. In the model, the isochrones are regarded as imaginary boundaries between soil layers.

Each of the soil layers may be regarded as a perfectly mixed reservoir. Part of the inflow is conveyed to underlying soil layers, the remainder flows horizontally to the water course or drainage tube. Assuming a steady state situation and equal distances between the soil layers, the displacement of a non-reactive solute through this system may be described by a set of linear differential equations. For the first reservoir, the following equation applies:

$$\frac{\varepsilon D}{N} \frac{dc_1}{dt} = Rc_{\text{inp}} - Rc_1 \quad (4.62)$$

where N is the number of soil layers and c_{inp} is the input concentration. For an arbitrary reservoir i , the change in concentration is described by:

$$\frac{\varepsilon D}{N} \frac{dc_i}{dt} = \frac{N-i+1}{N} Rc_{i-1} - \frac{N-i+1}{N} Rc_i \quad (4.63)$$

Assuming an initial concentration c_0 uniform over the entire depth, the solution to the differential equations yields the concentration course over time in reservoir j :

$$\frac{c_j(t) - c_{\text{inp}}}{c_0 - c_{\text{inp}}} = \sum_{i=1}^j \binom{N}{i-1} \binom{N-i}{j-i} (-1)^{i+1} e^{-\frac{(N-i+1)Rt}{\varepsilon D}} \quad (4.64)$$

Since the outflows of all reservoirs are assumed to be equal, the resulting concentration in drainage discharge can be found as the average of all reservoirs. Lengthy, but straight forward algebraic summation of the binomial series in Eq. (4.63) yields a simple relation for the concentration in drainage water:

$$\frac{c_d(t) - c_{\text{inp}}}{c_0 - c_{\text{inp}}} = \frac{1}{N} \sum_{j=1}^N \frac{c_j(t) - c_{\text{inp}}}{c_0 - c_{\text{inp}}} = e^{-\frac{Rt}{\varepsilon D}} \quad (4.65)$$

This relation is also found if the concentration in the drainage water is modelled by describing the groundwater system as one perfectly stirred reservoir. Breakthrough curves of the individual reservoirs as denoted in Figure 24 are presented in Figure 25. The flow

averaged concentration (indicated by circles) fits to the concentration relation for the single reservoir approach. Overall effects of vertical dispersion which are introduced by defining distinct soils layers can thus be described by using one single reservoir. For the single drainage system, the simulation of solute migration by describing a vertical column with uniform lateral outflow agrees with the solutions found by Gelhar and Wilson (1974), Raats (1978) and Van Ommen (1986).

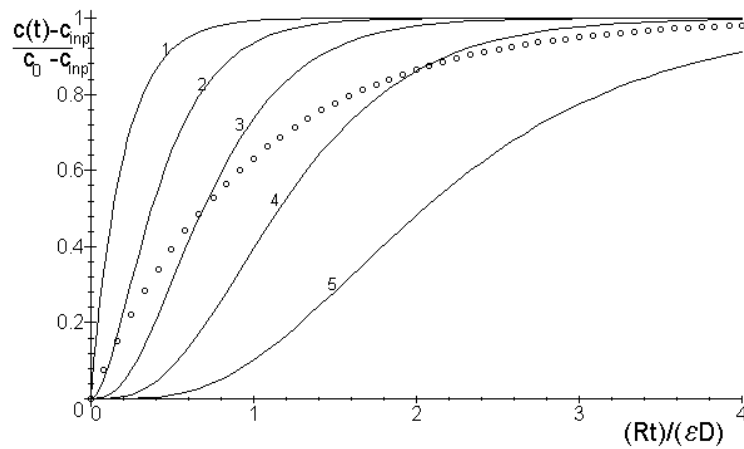


Figure 25 Step response of outflow concentrations per soil layer (numbered lines) and step response of the averaged concentration which enters the drains (circles)

4.3.5 Discussion

As a consequence of a number assumptions and schematization of the flow pattern, the model user should be aware of the following limitations:

- assumption of steady state during the time increment;
- constant depth of the drainage base;
- assumption of perfect drains;
- uniform thickness of the hydrological profile.

In most of the applications of the regional water quality model, the time step is set at 1 day up to 10 days. During an interval of 10 days, the drainage flux may vary as a result of variation of the meteorological conditions. For chemical substances which are bounded in the upper soil layers, the assessment of the solute discharge to the surface water may lead to considerable inaccuracies.

The boundary between the groundwater flow affected by the 'local' drainage system and the regional flow can be defined as the depth in the soil profile below which no direct discharge to surface water occurs (Figure 19). Above this depth, the larger part of the precipitation surplus flows to water courses and other drainage systems. This boundary depends on the deepest streamline discharging water to the drainage systems. It can be expected that the size of the subregion influences the depth of the boundary surface. With larger schematized areas, discharge water can originate from greater distances, having deeper streamlines. The influence of the seasonal variation of trans-boundary fluxes at the lower boundary of the modelled soil profile is not considered.

The uniform distribution of the lateral flux pattern is based on the assumption of perfect drains. In reality, the flow pattern converges in the surrounding area of the drain. The soil profile has a uniform depth. When the height difference between maximum groundwater level and drainage level is larger than a certain fraction of the depth of the saturated profile, this assumption may not be valid. In theory, these effects can be simulated by defining a correction function for the lateral flux relation with depth. From the point of view of data acquisition and validation of hydro-geological parameters, refinement of this relationship is questionable.

The Dupuit-assumption has been applied implicitly by assuming horizontal discharge layers. The discharge layer which corresponds to the channel system has been defined as a horizontal layer at the bottom of the local flow system. In reality, the water discharging to canals at larger distances infiltrates into the saturated zone. This water takes up some space in the upper zone of the groundwater system. A way to validate the 'discharge layer' approach presented above is by comparing a set of simulation results with the outcome of three dimensional streamline models at regional scale.

5 Soil water – groundwater interaction

J.G. Kroes, J.C. van Dam

5.1 Introduction

In the unsaturated zone water flow and solute transport occur mainly in the vertical direction. Once in the saturated zone, water starts to move in a three dimensional pattern, following the prevailing pressure gradients. The bottom boundary of the one-dimensional SWAP is either in the unsaturated zone or in the upper part of the saturated zone where the transition takes place to three-dimensional groundwater flow.

At the lower boundary we can define three types of conditions:

- Dirichlet condition, the pressure head h is specified;
- Neumann condition, the flux q is specified;
- Cauchy condition, the flux depends on the groundwater level.

The *Dirichlet* condition is a prescribed pressure head, often as a recorded phreatic surface of a present groundwater table.

The *Neumann* condition is usually applied when a no-flow boundary (e.g. an impermeable layer) can be identified, or in case of a deep groundwater table, resulting in free drainage.

The *Cauchy* condition is used when unsaturated flow models are combined with models for regional groundwater flow or when effects of surface water management are to be simulated. The relation between flux and groundwater level can be obtained from drainage formulae (see Par. 4.2.2) and/or from regional groundwater flow models (e.g. Van Bakel, 1986).

SWAP offers eight options to prescribe the lower boundary condition (Table 3), which each have their typical scale of application.

Table 3. Eight options for the lower boundary condition

| Lower boundary condition (input switch SwBotb) | Description | Type of condition | Typical scale of application |
|--|---|-------------------|------------------------------|
| 1 | Prescribe groundwater level | Dirichlet | field |
| 2 | Prescribe bottom flux (q_{bot}) | Neumann | region |
| 3 | Calculate bottom flux from hydraulic head of deep aquifer | Cauchy | region |
| 4 | Calculate bottom flux as function of groundwater level | Cauchy | region |
| 5 | Prescribe soil water pressure head of bottom compartment | Cauchy | field |
| 6 | Bottom flux equals zero | Neumann | field |
| 7 | Free drainage of soil profile | Neumann | field |
| 8 | Free outflow at soil-air interface | Neumann | field |

In case of options 1, 2, 3, 5 and 6, in addition to the bottom flux (q_{bot}), a drainage flux (q_{drain}) can be defined (Par. 4.2). In case of option 4 the lower boundary includes drainage to local ditches or drains so q_{drain} should not be defined separately. In case of options 7 and 8, the simulated soil profile is unsaturated, so lateral drainage will not occur.

5.2 Field scale

When the model is applied at field scale with locally known/measured data, the following 5 options are commonly applied:

- Prescribe groundwater level (SwBotB = 1)
- Prescribe soil water pressure head of bottom compartment (SwBotB = 5)
- Bottom flux equals zero (SwBotB = 6)
- Free drainage of soil profile (SwBotB = 7)
- Free outflow at soil-air interface (SwBotB = 8)

Prescribed water levels (ϕ_{avg}) are given as a function of time. This groundwater level represents a field average groundwater level. For days with unknown values a linear interpolation occurs between the days with known values. The main advantage of this boundary condition is the easy recording of the phreatic surface in case of a present groundwater table. A drawback is that at shallow groundwater tables the simulated phreatic surface fluctuations are very sensitive to the soil hydraulic functions. This condition may result in strong fluctuations of the water fluxes across the lower boundary, which may not be desirable. Especially when the output of the Swap model is used as input in water quality calculations, it is generally recommended to use another type of lower boundary condition.

| <i>Model input</i> | | | |
|----------------------|---------|---|----------------|
| <i>Variable Code</i> | | <i>Description</i> | <i>Default</i> |
| ϕ_{avg} | GWLEVEL | Groundwater level as function of time (cm below soil surface) | - |

Prescribed soil water pressure heads of bottom compartment (h_n) are input to the model and. The soil water pressure head is assigned to the lowest compartment. For days with unknown values a linear interpolation occurs between the days with known values.

| <i>Model input</i> | | | |
|----------------------|-------|--|----------------|
| <i>Variable Code</i> | | <i>Description</i> | <i>Default</i> |
| h_n | HOBTS | Soil water pressure head of bottom compartment as function of time (cm)- | |

A *bottom flux* (q_{bot}) of zero may be applied when an impervious layer exists at the bottom of the profile. This option is implemented with a simple switch, which forces q_{bot} to zero.

In case of *free drainage of a soil profile*, unit gradient is assumed at the bottom boundary and the bottom flux depends directly from the hydraulic conductivity of the lowest compartment:

$$\frac{\partial H}{\partial z} = 1 \quad \text{thus: } q_{\text{bot}} = -K_n \quad (5.1)$$

In case of *free outflow at soil-air interface*, drainage will only occur if the pressure head in the bottom compartment (h_n) increases until above zero. During drainage and after a drainage event, h_n is set equal to zero and q_{bot} is calculated by solving the Richards' equation. This option is commonly applied for lysimeters, where outflow only occurs when the lowest part of the lysimeter becomes saturated.

5.3 Regional scale

At regional scale the lower condition will generally be used describe the interaction with a regional groundwater system. In these cases 3 options are common:

- Prescribe bottom flux (SwBotB = 2)
- Calculate bottom flux from hydraulic head of deep aquifer (SwBotB = 3)
- Calculate bottom flux as function of groundwater level (SwBotB = 4)

Prescribed bottom flux

In this case the bottom flux (q_{bot}) is input to the model and should be given as a function of time. For days with unknown values a linear interpolation occurs between the days with known values. This option has a similar disadvantage as previously described option with the prescribed groundwater level. When a mismatch occurs between boundary conditions and soil physical properties the result may be a continuously declining or increasing groundwater level. Especially when the output of the Swap model is used as input in water quality calculations, it is generally recommended to use another type of lower boundary condition.

| <i>Model input</i> | | |
|--------------------------------|--|----------------|
| <i>Variable Code</i> | <i>Description</i> | <i>Default</i> |
| SW2 | Switch for kind of input: as sinus or as table | |
| When SW2=1: | | |
| SINAVE | Average value of bottom flux (cm d ⁻¹) | - |
| SINAMP | Amplitude of bottom flux (cm d ⁻¹) | - |
| SINMAX | Time of the year with maximum value of bottom flux (daynr from Jan 1)- | |
| When SW2=2 then enter a table: | | |
| q_{bot} | QBOT2 Average value of bottom flux (cm d ⁻¹) | - |

Calculate bottom flux from hydraulic head of deep aquifer

This Par. discusses how a Cauchy condition may be applied to determine the bottom boundary flux q_{bot} , starting from a given hydraulic head of a deep aquifer.

To illustrate this option Figure 26 shows a soil profile which is drained by ditches and which receives a seepage flux from a semi-confined aquifer. SWAP makes a distinction

between the local drainage flux to ditches and drains q_{drain} , as calculated according to chapter 4, and the bottom flux due to regional groundwater flow, q_{bot} .

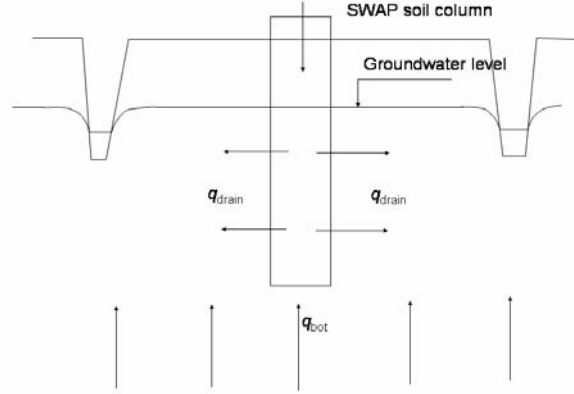


Figure 26 Pseudo two-dimensional Cauchy lower boundary conditions, in case of drainage to ditches and seepage from a deep aquifer

The bottom flux q_{bot} depends on the average groundwater level, the hydraulic head in the semi-confined aquifer, and the resistance of the semi-confining layer. The bottom flux q_{bot} is calculated by:

$$q_{bot} = \frac{\phi_{aquif} - \phi_{avg}}{c_{conf}} \quad (5.2)$$

where ϕ_{aquif} is the hydraulic head in the semi-confined aquifer (cm), ϕ_{avg} is the average groundwater level, and c_{conf} is the semi-confining layer resistance (d).

The hydraulic head in the aquifer may be prescribed using a sinusoidal wave:

$$\phi_{aquif} = \phi_{aquif,m} + \phi_{aquif,a} \cos\left(\frac{2\pi}{\phi_{aquif,p}}(t - t_{max})\right) \quad (5.3)$$

where $\phi_{aquif,m}$, $\phi_{aquif,a}$, and $\phi_{aquif,p}$ are the mean (cm), amplitude (cm) and period (d) of the hydraulic head sinus wave in the semi-confined aquifer, and t_{max} is a time (d) at which ϕ_{aquif} reaches its maximum.

The average phreatic head, ϕ_{avg} (cm), is calculated as:

$$\phi_{avg} = \phi_{drain} + \beta_{gwl} (\phi_{gwl} - \phi_{drain}) \quad (5.4)$$

with ϕ_{drain} is the hydraulic head of the drain (cm) and β_{gwl} the groundwater shape factor (-). Possible values for β_{gwl} are 0.66 (parabolic), 0.64 (sinusoidal), 0.79 (elliptic) and 1.00 (no drains).

| <i>Model input</i> | | | |
|-------------------------------------|---------------|---|----------------|
| <i>Variable Code</i> | | <i>Description</i> | <i>Default</i> |
| β_{gwl} | <i>SHAPE</i> | Shape factor to derive average groundwater level (-) | 1.0 |
| ϕ_{drain} | <i>HRAIN</i> | Mean drain base to correct for average groundwater level (cm) | - |
| c_{conf} | <i>RIMLAY</i> | Vertical resistance of aquitard (d) | - |
| - | <i>SW3</i> | Switch for kind of input: as sinus or as table | - |
| When SW3=1 then enter a sinus wave: | | | |
| $\phi_{\text{aquif,m}}$ | <i>AQAVE</i> | Average value of hydraulic head in underlying aquifer (cm) | - |
| $\phi_{\text{aquif,a}}$ | <i>AQAMP</i> | Amplitude of hydraulic head sinus wave (cm) | - |
| t_{max} | <i>AQTMAX</i> | First time of the year with maximum hydraulic head (daynr from Jan 1) | - |
| $\phi_{\text{aquif,p}}$ | <i>AQPER</i> | Period hydraulic head sinus wave (d) | - |
| When SW3=2 then enter a table: | | | |
| ϕ_{aquif} | <i>HAQUIF</i> | Average value of hydraulic head in underlying aquifer (cm) | - |

Calculate bottom flux as function of groundwater level

Calculate q_{bot} from an exponential flux - average groundwater relationship, which is valid for deep sandy areas:

$$q_{\text{bot}} = a_{\text{qbot}} e^{b_{\text{qbot}}|\phi_{\text{avg}}|} \quad (5.5)$$

where a_{qbot} (cm d^{-1}) and b_{qbot} (cm^{-1}) are empirical coefficients. For additional data of q_{bot} - ϕ_{avg} relationships, see Massop and De Wit (1994).

| <i>Model input</i> | | | |
|----------------------|---------------|--------------------------------------|----------------|
| <i>Variable Code</i> | | <i>Description</i> | <i>Default</i> |
| a_{qbot} | <i>COFQHA</i> | Coefficient A (cm d^{-1}) | - |
| b_{qbot} | <i>COFQHB</i> | Coefficient B (cm^{-1}) | - |

6 Soil heterogeneity

J.C. van Dam, R.F.A. Hendriks

6.1 Introduction

In many cases SWAP is used at field scale level, which can be viewed as a natural basic unit of larger regions. Most natural or cultivated fields have one cropping pattern, soil profile, drainage condition and management scheme. This information comes increasingly available in geographical data bases. Geographical information systems can be used to generate input data for field scale models, to run these models for fields with unique boundary conditions and physical properties, and to compile regional results of viable management scenarios. The regional scale is of most interest to water managers and politicians. In order the use SWAP at field scale level, we should consider the natural soil heterogeneity within a field. SWAP has options to accommodate hysteresis in the retention function, spatial variability of soil hydraulic functions, preferential flow in water repellent soils and in soils with macropores.

6.2 Hysteresis

Hysteresis refers to non-uniqueness of the $\theta(h)$ relation and is caused by variations of the pore diameter (inkbottle effect), differences in radii of advancing and receding meniscus, entrapped air, thermal gradients and swelling/shrinking processes (Hillel, 1980; Feddes et al., 1988). Gradual desorption of an initially saturated soil sample gives the main drying curve, while slow absorption of an initially dry sample results in the main wetting curve. In the field partly wetting and drying occurs in numerous cycles, resulting in so-called drying and wetting scanning curves lying between the main drying and the main wetting curves (Figure 27).

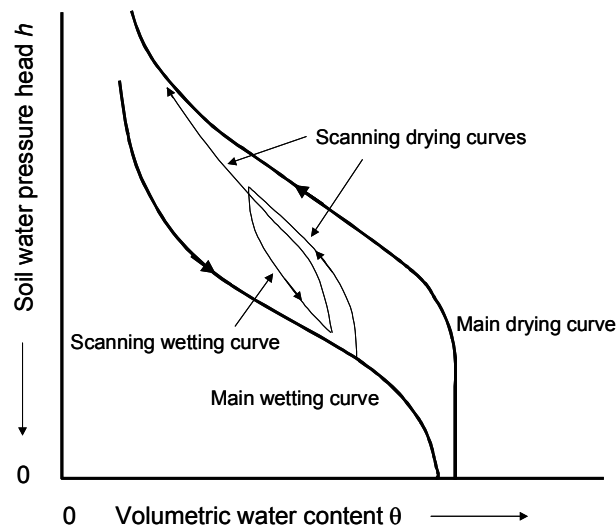


Figure 27 Water retention function with hysteresis, showing the main wetting, main drying and scanning curves

In simulation practice, often only the main drying curve is used to describe the $\theta(h)$ relation. This is mainly due to the time and costs involved in measurement of the complete $\theta(h)$ relationship, including the main wetting, the main drying and the scanning curves, especially in the dry range. For instance, a generally applied soil hydraulic data base in The Netherlands, known as the Staring series (Wösten et al., 1994), contains only $\theta(h)$ data of the main drying curve. Nevertheless, it is obvious that the simulation of infiltration events with the main drying curve can be inaccurate. Kaluarachchi and Parker (1987) showed that during infiltration the type of boundary condition at the soil surface determines the effect of hysteresis. A head-type boundary condition at the soil surface has more influence than a flux-type boundary condition. Dirksen (1987) could not explain his detailed experimental data on root water uptake in saline conditions without taking into account hysteresis. Hopmans et al. (1991) showed in case of trickle and furrow irrigation that hysteresis affects the water balance, although these effects were overwhelmed by spatial variability of the soil hydraulic functions.

To circumvent the tedious laboratory analysis, empirical hysteresis models with a limited number of parameters have been developed. Jaynes (1984) compared four of these models, which use the main wetting and main drying curve to generate scanning curves. None of the models was consistently better than the others for simulating primary wetting or drying curves for three test soils. Also each model performed equally well when used as part of a numerical model for simulating hysteretic flow. Scott et al. (1983) derived scanning curves by rescaling the main wetting or the main drying curve to the actual water content. Among others, Kool and Parker (1987) obtained acceptable results with Scott's method in the case of eight soils. The scaling method of Scott has been implemented into SWAP.

The main drying and main wetting curve should be measured in the laboratory and are described analytically with the Mualem-van Genuchten parameters (α , n , θ_{res} , θ_{sat} , K_{sat} , and λ) according to Eqs. (2.20) and (2.22). Some of the parameters describing the main wetting and main drying curve are related. We will assume θ_{res} and θ_{sat} to be equal for both curves. In general θ_{sat} will be somewhat less than porosity due to air entrapment under field conditions with intensive rainfall. Usually the $K(\theta)$ function shows only minor hysteresis effects. As Eq. (2.22) shows, this can be achieved by choosing for the main wetting and main drying curve a common value for n . Ultimately the two curves only differ in the parameter α , as depicted in Figure 28.

The scanning curves are derived by linear scaling of either the main wetting or main drying curve, such that the scanning curve includes the current θ - h combination and approaches the main wetting curve in case of a wetting scanning curve and the main drying curve in case of a drying scanning curve.

Figure 28A shows the scaling principle in case of a drying scanning curve. Based on its wetting and drying history, at a certain time and depth the soil shows an actual water content θ_{act} at the soil water pressure head h_{act} . The valid drying scanning curve should pass through the point (θ_{act}, h_{act}) , and approach the main drying curve at smaller water contents. We may define θ_{md} as the water content of the main drying curve at h_{act} , and θ_{sat}^* as the saturated water content of the drying scanning curve. Linear scaling of the main drying curve with respect to the vertical axis $\theta = \theta_{res}$ gives (Figure 28A):

$$\frac{\theta_{sat}^* - \theta_{res}}{\theta_{sat} - \theta_{res}} = \frac{\theta_{act} - \theta_{res}}{\theta_{md} - \theta_{res}} \Rightarrow \theta_{sat}^* = \theta_{res} + (\theta_{sat} - \theta_{res}) \frac{\theta_{act} - \theta_{res}}{\theta_{md} - \theta_{res}} \quad (6.1)$$

The only unknown in Eq.(6.1) is θ_{sat}^* , which can be directly solved. The drying scanning curve is accordingly described with the parameters $(\alpha_{dry}, n, \theta_{res}, \theta_{sat}^*)$. As long as the soil keeps drying, this drying scanning curve is valid.

The opposite occurs when the soil gets wetter. Again we start from the arbitrary actual water content θ_{act} at the soil water pressure head h_{act} , and now define θ_{mw} as the water content of the main wetting curve at h_{act} , and θ_{res}^* as the residual water content of the wetting scanning curve.

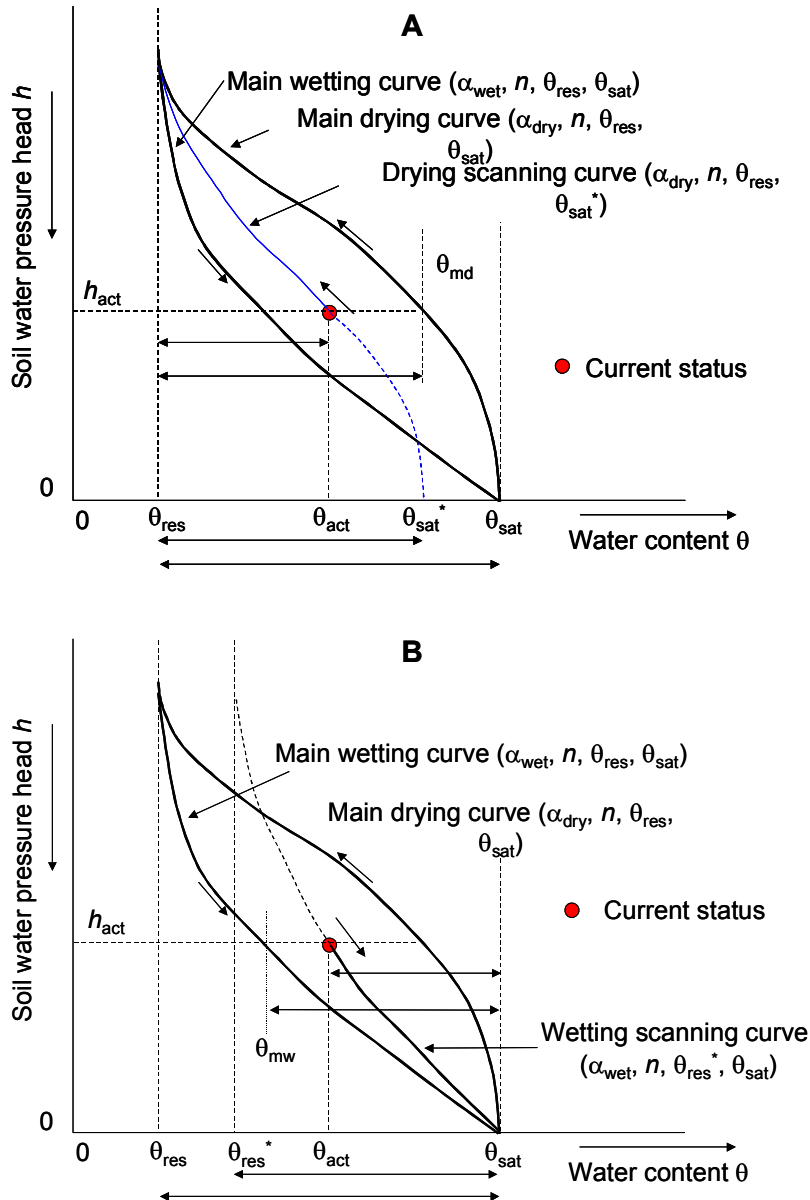


Figure 28 (A) Linear scaling of the main drying water retention curve in order to derive a drying scanning curve; (B) Linear scaling of the main wetting water retention curve in order to derive a drying wetting curve.

Linear scaling of the main wetting curve with respect to the vertical axis $\theta = \theta_{\text{sat}}$ gives (Figure 28B):

$$\frac{\theta_{\text{sat}} - \theta_{\text{res}}^*}{\theta_{\text{sat}} - \theta_{\text{res}}} = \frac{\theta_{\text{sat}} - \theta_{\text{act}}}{\theta_{\text{sat}} - \theta_{\text{mw}}} \Rightarrow \theta_{\text{res}}^* = \theta_{\text{sat}} - (\theta_{\text{sat}} - \theta_{\text{res}}) \frac{\theta_{\text{sat}} - \theta_{\text{act}}}{\theta_{\text{sat}} - \theta_{\text{mw}}} \quad (6.2)$$

From Eq.(6.2), θ_{res}^* can be directly solved. The wetting scanning curve is accordingly described with the parameters $(\alpha_{\text{wet}}, n, \theta_{\text{res}}^*, \theta_{\text{sat}})$, and is valid as long as the soil keeps wetting. As the wetting-drying history is different at each soil depth, each node may show a different scanning curve. The unique $K(\theta)$ relation of a soil layer always follows from the parameter set $(n, \theta_{\text{res}}, \theta_{\text{sat}}, K_{\text{sat}}, \lambda)$ according to Eq. (2.22).

| <i>Model input</i> | | | |
|-----------------------|-------------|--|---|
| <i>Variable</i> | <i>Code</i> | <i>Description</i> | <i>Default</i> |
| α_{dry} | ALFA | shape parameter alfa of main drying curve (cm^{-1}) | |
| α_{wet} | ALFAW | shape parameter alfa of main drying curve (cm^{-1}) | $\alpha_{\text{wet}} = 2 \alpha_{\text{dry}}$ |
| | SWHYST | initial condition wetting or drying | drying |
| | TAU | minimum pressure head difference to change wetting-drying (cm) | 0.2 |

6.3 Scaling of soil hydraulic properties

6.3.1 Introduction

Most models of the unsaturated zone are one-dimensional. The hydrological and drainage problems that have to be modelled however, are two- or three-dimensional and thus have a spatial component, be it a local or a regional one. If the area is homogeneous in all its components, a point simulation is representative of an entire region. The soil however, is never homogeneous, but is subject to spatial variability. It is not feasible to model the actual heterogeneity in a deterministic way as this would require enormous amounts of data and too much computational effort (Hopmans and Stricker, 1989). As the flow and transport processes in the unsaturated zone are strongly non-linear, in general the mean input of soil hydraulic functions will deviate from the areal mean water and solute balance. Various theoretical frameworks have emerged to model water flow and solute transport in heterogeneous soils. The most important concepts are summarized below.

One option to deal with the variability of the soil hydraulic and transport parameters is to treat them as random variables. Spatial patterns of these parameters can be produced by drawing from the statistical distributions of the parameters. This method (distributed modeling) is computationally very demanding, since numerous fields have to be simulated to produce the mean and standard deviation of the variables of interest. A simpler approach is to assume vertical flow only (which is quite realistic for unsaturated flow) and view the field as a collection of non-interacting columns with variable properties but without horizontal variations (Bresler and Dagan, 1981). This greatly reduces calculation time.

The geometrically similar media scaling technique (Miller and Miller, 1956) is an efficient way to describe the variability of the soil hydraulic properties. In its simplest form, the

technique assumes that the $\theta(h)$ and $K(\theta)$ functions at any point in the field are linear transformations of those at any other point. This technique will be described in the next Par..

Another much used approach is to view the soil as a combination of two or more parallel, homogeneous flow domains with contrasting soil properties (multi-domain models). Flow is vertical in each domain. The solute behavior is the result of the size of each domain and the function that defines solute exchange between domains (usually a simple diffusion process). Even with simple exchange functions, this type of models can produce a wide variety of breakthrough curves (Van Genuchten and Wierenga, 1976; Gerke and Van Genuchten, 1993). In SWAP the mobile-immobile concept is employed to mimic this type of flow and transport in water repellent soil (Par. 6.4). The fast and slow soil water flow in case of cracked clay soils is approached in SWAP employing the shrinkage characteristic and macropore flow theory (Par. 6.5).

6.3.2 Similar media scaling

Miller and Miller (1956) used the concept of geometrically similar media to deduce macroscopic equations governing the viscous flow phenomena. They showed that the variability in both the $\theta(h)$ and $K(\theta)$ relation might be described by just one dimensionless scale factor. The scale factor ρ_i at a certain location i is equal to:

$$\rho_i = \frac{\lambda_i}{\lambda_{\text{ref}}} \quad (6.3)$$

where (see Figure 29) λ_i is a characteristic length at location i , and λ_{ref} is the same characteristic length of a reference soil. Then, applying theory of capillary retention, if the soil at location i and the reference soil have the same water contents, their pressure heads are related according to:

$$h_i = \frac{h_{\text{ref}}}{\rho_i} \quad (6.4)$$

Using Poiseuille's law and again at the same water content in both soils, the hydraulic conductivities are related as:

$$K_i = \rho_i^2 K_{\text{ref}} \quad (6.5)$$

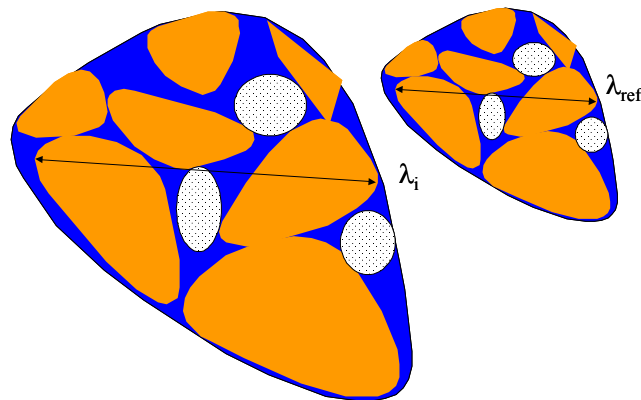


Figure 29 Characteristic lengths λ_i in geometrically similar media (Miller and Miller, 1956)

Natural soils will to some degree deviate from geometrically similar media. This is clear when we consider the saturated water content. If the similar media concept would apply strictly, the saturated water content should be the same for all soils. We know this is not the case. Jury et al. (1987) point out that due to dissimilarity, scaling of different soil properties, e.g. h and K , might result in different statistical properties of each scale factor's distribution. Youngs and Price (1981) measured microscopic characteristic lengths for porous materials ranging from glass beads and washed sands to sieved arable soils. They concluded that even for dissimilar soils the scaling concept is a good approximation.

In order to derive scale factors ρ_i and their statistical distribution, one should have $\theta(h)$ and $K(\theta)$ data of a series of soil samples. Clausnitzer et al. (1992) developed an efficient program for scaling $\theta(h)$ and $K(\theta)$ data of a series of soil samples. In their scaling approach, first a mean curve is fit to all the data available. Because natural soils don't have identical porosities, h and k are written as functions of the relative saturation $\theta/\theta_{\text{sat}}$ rather than as functions of the volumetric water content θ . In the second step, the corresponding set of scale factors is calculated for each soil sample. The scaled hydraulic data ($h_i\rho_i$ and K_i/ρ_i^2 , respectively) coalesce and allow an improved calculation of the mean curve. Therefore in the next step a new mean curve is fitted through the scaled hydraulic data, after which the scale factors are determined again. These steps are repeated until both the mean curve and the scale factors converge. Finally the stochastic distribution of the scale factors (generally log-normal), its mean and standard deviation are calculated.

Scaling is generally applied to determine the variability of the water balance components due to spatial variation of $\theta(h)$ and $K(\theta)$ (e.g. Peck et al., 1977; Hopmans and Stricker, 1989). SWAP will generate the water and solute balance for each scale factor that is provided. In areas without surface runoff, scaling might also be used to derive an equivalent curve for a field or a catchment (Feddes et al., 1993, Kim, 1995).

| <i>Model input</i> | | | |
|--------------------|-------------|--|----------------|
| <i>Variable</i> | <i>Code</i> | <i>Description</i> | <i>Default</i> |
| | NSCALE | number of scale factors and SWAP simulations (-) | |
| ρ_i | SOILI | NSCALE scale factors for each soil layer (-) | |

6.4 Mobile/immobile flow

6.4.1 Introduction

In field soils soil water may bypass large parts of the unsaturated soil domain. This phenomenon is generally called preferential flow and has a large effect on the leaching of nutrients, salts and pesticides to the saturated zone. Preferential flow can be caused by macropores in structured soils (Par. 6.5) or by unstable wetting fronts in unstructured soils that originate from soil layering, air entrapment and water repellency (Raats, 1973; Ritsema et al., 1993). In SWAP attention is paid to water repellency, which is attributed to organic coatings of soil particles, to organic matter and to specific micro flora. Water repellency is widespread in dry top soils and can be quantified by water drop penetration time tests (Krammes and DeBano, 1965; Dekker and Jungerius, 1990). More than 75 % of the

cropland and grassland top soils in the Netherlands are slightly to extremely water repellent, whereas more than 95 % of the top soils in nature reserves are strongly to extremely water repellent (Dekker and Ritsema, 1994).

De Rooij (1996) provides an overview of theories and experiments with respect to preferential flow due to water repellency. The same author performed an extensive lysimeter experiment which showed the large heterogeneity of water and solute fluxes at the 5 cm scale. De Rooij (1996) developed an analytical three region model, which could be applied to the collected lysimeter data, but which is less suitable for fields with transient flow and fluctuating groundwater levels. A large amount of field data and water repellency phenomena have been collected by Dekker (1998) and Ritsema (1998).

Numerically, flow in water repellent soil might be simulated with a dual-porosity model as has been used for macropores in structured soils (Gerke and Van Genuchten, 1993; Saxena et al., 1994). However, the water exchange between the mobile and immobile domains in the case of water repellent soils is difficult to simulate. Also field observations show a time dependent preferential flow path volume (Ritsema and Dekker, 1994) while dual-porosity models assume a constant volume of the preferential flow path. Another limitation of dual-porosity models is that they require twice as many soil physical parameters as single porosity models.

Another approach is the *mobile-immobile concept*. This concept has been used to explain accelerated breakthrough in the case of steady state solute transport (De Smedt and Wierenga, 1979; Van Genuchten and Wagenet, 1989). Van Dam et al. (1990, 1996) extended the mobile-immobile concept to both water flow and solute transport and to transient flow conditions. Their concept of preferential flow is easy to conceive, uses a limited number of physically based and easy to measure parameters (e.g. the soil volume fraction in which water is mobile), is applicable to transient flow conditions and can relatively easily be implemented in current one-dimensional soil water flow and solute transport codes. The concept has been applied to bromide tracer experiments in water repellent soils in lysimeters (Saxena et al., 1994) and in field soils (Van Dam et al. 1990, 1996). In the next Par.s we elaborate on the mobile-immobile concept for soil water fluxes and solute transport as implemented in SWAP.

6.4.2 Water flow

Usually in the laboratory, when measuring the retention function and the hydraulic conductivity curve, soil samples are first brought to saturation and during the experiment relatively long equilibrium times are allowed. These conditions suppress effects of water repellency. The soil hydraulic functions measured in the laboratory will be denoted as $\theta_{lab}(h)$ and $K_{lab}(h)$.

In the field, immobile soil domains may occur either as large, separate volumes (Figure 30) or as numerous small volumes corresponding to less accessible pores. We will assume that the soil hydraulic functions as measured in the laboratory are valid in the preferential flow domains. A second assumption is that the water content in the immobile region, θ_{im} ($\text{cm}^3 \text{cm}^{-3}$) remains constant in time. Then the bulk field water retention function $\theta_{bulk}(h)$ can be calculated as (Figure 30):

$$\theta_{\text{bulk}}(h) = F_{\text{mob}}\theta_{\text{lab}} + (1 - F_{\text{mob}})\theta_{\text{im}} \quad (6.6)$$

where F_{mob} equals the mobile fraction of the soil volume ($\text{cm}^3 \text{cm}^{-3}$) through which flow actually occurs. The factor F_{mob} can roughly be estimated by visual observation of dry and wet spots in the field shortly after precipitation, and more accurately with tracer colour tests, e.g. with iodide (Van Ommen et al., 1989b) or Brilliant Blue (Flury and Flühler, 1995), with a disc permeameter in combination with a tracer (Clothier et al., 1992), or by model calibration (Van Dam et al., 1990).

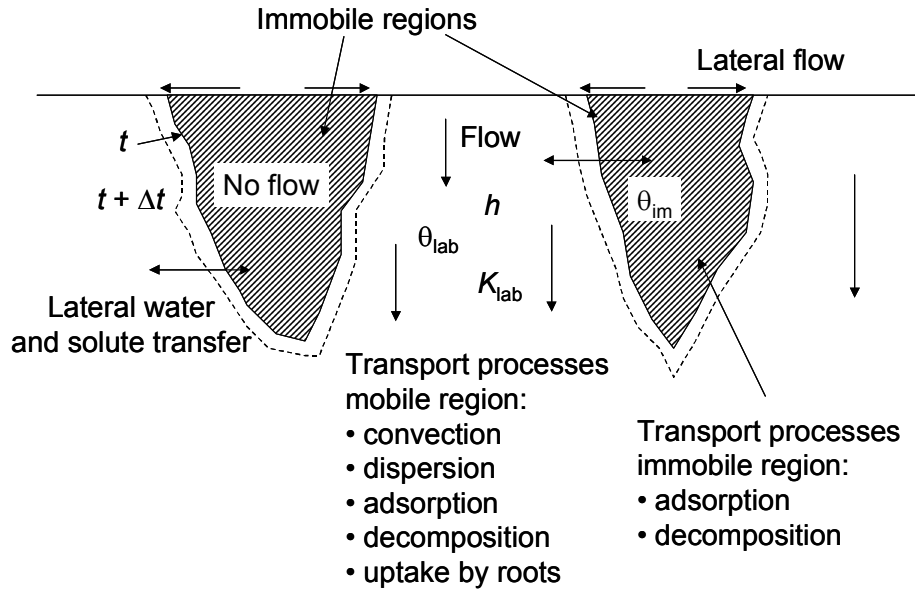


Figure 30 Schematization of mobile and immobile regions for flow and transport in water repellent soils

Richards' equation only applies to the mobile region. Therefore the effective retention function, which is used to solve Richards' equation, follows simply from:

$$\theta(h) = F_{\text{mob}}\theta_{\text{lab}}(h) \quad (6.7)$$

We may assume that the soil texture and the unsaturated hydraulic conductivity curves of the mobile and immobile regions are identical. In that case the soil water flux density q at a certain gradient $\partial H/\partial z$ will be reduced by the factor F_{mob} due to the reduction in flow domain. Thus, the effective field conductivity curve $K(h)$ which should be used in the solution of Richards' equation, is related to $K_{\text{lab}}(h)$ measured in the laboratory as:

$$K(h) = F_{\text{mob}}K_{\text{lab}}(h) \quad (6.8)$$

In this way the acceleration of soil water flow due to a smaller flow volume is taken into account. The time needed for some lateral soil water flow at depths where F_{mob} either increases or decreases with depth, is neglected. This convergent or divergent flow would require a more complicated three-dimensional analysis, as e.g. performed by De Rooij (1996).

Field studies (Ritsema and Dekker, 1994) show that the mobile fraction F_{mob} varies in time. In general, when the soil becomes wetter, F_{mob} increases. We might approximate this by a

linear relationship between $\log(-h)$ and F_{mob} . Notice that when the immobile regions contain water, variation of F_{mob} with h induces exchange of water between the mobile and immobile soil volumes (Figure 30). This exchange is included as an extra loss term G_w in the Richards' equation:

$$\frac{\partial \theta}{\partial t} = \frac{\partial \left[K \left(\frac{\partial h}{\partial z} + 1 \right) \right]}{\partial z} - S_a + \frac{\partial F_{\text{mob}}}{\partial t} \theta_{\text{im}} \quad (6.9)$$

where S_a the actual rootwater extraction rate (d^{-1}) and the last term in the right hand side of Eq. (6.9) accounts for the water amount transferred (d^{-1}) from the immobile to the mobile region.

| <i>Specify for each soil layer:</i> | | | |
|-------------------------------------|--------------------|--|----------------|
| <i>Variable Code</i> | <i>Description</i> | | <i>Default</i> |
| | PF1 | first $\log(-h)$ value (-) | 0.0 |
| F_{mob} | FM1 | mobile fraction at first $\log(-h)$ value (-) | 1.0 |
| | PF1 | second $\log(-h)$ value (-) | 3.0 |
| F_{mob} | FM2 | mobile fraction at second $\log(-h)$ value (-) | 1.0 |
| θ_{im} | THETIM | volumetric water content in immobile soil volume | 0.0 |

6.5 Macropore flow

6.5.1 Introduction

In structured soils (clay and peat soils), flow occurs preferential through large pores or macropores in the unsaturated soil matrix, a process known as 'bypass flow' or 'short-circuiting' (Hoogmoed and Bouma, 1980). Due to the very rapid flow through these macropores solutes can reach large depths almost immediately after the start of a shower, bypassing the capacity of the soil matrix for storage, adsorption and transformation of potential pollutants. This macroporosity can be caused by shrinking and cracking of soil, by plant roots, by soil fauna, or by tillage operations. Because macropores may have a large impact on water flow and solute transport through the vadose zone they should be included in generally applied agrohydrologic models like SWAP. Empirical models incorporating the bypass through macropores in a simplified way can be calibrated for specific soil samples or fields. However, because of their empirical character, the use of these models for predictive purposes is limited. Models that simulate the general physical processes are more reliable for use in scenario studies. Unfortunately, detailed simulation of the physical transport processes in cracked and macroporous soils is not feasible, as the chaotic and dynamic morphology of each location would require a huge amount of data. We may therefore search for some systematic behaviour on a larger scale, in the same way as Darcy's law incorporates complicated, unpredictable pore geometry at a scale where a continuum of water, solid material and air applies. In experimental fields with cracked clay, various locations show at the same soil depth a large variability of water contents and solute concentrations (Beven and Germann, 1982; Bronswijk et al., 1995). Instead of trying to describe water flow and solute transport at the various locations, the field average behaviour

might be more easy to catch in a model. In order to make the model suitable for process and scenario analysis, concepts should be used that are generally applicable, thus physically based. Furthermore, model calibration requires a limited number of parameters, and preferably parameters that can be measured directly in the field.

The importance of shrinkage cracks was already shown by Bronswijk, who implemented a concept for preferential flow through shrinkage cracks in the FLOCR model (Bronswijk, 1988). A modified version of this concept was implemented in SWAP by Van Dam (2000) and is included in this version of SWAP as option 1 for macropore flow: Simple macropore flow (Par. 6.5.2). Hendriks et al. (1999) showed the importance of permanent or static macropores (e.g. structural cracks, worm and root holes) beside the dynamic shrinkage cracks, with an extended version of the macropore concept of FLOCR. An adapted version of this more general concept for macropore flow is now implemented in this version of SWAP as option 2 for macropore flow: Advanced macropore flow (Par. 6.5.3). This option is yet in the testing phase and therefore still under construction.

6.5.2 Simple macropore flow

6.5.2.1 Introduction

In the simple macropore flow model shrinkage cracks are the sole macropores that are considered. The shrinkage characteristic is used to describe the swelling and shrinking of a clay soil, including its crack volume and crack depth. Water flow and solute transport are described with basic physics, employing ordinary numerical procedures. The model concept was developed to simulate the field average behaviour of a field with cracks, rather than the flow and transport at a single plot. Van Dam (2000) applied the model to an extensive field experiment, which was performed and described by Bronswijk et al. (1995).

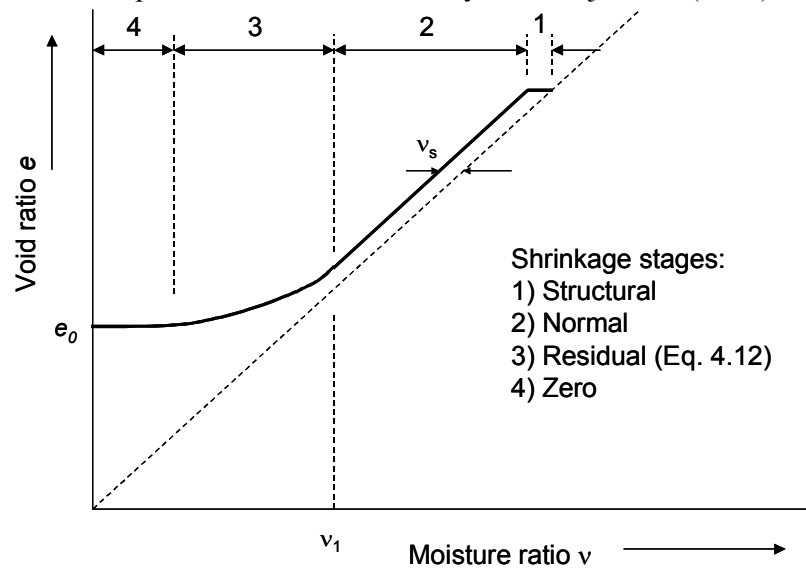


Figure 31 Void ratio e as function of moisture ratio v , showing four stages of a typical shrinkage characteristic (after Bronswijk, 1988)

6.5.2.2 Shrinkage characteristic

A shrinkage characteristic describes the relation between the amount of pores, as expressed by the void ratio, and the amount of water, as expressed by the moisture ratio (Bronswijk, 1988). The void ratio e ($\text{cm}^3 \text{cm}^{-3}$) is defined as:

$$e = \frac{V_p}{V_s} \quad (6.10)$$

and the moisture ratio v ($\text{cm}^3 \text{cm}^{-3}$) as:

$$v = \frac{V_w}{V_s} \quad (6.11)$$

where V_p is the total pore volume ($\text{cm}^3 \text{cm}^{-3}$) either filled with air or water, V_w the water volume ($\text{cm}^3 \text{cm}^{-3}$) and V_s the solid volume ($\text{cm}^3 \text{cm}^{-3}$). Figure 31 shows a typical shrinkage characteristic. Four stages can be distinguished (Stroosnijder, 1975; Bronswijk, 1988):

- 1) Structural shrinkage. When saturated soils dry, large water filled pores may be emptied. As a result, aggregates can get a somewhat denser packing. On the whole, the volume changes in this shrinkage phase are negligible, but water losses can be considerable.
- 2) Normal shrinkage. Volume decrease of clay aggregates is equal to moisture loss. The aggregates remain fully saturated.
- 3) Residual shrinkage. Upon drying the volume of the aggregates still decreases, but moisture loss is greater than volume decrease. Air enters the pores of the aggregates.
- 4) Zero shrinkage. The soil particles reached their densest configuration. Upon further moisture extraction, the volume of the aggregates remains constant. Moisture loss is equal to air volume increase of the aggregates. Rigid soils, like sands, only show this stage.

To facilitate input and data analysis in SWAP, an exponential relationship is employed for the residual shrinkage stage (Kim, 1992):

$$e = \alpha_{sh} e^{-\beta_{sh} v} + \gamma_{sh} v \quad (6.12)$$

with α_{sh} , β_{sh} , and γ_{sh} dimensionless, empirical parameters. The SWAP user needs to specify the void ratio e_0 at $v = 0$, the moisture ratio v_1 at the transition of residual to normal shrinkage, and the structural shrinkage, v_s (Figure 31). With these three input data, SWAP generates the parameters α_{sh} , β_{sh} , and γ_{sh} , and describes the $e(v)$ relationship.

Measured shrinkage characteristics of seven clay profiles in the Netherlands, as described by Bronswijk and Evers-Vermeer (1990), are listed in Appendix 5. Yule and Ritchie (1980a, 1980b) described shrinkage characteristics of eight Texas Vertisols, using small and large cores. Garnier et al. (1997) propose a simple evaporation experiment to determine simultaneously the moisture retention curve, hydraulic conductivity function and shrinkage characteristic.

The shrinkage characteristic enables us to calculate the crack volume and depth. Imagine a soil cube with sides z (cm) and volume $V = z^3$ (cm^3). In case of isotropic shrinkage of volume ΔV (cm^3) we may derive:

$$V = z^3, \quad V - \Delta V = (z - \Delta z)^3 \quad \text{and} \quad \Delta V = z^3 - (z - \Delta z)^3 \quad (6.13)$$

with Δz the change of each side length (cm). Therefore:

$$1 - \frac{\Delta V}{V} = \left(1 - \frac{\Delta z}{z}\right)^3 \quad (6.14)$$

In the case of one-dimensional subsidence without cracking, the following relation applies:

$$1 - \frac{\Delta V}{V} = \left(1 - \frac{\Delta z_{\text{ver}}}{z}\right)^1 \quad (6.15)$$

where Δz_{ver} is the vertical subsidence (cm). In a study on pedogenetically unripened soils, Rijniersce (1983) called the exponent in Eqs. (6.14) and (6.15) the geometry factor r_s . This results in a general relation between volume change ΔV and subsidence Δz_{ver} of a clay soil volume:

$$1 - \frac{\Delta V}{V} = \left(1 - \frac{\Delta z_{\text{ver}}}{z}\right)^{r_s} \quad (6.16)$$

In case of three-dimensional isotropic shrinkage, $r_s = 3$. When cracking dominates subsidence $r_s > 3$, when subsidence dominates cracking $1 < r_s < 3$. In case of subsidence only, $r_s = 1$.

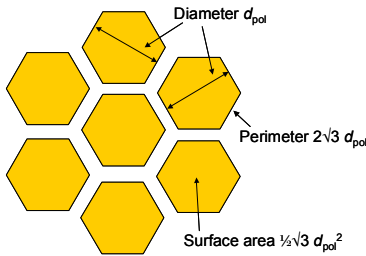


Figure 32 Geometry of soil matrix hexagons at a cracked clay soil

In order to calculate the lateral infiltration rate of water collected in cracks, we need to derive the vertical crack wall area. Consider a crack pattern of hexagons with diameter d_{pol} (cm) as depicted in Figure 32. We may derive that per unit depth the relative area of the vertical crack walls with respect to the horizontal surface area, $A_{\text{wall,rel}}$ ($\text{cm}^2 \text{ cm}^{-2}$), equals:

$$A_{\text{wall,rel}} = \frac{2\sqrt{3} d_{\text{pol}}}{\frac{1}{2}\sqrt{3} d_{\text{pol}}^2} = \frac{4}{d_{\text{pol}}} \quad (6.17)$$

6.5.2.3 Water flow concept

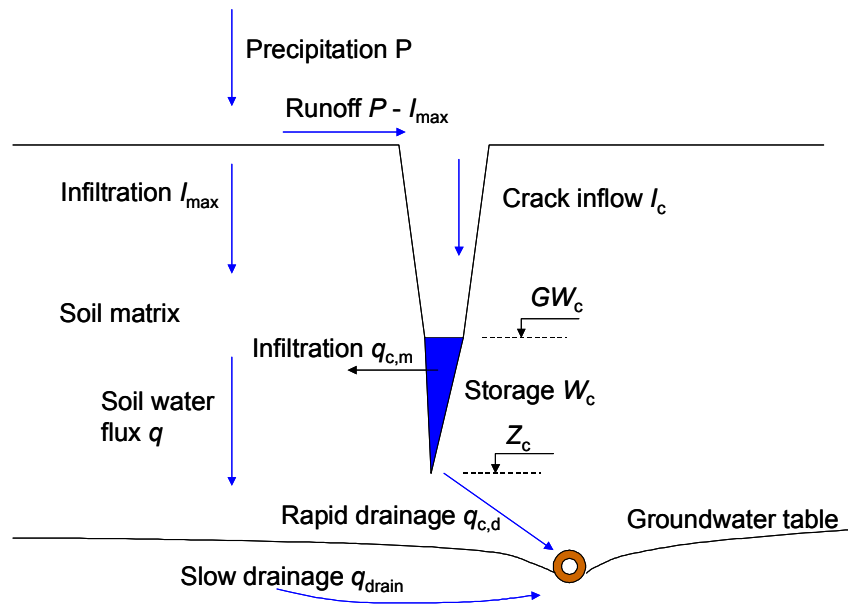


Figure 33 Concept of water flow in a cracked clay soil as applied in the simple macro pore concept. The variables are explained in the text.

The matrix and crack infiltration at a given rainfall intensity P can be calculated as (Bronswijk, 1988):

$$\begin{aligned}
 P < I_{max} : \quad I_m &= A_m P \\
 &I_c = A_c P \\
 P > I_{max} : \quad I_m &= A_m I_{max} \\
 &I_c = A_m (P - I_{max}) + A_c P
 \end{aligned}
 \tag{6.18}$$

with P the rainfall intensity (cm d^{-1}), I_{max} the maximum infiltration rate of the soil matrix (cm d^{-1}), I_m the infiltration rate into the soil matrix (cm d^{-1}), I_c infiltration rate into the cracks (cm d^{-1}), and A_m and A_c relative areas of soil matrix and cracks, respectively ($\text{cm}^2 \text{cm}^{-2}$).

Figure 33 shows the concept of water flow in a cracked clay soil as implemented in SWAP. Precipitation in excess of the infiltration rate flows as runoff to the cracks, as described by Eq. (6.18). The time needed for ponding water to flow on the soil surface to the cracks is probably negligible. A small time delay can be created by defining a threshold ponding height, which should be reached before runoff to the cracks starts. The maximum infiltration rate I_{max} is derived from an accurate solution of Richards' equation near the soil surface (see Par. 2.2). In order to do so, the nodal spacing near the soil surface should not exceed 1 cm, and the saturated hydraulic conductivity K_{sat} should be determined for the clay

matrix without cracks. Actual rainfall rates should be used, as daily rainfall rates underestimate seriously runoff amounts to the cracks.

Using the shrinkage characteristic and the actual water contents, the following steps are made to derive the amount of shrinkage ΔV , subsidence Δz_{ver} and relative, horizontal crack area A_c ($\text{cm}^2 \text{cm}^{-2}$) at a certain soil depth or node i :

- 1) Solid volume $V_s = 1.0 - \theta_{sat}$, where θ_{sat} is saturated water content ($\text{cm}^3 \text{cm}^{-3}$) of the considered soil layer;
- 2) Moisture ratio $\nu = \theta_i / V_s$, with the water content θ_i ($\text{cm}^3 \text{cm}^{-3}$) of node i , following from the solution of the Richards' equation at this time step;
- 3) Calculate void ratio e from the specified shrinkage characteristic $e(\nu)$;
- 4) Total pore volume $V_p = e V_s$;
- 5) Shrinkage soil volume with respect to maximum soil volume $\Delta V = \theta_{sat} - V_p$; vertical subsidence Δz_{ver} follows from Eq. (6.16);
- 6) Volume vertical crack $V_c = \Delta V - 1.0 \Delta z_{ver}$ ($\text{cm}^3 \text{cm}^{-3}$);
- 7) Relative horizontal crack area $A_c = 1.0 V_c / (1.0 - \Delta z_v)$ ($\text{cm}^2 \text{cm}^{-2}$).

In this procedure the water contents of the soil matrix are not adjusted for the shrinkage itself, which will change the vertical and horizontal co-ordinates. A study by Peerboom (1987) showed that the effects of these co-ordinate changes on simulated water contents and soil water movement inside the clay matrix are minor, while the numerical coding of this correction is substantial. Therefore this correction has been skipped, which results in the above listed straightforward procedure.

According to the described theoretical shrinkage characteristic (Figure 31), a crack volume would exist when $\theta_i < \theta_{sat}$. This would imply that as soon as the clay matrix is unsaturated ($h < 0$) cracks are formed. Field soils may deviate from this behaviour, showing crack bottoms higher and lower than the groundwater level. In the SWAP program we took this into account by calculating a crack volume if $\theta < \theta_{crit}$, where θ_{crit} is the critical water content for cracking derived from measurements. The concept of the shrinkage characteristic does not allow for the existence of cracks below the groundwater level ($\theta_{crit} \leq \theta_{sat}$), which is maintained in the SWAP program. In this way the level of the crack bottom Z_c is calculated as function of time.

Water collected in the cracks, will either infiltrate laterally to the soil matrix or flow rapidly to nearby drains and/or ditches, as depicted in Figure 33. The infiltration rate $q_{c,i}$ (cm d^{-1}) at node i can be derived straight from Darcy, if we assume a linear lateral pressure gradient in the soil matrix polygon and infiltration from each side:

$$q_{c,i} = -K(h_i) \frac{\partial H}{\partial x} = -6K(h_i) \frac{(h_i - h_{c,i})}{d_{pol}} \quad (6.19)$$

where K is the unsaturated hydraulic conductivity (cm d^{-1}), H the soil hydraulic head (cm), x the horizontal distance (cm), and h_i and $h_{c,i}$ are the nodal water pressure heads (cm) in the soil matrix and in the crack, respectively. The factor 6 accounts for water adsorption from all sides in the horizontal plane of the polygon. The water level in the cracks, GW_c (cm), can be calculated using the crack volume as function of depth as described earlier and the actual

crack water storage. The total lateral infiltration rate, $q_{c,m}$ (cm d⁻¹), is derived by the summation (Figure 33):

$$q_{c,m} = \sum_{z=Z_c}^{z=GW_c} q_{c,i} A_{\text{wall,rel}} \quad (6.20)$$

where Z_c is the crack depth (cm). The lateral infiltration rate is added as a source term $q_{c,i}/\Delta z_i$ to the Richards' equation for the water movement in the clay matrix:

$$\frac{\Delta \theta_i}{\Delta t} = \frac{\Delta}{\Delta z_i} \left[K(h_i) \left(\frac{\Delta h_i}{\Delta z_i} + 1 \right) \right] - S_a(h_i) + \frac{q_{c,i}}{\Delta z_i} \quad (6.21)$$

where S_a is the root water extraction rate (cm³ cm⁻³ d⁻¹). Field observations show that in cracked clay fields, water may flow directly from the cracks to drains or ditches, without entering the soil matrix. Hendriks et al. (1999) discussed an extensive concept for this so-called rapid drainage rate. In SWAP the rapid drainage rate, $q_{c,d}$ (cm d⁻¹), is calculated as function of the water collected in the cracks and with a linear rate coefficient f_{rapid} (d⁻¹):

$$q_{c,d} = f_{\text{rapid}} W_c \quad (6.22)$$

where W_c is the crack water storage (cm). Finally the change of water storage in the cracks, ΔW_c (cm), follows from the balance (Figure 33):

$$\Delta W_c = (I_c - q_{c,m} - q_{c,d}) \Delta t \quad (6.23)$$

Note that different from the earlier concept of Hoogmoed and Bouma (1980), water adsorption above the water level in the cracks is not included. Bouma and Dekker (1978) already concluded that the contact area between preferential flow and soil matrix forms only a small fraction of the total area available in the vertical ped surfaces. This complicates the calculation of horizontal adsorption. Booltink and Bouma (1993) applied the model with water adsorption to soil types ranging from loamy sand to clay and found that the lateral adsorption during bypass flow was always less than 1 percent. Therefore lateral adsorption was not included in this simple macropore model.

| <i>Model input</i> | | | |
|-------------------------------------|-------------|---|----------------|
| <i>Variable</i> | <i>Code</i> | <i>Description</i> | <i>Default</i> |
| e_0 | SHRINA | void ratio at zero water content (cm ³ cm ⁻³) | |
| v_1 | MOISR1 | moisture ratio at transition residual to normal shrinkage (cm ³ cm ⁻³) | |
| v_s | MOISRD | amount of structural shrinkage (cm ³ cm ⁻³) | |
| | ZNCRACK | depth at which crack area of soil surface is calculated (cm) | -5.0 |
| r_s | GEOMF | geometry factor (-) | 3.0 |
| d_{pol} | DIAMPOL | diameter of soil matrix polygon (cm) | |
| f_{rapid} | RAPCOEF | rate coefficient of bypass flow from cracks to surface water (d ⁻¹) | |
| <i>Specify for each soil layer:</i> | | | |
| | THETCR | critical water content below which cracks are formed (cm ³ cm ⁻³) | |

6.5.3 Advanced macropore flow

6.5.3.1 Introduction

It is known from the literature that other forms of macropores besides shrinkage cracks, such as structural cracks and worm and root holes, are of major importance for preferential flow in structured soils (see Hendriks et al., 1999). Therefore, the advanced macropore flow concept in SWAP contains these permanent macropores as well as temporary shrinkage cracks. This approach was taken from an adapted version of the FLOCR model (Hendriks et al., 1999) and is now implemented in SWAP. This option is yet in the testing phase and therefore still under construction. This applies as well to the description of this concept.

In many models, vertical water transport through macropores is calculated with Poiseuille's law and lateral infiltration into the unsaturated matrix of water trapped in non-continuous macropores at different depths (internal catchment) is accounted for by a tortuosity factor (e.g. Beven and Germann, 1981, Jarvis, 1989). In the SWAP model, a different approach is implemented, that is based on the geometry of the macropore structure. In this approach water flowing into the macropores is instantaneously added to the water storage at the bottom of the macropores. Lateral infiltration into crack walls of water running rapidly downwards along cracks is neglected, since according to Hoogmoed and Bouma (1980) and Booltink (1993) this infiltration is small. However, some of the macropore inflow will be trapped in non-continuous macropores and is therefore forced to infiltrate into the unsaturated matrix at different depths. Bouma and Dekker (1978), Van Stiphout et al. (1987) and Bouma (1990) call this process 'internal catchment'. In SWAP this process is explicitly implemented on the basis of the description of the macropore geometry.

6.5.3.2 Macropore geometry

In order to describe the geometry of the macropore structure the macropore volume is partitioned according to two properties:

I. Continuity:

- 1) main bypass flow domain: a network of continuous macropores (structural and shrinkage cracks);
- 2) internal catchment domain: discontinuous macropores ending at different depths;

II. Persistency:

- 1) static macropore volume: macropores that are permanent present;
- 2) dynamic macropore volume: shrinkage cracks.

Two classes of macropore are distinguished with respect to pore continuity. The first domain represents the main system of continuous and interconnected structural and shrinkage cracks that penetrate relatively deeply into the soil profile (i.e. the main bypass domain). The second domain represents macropores ending at different depths in the profile, resulting in 'internal catchment' (i.e. the internal catchment domain). Figure 34 shows a conceptual visualisation of these two classes of macropores. As shown in this figure, the volume of macropores in the main bypass domain consists of a network of interconnected macropores (e.g. structural and shrinkage cracks). It is constant with depth up to the depth where the internal catchment domain stops; thereafter the volume of pores in the main bypass domain decreases linearly with depth. The volume of the internal catchment consists of macropores that are not interconnected and that end at different

depths. The decline of the number of internal catchment macropores is described by a power law function (Figure 35). The internal catchment domain can be divided in a number of subdomains (horizontal discretisation). For each (sub)domain, the macropores in the various compartments are vertically interconnected.

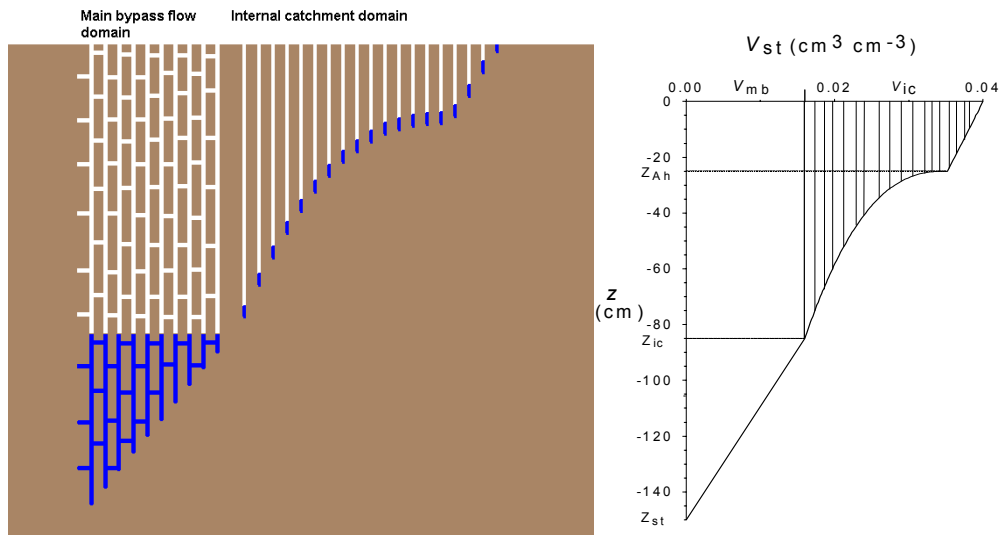


Figure 34 Schematic representation of the 2 domains: 1) main bypass flow domain (left part): transporting water and solutes deeper into profile and rapid drainage, 2) internal catchment (right part) domain: infiltration of trapped water into unsaturated matrix at different depths. The figure on the left gives a graphical representation of the two domains.

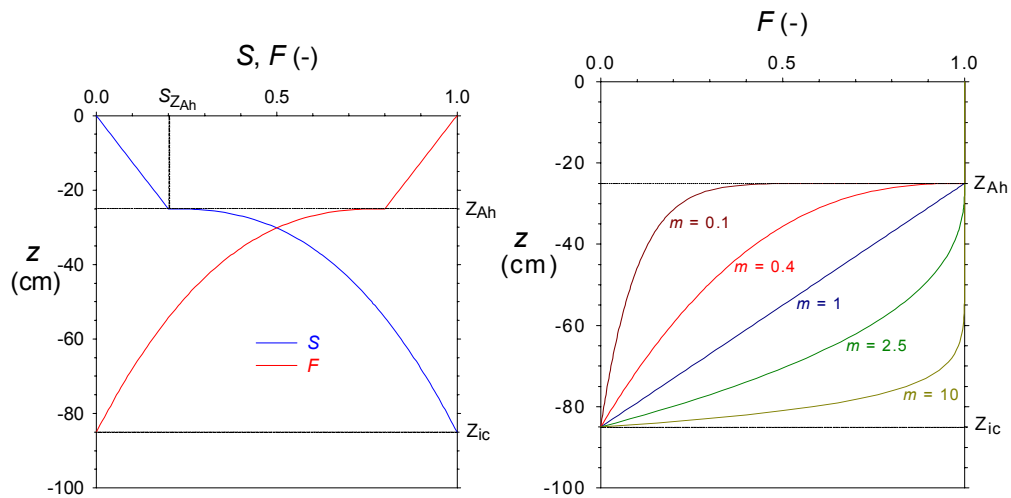


Figure 35 The decline of the number of internal catchment macropores is described by a power law function with power m . $m = 1$ represents a linear decline, while $m < 1$ represents a shallow system and $m > 1$ a deep system. ' $S_{Z_{Ah}}$ ' in the figure is similar to ' $R_{Z_{Ah}}$ ' in the list of Model input in 6.4.3.4.

Two types of macropore are included in the model to describe the dynamics of the macropore volume resulting from swelling and shrinking: a permanent static macropore volume independent of the soil moisture status and dynamic shrinkage cracks whose volume depends on the shrinkage characteristic and the current soil moisture content.

SWAP simulates the swelling and shrinking dynamics via a simplified procedure: the soil level remains fixed and swelling and shrinking influences only the pore volumes. For clay Eq. (6.12) is used to describe the shrinkage characteristic, and consequently the same input parameters are required as described in Par. 6.5.3.4. The shrinkage characteristic of peat differs strongly from the characteristic of clay. An analytical function for describing the peat characteristic is being developed. Figure 36 visualises the static and the dynamic macropore volumes. For each model compartment, a fraction of the volume per unit of horizontal area is considered to represent static macropores. In compartments with shrinkage cracks, the volume of the permanent macropores is added to the volume of the shrinkage cracks, resulting in a total macropore volume.

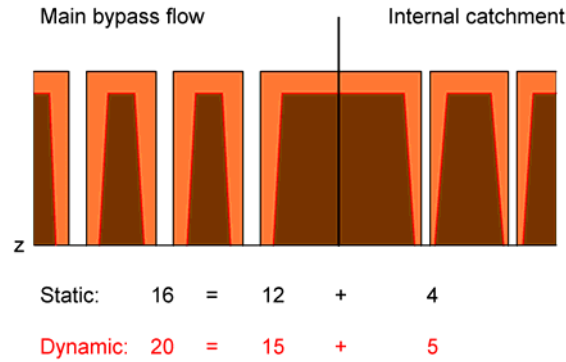


Figure 36 Partition between static and dynamic macropore volume: white area represents static and grey area dynamic macropore volume. Dark colour is the soil matrix.

6.5.3.3 Water flow

Figure 37 illustrates the different water flows into and from macropores in the SWAP advanced macropore concept. The amount of water routed into the macropores (I_{mp1} and I_{mp2}) at a given rainfall intensity P is calculated as described by Bronswijk (1988):

$$\begin{aligned}
 P \leq I_{\max} : \quad & I_m = A_m P \\
 & I_{mp1} = 0 \\
 & I_{mp2} = A_{mp} P \\
 P > I_{\max} : \quad & I_m = A_m I_{\max} \\
 & I_{mp1} = A_m (P - I_{\max}) \\
 & I_{mp2} = A_{mp} P \\
 I_{mp} &= I_{mp1} + I_{mp2}
 \end{aligned} \tag{6.24}$$

with P the rainfall intensity (cm d^{-1}), I_{\max} the maximum infiltration rate of the soil matrix (cm d^{-1}), I_m the infiltration rate into the soil matrix (cm d^{-1}), I_{mp} total infiltration rate into the macropores (cm d^{-1}), and A_m and A_{mp} relative areas of soil matrix and macropores, respectively ($\text{cm}^2 \text{cm}^{-2}$).

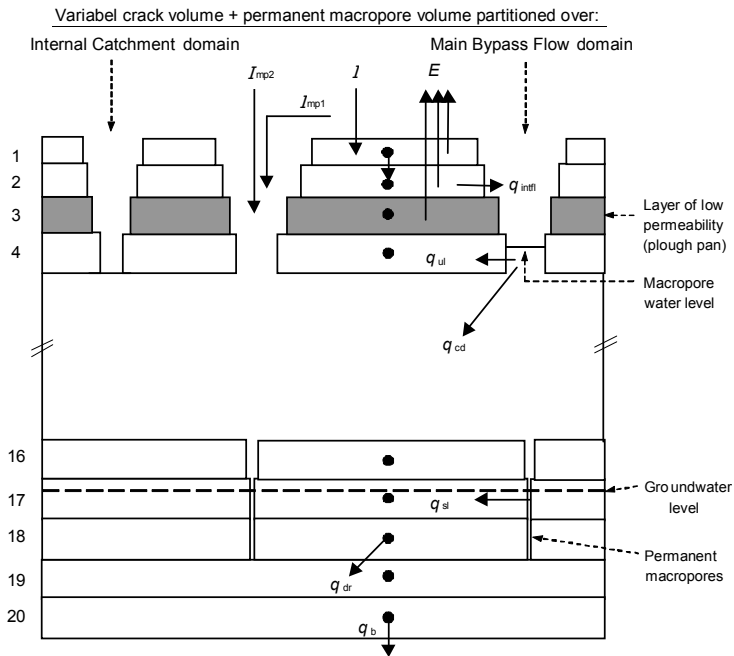


Figure 37 Schematic representation of the soil profile with the soil matrix, divided in 20 model compartments, and macropores and the various water fluxes ($m d^{-1}$) within the soil profile: I is infiltration rate into the soil matrix, I_{mp1} is part of total crack infiltration caused by rainfall intensity exceeding the maximum infiltration rate of the soil matrix, I_{mp2} is part of total crack infiltration caused by rain falling directly into the cracks, E is actual evapotranspiration, q_i is Darcy flux between two nodal points, q_b is bottom boundary flux, q_{inft} is interflow over layer of low permeability into macropores, q_{cd} is drainage flux via cracks, q_{ul} is lateral infiltration out of macropores into unsaturated matrix, q_{sl} is lateral infiltration out of macropores into saturated matrix.

The distribution of the total inflow into the macropores at the soil surface over the different domains is determined by the ratio of the volume fractions of the domains in the first compartment. Water flowing into the macropore domains accumulates at the bottom of the macropores. Some of the stored water can infiltrate laterally into the soil matrix that is in contact with this water, and, only in the case of the first domain, some of it can drain rapidly to the drainage systems. Water that has not infiltrated or drained within one time step is saved as storage for the next time step. A separate water balance is calculated for each (sub)domain. From saturated model compartments, water can exfiltrate into the macropores if the water potential in the macropores is lower than that in the soil matrix. This can happen in the case of a rising groundwater table in the matrix, but also when top compartments overlying a soil layer of relatively low permeability (e.g. a plough pan) become saturated and interflow occurs from these compartments into the macropores.

Unsaturated lateral infiltration

The calculation of the lateral infiltration through the macropore wall into the unsaturated soil compartments is based on the sorptivity (Philip, 1957):

$$I_{ul,i}(t) = \frac{4 S_i(\theta_{0,i}) \sqrt{t - t_{0,i}}}{d_{a,i}} D_i \quad (6.25)$$

where i is the compartment number; $I_{ul,i}$ is the unsaturated lateral infiltration (m), cumulative from time $t = t_{0,i}$ to $t = t$ (d); $S_i(\theta_{0,i})$ is Philip's sorptivity ($\text{cm d}^{-0.5}$) as a function of $\theta_{0,i}$, the initial volumic water content ($\text{cm}^3 \text{cm}^{-3}$) at $t = t_{0,i}$ the time of first contact of macropore water with the matrix; $d_{a,i}$ is the diameter of the aggregates (cm) and D_i is the thickness of the compartment (cm).

Sorptivity as a function of the initial volumic water content $\theta_{0,i}$ is derived from an empirical relation developed by Greco et al. (1996):

$$S_i(\theta_{0,i}) = S_{d,i} \left(1 - \frac{\theta_{0,i}}{\theta_{s,i}} \right)^{\alpha_i} \quad (6.26)$$

where $S_{d,i}$ is the sorptivity when $\theta_{0,i} = 0$; $\theta_{s,i}$ is the volumic water content at saturation; α_i is a fitting parameter (-).

The infiltration rate during the time step Δt is linearised to obtain an average, constant rate $q_{ul,i}(t)$ (cm.d^{-1}):

$$q_{ul,i}(t) = - \frac{I_{ul,i}(t + \Delta t) - I_{ul,i}(t)}{\Delta t} \quad (6.27)$$

The advantage of this approach is that measured values can be used for the sorptivity in relation to the initial moisture content. These measured sorptivities reflect the influence of water-repellent coatings on the surface of the clay aggregates which often hamper infiltration into these aggregates (Thoma et al., 1992; Dekker and Ritsema, 1996). If measured sorptivities are not available, the sorptivity in relation to the moisture content can be derived from the soil hydraulic functions (Parlange, 1975).

Saturated lateral infiltration

From the permanent macropores below the groundwater table, water can infiltrate laterally into the saturated matrix. The infiltration rate can be described by Darcy's law:

$$q_{sl,i} = - \frac{\delta k_{s,i} D_i h_{mg}}{d_{ap,i}^2} \quad (6.28)$$

where $q_{sl,i}$ is the saturated lateral infiltration flux (cm d^{-1}); $k_{s,i}$ is the saturated hydraulic conductivity (cm d^{-1}); D_i is the thickness of the compartment (cm); h_{mg} is the difference in potential (cm) between the water in the macropores and the groundwater; $d_{ap,i}$ is the effective diameter (cm) of aggregates in the zone with permanent macropores.

If the matrix water potential is higher than the macropore water potential, h_{mg} is negative and exfiltration from the matrix into the macropores occurs.

Rapid drainage

Rapid drainage via a network of cracks is calculated according to the drainage theory with one calibration parameter: the reference drainage resistance γ_{ref} (d^{-1}) for rapid drainage at field capacity (pF = 2). The rapid drainage flux q_{cd} (cm d^{-1}) is calculated from the crack water level h_{cd} (cm) above drain level and the actual drainage resistance γ_{act} (d^{-1}) at actual moisture content:

$$q_{cd} = \frac{h_{cd}}{\gamma_{\text{act}}} \quad (6.29)$$

The actual drainage resistance is calculated from the reference drainage resistance according to the ratio between actual and reference (at $pF = 2$) transmissivity kD ($\text{cm}^2 \text{d}^{-1}$):

$$\gamma_{\text{act}} = \frac{kD_{\text{ref}}}{kD_{\text{act}}} \gamma_{\text{ref}}, \text{ with} \quad (6.30)$$

$$kD_{\text{ref}} = \sum_{i=1}^{nd} k_{\text{ref},i} D_i \quad \text{and} \quad kD_{\text{act}} = \sum_{i=nt}^{nb} k_{\text{act},i} D_i$$

nd and nb are the numbers of respectively the compartment with the drainage level and the bottom compartment with water in macropores. The horizontal saturated hydraulic conductivity of the cracks k_i (cm d^{-1}) is a function of the dynamic crack width and as such is based on a slit model presented by Bouma and Anderson (1973) with r (-) is a reaction coefficient that determines the reaction of k to changes of the crack width w_i (with C is a system depending constant):

$$k_{\text{ref},i} = C \frac{(w_{\text{ref},i})^r}{d_i} \quad \text{and} \quad k_{\text{act},i} = C \frac{(w_{\text{act},i})^r}{d_i} \quad (6.31)$$

The crack width $w_{c,i}$ (cm) can be calculated from the relative volume of cracks $V_{c,i}$ ($\text{cm}^3 \text{cm}^{-2}$):

$$w_{c,i} = d_a \left(1 - \sqrt{1 - \frac{V_{c,i}}{D_i}} \right) \quad (6.32)$$

The diameter d_i of the soil polynomes (cm) per compartment i is calculated from the maximum d_{max} and minimum diameter d_{min} , and the number of domains $N_{d,i}$ in compartment i and the maximum number of domains $N_{d,\text{max}} = 1 + N_{\text{sd}}$ (number of subdomains in internal catchment domain):

$$d_i = d_{\text{min}} + \frac{N_{d,\text{max}} - N_{d,i}}{N_{d,\text{max}} - 1} \cdot (d_{\text{max}} - d_{\text{min}}) \quad (6.33)$$

All flows out of the macropores occur simultaneously. The distribution of drainage and the two forms of lateral infiltration depends on the rates of these processes.

6.5.3.4 Parameterisation of model input

| <i>Model input</i> | | | |
|-------------------------------------|----------------------|--|----------------|
| <i>Variable</i> | <i>Code</i> | <i>Description</i> | <i>Default</i> |
| Z_{Ah} | Z_Ah | depth bottom A-horizon (cm) | |
| Z_{Ic} | Z_Ic | depth bottom Internal Catchment (IC) domain (cm) | |
| Z_{St} | Z_St | depth bottom static macropores (cm) | |
| $V_{St,0}$ | VIMpStSs | volume of static macropores at soil surface ($\text{cm}^3 \text{cm}^{-3}$) | |
| $P_{Ic,0}$ | PpIcSs | proportion of IC domain at soil surface (-) | |
| N_{sd} | NumSbDm | number of subdomains in IC domain (-) | |
| m | PowM | power M for frequency distribut. curve IC domain (-) | 1.0 |
| R_{ZAh} | RZAh | fraction macropores ended at bottom A-horizon (-) Optional | 0.0 |
| S | Spoint | symmetry point for freq. distr. curve (-) Optional | 1.0 |
| - | SwPowM | switch for double convex/concave freq. distr. curve (-) Optional | 0 |
| d_{min} | DiPoMi | minimal diameter soil polygons (shallow) (-) | |
| d_{max} | DiPoMa | maximal diameter soil polygons (deep) (-) | |
| - | ZnCrAr | depth at which crack area of soil surface is calculated (cm) | -5.0 |
| - | CofAniMp | coefficient of anisotropy for Ksat | 1.0 |
| - | SwDrRap | switch for kind of drainage function TEMPORARY: TEST (-) | |
| γ_{ref} | RapDraResRef | reference rapid drainage resistance (d^{-1}) | |
| r | RapDraReaCof | reaction coefficient for rapid drainage (-) | |
| <i>Specify for each soil layer:</i> | | | |
| - | SwSoilShr | switch for kind of soil for determining shrinkage curve (-): 0 = rigid soil, 1 = clay, 2 peat | |
| - | SWSshrInp | switch for determining shrinkage curve (-): 1 = parameters for curve; 2 = typical points of curve | |
| - | ThetCrMP | critical water content below which cracks are formed ($\text{cm}^3 \text{cm}^{-3}$) | |
| r_s | GeomFac | geometry factor (-) | 3.0 |
| - | ShrParA - ShrParE | 5 possible parameters for describing shrinkage characteristics | |
| - | SWSorp | switch for kind of sorptivity function (-) 0 = Parlange, 1 = sorptivity curve | |
| - | SorpFacParl | factor for modifying Parlange function (-) | 1.0 |
| $S_{d,i}$ | SorpMax | maximal sorptivity at theta residual ($\text{cm d}^{0.5}$) | |
| α_i | SorpAlfa | fitting parameter for empirical sorptivity curve (-) | |

6.5.3.5 Output for solute transport models

Output of this module can be used as hydrological input in other models. For this purpose all in- and outgoing flows from matrix compartments, macropore domains and drains are accumulated over each output interval. In order to limit the total output, the water balance terms of the internal catchment macropore domains are lumped together in one domain (Appendix 16). The purpose of distinguishing different domains to describe internal catchment is to allow simulation of lateral infiltration and macropore water storage at increasing depths. Water flowing into the different domains basically has the same solute concentration, which will only change during storage. It is assumed that the storage time in

the shallow internal catchment domains is relatively small. For the purpose of calculating solute transport, therefore these domains can be treated as one integrated domain without introducing large errors. Since the storage time in the deep first domain, which often penetrates into the groundwater, is much larger, it remains necessary for solute transport simulation to distinguish this domain from the integrated internal catchment domain.

7 Crop growth

J.C. van Dam, J.C. van Diepen, J. Huygen

7.1 Introduction

SWAP contains three crop growth routines: a simple model, a detailed model (WOFOST), and the same model attuned to simulate grass growth. The simple model prescribes crop development, independent of external stress factors. The main function is to provide proper upper boundary conditions for soil water movement.

WOFOST simulates in detail photosynthesis and crop development, and takes into account the effects of water and salt stress on crop development. WOFOST (WORLD FOOD STUDIES) originated in the framework of an interdisciplinary study on the potential world food production by the Centre for World Food Studies (CWFS) in cooperation with the Wageningen Agricultural University, Department of Theoretical Production Ecology (WAU-TPE) and the DLO-Centre for Agrobiological Research (CABO-DLO, currently Plant Research International), Wageningen, the Netherlands. After cessation of the CWFS in 1988, the model was further developed at the DLO-Winand Staring Centre (SC-DLO) in cooperation with AB-DLO and WAU-TPE. Related models to WOFOST are the successive SUCROS (Simple and Universal Crop Simulator) models (Spitters et al., 1989; Van Laar et al., 1992), Arid Crop (Van Keulen, 1975; Van Keulen et al., 1981), Spring wheat (Van Keulen and Seligman, 1987), MACROS (Penning de Vries et al., 1989) and ORYZA1 (Kropff et al., 1993). All these Wageningen models follow the hierarchical distinction between potential and actual production, and share similar crop growth submodels, with light interception and CO₂ assimilation as growth driving processes, and crop phenological development as growth controlling process.

In SWAP, WOFOST 6.0 has been implemented. The description in Par. 7.3 is based on Spitters et al. (1989), Supit et al. (1994) and the program source code. A user's guide of WOFOST 6.0 was written by Hijmans et al. (1994). Boons-Prins et al. (1993) documented specific parameters for the crops winter wheat, grain maize, spring barley, rice, sugar beet, potato, field bean, soy bean, winter oilseed rape and sunflower. WOFOST input files for these crops will be provided with the SWAP program.

7.2 Simple crop module

This option is useful when crop growth doesn't need to be simulated or when crop growth input data are insufficient. The simple crop growth model represents a green canopy that intercepts precipitation, transpires and shades the ground. The user specifies leaf area index, crop height and rooting depth as function of development stage. In stead of the leaf area index also the soil cover fraction can be provided (see Par. 0). The development stage can be controlled either by the temperature sum or can be linear in time.

When the simple crop model is used in combination with the reference evapotranspiration, the crop factor should be given of the particular crop completely covering the soil and with optimal water supply.

The simple model does not calculate the crop potential or actual yield. However, the user may define yield response factors (Doorenbos and Kassam, 1979; Smith, 1992) for various growing stages as function of development stage. Each growing stage k the actual yield $Y_{a,k}$ (kg ha^{-1}) relative to the potential yield $Y_{p,k}$ (kg ha^{-1}) during this growing stage is calculated by:

$$1 - \frac{Y_{a,k}}{Y_{p,k}} = K_{y,k} \left(1 - \frac{T_{a,k}}{T_{p,k}} \right) \quad (7.1)$$

where $K_{y,k}$ (-) is the yield response factor of growing stage k , and $T_{p,k}$ (cm) and $T_{a,k}$ (cm) are the potential and actual transpiration, respectively, during growing period k .

The relative yield of the whole growing season is calculated as product of the relative yields of each growing stage:

$$\frac{Y_a}{Y_p} = \prod_{k=1}^n \left(\frac{Y_{a,k}}{Y_{p,k}} \right) \quad (7.2)$$

where Y_a is the cumulative actual yield (kg ha^{-1}) of the whole growing season, Y_p is the cumulative potential yield (kg ha^{-1}) of the whole growing season, index k is the growing stage and n is the number of defined growing stages.

In case of a linear relation between Y_a/Y_p and T_a/T_p during the whole growing period, or when no information is available of the yield response factors as function of development stage D_s for the particular crop, specify $K_{y,k} = 1$ for $0 < D_s < 2$ and specify one growing stage k . Mind that increase of the number of growing stages k , reduces the relative yield as calculated by Eq. (7.1).

| <i>Model input for each crop</i> | | | |
|----------------------------------|-------------|--|----------------|
| <i>Variable</i> | <i>Code</i> | <i>Description</i> | <i>Default</i> |
| | LCC | length of crop cycle (d) (optional) | |
| | TSUMEA | temperature sum from emergence to anthesis ($^{\circ}\text{C}$) (optional) | |
| | TSUMAM | temperature sum from anthesis to maturity ($^{\circ}\text{C}$) (optional) | |
| K_{df} | KDIF | extinction coefficient for diffuse visible light (-) (optional) | 0.60 |
| K_{dir} | KDIR | extinction coefficient for direct visible light (-) (optional) | 0.72 |
| <i>LAI</i> | LAI | leaf area index as function of development stage ($\text{m}^2 \text{m}^{-2}$) (optional) | |
| <i>SC</i> | SCF | soil cover fraction as function of development stage (-) (optional) | |
| k_c | CF | crop factor as function of development stage (-) (optional) | |
| h_{crop} | CH | crop height as function of development stage (cm) (optional) | |
| D_{root} | RD | rooting depth as function of development stage (cm) | |
| $K_{y,k}$ | KY | yield response factor as function of development stage (-) | 1.0 |

Other input parameters are related to water stress (Par. 2.4) and to interception (Par. 3.3)

7.3 Detailed crop module

Figure 38 shows the processes and relations incorporated in WOFOST. The radiation energy absorbed by the canopy is a function of incoming radiation and crop leaf area. Using the absorbed radiation and taking into account photosynthetic leaf characteristics the potential gross photosynthesis is calculated. The latter is reduced due to water and/or salinity stress, as quantified by the relative transpiration, and yields the actual gross photosynthesis. The actual gross photosynthesis is reduced by maintenance respiration and growth respiration to yield the dry matter increase. The dry matter increase is partitioned among roots, stems, storage organs, and leaves. The partitioning to leaves determines leaf area development and hence the dynamics of light interception. The dry weights of the plant organs are obtained by integrating their growth rates over time. During the development of the crop, part of living biomass dies due to senescence.

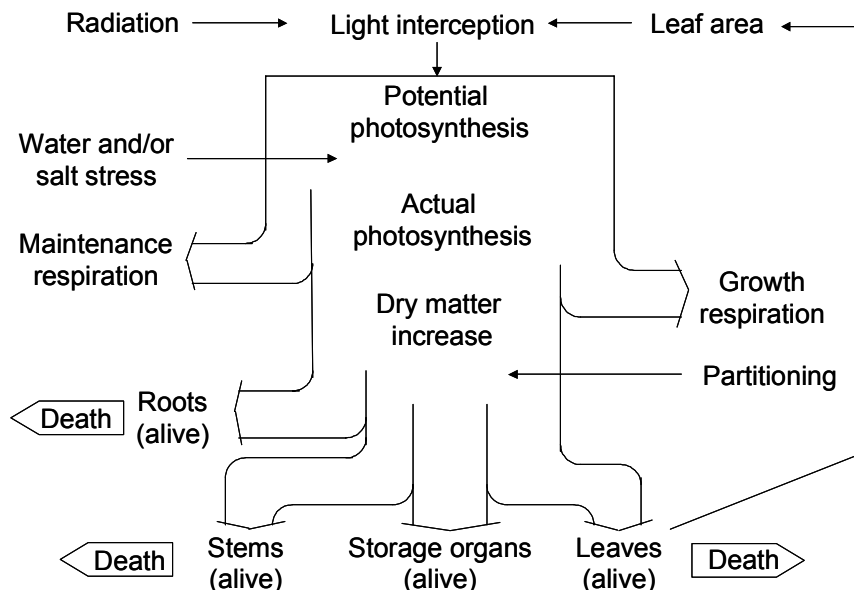


Figure 38 Schematization of the crop growth processes incorporated in WOFOST

Part of the carbohydrates (CH_2O) produced are used to provide energy for the maintenance of the existing live biomass (maintenance respiration). The remaining carbohydrates are converted into structural matter. In this conversion, some of the weight is lost as growth respiration. The dry matter produced is partitioned among roots, leaves, stems and storage organs, using partitioning factors that are a function of the phenological development stage of the crop (Spitters et al., 1989). The fraction partitioned to the leaves, determines leaf area development and hence the dynamics of light interception. The dry weights of the plant organs are obtained by integrating their growth rates over time. During the development of the crop, part of living biomass dies due to senescence.

Some simulated crop growth processes are influenced by temperature, like for example the maximum rate of photosynthesis and the maintenance respiration. Other processes, like the partitioning of assimilates or decay of crop tissue, are steered by the phenological development stage.

7.3.1 Phenological development stage

As many physiological and morphological processes change with the phenological stage of the plant, quantification of phenological development is essential in any crop growth simulation model. For many annual crops, the phenological development can conveniently be expressed in development stage D_s (-), having the value 0 at seedling emergence, 1 at flowering and 2 at maturity (Van Heemst, 1986a; 1986b). The most important phenological

change is the one from vegetative ($0 < D_s < 1$) to reproductive stage ($1 < D_s < 2$), which changes drastically the dry matter allocation to organs.

WOFOST starts crop growth simulation at emergence, which date should be specified by the user. A crop passes through successive phenological development stages from 0 to 2. The length of these stages depends on the development rate. Development rates before and after floral initiation or anthesis ($D_s = 1$) are controlled by day length and/or temperature. In the model, before anthesis both factors can be active. After anthesis only temperature will affect development rate.

Higher temperatures accelerate the development rate, leading to shorter growing periods. This rate responds to temperature according to a curvilinear relationship. However, it has often been demonstrated, that over a wide range of temperatures, the development rate increases more or less linearly with temperature (Van Dobben, 1962; Van Keulen and Seligman, 1987). WOFOST uses the temperature sum to determine the development stage. An effective temperature T_{eff} (°C) is calculated as function of daily average temperature T_{air} (°C). For species originating from temperate regions $T_{\text{eff}} = 0$ at $T_{\text{air}} = 0-3$ °C, while for species of subtropical and tropical origins $T_{\text{eff}} = 0$ at $T_{\text{air}} = 9-14$ °C (Angus et al., 1981). Within a species, cultivars may vary substantially in their temperature requirements. The temperature sum, therefore, is characteristic for each cultivar. Accordingly, the development stage, D_s (-), is calculated as:

$$D_s^{j+1} = D_s^j + \frac{T_{\text{eff}}}{T_{\text{sum},i}} \quad (7.3)$$

where superscript j is the day number and $T_{\text{sum},i}$ is the temperature sum required to complete either the vegetative or the reproductive stage.

For certain species or cultivars, during the vegetative stage, the effect of day length should be taken into account. Approaches that describe such effects quantitatively are given, amongst others, by Weir et al. (1984), Hadley et al. (1984) and Reinink et al. (1986). In the model, a reduction factor for the development rate as function of day length f_{lday} (-) is introduced:

$$f_{\text{lday}} = \frac{L_{\text{day}} - L_{\text{cday}}}{L_{\text{oday}} - L_{\text{cday}}} \quad \text{with} \quad 0 < f_{\text{lday}} < 1 \quad (7.4)$$

with L_{day} the actual day length (d), L_{cday} the shortest day length for any development (d), and L_{oday} the minimum day length for optimum development (d).

The user should provide information whether the development rate depends on temperature, on day length or on both. Note that in modern cultivars, photosensitivity is much less pronounced than in traditional cultivars, and that for the purpose of modelling the day length influence can be ignored by choosing an appropriate temperature sum, which leads to an equivalent crop life cycle.

The simulation of crop growth stops when the development stage reaches the stage at which the crop will be harvested. The development stage at harvest time should be provided by the user.

Model input for each crop

| <i>Variable</i> | <i>Code</i> | <i>Description</i> |
|---------------------|-------------|---|
| T_{eff} | DTSM | effective temperature as function of daily temperature(°C) (optional) |
| $T_{\text{sum}, 1}$ | TSUMEA | temperature sum from emergence to anthesis (°C) (optional) |
| $T_{\text{sum}, 2}$ | TSUMAM | temperature sum from anthesis to maturity (°C) (optional) |
| L_{oday} | DLO | minimum day length for optimum crop development (h) (optional) |
| L_{cday} | DLO | shortest day length for any crop development (h) (optional) |
| | DVSEND | crop development stage at harvest (-) |

7.3.2 Radiation fluxes above the canopy

Measured or estimated daily global solar radiation (wavelength 300-3000 nm) is input for the model. Incoming radiation is partly direct, with the angle of incidence equal to the angle of the sun, and partly diffuse, with incidence under various angles. The sine of solar elevation as a function of the day hour, can be calculated with:

$$\sin \beta_{\text{sun}} = \sin L_g \sin \sigma_{\text{sun}} + \cos L_g \cos \sigma_{\text{sun}} \cos \left(\frac{2\pi (t_h + 12)}{24} \right) \quad (7.5)$$

with β_{sun} the solar elevation (degrees), σ_{sun} is solar declination (degrees), L_g is geographic latitude (degrees) and t_h is hour of the day.

Only 50 percent of the global solar radiation (wavelength 300-3000 nm) is photosynthetically active (PAR, Photosynthetically Active Radiation, wavelength 400-700 nm). This fraction, is generally called 'light' or 'visible radiation'.

The instantaneous incoming photosynthetically active radiation PAR ($\text{J m}^{-2} \text{d}^{-1}$) is calculated by multiplying half of the daily global radiation with the ratio of the actual effective solar elevation and the integral of the effective solar height, taking into account reduced atmospheric transmission at low solar elevations:

$$PAR = 0.5 R_s \frac{\sin \beta_{\text{sun}} (1 + 0.4 \sin \beta_{\text{sun}})}{\int \sin \beta_{\text{mod, sun}}} \quad (7.6)$$

where R_s is global radiation flux density ($\text{J m}^{-2} \text{d}^{-1}$) and $\int \sin \beta_{\text{mod, sun}}$ the integral of $\sin \beta_{\text{sun}}$ over the day (-) which is corrected for reduced atmospheric transmission at low solar elevations.

A diffuse radiation flux results from scattering of sun rays by clouds, gases and dust in the atmosphere. To quantify the degree of scattering, the measured daily total radiation is compared with the amount that would have reached the earth's surface in the absence of an atmosphere, S_{sun} , which can be calculated from theoretical considerations:

$$S_{\text{sun}} = 1.18 \cdot 10^8 \left(1 + 0.033 \left(\frac{2j\pi}{365} \right) \right) \quad (7.7)$$

where S_{sun} is the solar constant ($\text{J m}^{-2} \text{d}^{-1}$) and j the Julian day number. The ratio of potential and measured daily total radiation is called atmospheric transmission A_t (-). The proportion of diffuse radiation, I_{dif} (-), is derived from the atmospheric transmission by an empirical relationship (Spitter et al., 1986). Taking also into account that only 50 percent of the solar radiation is photosynthetically active, the diffuse photosynthetic active radiation PAR_{dif} ($\text{J m}^{-2} \text{d}^{-1}$) can thus be calculated by:

$$PAR_{\text{dif}} = 0.5 I_{\text{dif}} A_t S_{\text{sun}} \sin \beta_{\text{sun}} \quad (7.8)$$

The direct radiation flux, PAR_{dir} ($\text{J m}^{-2} \text{d}^{-1}$), is obtained by subtracting the diffuse part from the photosynthetically active radiation flux:

$$PAR_{\text{dir}} = PAR - PAR_{\text{dif}} \quad (7.9)$$

7.3.3 Radiation profiles within the canopy

The total incoming photosynthetically active radiation flux is partly reflected by the canopy. The reflection coefficient is defined as the fraction of the downward radiation flux that is reflected by the whole canopy. According to Goudriaan (1977), the reflection coefficient of a green leaf canopy with a random spherical leaf angle, ρ_{rad} (-), equals:

$$\rho_{\text{rad}} = \left(\frac{1 - \sqrt{1 - \sigma_{\text{leaf}}}}{1 + \sqrt{1 - \sigma_{\text{leaf}}}} \right) \left(\frac{2}{1 + 1.6 \sin \beta_{\text{sun}}} \right) \quad (7.10)$$

with σ_{leaf} the scattering coefficient of single leaves for visible radiation (-), which is taken to be 0.2. The first term of Eq. (7.10) denotes the reflection of a canopy of horizontal leaves and the second term is the approximate correction factor for a spherical leaf angle distribution. The fraction $(1 - \rho_{\text{rad}})$ of the incoming visible radiation is potentially available for absorption by the canopy.

Light intensity, adjusted for crop reflection, decreases approximately exponentially with leaf area index when going deeper into the canopy:

$$PAR_L = (1 - \rho_{\text{rad}}) PAR e^{-\kappa L} \quad (7.11)$$

where PAR_L is the net light intensity ($\text{J m}^{-2} \text{d}^{-1}$) at depth L , κ is the radiation extinction coefficient (-) and L is the cumulative leaf area index, ΣLAI ($\text{m}^2 \text{ leaf m}^{-2} \text{ ground}$), counted from the top of the canopy downwards.

The profiles of the net diffuse flux and the net flux caused by direct irradiance can be characterized analogously (Goudriaan, 1982). Diffuse and direct fluxes each attenuate at a different rate. For a spherical leaf angle distribution with leaves distributed randomly within the canopy volume, the extinction coefficients of the direct component of the direct flux, κ_{dir} (-), is approximated by (Goudriaan, 1977, 1982):

$$\kappa_{\text{dir}} = \frac{0.5}{\sin \beta_{\text{sun}}} \quad (7.12)$$

and the extinction coefficient of the diffuse flux, κ_{df} (-), is calculated as:

$$\kappa_{df} = \kappa_{dir} \sqrt{1 - \sigma_{leaf}} \quad (7.13)$$

In Eq. (7.12), the factor 0.5 represents the average projection on the ground surface of leaves showing a spherical angle distribution. Averaging $0.5/\sin\beta$ during a day with an overcast sky, gives a value of $\kappa_{dir} = 0.8$ (-). In SWAP, κ_{df} should be given as an input by the user. It's value can be measured directly under diffuse sky conditions. The average value is about 0.72 (-) (Goudriaan, 1977).

In many situations, the leaf angle distribution is not spherical. In the model, therefore, the actual leaf angle distribution is accounted for by using a so called cluster factor which is the measured extinction coefficient for diffuse radiation flux, relative to the theoretical one for a spherical leaf area distribution.

On its way through the canopy, part of the direct flux is intercepted and scattered by the leaves; hence, the direct flux segregates into a diffused, scattered component and another component which remains direct. Attenuation of the direct component of the direct flux proceeds equally to the attenuation of light in a hypothetical canopy of black, non scattering leaves. The diffused component is obtained as the difference between the total direct flux and its direct component.

The decline of the radiation flux reflects the amount of absorption. The rate of absorption at a depth L in the canopy, $PAR_{L,a}$ ($J\ m^{-2}\ leaf\ d^{-1}$), is obtained by taking the derivative of Eq. (7.11) with respect to L :

$$PAR_{L,a} = \kappa(1 - \rho_{rad}) PAR e^{-\kappa L} \quad (7.14)$$

Similar expressions can be derived for the separate light components: the diffuse flux, the total direct radiation flux and the direct component of the direct radiation flux. The absorbed diffused component of the direct flux is obtained by subtracting the direct component from the total direct flux.

Two leaf area classes are distinguished: shaded leaf area and sunlit leaf area. The shaded leaf area absorbs the diffuse flux and the diffused component of the direct flux. The sunlit leaf area receives diffuse and direct radiation. At every horizon within the canopy, the intensity of the unobstructed direct beam equals its intensity above the crop.

| <i>Model input for each crop</i> | | | |
|----------------------------------|-------------|---|----------------|
| <i>Variable</i> | <i>Code</i> | <i>Description</i> | <i>Default</i> |
| κ_{df} | KDIF | extinction coefficient for diffuse visible light (-) (optional) | 0.60 |
| κ_{dir} | KDIR | extinction coefficient for direct visible light (-) (optional) | 0.72 |

7.3.4 Instantaneous assimilation rates per leaf layer

The CO_2 assimilation rate of a canopy layer is obtained by substituting the absorbed amount of light energy into the assimilation-light response of single leaves. Of the two-parameter response functions, the asymptotic exponential function appears to be the most satisfactory (Peat, 1970):

$$A_L = A_{\max} \left(1 - e^{-\frac{\varepsilon_{\text{PAR}} PAR_{L,a}}{A_{\max}}} \right) \quad (7.15)$$

where A_L is the gross assimilation rate ($\text{kg CO}_2 \text{ m}^{-2} \text{ leaf d}^{-1}$), A_{\max} the gross assimilation rate at light saturation ($\text{kg CO}_2 \text{ m}^{-2} \text{ leaf d}^{-1}$), and ε_{PAR} the initial slope or light use efficiency ($\text{kg CO}_2 \text{ J}^{-1}$ absorbed).

Substitution into Eq. (7.15) the absorbed amount of radiation by shaded leaves and by sunlit leaves, yields the assimilation rates of sunlit and shaded leaves. The shaded leaf area receives the diffuse flux and the scattered component of the direct flux. The sunlit leaf area receives both diffuse and direct flux. Illumination intensity of sunlit leaves varies strongly with leaf angle. In the model, the assimilation rate of the sunlit leaf area is therefore integrated over the leaf angle distribution.

The assimilation rate per unit leaf area in a canopy, is the sum of the assimilation rates of sunlit and shaded leaves, taking into account their proportion in each layer. The proportion of sunlit leaf area at depth L in the canopy equals the proportion of the direct component of the direct flux reaching that depth. This proportion is calculated in analogy to Eq. (7.14), using the extinction coefficient of the direct radiation component.

Model input for each crop

| <i>Variable Code</i> | <i>Description</i> |
|--------------------------------|--|
| A_{\max} AMAX | maximum CO_2 assimilation rate as function of development stage (-) |
| ε_{PAR} EFF | light use efficiency ($\text{kg CO}_2 \text{ J}^{-1}$ adsorbed) |

7.3.5 Daily gross assimilation rate of the canopy

The instantaneous rates per leaf layer need to be integrated over the canopy leaf area index and over the day. This is efficiently achieved with the Gaussian integration method (Press et al., 1989). This method specifies the discrete points at which function values have to be calculated, and the weighting factors with which the function values have to be multiplied in order to attain minimum deviation from analytical integration. A three-point algorithm evaluates the function at $0.1127a$, $0.5a$ and $0.8873a$ of the interval $(0,a)$, with weighting coefficients 1.0, 1.6 and 1.0, respectively. The Gaussian integration method is remarkable accurate in case of trigonometric (radiation) and exponential (light absorption) functions. WOFOST computes at three selected moments of the day incoming PAR just above the canopy. Using this radiation, assimilation is computed at three selected depths in the canopy (Spitters et al., 1989). Gaussian integration of these values results in the daily rate of potential gross CO_2 assimilation, A_{pgross} ($\text{kg CO}_2 \text{ ha}^{-1} \text{ d}^{-1}$).

Until now the assimilation has been treated as a function of the intercepted light and of photosynthetic crop characteristics such as initial light use efficiency and maximum leaf CO_2 assimilation at light saturation. Other factors that may reduce the daily assimilation rate are typical crop characteristics, unfavourable temperatures and water stress.

Crop characteristics depend on the phenological crop stage. This is taken into account by specifying the maximum assimilation rate, A_{\max} ($\text{kg CO}_2 \text{ ha}^{-1} \text{ d}^{-1}$), as function of development stage.

A reduction factor f_{tday} (-), which is a function of the average daytime temperature T_{day} ($^{\circ}\text{C}$), accounts for sub-optimum temperatures. T_{day} is calculated by:

$$T_{\text{day}} = 0.75 T_{\max} + 0.25 T_{\min} \quad (7.16)$$

where T_{\max} and T_{\min} ($^{\circ}\text{C}$) are the daily maximum and minimum temperature, respectively.

The crop characteristics and the day temperature result in a reduction of A_{pgross} to A_{pgross}^1 ($\text{kg CO}_2 \text{ ha}^{-1} \text{ d}^{-1}$):

$$A_{\text{pgross}}^1 = \max(A_{\text{pgross}}, f_{\text{tday}}, A_{\max}) \quad (7.17)$$

In addition, low nighttime temperatures affect assimilation. At night, assimilates produced during daytime, are transformed into structural biomass. This process is hampered by low temperature. If these low temperatures prevail for a several days, the assimilates accumulate in the plant and the assimilation rate diminishes and ultimately halts. In the model, this temperature effect is accounted for by a reduction factor $f_{7\min}$, which is a function of the minimum temperature during the last seven days.

Another important factors that may reduce assimilation, is water and/or salinity stress. WOFOST uses the ratio of actual transpiration and potential transpiration, T_a/T_p , as reduction coefficient.

Reduction due to low minimum temperatures, water stress, and salinity stress, and taking into account that for each kg CO_2 30/44 kg biomass (CH_2O) is formed, results in the following equation for the daily gross assimilation rate A_{gross} ($\text{kg ha}^{-1} \text{ d}^{-1}$):

$$A_{\text{pgross}} = \frac{30}{40} f_{7\min} \frac{T_a}{T_p} A_{\text{pgross}}^1 \quad (7.18)$$

Model input for each crop

| <i>Variable</i> | <i>Code</i> | <i>Description</i> |
|-------------------|-------------|---|
| f_{tday} | TMPF | reduction factor of AMAX as function of average day temperature (-) |
| $f_{7\min}$ | TMNF | reduction factor of AMAX as function of minimum day temperature (-) |

7.3.6 Maintenance respiration

Some of the carbohydrates formed are respired to provide energy for maintaining the existing bio structures. This maintenance respiration consumes roughly 15 - 30% of the carbohydrates produced by a crop in a growing season (Penning de Vries et al., 1979). This indicates the importance of accurate quantification of this process in the model.

The maintenance costs may be estimated from the quantities of proteins and minerals present in the biomass and from crop metabolic activity, as presented by De Wit et al. (1978). This method, however, requires information on the vegetation nitrogen and mineral

contents. Based on De Wit et al. (1978), typical values for the maintenance coefficients of various plant organs have been derived by Penning de Vries and Van Laar (1982). These coefficients should be specified by the user in WOFOST. According to this approach, the reference maintenance requirements R_{mref} ($\text{kg ha}^{-1} \text{d}^{-1}$) are proportional to the dry weights of the plant organs to be maintained:

$$R_{mref} = c_{m,leaf} W_{leaf} + c_{m,stem} W_{stem} + c_{m,stor} W_{stor} + c_{m,root} W_{root} \quad (7.19)$$

where $c_{m,i}$ denotes the maintenance coefficient of organ i ($\text{kg kg}^{-1} \text{d}^{-1}$) and W_i the organ dry weight (kg ha^{-1}).

The maintenance respiration rate still has to be corrected for senescence and temperature. The reduction factor for senescence f_{senes} (-) is crop specific and is defined as a function of development stage. Higher temperatures accelerate the turnover rates in plant tissue and hence the costs of maintenance. An increase in temperature of 10°C increases maintenance respiration by a factor of about 2 (Kase and Catsky, 1984; Penning de Vries and Van Laar, 1982). To be more flexible, the user may specify the increase factor of the respiration rate per 10°C temperature increase, Q_{10} (-):

$$R_m = f_{senes} R_{mref} Q_{10}^{\frac{T_{avg} - 25}{10}} \quad (7.20)$$

where R_m is the actual maintenance respiration rate ($\text{kg ha}^{-1} \text{d}^{-1}$).

Thus, the maintenance respiration rate depends on the amount of dry matter in the various organs, the relative maintenance rate per organ and the temperature. We may assume that the vegetation will not be 'self-consuming' in terms of carbohydrates. Therefore the maintenance respiration rate cannot exceed the gross assimilation rate.

Gross assimilation rate A_{gross} minus maintenance respiration rate R_m results in the net assimilation rate A_{net} ($\text{kg ha}^{-1} \text{d}^{-1}$), the amount of carbohydrates available for conversion into structural material:

$$A_{net} = A_{gross} - R_m \quad \text{with} \quad A_{net} \geq 0 \quad (7.21)$$

Model input for each crop

| <i>Variable</i> | <i>Code</i> | <i>Description</i> |
|-----------------|-------------|---|
| $c_{m,leaf}$ | RML | relative maintenance respiration rate of leaves ($\text{kg H}_2\text{O kg}^{-1} \text{d}^{-1}$) |
| $c_{m,stor}$ | RMO | relative maintenance respiration rate of storage organs ($\text{kg H}_2\text{O kg}^{-1} \text{d}^{-1}$) |
| $c_{m,root}$ | RMR | relative maintenance respiration rate of roots ($\text{kg H}_2\text{O kg}^{-1} \text{d}^{-1}$) |
| $c_{m,stem}$ | RMS | relative maintenance respiration rate of stems ($\text{kg H}_2\text{O kg}^{-1} \text{d}^{-1}$) |
| f_{senes} | RFSE | reduction factor of senescence as function of development stage (-) |
| Q_{10} | Q10 | relative increase in respiration rate with temperature (10°C^{-1}) |

7.3.7 Dry matter partitioning and growth respiration

The primary assimilates in excess of the maintenance costs, are available for conversion into structural plant material. In this conversion process of the glucose molecules, CO_2 and H_2O are released. This is a partial combustion of glucose to provide energy required in the various biochemical pathways. Hence, biosynthesis of the various structural compounds can

be considered as a process of cut and paste, the scraps representing the weight lost in growth respiration.

The magnitude of growth respiration is determined by the composition of the end product formed (Penning de Vries et al., 1974). Thus the weight efficiency of conversion of primary photosynthates into structural plant material varies with the composition of that material. Fats and lignin are produced at high costs; structural carbohydrates and organic acids are relatively cheap. Proteins and nucleic acids form an intermediate group.

At higher temperatures the conversion processes are accelerated, but the pathways are identical (Spitters et al. 1989). Hence, the assimilate requirements do not vary with temperature.

The increase in total dry weight of the crop is partitioned over the plant organs: roots, leaves, stems and storage organs. This is correct simulation of what occurs during the vegetative phase. Storage organs, however, may not only be formed from current photosynthates but also from carbohydrates and proteins that have been stored temporarily in vegetative parts and that are redistributed during the reproductive stage. In the model, the latter process is not incorporated: the total growth of the crop is partitioned among the plant organs according to partitioning factors that are introduced as forcing functions; their values only change with the development stage of the crop.

In the model, average (crop specific) conversion factors $C_{e,i}$ (kg kg^{-1}) are used for leaf, storage organ, stem and root biomass. A weighted average, C_e (kg kg^{-1}), of these organ specific conversion factors is calculated by multiplying the organ specific values with the partitioning factors :

$$C_e = \frac{1}{\left(\frac{\xi_{\text{leaf}}}{C_{e,\text{leaf}}} + \frac{\xi_{\text{stor}}}{C_{e,\text{stor}}} + \frac{\xi_{\text{stem}}}{C_{e,\text{stem}}} \right) (1 - \xi_{\text{root}}) + \frac{\xi_{\text{root}}}{C_{e,\text{root}}}} \quad (7.22)$$

where ξ_i is the partitioning factor for organ i .

The gross dry matter growth rate w_{gross} ($\text{kg ha}^{-1} \text{d}^{-1}$) is related to the net assimilation rate A_{net} by:

$$w_{\text{gross}} = C_e A_{\text{net}} \quad (7.23)$$

Gross dry matter growth is first partitioned between shoots (leaves, stems and storage organs together) and roots:

$$w_{\text{gross,root}} = \xi_{\text{root}} w_{\text{gross}} \quad \text{and} \quad w_{\text{gross,sh}} = (1 - \xi_{\text{root}}) w_{\text{gross}} \quad (7.24)$$

where ξ_{root} is the partitioning factor for roots (-) and $w_{\text{gross,root}}$ and $w_{\text{gross,sh}}$ are the gross growing rates ($\text{kg ha}^{-1} \text{d}^{-1}$) of the roots and the shoots, respectively. The gross growth rate of leaves, stems and storage organs is simply the product of the gross dry matter growth rate of the shoots and the fraction allocated to these organs. The partitioning factors are a function of development stage and are crop specific. Mind that the sum of ξ_{leaf} , ξ_{stem} and ξ_{stor} at any development stage should be one!

Model input for each crop

| <i>Variable</i> | <i>Code</i> | <i>Description</i> |
|---------------------|-------------|---|
| ξ_{root} | FR | fraction of total dry matter increase partitioned to roots (-) |
| ξ_{leaf} | FL | fraction of total above ground dry matter increase part. to leaves (-) |
| ξ_{stem} | FS | fraction of total above ground dry matter increase part. to stems (-) |
| ξ_{stor} | FO | fraction of total above ground dry matter incr. part. to st. organs (-) |
| $C_{e,\text{leaf}}$ | CVL | efficiency of conversion into leaves (kg kg ⁻¹) |
| $C_{e,\text{stor}}$ | CVO | efficiency of conversion into storage organs (kg kg ⁻¹) |
| $C_{e,\text{root}}$ | CVR | efficiency of conversion into roots (kg kg ⁻¹) |
| $C_{e,\text{stem}}$ | CVS | efficiency of conversion into stems (kg kg ⁻¹) |

7.3.8 Senescence

The death rate of storage organs is considered to be zero. The death rate of stem and roots is crop specific and is defined as the daily amount of the living biomass which no longer participates in the plant processes. The death rate of stems and roots is considered to be a function of development stage as specified by the user.

The death rate of leaves is more complicated. Leaf senescence occurs due to water stress, shading (high LAI), and also due to exceedance of the life span.

The potential death rate of leaves due to water stress $\zeta_{\text{leaf},\text{water}}$ (kg ha⁻¹ d⁻¹) is calculated as:

$$\zeta_{\text{leaf},\text{w}} = W_{\text{leaf}} \left(1 - \frac{T_a}{T_p} \right) \zeta_{\text{leaf},\text{p}} \quad (7.25)$$

where W_{leaf} is the leaf dry matter weight (kg ha⁻¹), T_a and T_p are the actual and potential transpiration rates (cm d⁻¹), respectively, and $\zeta_{\text{leaf},\text{p}}$ is the maximum relative death rate of leaves due to water stress (kg kg⁻¹ d⁻¹). The latter is crop specific and should be provided by the user.

A potential death rate due to self-shading, $\zeta_{\text{leaf},\text{shade}}$ (kg ha⁻¹ d⁻¹), is defined which increases linearly from zero at a certain critical leaf area index, to its maximum value at twice this critical leaf area index:

$$\zeta_{\text{leaf},\text{shade}} = 0.03 W_{\text{leaf}} \left(\frac{\text{LAI} - \text{LAI}_c}{\text{LAI}_c} \right) \quad \text{with} \quad 0 < \left(\frac{\text{LAI} - \text{LAI}_c}{\text{LAI}_c} \right) < 1 \quad (7.26)$$

where LAI_c is the critical leaf area index (-).

LAI_c is set equal to $3.2/\kappa_{\text{df}}$, with κ_{df} the extinction coefficient (-) for diffuse radiation (Par. 7.4). Typical values for $\zeta_{\text{leaf},\text{p}}$ and LAI_c are 0.03 d⁻¹ and 4 ha ha⁻¹, respectively (Spitters et al., 1989).

WOFOST uses the highest value of $\zeta_{\text{leaf},\text{w}}$ and $\zeta_{\text{leaf},\text{shade}}$ for the combined effect of water stress and mutual shading.

Leaves that have escaped from premature death due to water stress or mutual shading, inevitably die due to exceedance of the life span for leaves (i.e. physiologic ageing). Life span is defined as the maximum time a leaf can live at a constant temperature of 35°C. Life span is crop specific. A physiologic ageing factor, f_{age} (-), is calculated each day:

$$f_{age} = \frac{T - T_{b,age}}{35 - T_{b,age}} \quad \text{with} \quad f_{age} \geq 0 \quad (7.27)$$

with $T_{b,age}$ the lower threshold temperature for physiologic ageing (°C), which is crop specific and should be provided by the user.

The integral of the physiologic ageing factor over time yields the physiologic age, P_{age} (d):

$$P_{age}^{j+1} = P_{age}^j + f_{age} \Delta t \quad (7.28)$$

In order to correct for leaf senescence, the specific leaf area of each day, S_{la}^j (ha kg⁻¹), the growth of the dry matter weight of leaves per day, w_{leaf} , and the physiological age, P_{age} , are stored in three different arrays. The first element of the arrays represents the most recent day and the last element of the arrays represents the oldest day.

The weight of the leaves that have died during a day due to water stress or mutual shading is subtracted from the weight of the oldest leaf class. If there is only one class, the result should be positive. When more leaf classes exist, the oldest leaf class may be emptied completely, and the remainder is subtracted from the next leaf class. Emptying the oldest leaf class continues, until the original amount is dissipated completely or the remaining amount of leaves becomes zero.

Leaves may attain the age defined by the crop specific life span. However, they can not exceed this age. The model checks the leaf classes ages. The first class younger than the defined life span becomes the oldest class.

Model input for each crop

| <i>Variable</i> | <i>Code</i> | <i>Description</i> |
|------------------|-------------|--|
| | RDRR | relative death rate of roots as function of development stage (kg kg ⁻¹ d ⁻¹) |
| | RDRR | relative death rate of stems as function of development stage (kg kg ⁻¹ d ⁻¹) |
| $\zeta_{leaf,p}$ | PERDL | maximum relative death rate of leaves due to water stress (d ⁻¹) |
| $T_{b,age}$ | TBASE | lower threshold temperature for ageing of leaves (°C) |
| | SPAN | life span of leaves at optimum growth conditions (d) |

7.3.9 Net growth

The initial amount of total dry crop weight should be provided by the user. This amount is multiplied by the partitioning factors, ξ_i , to yield the dry weight values at emergence.

The net growth rates of the plant organs, $w_{net,i}$ (kg ha⁻¹ d⁻¹) result from the gross growth rates (Par. 7.8) and the senescence rates, ζ_i (kg kg⁻¹ d⁻¹):

$$w_{net,i} = w_{gross,i} - \zeta_i W_i \quad (7.29)$$

By integrating $w_{\text{net},i}$ over time, the dry matter weight of organ i , W_i (kg ha^{-1}), is calculated.

An exception has to be made for the growth of leaves. In the initial stage, the rate of leaf appearance and final leaf size are constrained by temperature through its effect on cell division and extension, rather than by the supply of assimilates. For a relative wide range of temperatures the growth rate responds more or less linearly to temperature (Hunt et al., 1985; Causton and Venus, 1981; Van Dobben, 1962). The growth rate of the leaf area index, w_{LAI} ($\text{ha ha}^{-1} \text{d}^{-1}$), in this so-called exponential stage, is described by:

$$w_{\text{LAI}} = \text{LAI} w_{\text{LAI,max}} T_{\text{eff}} \quad (7.30)$$

where $w_{\text{LAI,max}}$ is the maximum relative increase of leaf area index ($^{\circ}\text{C}^{-1} \text{d}^{-1}$).

WOFOST assumes that the exponential growth rate of leaf area index will continue until it equals the assimilation limited growth rate of the leaf area index. During this second, source limited growth stage, w_{LAI} is described by:

$$w_{\text{LAI}} = w_{\text{net,leaf}} S_{\text{la}} \quad (7.31)$$

where S_{la} is the specific leaf area (ha kg^{-1}).

The green parts of stems and storage organs, may absorb a substantial amount of radiation. Therefore the so-called green area index GAI_i (ha ha^{-1}) should be added to the leaf area index. The green area index of the stems and storage organs, are calculated from the dry matter weights of the organs:

$$GAI_i = S_{\text{ga},i} W_i \quad (7.32)$$

with $S_{\text{ga},i}$ the specific green area (ha kg^{-1}) of either stems or storage organ. $S_{\text{ga},i}$ are crop specific and should be provided by the user.

Model input for each crop

| <i>Variable</i> | <i>Code</i> | <i>Description</i> |
|-----------------------|-------------|--|
| $w_{\text{LAI,max}}$ | RGRLAI | maximum relative increase of leaf area index ($^{\circ}\text{C}^{-1} \text{d}^{-1}$) |
| S_{la} | SLA | specific leaf area as function of development stage (ha kg^{-1}) |
| $S_{\text{ga, stor}}$ | SPA | specific pod area (ha kg^{-1}) |
| $S_{\text{ga, stem}}$ | SSA | specific stem area (ha kg^{-1}) |
| | TDWI | initial total crop dry weight (kg ha^{-1}) |
| | LAIEM | leaf area index at emergence ($\text{m}^2 \text{m}^{-2}$) |

7.3.10 Root growth

Root extension is computed in a straightforward way. The user needs to specify the initial rooting depth, the maximum rooting depth as determined by the crop and by the soil, and the maximum daily increase in rooting depth, $d_{\text{root,max}}$ (cm). Daily increase in rooting depth is equal to the maximum daily increase, unless maximum rooting depth is reached or no assimilates are available for root growth:

$$D_{\text{root}}^{j+1} = D_{\text{root}}^j + d_{\text{root,max}} \quad \text{if} \quad D_{\text{root}}^{j+1} \leq D_{\text{root,max}} \quad \text{and} \quad w_{\text{net,root}} \geq 0 \quad (7.33)$$

where D_{root}^j is the rooting depth (cm) at day j .

Model input for each crop

| <i>Variable</i> | <i>Code</i> | <i>Description</i> |
|------------------------|-------------|---|
| | RDI | initial rooting depth (cm) |
| $D_{\text{root, max}}$ | RDC | maximum rooting depth of particular crop (cm) |
| $d_{\text{root, max}}$ | RRI | maximum daily increase in rooting depth (cm d ⁻¹) |

8 Solute transport

J.C. van Dam, J.J.T.I. Boesten

8.1 Introduction

Many solutes enter the natural system at the soil surface. The solute residence time in the unsaturated zone is important for soil- and groundwater pollution management. For instance organic compounds are mainly decomposed in the unsaturated zone, where the biological activity is concentrated. Most plants are able to extract water and nutrients from the soil only in the unsaturated zone. In irrigated areas, the long term salinity in the root zone will depend on the amount of percolation from the unsaturated zone. Whereas in the unsaturated zone the transport of solutes is predominantly vertical, once being in the groundwater solutes may diverge in any direction, threatening surface waters, nature reserves and drinking wells. Using an analytical model, Beltman et al. (1995) show the importance of the transport processes in the unsaturated zone as compared to the transport processes in the saturated zone. It is clear that a thorough understanding is needed of the processes that govern the transport, adsorption, root uptake and decomposition of the solutes in the unsaturated zone, in order to analyse and manage soil and water related environmental problems.

SWAP is designed to simulate transport processes at field scale level. Although for management purposes most farmers try to have more or less the same soil and drainage condition per field, still the existing soil spatial heterogeneity within a field may cause a large variation of solute fluxes (Biggar and Nielsen, 1976; Van de Pol et al., 1977; Van der Zee and Van Riemsdijk, 1987). Most of this variation is caused by spatial variation of the soil hydraulic functions (Par. 6.3), preferential flow due to macropores in structured soils (Par. 6.5) or unstable wetting fronts in unstructured soils (Par. 6.4). In many cases it will not be possible to determine the variation (including the correlations) of all the physical parameters. One approach is to measure for a period of time the solute concentrations in the soil profile and drainage water and apply calibration or inverse modelling to determine 'effective' transport parameters (Groen, 1997). Another approach is the use of Monte Carlo simulations, where the variation of the transport parameters is derived from comparable fields (Boesten and Van der Linden, 1991). Jury (1982) proposed to use transfer functions, which don't explicitly describe the transport processes within the soil, but just describe the relation between solutes that enter and that leave a soil profile. Some limitations of the transfer function approach are that it requires a field experiment for calibration and that extrapolation to other circumstances is risky because of its stochastic rather than physical basis. SWAP confines to the physical processes in order to be flexible in parameter input and allow the simulation of all kind of design and management scenario's. The spatial variability can be taken into account by calibration, inverse modelling or Monte Carlo simulation.

SWAP is focused on the transport of salts, pesticides and other solutes that can be described with relatively simple kinetics. Processes that are not considered in SWAP are:

- volatilization and gas transport
- transport of non-mixing or immiscible fluids (e.g. oil and water)
- chemical equilibria of various solutes (e.g. between Na^+ , Ca^{2+} and Mg^{2+})

- chemical and biological chain reactions (e.g. mineralization, nitrification)

In case of advanced pesticide transport, including volatilization and kinetic adsorption, SWAP can be used in combination with the model PESTLA (Van den Berg and Boesten, 1998) and PEARL (Leistra et al., 2000; Tiktak et al., 2000). For nutrient transport (nitrogen and phosphorus), SWAP can be used in combination with the model ANIMO (Rijtema et al., 1997; Kroes and Roelsma, 1998).

First we describe the transport processes that are considered in SWAP. Next we discuss the applied boundary conditions. Finally we consider how SWAP deals with solute transport in water repellent soils and in cracked clay soils.

8.2 Basic equations

8.2.1 Transport processes

The three main solute transport mechanisms in soil water are diffusion, convection and dispersion. *Diffusion* is solute transport which is caused by the solute gradient. Thermal motion of the solute molecules within the soil solution cause a net transport of molecules from high to low concentrations. The solute flux J_{dif} ($\text{g cm}^{-2} \text{d}^{-1}$) is generally described by Fick's first law:

$$J_{\text{dif}} = -\theta D_{\text{dif}} \frac{\partial c}{\partial z} \quad (8.1)$$

with D_{dif} the diffusion coefficient ($\text{cm}^2 \text{d}^{-1}$) and c the solute concentration in soil water (g cm^{-3}). D_{dif} is very sensitive to the actual water content, as it strongly affects the solute transport path and the effective cross-sectional transport area. In SWAP we employ the relation proposed by Millington and Quirk (1961):

$$D_{\text{dif}} = D_w \frac{\theta^{7/3}}{\phi_{\text{por}}^2} \quad (8.2)$$

with D_w the solute diffusion coefficient in free water ($\text{cm}^2 \text{d}^{-1}$) and ϕ_{por} the soil porosity ($\text{cm}^3 \text{cm}^{-3}$).

The bulk transport of solutes occurs when solutes are carried along with the moving soil water. The mean flux of this transport is called the *convective* flux, J_{con} ($\text{g cm}^{-2} \text{d}^{-1}$), and can be calculated from the average soil water flux:

$$J_{\text{con}} = qc \quad (8.3)$$

When describing water flow, we usually consider the Darcy flux q (cm d^{-1}), which is averaged over a certain cross section. In case of solute transport, we need to consider the water velocity variation between pores of different size and geometry and also the water velocity variation inside a pore itself. The variety of water velocities cause some solutes to advance faster than the average solute front, and other solutes to advance slower. The overall effect will be that steep solute fronts tends to smoothen or to disperse. Solutes seem to flow from high to low concentrations. If the time required for solutes to mix in the transverse direction is small, compared to the time required for solutes to move in the flow

direction by mean convection, the *dispersion* flux J_{dis} ($\text{g cm}^{-2} \text{d}^{-1}$) is proportional to the solute gradient (Bear, 1972):

$$J_{\text{dis}} = -\theta D_{\text{dis}} \frac{\partial \theta}{\partial z} \quad (8.4)$$

with D_{dis} the dispersion coefficient ($\text{cm}^2 \text{d}^{-1}$). Under laminar flow conditions D_{dis} itself is proportional to the pore water velocity $v = q/\theta$ (Bolt, 1979):

$$D_{\text{dis}} = L_{\text{dis}} |v| \quad (8.5)$$

with L_{dis} the dispersion length (cm). Dispersion length depends on the scale over which the water flux and solute convection are averaged. Typical values of L_{dis} are 0.5 - 2.0 cm in packed laboratory columns and 5-20 cm in the field, although they can be considerably larger in regional groundwater transport (Jury et al., 1991). Unless water is flowing very slowly through repacked soil, the dispersion flux is usually much larger than the diffusion flux.

The total solute flux J ($\text{g cm}^{-2} \text{d}^{-1}$) is therefore described by:

$$J = J_{\text{dif}} + J_{\text{con}} + J_{\text{dis}} = qc - \theta (D_{\text{dif}} + D_{\text{dis}}) \frac{\partial c}{\partial z} \quad (8.6)$$

| <i>Model input</i> | | | |
|--------------------|-------------|--|----------------|
| <i>Variable</i> | <i>Code</i> | <i>Description</i> | <i>Default</i> |
| D_w | DDIF | solute diffusion coefficient in free water ($\text{cm}^2 \text{d}^{-1}$) | 0.0 |
| | LDIS | solute dispersion length (cm) | 5.0 |

8.2.2 Continuity and transport equation

By considering conservation of mass in an elementary volume, we may derive the continuity equation for solute transport:

$$\frac{\partial X}{\partial t} = -\frac{\partial J}{\partial z} - S_s \quad (8.7)$$

with X being the total solute concentration in the soil system (g cm^{-3}) and S_s the solute sink term ($\text{g cm}^{-3} \text{d}^{-1}$) accounting for decomposition and uptake by roots.

The solutes may be dissolved in the soil water and/or may be adsorbed to organic matter or to clay minerals:

$$X = \theta c + \rho_b Q \quad (8.8)$$

with ρ_b being the dry soil bulk density (g cm^{-3}) and Q the amount adsorbed (g g^{-1}). The adsorption isotherm describes the amount of solutes adsorbed in equilibrium with the dissolved concentration. At this stage we will assume instantaneous equilibrium between c and Q and use the non-linear Freundlich equation, which is a flexible function for many organic and inorganic solutes. However the mobile-immobile concept as implemented in SWAP, allows the transfer of solutes from the dissolved state to the adsorbed state and vice versa at a certain rate (Par. 6.4 and 8.3). Freundlich adsorption can be written as:

$$Q = K_f c_{\text{ref}} \left(\frac{c}{c_{\text{ref}}} \right)^{N_f} \quad (8.9)$$

with K_f the Freundlich coefficient ($\text{cm}^3 \text{g}^{-1}$), N_f is the Freundlich exponent (-) and c_{ref} is a reference value of the solute concentration (g cm^{-3}) which is used to make N_f dimensionless.

The solute sink term S_s can be written as:

$$S_s = \mu(\theta c + \rho_b Q) + K_r S c \quad (8.10)$$

where μ is the first order rate coefficient of transformation (d^{-1}), K_r is the root uptake preference factor (-) and S the root water extraction rate (d^{-1}). At the right hand side of Eq. (8.10), the first term accounts for linear decomposition and the second term for root uptake proportional to water uptake. K_r accounts for positive or negative selection of solute ions relative to the amount of soil water that is extracted.

The coefficient μ is affected by soil temperature, water content and depth. Analogous to Boesten and Van der Linden (1991), SWAP calculates μ from:

$$\mu = f_T f_\theta f_z \mu_{\text{ref}} \quad (8.11)$$

in which f_T is a soil temperature factor (-), f_θ and f_z are reduction factors (-) accounting for the effect of soil water content and soil depth, and μ_{ref} (d^{-1}) is μ at reference conditions (e.g. soil from the plough layer at 20 °C and at suction $h = -100$ cm).

The factor f_T is described according to Boesten (1986) as:

$$f_T = e^{\gamma_T (T-20)} \quad (8.12)$$

where γ_T is a parameter ($^{\circ}\text{C}^{-1}$), and T is the soil temperature in $^{\circ}\text{C}$.

Wolfe et al. (1990) describe the importance of the water content in transformation processes. Realizing that it is a large simplification, in SWAP we adopt the relation as proposed by Walker (1974) :

$$f_\theta = \left(\frac{\theta}{\theta_{\text{ref}}} \right)^B \quad \text{with} \quad f_\theta \leq 1.0 \quad (8.13)$$

where θ_{ref} is θ at $h = -100$ cm and B is a constant (-).

The transformation reduction factor for soil depth, f_z , should be derived from in situ measurements. The user may specify f_z as function of soil depth in the input file.

Combination of Eq. (8.6), (8.7), (8.8), and (8.10), yields the transport equation applied in SWAP which is valid for dynamic, one-dimensional, convective-dispersive mass transport, including non-linear adsorption, linear decay and proportional root uptake in unsaturated/saturated soil (Van Genuchten and Cleary, 1979; Nielsen et al., 1986; Boesten and Van der Linden, 1991):

$$\frac{\partial(\theta c + \rho_b Q)}{\partial t} = -\frac{\partial(qc)}{\partial z} + \frac{\partial\left[\theta(D_{\text{dif}} + D_{\text{dis}})\frac{\partial c}{\partial z}\right]}{\partial z} - \mu(\theta c + \rho_b Q) - K_r S c \quad (8.14)$$

An explicit, central finite difference scheme is used to solve Eq. (8.14):

$$\frac{\theta_i^{j+1} c_i^{j+1} + \rho_b Q_i^{j+1} - \theta_i^j c_i^j - \rho_b Q_i^j}{\Delta t^j} = \frac{q_{i-1/2}^j c_{i-1/2}^j - q_{i+1/2}^j c_{i+1/2}^j}{\Delta z_i} + \frac{1}{\Delta z_i} \left[\frac{\theta_{i-1/2}^j D_{i-1/2}^j (c_{i-1}^j - c_i^j)}{\Delta z_u} - \frac{\theta_{i+1/2}^j D_{i+1/2}^j (c_i^j - c_{i+1}^j)}{\Delta z_\ell} \right] - \mu_i^j (\theta_i^j c_i^j + \rho_b Q_i^j) - K_r S_i^j c_i^j \quad (8.15)$$

where D ($= D_{\text{dif}} + D_{\text{dis}}$) is the overall dispersion coefficient ($\text{cm}^2 \text{d}^{-1}$); the superscript j denotes the time level, subscript i the node number and subscripts $i-1/2$ and $i+1/2$ refer to linearly interpolated values at the upper and lower compartment boundary, respectively. Compared to an implicit, iterative scheme, above explicit scheme has the advantage that incorporation of non-linear adsorption, mobile/immobile concepts, and other non-linear processes is relatively easy. In order to ensure stability of the explicit scheme, the time step Δt^j should meet the criterium (Van Genuchten and Wierenga, 1974):

$$\Delta t^j \leq \frac{\Delta z_i^2 \theta_i^j}{2D_i^j} \quad (8.16)$$

This stability criterium applies to non-sorbing substances and is therefore also safe for sorbing substances.

| <i>Model input</i> | | | |
|-----------------------|-------------|--|----------------|
| <i>Variable</i> | <i>Code</i> | <i>Description</i> | <i>Default</i> |
| K_f | KF | Freundlich adsorption coefficient ($\text{cm}^3 \text{mg}^{-1}$) | |
| N_f | FREXP | Freundlich exponent (-) | |
| c_{ref} | CREF | reference solute concentration for adsorption (mg cm^{-3}) | |
| K_r | TSCF | relative uptake of solutes by roots | 0.0 |
| μ_{ref} | DEC POT | decomposition rate at reference conditions (d^{-1}) | |
| γ_T | GAMPAR | factor for reduction of decomposition due to temperature ($^{\circ}\text{C}^{-1}$) | |
| θ_{ref} | RTHETA | minimum water content for maximum decomposition ($\text{cm}^3 \text{cm}^{-3}$) | |
| B | BEXP | exponent for reduction of decomposition due to dryness (-) | |
| f_z | FDEPTH | reduction of ref. decomposition in each soil layer | |

8.3 Boundary conditions

As *initial condition*, the user needs to specify the solute concentrations, c_i (g cm^{-3}), in the soil water and the average solute concentration, c_{gr} (g cm^{-3}), in the groundwater.

For the *top boundary condition*, the solute concentrations in irrigation and rain water, c_{irr} and c_{prec} (g cm^{-3}), need to be specified. During evaporation no solutes enter the soil profile

at the surface. During infiltration, the solute concentration of water that enters the soil profile at the top, c_{pond} (g cm^{-3}), is affected by the ponding layer and its concentration at the former time step, the solute amounts coming in by rain and irrigation, and the solute amounts transported laterally to cracks:

$$c_{\text{pond}}^j = \frac{(P_{\text{net}}^j c_{\text{prec}} + I_{\text{net}}^j c_{\text{irr}}) \Delta t^j + h_{\text{pond}}^{j-1} c_{\text{pond}}^{j-1}}{h_{\text{pond}}^j - (q_{\text{top}} + q_{\text{lat}}) \Delta t^j} \quad (8.17)$$

where P_{net} is the net precipitation rate (cm d^{-1} , see Par. 3.3), I_{net} is the net irrigation rate (cm d^{-1}), h_{pond} is the height of water ponding on the soil surface, q_{top} is the water flux at the soil surface (cm d^{-1} , positive upward) and q_{lat} is the water flux flowing to cracks (cm d^{-1} , see Par. 8.5). The solute flux J_{top} (g cm^{-2}) entering the soil at the surface, equals:

$$J_{\text{top}} = q_{\text{top}} c_{\text{pond}} (1.0 - A_c) \quad (8.18)$$

where A_c is the relative crack area ($\text{cm}^2 \text{cm}^{-2}$). The solute flux that enters the cracks is described in Par. 6.5.3.5.

For the *drainage boundary condition*, SWAP assumes that the lateral drainage flux leaves the soil profile laterally at the lowest compartment. During drainage ($q_{\text{drain}} > 0$), the solute flux J_{drain} (g cm^{-2}) that leaves the one-dimensional soil profile is calculated as:

$$J_{\text{drain}} = q_{\text{drain}} c_n \quad (8.19)$$

where c_n is the solute concentration in the lowest compartment. During infiltration ($q_{\text{drain}} < 0$), J_{drain} follows from:

$$J_{\text{drain}} = q_{\text{drain}} c_{\text{gr}} \quad (8.20)$$

where c_{gr} is the average solute concentration in the groundwater (g cm^{-3}).

For the *bottom boundary condition*, SWAP uses the flux through the bottom of the soil profile q_{bot} (cm d^{-1} , see Chapter 5). In case of upward flow ($q_{\text{bot}} > 0$), the solute flux J_{bot} (g cm^{-2} , positive is upwards) equals:

$$J_{\text{bot}} = q_{\text{bot}} c_{\text{gr}} \quad (8.21)$$

If q_{bot} is directed downwards ($q_{\text{bot}} < 0$), the solute flux J_{bot} (g cm^{-2}) equals:

$$J_{\text{bot}} = q_{\text{bot}} c_n \quad (8.22)$$

| <i>Model input</i> | | | |
|--------------------|-------------|--|----------------|
| <i>Variable</i> | <i>Code</i> | <i>Description</i> | <i>Default</i> |
| c_i | CML | initial solute concentrations (mg cm^{-3}) | |
| c_{prec} | CPRE | solute concentration in precipitation (mg cm^{-3}) | 0.0 |
| c_{irr} | IRCONC | solute concentration in irrigation water (mg cm^{-3}) | |
| c_{gr} | CDRAIN | solute concentration in groundwater (mg cm^{-3}) | |

8.4 Mobile/immobile solute transport

The water flow in soils with mobile/immobile flow has been described in Par. 6.4. In the mobile region the transport of solutes is affected by convection, dispersion, adsorption, decomposition and root water uptake (Figure 30). These processes are included in the solute transport equation, but corrections are needed as only the soil volume fraction F_{mob} is mobile:

$$\frac{\partial \left(\theta c + F_{\text{mob}} \rho_b K_f c_{\text{ref}} \left(\frac{c}{c_{\text{ref}}} \right)^{N_f} \right)}{\partial t} = - \frac{\partial qc}{\partial z} + \frac{\partial \left(\theta D \frac{\partial c}{\partial z} \right)}{\partial z} - \mu \left(\theta c + F_{\text{mob}} \rho_b K_f c_{\text{ref}} \left(\frac{c}{c_{\text{ref}}} \right)^{N_f} \right) - K_r S_a c - G_c \quad (8.23)$$

with c the solute concentration in the mobile soil water (g cm^{-3}), ρ_b the soil dry bulk density (g cm^{-3}), K_f the Freundlich coefficient ($\text{cm}^3 \text{g}^{-1}$), c_{ref} the reference concentration for adsorption (g cm^{-3}), N_f the Freundlich exponent (-), t the time (d), D the overall dispersion coefficient ($\text{cm}^2 \text{d}^{-1}$), μ the first order rate coefficient for decomposition (d^{-1}), K_r the root uptake preference factor (-), and G_c the transfer rate of solutes from the mobile to the immobile region ($\text{g cm}^{-3} \text{d}^{-1}$). G_c contains a diffusion term and a term that accounts for solute transfer due to variation of F :

$$G_c = K_{\text{dif}} (c - c_{\text{im}}) + G_w c_x \quad (8.24)$$

with K_{dif} a solute transfer coefficient (d^{-1}) between the mobile and immobile region, c_{im} is the solute concentration in the immobile region and c_x equals c if G_w is positive (mobile region decreases) and equals c_{im} if G_w is negative (mobile region increases).

In the immobile region, water flow is absent and transport of solutes will occur by diffusion only. The roots are assumed to avoid largely the immobile regions. Hence rootwater uptake in the immobile region is small and can be neglected. The change of solute amounts in the immobile region is therefore governed by solute transfer between mobile and immobile regions and by solute decomposition:

$$\frac{\partial (1 - F_{\text{mob}}) \left(\theta_{\text{im}} c_{\text{im}} + \rho_b K_f c_{\text{ref}} \left(\frac{c_{\text{im}}}{c_{\text{ref}}} \right)^{N_f} \right)}{\partial t} = -\mu (1 - F_{\text{mob}}) \left(\theta_{\text{im}} c_{\text{im}} + \rho_b K_f c_{\text{ref}} \left(\frac{c_{\text{im}}}{c_{\text{ref}}} \right)^{N_f} \right) + G_c \quad (8.25)$$

Equations (8.23) and (8.24) are solved with the previously described explicit central finite difference scheme.

| <i>Model input</i> | | |
|-------------------------|---|----------------|
| <i>Variable Code</i> | <i>Description</i> | <i>Default</i> |
| K_{dif} KMOBIL | solute transfer between mobile and immobile parts (d^{-1}) | |

8.5 Crack solute transport

In current SWAP version solute transport in cracked clay soils can only be calculated in combination with the simple macro pore flow model (Par. 6.5.2). The transport processes incorporated are described hereafter. If you want to calculate solute transport in combination with the advanced macro pore flow model, SWAP may generate soil water fluxes which are input to the pesticide model PEARL or the nutrient model ANIMO.

The solutes that enter the cracks may originate from the precipitation directly falling into the cracks, or from runoff water when the infiltration capacity at the soil surface is exceeded ($P > I_{\max}$). The solute concentration of the water entering the cracks, c_{in} (g cm^{-3}), equals:

$$c_{\text{in}} = \frac{A_m (P - I_{\max}) c_{\text{pond}} + A_c P c_{\text{prec}}}{I_c} \quad (8.26)$$

with c_{pond} and c_{prec} solute concentrations (g cm^{-3}) of water ponding on the soil surface and of the precipitation, respectively.

When water flows down the cracks during intensive rain showers, solutes are leached out of the crack walls and transported quickly to the subsoil (e.g. Bronswijk et al., 1995). Therefore, lateral solute transfer between the soil matrix and water flowing down the cracks should be taken into account. The lateral solute transfer, $s_{\text{lat},i}$ ($\text{g cm}^{-2} \text{d}^{-1}$), for the nodes $GW_c < z < 0$ is calculated by:

$$s_{\text{lat},i} = D_{\text{lat}} I_c (c_i - c_{\text{in}}) \Delta z_i \quad (8.27)$$

where D_{lat} is the lateral transfer coefficient (cm^{-1}) and c_i the solute concentration in the soil matrix (g cm^{-3}). D_{lat} is a function of crack morphology and transmitting properties of the crack wall and has to be derived from field or laboratory measurements. The amount of solutes that enter the water reservoir in the cracks, $s_{\text{c,in}}$ ($\text{g cm}^{-2} \text{d}^{-1}$), equals:

$$s_{\text{c,in}} = I_c c_{\text{in}} + \sum_{z=GW_c}^{z=0} s_{\text{lat},i} \quad (8.28)$$

In the crack water reservoir the solutes are mixed. Part of the solutes will enter the soil matrix along the crack wall in contact with the water. Another part is transported with the bypass flow directly to the drains and/or ditches (Figure 33):

$$s_{\text{c,out}} = c_c (q_{\text{c,m}} + q_{\text{c,d}}) \quad (8.29)$$

with $s_{\text{c,out}}$ the total flux of solutes leaving the crack reservoir ($\text{g cm}^{-2} \text{d}^{-1}$) and c_c the solute concentration in the crack reservoir (g cm^{-3}).

Change of solute storage in the cracks S_c (g cm^{-2}) is straightforwardly calculated as:

$$\Delta S_c = (s_{\text{c,in}} - s_{\text{c,out}}) \Delta t \quad (8.30)$$

In the soil matrix the convection-dispersion equation is applied, as described in Par. 8.2.2. The lateral diffused solute amounts due to water flowing down the cracks, $c_{\text{lat},i}$, and the

adsorbed solutes from the water reservoir in the cracks, $q_{c,i}c_c$, are added as a source term to Eq. (8.14).

| <i>Model input</i> | | |
|----------------------|--|----------------|
| <i>Variable Code</i> | <i>Description</i> | <i>Default</i> |
| D_{lat} | DIFDES effective lateral transfer coefficient (cm^{-1}) | |

8.6 Residence time in the saturated zone

In case of heterogeneous groundwater flow or multi-level drainage, the residence time approach described in chapter 4 can be used. This paragraph describes a concept assuming a homogeneous aquifer and field drainage at one level.

In the saturated zone, prevailing soil water pressure gradients will induce a three-dimensional flow and transport pattern. A strict deterministic approach would require a coupling of the one-dimensional agrohydrological model with a two- or three-dimensional model for the saturated zone. In many situations this is not feasible due to limitations of data, time, computer resources or experience. Also the required accuracy of the analysis might not justify such a detailed approach. Therefore in SWAP a simplified approach is followed to calculate the transport of solutes to drains or ditches.

Ernst (1973) and Van Ommen (1985) showed that the breakthrough curve of a field with fully penetrating drainage canals, is identical to the breakthrough curve of a reservoir with complete mixing. This is also valid if linear adsorption and transformation at first order rate take place (Van Ommen, 1985). Linear adsorption might be described by:

$$Q = k_{ads} c_{gr} \quad (8.31)$$

where k_{ads} is the linear adsorption coefficient in the saturated zone ($\text{cm}^3 \text{g}^{-1}$) and c_{gr} is the average solute concentration in the groundwater (g cm^{-3}). Numerical analysis by Duffy and Lee (1992) showed that dispersion in the saturated zone has only a minor effect for $L_{drain}/d_{aquif} \geq 10$, where L_{drain} is the distance between the drainage canals (cm) and d_{aquif} the thickness of the aquifer (cm). Generally L_{drain}/d_{aquif} will be around 10 or larger, therefore dispersion might be ignored.

In order to derive the breakthrough curve, we will use the similarity between breakthrough curves of drained fields and mixed reservoirs. Starting point is the solute transport equation of the unsaturated zone, Eq. (8.14). Replacement of non-linear adsorption by linear adsorption, and omission of dispersion and root water uptake, results in the mass balance equation of the saturated zone:

$$\frac{\partial(\theta_s c_{gr} + \rho_b k_{ads} c_{gr})}{\partial t} = \frac{q_{drain}}{d_{aquif}} (c_{in} - c_{gr}) - \mu_{gr} (\theta_s c_{gr} + \rho_b k_{ads} c_{gr}) \quad (8.32)$$

where θ_s is the saturated water content ($\text{cm}^3 \text{cm}^{-3}$), q_{drain} is the drainage flux (cm d^{-1}), c_{in} is the solute concentration of water percolating from the unsaturated zone (g cm^{-3}) and μ_{gr} is the first order rate coefficient for transformation in the saturated zone (d^{-1}). Eq. (8.32) applies to a drainage situation ($q_{drain} > 0$). In case of infiltration ($q_{drain} < 0$), SWAP assumes the infiltrating water from the drainage system to be solute free, and Eq. (8.32) transforms to:

$$\frac{\partial(\theta_s c_{gr} + \rho_b k_{ads} c_{gr})}{\partial t} = \frac{q_{drain}}{d_{aquif}} c_{gr} - \mu_{gr} (\theta_s c_{gr} + \rho_b k_{ads} c_{gr}) \quad (8.33)$$

Eq. (8.32) and (8.33) are discretized as an explicit, forward difference scheme. For instance, SWAP discretizes Eq. (8.32) as follows:

$$\frac{c_{gr}^{j+1} - c_{gr}^j}{\Delta t^j} (\theta_s + \rho_b k_{ads}) = \frac{q_{drain}^j}{d_{aquif}} (c_{in}^j - c_{gr}^j) - \mu_{gr} (\theta_s c_{gr}^j + \rho_b k_{ads} c_{gr}^j) \quad (8.34)$$

The stability of Eq. (8.34) depends on the size of the time step. In SWAP, the time step will be limited by the soil water dynamics and solute transport near the soil surface, and no stability problems are expected. The boundary conditions that apply to the saturated zone, are included in (8.32) and (8.33).

9 Soil temperature

J.C. van Dam

9.1 Introduction

Soil temperature affects many physical, chemical and biological processes in the top soil, for instance the surface energy balance, soil hydraulic properties, decomposition rate of solutes and growth rate of roots. Currently SWAP uses the soil temperatures only to adjust the solute decomposition rate, but other temperature relations may readily be included. SWAP calculates the soil temperatures either analytically or numerically. In the following sections the heat flow equations and the applied analytical and numerical solutions are discussed.

9.2 Temperature conductance equation

Commonly, heat flow by radiation, convection and conduction is modeled by the conduction equation alone. According to De Vries (1975), the rate of heat transfer by water vapour diffusion is small and proportional to the temperature gradient. Therefore, such diffusion might be taken into account by slightly increasing the soil thermal diffusivity. This approach is followed in SWAP as well. Apparent thermal properties rather than real thermal properties are assumed to account for both conductive and non-conductive heat flow.

The one-dimensional soil heat flux, q_{heat} ($\text{J cm}^{-2} \text{d}^{-1}$), is described as:

$$q_{\text{heat}} = -\lambda_{\text{heat}} \frac{\partial T}{\partial z} \quad (9.1)$$

where λ_{heat} is the thermal conductivity ($\text{J cm}^{-1} \text{°C}^{-1} \text{d}^{-1}$) and T is the soil temperature (°C).

Conservation of energy results in:

$$C_{\text{heat}} \frac{\partial T}{\partial t} = \frac{-\partial q_{\text{heat}}}{\partial z} \quad (9.2)$$

where C_{heat} is the soil heat capacity ($\text{J cm}^{-3} \text{°C}^{-1}$).

Combination of Eq. (9.1) and (9.2) yields the differential equation for soil heat flow:

$$C_{\text{heat}} \frac{\partial T}{\partial t} = \frac{\partial \left(\lambda_{\text{heat}} \frac{\partial T}{\partial z} \right)}{\partial z} \quad (9.3)$$

9.3 Analytical solution (sinus wave)

If the values of λ and C_h are considered to be constant with depth and time, the soil thermal diffusivity D_{heat} ($\text{cm}^2 \text{d}^{-1}$) can be defined as:

$$D_{\text{heat}} = \frac{\lambda_{\text{heat}}}{C_{\text{heat}}} \quad (9.4)$$

and Eq. (9.3) simplifies to:

$$\frac{\partial T}{\partial t} = D_{\text{heat}} \frac{\partial^2 T}{\partial z^2} \quad (9.5)$$

This partial differential equation can be solved for simple boundary conditions, assuming D_{heat} constant or very simple functions for D_{heat} (Van Wijk, 1966; Feddes, 1971; Wesseling, 1987). A commonly used top boundary condition is a sinusoidally varying soil surface temperature during the year:

$$T(0, t) = T_{\text{mean}} + T_{\text{ampl}} \sin\left(\frac{1}{2}\pi + \omega(t - t_{\text{max}})\right) \quad (9.6)$$

where T_{mean} is the mean yearly temperature ($^{\circ}\text{C}$), T_{ampl} is the wave amplitude ($^{\circ}\text{C}$), $\omega = 2\pi / \tau$ is the angular frequency, where τ is the period of the wave (365 d), t is time (d) starting January 1st and t_{max} equals t when the temperature reaches its maximum. In case of a semi-infinite soil profile with constant D_{heat} and subject to the top boundary condition according to Eq. (9.6), the solution to Eq. (9.5) is:

$$T(z, t) = T_{\text{mean}} + T_{\text{ampl}} e^{\frac{z}{d_{\text{temp}}}} \sin\left(\frac{1}{2}\pi + \omega(t - t_{\text{max}}) + \frac{z}{d_{\text{temp}}}\right) \quad (9.7)$$

where d_{temp} is the damping depth (cm), which equals:

$$d_{\text{temp}} = \sqrt{\frac{2D_{\text{heat}}}{\omega}} \quad (9.8)$$

Model input

| <i>Variable Code</i> | <i>Description</i> |
|--------------------------|---|
| SWHEA | Switch for simulation of heat transport |
| SWCALT | Switch for method: 1 = analytical method, 2 = numerical method |
| T_{ampl} TAMPLI | Amplitude of annual temperature wave at soil surface ($^{\circ}\text{C}$) |
| T_{mean} TMEAN | Mean annual temperature at soil surface ($^{\circ}\text{C}$) |
| t_{max} TIMREF | Time in the year with top of sine temperature wave (d) |
| d_{temp} DDAMP | Damping depth of temperature wave in soil (cm) |

9.4 Numerical solution

In reality, λ_{heat} and C_{heat} depend on the soil moisture content and vary with time and depth. Also the soil surface temperature will deviate from a sinus wave. Therefore higher accuracy

can be reached by numerical solution of the heat flow equation. Numerical discretization of Eq. (9.3) is achieved in a similar way as the discretization of the water flow equation (Eq. (2.3)). SWAP employs a fully implicit finite difference scheme as described by Wesseling (1998). The soil heat flow equation is written as:

$$C_i^{j+1} (T_i^{j+1} - T_i^j) = \frac{\Delta t^j}{\Delta z_i} \left[\lambda_{i-\frac{1}{2}}^{j+\frac{1}{2}} \frac{T_{i-1}^{j+1} - T_i^{j+1}}{\Delta z_u} - \lambda_{i+\frac{1}{2}}^{j+\frac{1}{2}} \frac{T_i^{j+1} - T_{i+1}^{j+1}}{\Delta z_\ell} \right] \quad (9.9)$$

where superscript j denotes the time level, subscript i is the node number, $\Delta z_u = z_{i+1} - z_i$ and $\Delta z_\ell = z_i - z_{i+1}$ (see Figure 3). The coefficients C_{heat} and λ_{heat} are not affected by the temperature, which makes Eq. (9.9) linear.

Both volumetric heat capacity and thermal conductivity depend on the soil composition. The volumetric heat capacity is calculated as weighted mean of the heat capacities of the individual components (De Vries, 1963):

$$C_{\text{heat}} = f_{\text{sand}} C_{\text{sand}} + f_{\text{clay}} C_{\text{clay}} + f_{\text{organic}} C_{\text{organic}} + \theta C_{\text{water}} + f_{\text{air}} C_{\text{air}} \quad (9.10)$$

where f and C on the right hand side of Eq. (9.10) are respectively the volume fraction ($\text{cm}^3 \text{cm}^{-3}$) and volumetric heat capacity ($\text{J cm}^{-3} \text{ }^\circ\text{C}^{-1}$) of each component. Table 4 gives values of the volumetric heat capacity for the different soil components.

Table 4 Volumetric heat capacity and thermal conductivity of the soil components.

| Component | Volumetric heat capacity ($\text{J cm}^{-3} \text{ }^\circ\text{C}^{-1}$) | Thermal conductivity ($\text{J cm}^{-1} \text{ }^\circ\text{C}^{-1} \text{ d}^{-1}$) |
|------------|--|---|
| Sand | 2.128 | 7603 |
| Clay | 2.385 | 2523 |
| Organic | 2.496 | 216 |
| Water | 4.180 | 492 |
| Air (20°C) | 1.212 | 22 |

In order to calculate C_{heat} (and λ_{heat}) in De Vries model, we need to input the percentage (by volume) of sand and clay, denoted VP_{sand} and VP_{clay} respectively. VP_{sand} and VP_{clay} are taken as percentages of the total *solid* soil matter and may differ for each soil layer. The total volume fraction of solid matter is given by:

$$\theta_{\text{solid}} = 1 - \theta_{\text{sat}} \quad (9.11)$$

where θ_{sat} is the saturated volumetric water content. The volume fraction of air is equal to the saturated minus the actual water content:

$$f_{\text{air}} = \theta_{\text{sat}} - \theta \quad (9.12)$$

f_{sand} , f_{clay} and f_{organic} are then calculated by:

$$f_{\text{sand}} = \frac{VP_{\text{sand}}}{100} \theta_{\text{solid}} \quad (9.13)$$

$$f_{\text{clay}} = \frac{VP_{\text{clay}}}{100} \theta_{\text{solid}} \quad (9.14)$$

$$f_{\text{organic}} = \theta_{\text{solid}} - f_{\text{sand}} - f_{\text{clay}} \quad (9.15)$$

where Eq. (9.15) assumes that solid matter that is not sand or clay, is organic.

As shown in Table 4, the thermal conductivities of the various soil components differ very markedly. Hence the space-average thermal conductivity of a soil depends upon its mineral composition and organic matter content, as well as the volume fractions of water and air. Since the thermal conductivity of air is very much smaller than that of water or solid matter, a high air content (or low water content) corresponds to a low thermal conductivity. The components which affect thermal conductivity λ_{heat} are the same as those which affect the volumetric heat capacity C_{heat} , but the measure of their effect is different so that the variation in λ_{heat} is much greater than of C_{heat} . In the normal range of soil wetness experienced in the field, C_{heat} may undergo a threefold or fourfold change, whereas the corresponding change in λ_{heat} may be hundredfold or more. One complicating factor is that, unlike heat capacity, thermal conductivity is sensitive not merely to the volume composition of a soil but also to the sizes, shapes, and spatial arrangements of the soil particles (Hillel, 1980). SWAP employs the method of De Vries (1975) as applied by Ten Berge (1986) to calculate the thermal conductivity. A clear description of the method is given in Ashby et al. (1996). The method requires no extra input data.

At the soil surface the daily average air temperature T_{avg} is used as boundary condition. At the bottom of the soil profile SWAP assumes $q_{\text{heat}} = 0.0$.

Application of Eq. (9.9) to each node and including the boundary conditions at the top and bottom of the soil profile, results in a tri-diagonal system of equations, as shown in Annex G. SWAP solves the equations with *LU*-decomposition for tridiagonal systems (Press et al., 1989).

Model input

| <i>Variable</i> | <i>Code</i> | <i>Description</i> |
|-------------------------------------|-------------|--|
| | SWCALT | Switch for method: 1 = analytical method, 2 = numerical method |
| T_i | TSOIL | initial temperature as function of soil depth ZH (°C) |
| <i>Specify for each soil layer:</i> | | |
| VP_{sand} | PSAND | Sand fraction in soil layer (g g ⁻¹ mineral parts) |
| VP_{silt} | PSILT | Silt fraction in soil layer (g g ⁻¹ mineral part) |
| VP_{clay} | PCLAY | Clay fraction in soil layer (g g ⁻¹ mineral part) |
| VP_{organic} | ORGMAT | Organic fraction in soil layer (g g ⁻¹ dry soil) |

10 Management aspects

J.G. Kroes, J.C. van Dam

10.1 Introduction

A dynamic model like SWAP can be applied in various ways to analyse water management aspects. The applications in this field may range from a simple static impression of a seasonal water balance to detailed assistance in timing aspects of fertilizer strategies. Due to the large range of its applications this chapter does not pretend to give a complete picture of all management aspects, but focusses on the most important items. Examples are given for: irrigation, drainage, land use and surface water management.

10.2 Sprinkling and surface irrigation

Water balance simulation models are applied for irrigation scheduling in order to develop optimal irrigation schedules by evaluating alternative water application strategies. A common objective at irrigation scheduling is to maximize net return. Other objectives may be: minimize irrigation costs, maximize yield, optimally distribute a limited water supply, minimize groundwater and surface water pollution, or optimize the production from a limited irrigation system capacity. In semi-arid and arid zones irrigation may cause salinity problems. If natural drainage for leaching is not present, artificial drainage has to be installed to create favourable moisture and salinity conditions in the root zone. SWAP can be used to support the design of a combined irrigation and drainage system, including sub-irrigation.

The appropriate management objective depends on the available water amounts and the irrigation costs. In many cases it is optimal to produce near maximum yields on the entire area that can be irrigated. Then the prime objective is to prevent crop water stress throughout the growing season. In case water supplies do not allow irrigation for maximum yield, or irrigation costs are that high, that the economic optimum level of irrigation is below the yield maximizing level, deficit irrigation must be practised. The objective of irrigation management under these conditions is to maximize the economic returns to water and generally three decision criteria are involved:

- how much area to irrigate;
- which crops to plant;
- how to distribute the available supply over the irrigable area during the season.

If land amount is limiting and water is available but expensive, net returns to land are to be optimized: maximum economic efficiency occurs when the cost of an additional unit of water just equals the value of the resulting crop yield increment.

10.2.1 Irrigation scheduling options

In SWAP irrigations may be prescribed at fixed times or scheduled according to a number of criteria. Also a combination of irrigation prescription and scheduling is possible. The scheduling criteria define the time when irrigation should take place, as well as the irrigation depth. A specified combination of timing and depth criteria is valid from a user defined date in the cropping season until the end of crop growth. Both timing and depth criteria may be dynamic i.e. be defined as a function of crop development stage. The reduced growth rate and final yield due to soil moisture stress will depend on the time of occurrence of the stress during the growth cycle. If the stress period occurs during rapid plant growth and high water demands, or when reproductive processes are critical, the effect of stress will be larger than during stress periods of similar length when growth and development are slow, such as near maturity.

The irrigation scheduling criteria applied in SWAP are similar to the criteria in CROPWAT (Smith, 1992), IRSIS (Raes et al., 1988), and the Hydra Decision Support System for Irrigation Water Management (Jacucci et al., 1994).

10.2.2 Timing criteria

Five different timing criteria can be selected to generate an irrigation schedule:

10.2.2.1 Allowable daily stress

Irrigation is applied whenever due to dryness conditions the actual transpiration rate T_a drops below a predetermined fraction f_1 (-) of the potential transpiration rate T_p :

$$T_a \leq f_1 T_p \quad (10.1)$$

This option is relevant for sub-optimal (deficit) irrigation when the water supply is limited.

10.2.2.2 Allowable depletion of readily available water in the root zone

Irrigation is applied whenever the water depletion in the root zone is larger than a fraction f_2 (-) of the readily available water amount:

$$(U_{\text{field}} - U_a) \geq f_2 (U_{\text{field}} - U_{h3}) \quad (10.2)$$

where U_a (cm) is the actual water storage in the root zone, U_{field} (cm) is the root zone water storage at $h = -100$ cm (field capacity), and U_{h3} (cm) is the root zone water storage at $h = h_3$, where root water extraction starts being reduced due to drought stress (Figure 5).

U_a is calculated by integrating numerically the water content in the rooting layer. This option is useful for optimal scheduling where irrigation is always secured before conditions of soil moisture stress occur. For deficit irrigation purposes, stress can be allowed by specifying $f_2 > 1$.

10.2.2.3 Allowable depletion of totally available water in the root zone

Irrigation is applied whenever the depletion is larger than a fraction f_3 (-) of the total available water amount between field capacity and permanent wilting point:

$$(U_{\text{field}} - U_a) \geq f_3 (U_{\text{field}} - U_{h4}) \quad (10.3)$$

where U_{h_4} is the root zone water storage at $h = h_4$, the pressure head at which root water extraction is reduced to zero (Figure 5).

10.2.2.4 Allowable depletion amount of water in the root zone

Irrigation is applied whenever a predetermined water amount, ΔU_{\max} (cm), is extracted below field capacity:

$$U_a \leq U_{\text{field}} - \Delta U_{\max} \quad (10.4)$$

This option is useful in case of high frequency irrigation systems (drip).

10.2.2.5 Critical pressure head or moisture content at sensor depth

Irrigation is applied whenever moisture content or pressure head at a certain depth in the root zone drops below a prescribed threshold value θ_{\min} ($\text{cm}^3 \text{cm}^{-3}$) or h_{\min} (cm):

$$\theta_{\text{sensor}} \leq \theta_{\min} \quad \text{or} \quad h_{\text{sensor}} \leq h_{\min} \quad (10.5)$$

This option may be used to verify field experiments or to simulate irrigation with automated systems.

10.2.3 Application depth criteria

Two irrigation depth criteria can be selected:

10.2.3.1 Back to Field Capacity (+/- specified amount)

The soil water content in the root zone is brought back to field capacity. An additional irrigation amount can be defined to leach salts, while the user may define a smaller irrigation amount when rainfall is expected. This option is useful in case of sprinkler and micro irrigation systems, which allow variation of irrigation application depth.

10.2.3.2 Fixed irrigation depth

A specified amount of water is applied. This option applies to most gravity systems, which allow little variation in irrigation application depth.

10.3 Design of field drainage

Drainage design can be evaluated using the equations of Hooghoudt and Ernst (paragraph 4.2.2). Using these formulae one may analyse the impact of various physical parameters (soil, crop, climate) on drain spacing and drain depth. More examples are extensively elaborated by Ritzema (1994).

Combining options for irrigation (paragraph 10.2) and salinity (chapter 8) one may analyse the relation between irrigation, drainage and field scale soil salinity.

This may be further elaborated towards the impact on crop production using the Wofost-options described in paragraph 7.3

10.4 Land use

The impact of land use alternatives can be analysed in many ways. Some examples are:

- introduce different crops and crop-rotations;
- change phenological parameters, such as time of emergence and/or harvest;
- vary temperature sums that determine crop development;

This can be carried out by changes on input parameters (paragraph 11.1) for simple or detailed crop module (for details see respectively paragraph 7.2 or 7.3).

10.5 Surface water management

The interaction between groundwater and surface water system may be analysed using the various options described in chapter 4. Examples of management strategies are:

- Change variations in the dynamics of surface water levels and analyse its impact on groundwater, and agricultural management or growth of natural vegetations;
- Change the inlet or outlet of a region and its corresponding surface water levels;
- Analyse impacts of weather extremes (dry or wet);
- Analyse a change in the variation of weather dynamics on surface and groundwater levels;
- Introduce shallow systems (trenches, ditches) and analyse its impact on the soil water balance;
- Simulate effects of poor maintenance of surface waters (tube drains or ditches) by adjusting drainage resistances;
- reconstruct drainage systems

For polder systems or other areas where a uniform waterlevel occurs in a larger area this can be carried out with the extended drainage option (paragraph 4.2.5). In other areas special care should be taken about the influence of the lower boundary condition on groundwater and surface water levels. If this influence is very large then it is recommended to use a regional groundwater model.

11 Program operation

M. Groenendijk, J.G. Kroes

11.1 Program input

A summary of all input files is given in Table 5, a more detailed description of these files is given in Appendix 6. Some files are required, other files are optional. The extensions of the files are fixed. The names of the input files can be freely chosen and have to be specified in the *.swp file.

Table 5 Input data files

| Input file | Description | Appendix | |
|------------|---------------------------|----------|----------|
| *.swp | Main input | 7 | Required |
| *.yyy | Daily meteorological data | 8 | Required |
| *.crp | Crop growth | 9 and 10 | Optional |
| *.dra | Drainage data | 11 | Optional |

In the input files of each parameter the symbolic name, a description and an identification is given. The identification between square brackets uses the following convention:

- 1) range
- 2) unit
- 3) data type (I = Integer, R = Real, Ax = character string of x positions)

For example: [-5000 .. 100 cm, R] means: value between -5000 and +100 with a unit in cm, given as a Real datatype (which means that a dot must be added).

Ranges of all input parameters are given in Appendix 17.

General rules for the formats of input files are:

- order of variables is fixed
- free format with the structure 'VariableName' = 'value' or in a table
- comment in lines is allowed starting with '*' or '!'
- blank lines are allowed.

The meteorological data must be specified in the *.yyy file separately for each year. The extension of these files consists of the last three digits of the year. Missing values should be indicated with -99.0 or lower. The following rules apply to missing meteo data:

- missing values of rainfall are never allowed
- if potential evapotranspiration must be calculated (specified in *.swp), no missing values are allowed of the data RAD, Tmin, Tmax, HUM and WIND
- no missing values for Tmin and Tmax are allowed if a crop is present or soil temperature must be simulated
- no missing values for RAD is allowed in case the detailed crop model or the detailed grass model is active.

Violation of these rules cause program termination, after first writing the date and cause of the fatal error to the log file.

11.2 Program execution

The *.swp file and the executable need to be present in the same directory. All other input files should exist on the directory, which has been specified in the file *.swp

A simulation can be executed by entering the name of the executable of SWAP from the command line, optionally followed by the name of the main input file. For the example file in Appendix 7 (Hupsel.swp) this would be:

```
Swap.exe Hupsel
```

Indirectly a simulation can be executed by entering the name of a batch file referring to the SWAP executable and the *.swp file.

In the *.swp file the names of the other files are given and also their location. Therefore it is possible to have a separate data directory with meteorological, crop and drainage data.

Output files will be generated in the same directory as the main input file. Also the log file will be placed here. This file (swap.log) contains a copy of the *.swp file and, errors and warnings, and when the simulation is successful, the following line:

```
'Swap simulation succesfully terminated!'
```

There are two types of warnings: fatal errors, the simulation will be terminated, and warnings with the advise to adapt the input data.

A third type of errors is generated by the utility library TTUTIL (Kraalingen & Rappoldt, 2000), and these handle the formats of the input data..

11.3 Program output

Table 6 Output data files

| Output file | Description | Optional |
|-------------|-----------------------------------|----------|
| *.bal | Short water and solute balance | No |
| *.blc | Extended water balance | Yes |
| *.inc | Incremental water balance | No |
| *.wba | Cummulative water balance | No |
| *.sba | Cummulative solute balance | Yes |
| *.ate | Soil temperatures | Yes |
| *.vap | Soil profiles | Yes |
| *.irg | Irrigation | Yes |
| *.crp | Crop growth | No |
| *.drf | Extended drainage components | Yes |
| *.swb | Surface water management 1 | Yes |
| *.man | Surface water management 2 | Yes |
| *.snw | Snowpack water balance | Yes |
| *.bma | Detailed water balance Macropores | Yes |
| swap.log | Log file | No |
| *.end | Final values of state variables | No |

Different ASCII output files (Table 6) can be generated which can be switched on or off by means of variables given in the main input file (when optional in the above table). All these files have the same header with the project name, file content, file name, model version, date of generation, period of calculations and the depth of the soil profile. Appendix 12 lists the variables which are printed in each output file.

Formatted and unformatted (binary) export files can be generated with data that cover the entire simulation period. These output files can be directly used as input for pesticide and nutrient models like PEARL (Leistra et al, 2001) and ANIMO (Groenendijk et al, 2003). A description of these files is given in Appendix 15 and Appendix 16)

References

- Abenney-Mickson, S., A. Yomota, and T. Miura, 1997. *Water balance of field plots planted with soybean and pumpkin*. Trans. ASAE, 40: 899-909.
- Allen, R.G., M.E. Wright and R.D. Burman, 1989. *Operational estimates of evapotranspiration*. Agron. J., 81, 650-662.
- Allen, R.G., 1991. *REF-ET Reference evapotranspiration calculator, version 2.1*. Utah State University, Logan, 39 pp.
- Allen, R.G., L.S. Pereira, D. Raes, and M. Smith, 1998. *Crop evapotranspiration. Guidelines for computing crop water requirements*. Irrigation and Drainage Paper 56, FAO, Rome, Italy, 300 p.
- Angus, J.F., R.B. Cunningham, M.W. Moncur and D.H. Mackenzie, 1981. *Phasic development in field crops. I. Thermal response in seedling phase*. Field Crops Research 3, 365-378.
- Ashby, M., A.J. Dolman, P. Kabat, E.J. Moors and M.J. Ogink-Hendriks, 1996. *SWAPS version 1.0. Technical reference manual*. Technical document 42, Winand Staring Centre, Wageningen.
- Bear, J., 1972. *Dynamics of fluids in porous media*. Elsevier, Amsterdam.
- Belmans, C., J.G. Wesseling and R.A. Feddes, 1983. *Simulation of the water balance of a cropped soil: SWATRE*. J. Hydrol., 63, 271-286.
- Beltman, W.H.J., J.J.T.I. Boesten and S.E.A.T.M. van der Zee, 1995. *Analytical modelling of pesticide transport from the soil surface to a drinking water well*. J. Hydrol., 169, 209-228.
- Beven, K. and P. Germann, 1982. *Macropores and water flow in soils*. Water Resour. Res., 18: 1311-1325.
- Biggar, J.W. and D.R. Nielsen, 1976. *The spatial variability of the leaching characteristics of a field soil*. Water Resour. Res., 12, 78-84.
- Black, T.A., W.R. Gardner and G.W. Thurtell, 1969. *The prediction of evaporation, drainage, and soil water storage for a bare soil*. Soil Sci. Soc. Am. J., 33, 655-660.
- Boesten, J.J.T.I., 1986. *Behaviour of herbicides in soil : Simulation and experimental assessment*. Ph.D. thesis Winand Staring Centre, Wageningen.
- Boesten, J.J.T.I. and L. Stroosnijder, 1986. *Simple model for daily evaporation from fallow tilled soil under spring conditions in a temperate climate*. Neth. J. Agric. Sci., 34, 75-90.
- Boesten, J.J.T.I. and A.M.A. van der Linden, 1991. *Modeling the influence of sorption and transformation on pesticide leaching and persistence*. J. Environ. Qual., 20, 425-435.
- Bolt, G.H., 1979. *Movement of solutes in soils: principles of adsorption/exchange chromatography*. In: G.H. Bolt (Ed.), Soil Chemistry B, Physico-Chemical Models. Elsevier, Amsterdam. p. 285-348.
- Booltink, H.W.G., 1993. *Morphometric methods for simulation of water flow*. PhD-thesis, Wageningen University, 169 p.
- Booltink, H.W.G. and J. Bouma, 1993. *Sensitivity analysis on processes affecting bypass flow*. Hydrol. Process., 7: 33-43.
- Boons-Prins, E.R., G.H.J. de Koning, C.A. van Diepen and F.W.T. Penning de Vries, 1993. *Crop specific simulation parameters for yield forecasting across the European Community*. Simulation Rep. 32, CABO-DLO and SC-DLO, Wageningen, The Netherlands.
- Bos, M.G., J. Vos and R.A. Feddes, 1996. *CRIWAR 2.0. A simulation model on crop irrigation water requirements*. ILRI publ. 46, Wageningen, The Netherlands.
- Bouma, J. and J.L. Anderson, 1973. *Relationships between soil structure characteristics and hydraulic conductivity*. p. 77-105. In: R.R. Bruce (ed.). Field soil moisture regime. SSSA Special Publ. no. 5. Am. Soc. of Agron. Madison, Wis.
- Bouma, J. and L.W. Dekker, 1978. *A case study on infiltration into a dry clay soil. I. Morphological observations*. Geoderma, 20: 27-40.

- Bouma, J., C. Belmans, L.W. Dekker and W.J.M. Jeurissen, 1983. *Assessing the suitability of soils with macropores for subsurface liquid waste disposal*. J. Environ. Qual. 12, 305-311.
- Bouma, J., 1990. *Using morphometric expressions for macropores to improve soil physical analyses of fields soils*. Geoderma 46, 3-11.
- Bouten, W., 1992. *Monitoring and modelling forest hydrological processes in support of acidification research*. Diss. Univ. A'dam. 218 pp.
- Braden, H., 1985. *Ein Energiehaushalts- und Verdunstungsmodell for Wasser und Stoffhaushaltsuntersuchungen landwirtschaftlich genutzter Einzugsgebiete*. Mittlungen Deutsche Bodenkundliche Gesellschaft, 42, 294-299.
- Bresler, E., and G. Dagan, 1983. *Unsaturated flow in spatially variable fields. 2. Application of water flow models to various fields*. Water Resour. Res., 19: 421-428.
- Bronswijk, J.J.B. 1988. *Modeling of water balance, cracking and subsidence of clay soils*. J. Hydrol., 97: 199-212.
- Bronswijk, J.J.B. and J.J. Evers-Vermeer, 1990. *Shrinkage of Dutch clay soil aggregates*. Neth. J. of Agric. Sci., 38, 175-194.
- Bronswijk, J.J.B., W. Hamminga and K. Oostindie, 1995. *Field-scale solute transport in a heavy clay soil*. Water Resour. Res., 31, 517-526.
- Brooks, R.H. and A.T. Corey, 1964. *Hydraulic properties of porous media*. Colorado State Univ., Hydrology paper no. 3, p. 27.
- Bruin, R.A., 1998. *Micrometeorology*. Lecture notes 06252207, Wageningen University, 156 p.
- Brunt, D., 1952. *Physical and dynamical meteorology*. Second edition, University Press, Cambridge, 428 pp.
- Burman, R.D., M.E. Jensen and R.G. Allen, 1987. *Thermodynamic factors in evapotranspiration*. In 'Proc. Irrig. and Drain. Spec. Conf.', L.G. James and M.J. English (Eds.), ASCE, Portland, Ore., July, p. 28-30.
- Carrera, J. and S.P. Neuman, 1986. *Estimation of aquifer parameters under transient and steady state conditions. 2. Uniqueness, stability, and solution algorithms*. Water Resour. Res. 22, 211-27.
- Carsel, R.F. and R.S. Parrish, 1988. *Developing joint probability distributions of soil water characteristics*. Water Resour. Res., 24, 755-769.
- Causton, D.R. and J.C. Venus, 1981. *The biometry of plant growth*. Edward Arnold, London. 307 pp.
- Celia, M.A., E.T. Bouloutas and R.L. Zarba, 1990. *A general mass-conservative numerical solution for the unsaturated flow equation*. Water Resour. Res., 26, 1483-1496.
- Clausnitzer, V., J.W. Hopmans and D.R. Nielsen, 1992. *Simultaneous scaling of soil water retention and hydraulic conductivity curves*. Water Resour. Res., 28, 19-31.
- Clothier, B.E., M.B. Kirkham and J.E. McLean, 1992. *In situ measurement of the effective transport volume for solute moving through soil*. Soil Sci. Soc. Am. J., 56, 733-736.
- Dane, J.H., and G.C. Topp, 2002. *Methods of soil analysis. Part 4. Physical methods*. SSSA Book series, number 5, Madison, Wisconsin, 1692 p.
- Dekker, L.W. and P.D. Jungerius, 1990. *Water repellency in the dunes with special reference to the Netherlands*. In 'Dunes of the European Coasts', Catena Suppl., 18, 173-183.
- Dekker, L.W. and C.J. Ritsema, 1994. *How water moves in a water repellent sandy soil. 1. Potential and actual water repellency*. Water Resour. Res., 30, 2507-2517.
- Dekker, L.W. and C.J. Ritsema, 1996. *Preferential flow paths in a water repellent clay soil with grass cover*. Water. Resour. Res. 32: 1239-1249.
- Dekker, L.W., 1998. *Moisture variability resulting from water repellency in Dutch soils*. PhD-thesis Wageningen University, 240 p.

- De Rooij, G.H., 1996. *Preferential flow in water-repellent sandy soils. Model development and lysimeter experiments*. Ph.D. thesis, Wageningen Agricultural University, The Netherlands, 229 p.
- Desbarats, A.J., 1995. *An interblock conductivity scheme for finite difference models of steady unsaturated flow in heterogeneous media*. Water Resour. Res., 31, 2883-2889.
- De Smedt, F. and P.J. Wierenga, 1979. *A generalized solution for solute flow in soils with mobile and immobile water*. Water Resour. Res., 1137-1141.
- De Vries, D.A., 1975. *Heat transfer in soils*. In 'Heat and mass transfer in the biosphere. I. Transfer processes in plant environment', De Vries, D.A. and N.H. Afgan (eds.), Scripta Book Company, Washington D.C., p. 5-28.
- De Wit, C.T. et al., 1978. *Simulation of assimilation and transpiration of crops*. Simulation Monographs, Pudoc, Wageningen, The Netherlands. 100 pp.
- Dirksen, C., 1979. *Flux-controlled sorptivity measurements to determine soil hydraulic property functions*. Soil Sci. Soc. Am. J., 43, 827-834.
- Dirksen, C., 1987. *Water and salt transport in daily irrigated root zone*. Neth. J. Agric. Sci., 35: 395-406.
- Dirksen, C., 1991. *Unsaturated hydraulic conductivity*. In 'Soil analysis, physical methods', K.A. Smith and C.E. Mullins (eds), Marcel Dekker, New York, p. 209-269.
- Dirksen, C., J.B. Kool, P. Koorevaar and M.Th. van Genuchten, 1993. *Hyswasor: simulation model of hysteretic water and solute transport in the root zone*. In: D. Russo and G. Dagan (Eds.), Water flow and solute transport in soils. Springer-Verlag, Adv. Series in Agric. Sci., 20, 99-122.
- Dirksen, C. and S. Matula, 1994. *Automatic atomized water spray system for soil hydraulic conductivity measurements*. Soil Sci. Soc. Am. J., 58, 319-325.
- Doorenbos, J. and W.O. Pruitt, 1977. *Guidelines for predicting crop water requirements*. Irrigation and Drainage Paper 24, FAO, Rome, Italy.
- Doorenbos, J. and A.H. Kassam, 1979. *Yield response to water*. FAO Irrigation and Drainage Paper 33, FAO, Rome, Italy.
- Elrick, D.E. and W.D. Reynolds, 1992. *Infiltration from constant-head well permeameters and infiltrometers*. In 'Advances in measurement of soil physical properties: bringing theory into practice', G.C. Topp, W.D. Reynolds and R.E. Green (eds.), SSSA special publication no. 30, p. 1-24.
- Ernst, L.F., 1956. *Calculation of the steady flow of groundwater in vertical cross-sections*. Netherlands Journal of Agricultural Science 4, 126-131.
- Ernst, L.F. 1962. *Groundwater flow in the saturated zone and its calculation when parallel open conduits are present*. Thesis (Dutch with English summary), University of Utrecht, 189 pp.
- Ernst, L.F., 1973. *The determination of residence times in case of groundwater flow*. Nota 755 I.C.W., now Winand Staring Centre, Wageningen (in Dutch).
- Ernst, L.F. 1978. *Drainage of undulating sandy soils with high groundwater tables. I en II*. Journal of Hydrology 39, 1-50.
- Ernst, L.F. and R.A. Feddes, 1979. *Invloed van grondwateronttrekking voor beregening en drinkwater op de grondwaterstand*. Report 1116, ICW (currently Winand Staring Centre), Wageningen, The Netherlands.
- Feddes, R.A., 1971. *Water, heat and crop growth*. Ph.D. thesis, Wageningen Agricultural University, The Netherlands.
- Feddes, R.A., P.J. Kowalik and H. Zaradny, 1978. *Simulation of field water use and crop yield*. Simulation Monographs. Pudoc. Wageningen. 189 pp.

- Feddes, R.A., 1987. *Crop factors in relation to Making reference crop evapotranspiration*. In 'Evaporation and weather', TNO Committee on Hydrological Research, Proceedings and information no 39, p. 33-46.
- Feddes, R.A., P. Kabat, P.J.T. van Bakel, J.J.B. Bronswijk and J. Halbertsma, 1988. *Modelling soil water dynamics in the unsaturated zone - state of the art*. J. Hydrol., 100, 69-111.
- Feddes, R.A., G.H. de Rooij, J.C. van Dam, P. Kabat, P. Droogers, and J.N.M. Stricker, 1993a. *Estimation of regional effective soil hydraulic parameters by inverse modelling*. In 'Water flow and solute transport in soils: modelling and application', D. Russo and G. Dagan (Eds.), Springer Verlag, Berlin, p. 211-231.
- Feddes, R.A., M. Menenti, P. Kabat, and W.G.M. Bastiaanssen, 1993b. *Is large scale inverse modelling of unsaturated flow with areal average evaporation and surface soil moisture as estimated from remote sensing feasible?* J. Hydrol., 143: 125-152.
- Feddes, R.A. and K.J. Lenselink, 1994. *Evapotranspiration*. In 'Drainage principles and applications', H.P. Ritzema (ed.), ILRI publication 16, second ed., Wageningen, p. 145-174.
- Fernández, A., 1998. *An Energy Balance Model of Seasonal Snow Evolution*. Physical Chemistry of the Earth 23, 5-6: 661-666.
- Flury, M. and H. Flüher, 1995. *Tracer characteristics of Brilliant Blue FCF*. Soil Sci. Soc. Am. J., 59, 22-27.
- Garnier, P., Rieu, M., Boivin, P., Vauclin, M., and Baveye, P. 1997. *Determining the hydraulic properties of a swelling soil from a transient evaporation experiment*. Soil Sci. Soc. Am. J., 61: 1555-1563.
- Gash, J.H.C., 1979. *An analytical model of rainfall interception by forests*. Q. J. R. Meteor. Soc. 105, 43-55.
- Gash, J.H.C., C.R. Lloyd and G. Lachaud, 1995. *Estimating sparse forest rainfall interception with an analytical model*. *Journal of Hydrology* 170 (1995) 79-86.
- Gelhar, L.W. and J.L. Wilson, 1974. *Groundwater quality modeling*. Ground Water, 12, 399-408.
- Gerke, H.H. and M.Th van Genuchten, 1993. *A dual-porosity model for preferential movement of water and solutes in structured porous media*. Water Resour. Res., 29, 305-319.
- Goudriaan, J., 1977. *Crop meteorology: a simulation study*. Simulation monographs, Pudoc, Wageningen.
- Goudriaan, J., 1982. *Some techniques in dynamic simulation*. In 'Simulation of plant growth and crop production', F.W.T. Penning de Vries and H.H. van Laar (Eds.), Simulation Monographs, Pudoc, Wageningen, p. 66-84.
- Greco, R., R.F.A. Hendriks and W. Hamminga, 1997. *Clay soil aggregate sorptivity measurements under different water contents*. Proceedings of the National Hydraulics Conference, Turin, Italy, November 1996.
- Groen, K.P., 1997. *Pesticide leaching in polders. Field and model studies on cracked clays and loamy sand*. PhD thesis, Wageningen Agricultural University, Wageningen, The Netherlands, 296 pp.
- Hadley, P., E.H. Roberts, R.J. Summerfield and F.R. Minchin, 1984. *Effects of temperature and photoperiod on flowering in soya bean: a quantitative model*. Annals of Botany, 53, 669-681.
- Hargreaves, G.L., and Z.A. Samani, 1985. *Reference crop evapotranspiration from temperature*. Applied Engineer. In Agric., 1, 2, 96-99.
- Harrison, L.P., 1963. *Fundamental concepts and definitions relating to humidity*. In 'Humidity and moisture', A. Wexler (Ed.), Vol. 3, Reinhold Publishing Company, New York.
- Haverkamp, R., M. Vauclin, J. Touma, P.J. Wierenga and G. Vachaud, 1977. *A comparison of numerical simulation models for one-dimensional infiltration*. Soil Sci. Soc. Am. J., 41, 285-294.

- Haverkamp, R., and M. Vauclin, 1979. *A note on estimating finite difference interblock hydraulic conductivity values for transient unsaturated flow problems*. Water Resour. Res., 15, 181-187.
- Hendriks, R.F.A., K. Oostindie, and P. Hamminga, 1999. *Simulation of bromide tracer and nitrogen transport in a cracked clay soil with the FLOCR/ANIMO model combination*. J. Hydrol., 215: 94-115.
- Hijmans, R.J., I.M. Guiking-Lens and C.A. van Diepen, 1994. *User's guide for the WOFOST 6.0 crop growth simulation model*. Technical Document 12, Winand Staring Centre, Wageningen, The Netherlands, 144 p.
- Hillel, D., 1980. *Fundamentals of soil physics*. Academic Press, San Diego, CA, 412 p.
- Hooghoudt, S.B., 1940. *Algemene beschouwing van het probleem van de detailontwatering en de infiltratie door middel van parallel lopende drains, greppels, sloten en kanalen*. Versl. Landbouwk. Onderz., 46, B, 193 p.
- Hoogmoed, W.B., and Bouma, J. 1980. *A simulation model for predicting infiltration into a cracked clay soil*. Soil Sci. Soc. Am. J., 44: 458-461.
- Homaee, M., 1999. *Root water uptake under non-uniform transient salinity and water stress*. PhD- thesis, Wageningen University, 173 p.
- Hopmans, J.W., and J.N.M. Stricker, 1989. *Stochastic analysis of soil water regime in a watershed*. J. Hydrol., 105, 57-84.
- Hopmans, J.W., K.C. Roy, and W.W. Wallender, 1991. *Irrigation water management and soil-water hysteresis - a computer modeling study with stochastic soil hydraulic properties*. Transactions of the ASAE, 34: 449-459.
- Hopmans, J.W., J.C. van Dam, S.O. Eching and J.N.M. Stricker, 1994. *Parameter estimation of soil hydraulic functions using inverse modeling of transient outflow experiments*. Trends in Hydrology, 1, 217-242.
- Hornung, U., and W. Messing, 1983. *Truncation errors in the numerical solution of horizontal diffusion in saturated/unsaturated media*. Adv. Water Resour., 6, 165-168.
- Huang, K., B.P. Mohanty and M.Th. van Genuchten, 1996. *A new convergence criterion for the modified Picard iteration method to solve the variably saturated flow equation*. J. Hydrol., 178, 69-91.
- Hunt, E.R., J.A. Weber and D.M. Gates, 1985. *Effects of nitrate application on Amaranthuspowellii Wats. I. Changes in photosynthesis, growth rates, and leaf area*. Plant Physiology 79, 609-613.
- Jacucci, G., P. Kabat, L. Pereira, P. Verrier, P. Steduto, C. Uhrík, G. Bertanzon, J. Huygen, B. van den Broek, J. Teixeira, R. Fernando, G. Giannerini, F. Carboni, M. Todorovic, G. Toller, G. Tziallas, E. Fragaki, J. Vera Munoz, D. Carreira, P. Yovchev, D. Calza, E. Valle and M. Douroukis, 1994. *The Hydra Project: a Decision Support System for Irrigation Water Management*. Proceedings of the International Conference on Land and Water Resources Management in the Mediterranean Region. 4-8 September 1994, Valenzano (Bari), Italy.
- Jarvis, N.J., 1989. *CRACK - A model of water and solute movement in cracking clay soils. Technical description and user notes*. Report 159, Dept. Soil Sci., Swedish Univ. Agric. Sci., Uppsala, Sweden, 37 pp.
- Jaynes, D.B., 1984. *Comparison of soil water hysteresis models*. J. Hydrol., 75, 287-299.
- Jensen, M.E., R.D. Burman and R.G. Allen, 1990. *Evapotranspiration and irrigation water requirements*. ASCE manuals and reports on engineering practice 70, ASCE, New York. 332 pp.
- Jury, W.A., 1982. *Simulation of solute transport using a transfer function mode*. Water Resour. Res., 18, 363-368.

- Jury, W.A., D. Russo and G. Sposito, 1987. *The spatial variability of water and solute transport properties in unsaturated soil, II Scaling of water transport*. Hilgardia, 55, 33-56.
- Jury, W.A., W.R. Gardner and W.H. Gardner, 1991. *Soil Physics*. Fifth edition. Wiley, New York. 330 pp.
- Kabat, P., B.J. Broek, van den and R.A. Feddes, 1992. *SWACROP: A water management and crop production simulation model*. ICID Bulletin 92, vol. 41 No. 2, 61-84.
- Kaluarachchi, J.J., and J.C. Parker, 1987. *Effects of hysteresis with air entrapment on water flow in the unsaturated zone*. Water Resour. Res., 23: 1967-1976.
- Kase, M. and J. Catský, 1984. *Maintenance and growth components of dark respiration rate in leaves of C₃ and C₄ plants as affected by leaf temperature*. Biologia Plantarum 26, 461-470.
- Kim, D.J., 1992. *Characterization of swelling and shrinkage behaviour, hydraulic properties and modelling of water movement in a physically ripening marine clay soil*. PhD thesis, Catholic University Leuven.
- Kim, R., 1995. *The water budget of heterogeneous areas*. Doctoral thesis. Wageningen Agricultural University, Wageningen, The Netherlands, 182 pp.
- Kool, J.B., J.C. Parker and M.Th. van Genuchten, 1985. *Determining soil hydraulic properties from One-step outflow experiments by parameter estimation: I. Theory and numerical studies*. Soil Sci. Soc. Am. J., 49, 1348-1354.
- Kool, J.B., and J.C. Parker, 1987. *Development and evaluation of closed form expressions for hysteretic soil hydraulic properties*. Water Resour. Res., 23, 105-114.
- Kool, J.B., J.C. Parker and M.Th. van Genuchten, 1987. *Parameter estimation for unsaturated flow and transport models - a review*. J. Hydrol., 91, 255-293.
- Kool, J.B., and M.Th. van Genuchten, 1991. *HYDRUS, One-dimensional variably saturated flow and transport model including hysteresis and root water uptake*. Research Report 124, U.S. Salinity Laboratory, USDA, ARS, Riverside, CA.
- Koorevaar, P., G. Menelik and C. Dirksen, 1983. *Elements of soil physics*. Developments in Soil Science 13, Elsevier, Amsterdam, p. 223.
- Klute, A., 1986. *Water retention: laboratory methods*. In 'Methods of soil analysis; Part 1; Physical and Mineralogical methods', A. Klute (Ed.), Agronomy series n. 9, ASA and SSSA, Madison, Wisconsin, p. 635-662.
- Klute, A., and C. Dirksen, 1986. *Hydraulic conductivity and diffusivity: laboratory methods*. In 'Methods of soil analysis; Part 1; Physical and Mineralogical methods', A. Klute (Ed.), Agronomy series n. 9, ASA and SSSA, Madison, Wisconsin, p. 687-734.
- Kraalingen, D. W. G. and C. Rappoldt, 2000. *Reference manual of the FORTRAN utility library TTUTIL v. 4*. Report 5. Plant Research International, Wageningen.
- Krammes, J.S., and L.F. DeBano, 1965. *Soil wettability: a neglected factor in watershed management*. Water Resour. Res., 1, 283-288.
- Kroes, J.G., and J. Roelsma, 1997. *User's Guide ANIMO 3.5; input instructions and technical programme description*. Technical Document 46, DLO Winand Staring Centre, Wageningen.
- Kroes, J.G., P.J.T. van Bakel, J. Huygen, T. Kroon en R. Pastoors, 2001. *Actualisatie van de hydrologie voor STONE 2.0*. Rapport 298, Alterra, Wageningen, 68 p.
- Kropff, M.J., H.H. van Laar and H.F.M. ten Berge (Eds.), 1993. *ORYZA1 A basic model for irrigated lowland rice production*. IRRI, Los Banos, The Philippines.
- Kustas, W., A. Rango, 1994. *A simple energy algorithm for the snowmelt runoff model*. Water Resources Research 30: 1515-1527.
- Leij, F.J., W.J. Alves, M. Th. van Genuchten and J.R. Williams, 1996. *The UNSODA Unsaturated Soil Hydraulic Database. User's manual Version 1.0*, Soil Salinity Laboratory, Riverside, California.

- Leistra, M., A.M.A. van der Linden, J.J.T.I. Boesten, A. Tiktak and F. van den Berg. 2001. *PEARL model for pesticide behaviour and emissions in soil-plant systems. Description of processes*. Alterra report 13, RIVM report 711401009, Alterra, Wageningen, 107 pp.
- Maas, E.V., and G.J. Hoffman, 1977. *Crop salt tolerance-current assessment*. J. Irrig. and Drainage Div., ASCE 103, 115-134.
- Maas, E.V., 1990. *Crop salt tolerance*. In 'Agricultural salinity assessment and management', K.K. Tanji (Ed.), ASCE Manuals and Reports on Engineering practice, No 71, New York.
- Makkink, G.F., 1957. *Testing the Penman formule by means of lysimeters*. J. Int. Water Eng., 11:277-288.
- Massop, H.Th.L., and P.A.J.W. de Wit, 1994. *Hydrologisch onderzoek naar de gewasweerstand van het tertiair ontwateringsstelsel in Oost-Gelderland*. Report 373, Winand Staring Centre, Wageningen, The Netherlands, 132 p.
- Miller, E.E., and R.D. Miller, 1956. *Physical theory for capillary flow phenomena*. J. Appl. Phys., 27, 324-332.
- Millington, R.J., and J.P. Quirk., 1961. *Permeability of porous solids*. Trans. Faraday Soc., 57, 1200-1207.
- Milly, P.C.D., 1985. *A mass conservative procedure for time-stepping in models of unsaturated flow*. Adv. Water Resour., 8, 32-36.
- Monteith, J.L., 1965. *Evaporation and the Environment*. In: G.E. Fogg (ed.), The state and movement of water in living organisms. Cambridge University Press, p. 205-234.
- Monteith, J.L., 1981. *Evaporation and surface temperature*. Quarterly J. Royal Soc., 107, 1-27.
- Mualem, Y., 1976. *A new model for predicting the hydraulic conductivity of unsaturated porous media*. Water Resour. Res., 12, 513-522.
- Murray, F.W., 1967. *On the computation of saturation vapor pressure*. J. Appl. Meteor., 6, 203-204.
- Nielsen, D.R., M.Th. van Genuchten and J.W. Biggar, 1986. *Water flow and solute transport in the unsaturated zone*. Water Resour. Res., 22, supplement, 89S-108S.
- Nimmo, J.R., J. Rubin and D.P. Hammermeister, 1987. *Unsaturated flow in a centrifugal field: Measurement of hydraulic conductivity and testing of Darcy's law*. Water Resour. Res., 32, 124-134.
- Parlange, J.Y., 1975. *On solving the flow equation in unsaturated soils by optimization: horizontal infiltration*. Soil Sci. Soc. Am. Proc. 39, 415-418.
- Peat, W.E., 1970. *Relationships between photosynthesis and light intensity in the tomato*. Annal Bot., 34, 319-328.
- Peck, A.J., R.J. Luxmoore and J.L. Stolzy, 1977. *Effects of spatial variability of soil hydraulic properties in water budget modeling*. Water Resour. Res., 13, 348-354.
- Peerboom, J. 1987. *Adaptions of the model SWATRE in order to simulate the behaviour of swelling and shrinking clay soils*. MSc-thesis, Subdep. Water Resources, Wageningen University, 104 p. (in Dutch)
- Penning de Vries, F.W.T., A.H.M. Brunsting and H.H. van Laar, 1974. *Products requirements and efficiency of biosynthesis: a quantitative approach*. Journal of Theoretical Biology 45, 339-377.
- Penning de Vries, F.W.T., J.M. Wiltage and D. Kremer, 1979. *Rates of respiration and of increase in structural dry matter in young wheat, ryegrass and maize plants in relation to temperature, to water stress and to their sugar content*. Annals of Botany (London) 44, 595-609.
- Penning de Vries, F.W.T. and H.H. van Laar, 1982. *Simulation of growth processes and the model BACROS*. In Penning de Vries, F.W.T. and H.H. van Laar (Eds.) Simulation of plant growth and crop production. Simulation Monographs, Pudoc, Wageningen, The Netherlands. p. 114-135.

- Penning de Vries, F.W.T., D.M. Jansen, H.F.M. ten Berge and A. Bakema, 1989. *Simulation of ecophysiological processes of growth in several annual crops*. Pudoc, Wageningen, the Netherlands, 271 pp.
- Penman, H.L., 1948. *Natural evaporation from open water, bare soil, and grass*. Proc. Royal Society, London 193, 120-146.
- Philip, J.R., 1957. *The theory of infiltration: 4. Sorptivity and algebraic infiltration equations*. Soil Science 84, 264-275.
- Press, W.H., B.P. Flannery, S.A. Teukolsky and W.T. Vetterling, 1989. *Numerical Recipes. The art of scientific computing*. Cambridge University Press. 702 pp.
- Priestley, C.H.B., and R.J. Taylor, 1972. *On the assessment of surface heat flux and evaporation using large scale parameters*. Mon. Weath. Rev., 100, 81-92.
- Raats, P.A.C., 1973. *Unstable wetting fronts in uniform and nonuniform soils*. Soil Sci. Soc. Am. J., 37, 681-685.
- Raes, D., H. Lemmens, P. van Aelst, M. van der Bult and M. Smith, 1988. *IRSIS (Irrigation Scheduling Information System), reference manual*. Laboratory of Land Management, K.U. Leuven, Belgium.
- Reinink, K., I. Jorritsma and A. Darwinkel, 1986. *Adaption of the AFRC wheat phenology model for Dutch conditions*. Neth. J. Agric. Science, 34, 1-13.
- Rijniersce, K., 1983. *A simulation model for physical ripening in the IJsselmeerpolders*. Rijksdienst voor IJsselmeerpolders. Lelystad, The Netherlands, 216 pp.
- Rijtema, P.E., P. Groenendijk and J.G. Kroes, 1997. *ANIMO, a dynamic simulation model for transport and transformation of nutrients and organic materials in soils*. Report 30, DLO Winand Staring Centre, Wageningen, in press.
- Ritchie, J.T., 1972. *A model for predicting evaporation from a row crop with incomplete cover*. Water Resour. Res., 8, 1204-1213.
- Ritsema, C.J., L.W. Dekker, J.M.H. Hendrickx and W. Hamminga, 1993. *Preferential flow mechanism in a water repellent sandy soil*. Water Resour. Res., 29, 2183-2193.
- Ritsema, C.J., and L.W. Dekker, 1994. *How water moves in a water repellent sandy soil. 2. Dynamics of fingered flow*. Water Resour. Res., 30, 2519-2531.
- Ritsema, C.J., 1998. *Flow and transport in water repellent sandy soils*. PhD-thesis Wageningen University, 213 p.
- Ritzema, H.P., 1994. *Subsurface flow to drains*. In 'Drainage principles and applications', H.P. Ritzema (Ed. in Chief), ILRI publication 16, second edition, Wageningen, p. 263-304.
- Ross, P.J., 1990. *Efficient numerical methods for infiltration using Richards' equation*. Water Resour. Res., 26, 279-290.
- Russo, D., E. Bresler, U. Shani and J. Parker, 1991. *Analysis of infiltration events in relation to determining soil hydraulic properties by inverse problem methodology*. Water Resour. Res., 27, 1361-1373.
- Saxena, R.K., N.J. Jarvis and L. Bergström, 1994. *Interpreting non-steady state tracer breakthrough experiments in sand and clay soils using a dual-porosity model*. J. Hydrol., 162, 279-298.
- Scott, P.S., G.J. Farquhar and N. Kouwen, 1983. *Hysteretic effects on net infiltration*. In 'Advances in infiltration', American Society of Agricultural Engineers, St. Joseph, Mich, p. 163-170.
- Shalhevet, J., 1994. *Using water of marginal quality for crop production: major issues*. Agric. Water Man., 25, 233-269.
- Singh, P., G. Spitzbart, H. Hübl, H. W. Weinmeister, 1997. *Hydrological response of snowpack under rain-on-snow events: a field study*. Journal of Hydrology 202: 1-20.

- Šimůnek, J., T. Vogel and M.Th. van Genuchten, 1992. *The SWMS-2D code for simulating water flow and solute transport in two-dimensional variably saturated media*. Version 1.1. Res. Rep. 126, U.S. Salinity Lab., Agric. Res. Ser., U.S. Dept. of Agric., Riverside, Calif.
- Šimůnek, J., R. Kodesova, M.M. Gribb and M.T. van Genuchten, 1999. *Estimating hysteresis in the soil water retention function from cone permeameter experiments*. Water Resour. Res., 35: 1329-1345.
- Smith, M., 1992. *CROPWAT, a computer program for irrigation planning and management*. FAO Irrigation and Drainage Paper 46. Rome, Italy.
- Spitters, C.J.T., H. van Keulen and D.W.G. van Kraalingen, 1989. *A simple and universal crop growth simulator: SUCROS87*. In: R. Rabbinge, S.A. Ward and H.H. van Laar (Eds.) *Simulation and systems management in crop protection*. Simulation Monographs, Pudoc, Wageningen, The Netherlands. p. 147-181.
- Stolte, J., J.I. Freijer, W. Bouten, C. Dirksen, J.M. Halbertsma, J.C. van Dam, J.A. van den Berg, G.J. Veerman and J.H.M. Wösten, 1994. *Comparison of six methods to determine unsaturated soil hydraulic conductivity*. Soil Sci. Soc. Am. J., 58, 1596-1603.
- Stroosnijder, L. 1975. *Infiltration and redistribution of water in the soil*. PhD-thesis, Wageningen University, 213 p. (in Dutch)
- Supit, I., A.A. Hooyer and C.A. van Diepen (Eds.), 1994. *System description of the WOFOST 6.0 crop simulation model implemented in CGMS. Vol. 1: Theory and algorithms*. EUR publication 15956, Agricultural series, Luxembourg, 146 p.
- Taylor, S.A., and G.M. Ashcroft, 1972. *Physical Edaphology*. Freeman and Co., San Francisco, California, p. 434-435.
- Ten Berge, H.F.M., 1986. *Heat and water transfer at the bare soil surface: aspects affecting thermal images*. PhD thesis, Wageningen Agricultural University, Wageningen, The Netherlands.
- Tetens, O., 1930. *Über einige meteorologische Begriffe*. Z. Geophys, 6, 297-309.
- Thoma, S.G., D.P. Gallegos and D.M. Smith, 1992. *Impact of fracture coatings on fracture/matrix flow interactions in unsaturated porous media*. Water Resources Res., 28, 1357-1367.
- Tiktak, A., F. van den Berg, J.J.T.I. Boesten, M. Leistra, A.M.A. van der Linden, and D. van Kraalingen, 2000. *Pesticide Emission at Regional and Local scales: Pearl version 1.1 User Manual*. RIVM report 711401008, report 29, Alterra Green World Research, Wageningen.
- Van Bakel, P.J.T., 1986. *Planning, design and operation of surface water management systems; a case study*. PhD thesis, Wageningen Agricultural University.
- Van Dam, J.C., J.M.H. Hendrickx, H.C. van Ommen, M.H. Bannink, M.Th. van Genuchten and L.W. Dekker, 1990. *Water and solute movement in a coarse-textured water-repellent field soil*. J. Hydrol., 120, 359-379.
- Van Dam, J.C., J.N.M. Stricker and P. Droogers, 1994. *Inverse method to determine soil hydraulic functions from multi-step outflow experiments*. Soil Sci. Soc. Am. J., 58, 647-652.
- Van Dam, J.C., J.H.M. Wösten and A. Nemes, 1996. *Unsaturated soil water movement in hysteretic and water repellent soils*. J. Hydrol., 184, 153-173.
- Van Dam, J.C., J. Huygen, J.G. Wesseling, R.A. Feddes, P. Kabat, P.E.V. van Walsum, P. Groenendijk and C.A. van Diepen, 1997. *Theory of SWAP version 2.0. Simulation of water flow, solute transport and plant growth in the Soil-Water-Atmosphere-Plant environment*. Wageningen University and Alterra. Technical Document 45.
- Van Dam, J.C., 2000. *Field scale water flow and solute transport. SWAP model concepts, parameter estimation and case studies*. PhD thesis, Wageningen Universiteit, 167 p.
- Van Dam, J.C., and R.A. Feddes, 2000. *Simulation of infiltration, evaporation and shallow groundwater levels with the Richards' equation*. J. of Hydrol., 233, 72-85.

- Van de Pol, R.M., P.J. Wierenga and D.R. Nielsen, 1977. *Solute movement in a field soil*. Soil Sci. Soc. Am. J., 41, 10-13.
- Van den Berg, F., and J.J.T.I. Boesten, 1998. *PEsticide Leaching and Accumulation model (PESTLA) version 3.4; description and user's guide*. Technical Document 43, Alterra Green World Research, Wageningen, 150 p.
- Van den Broek, B.J., J.C. van Dam, J.A. Elbers, R.A. Feddes, J. Huygen, P. Kabat and J.G. Wesseling, 1994. *SWAP 1993, input instructions manual*. Report 45, Dep. Water Resources, Wageningen Agricultural University.
- Van der Molen, W.H., and J. Wesseling, 1991. *A solution in closed form and a series solution to replace the tables for the thickness of the equivalent layer in Hooghoudt's drain spacing formula*. Agricultural Water Management 19, p. 1-16.
- Van der Zee, S.E.A.T.M., and W.H. van Riemsdijk, 1987. *Transport of reactive solute in spatially variable soil systems*. Water Resour. Res., 23, 2059-2069.
- Van Dobben, W.H., 1962. *Influence of temperature and light conditions on dry matter distribution, development rate and yield in arable crops*. Netherlands Journal of Agricultural Science 10, 377-389.
- Van Genuchten, M.Th., and P.J. Wieringa, 1974. *Simulation of one-dimensional solute transfer in porous media*. New Mexico State University Agric. Exp. Stn. Bull. 628, New Mexico.
- Van Genuchten, M.Th., and R.W. Cleary, 1979. *Movement of solutes in soil : computer simulated and laboratory results*. In: G.H. Bolt (Ed.), Soil Chemistry B, Physico-Chemical Models. Elsevier, Amsterdam, pp. 349-386.
- Van Genuchten, M.Th., 1980. *A closed form equation for predicting the hydraulic conductivity of unsaturated soils*. Soil Sci. Soc. Am. J., 44, 892-898.
- Van Genuchten, M.Th., 1982. *A comparison of numerical solutions of the one-dimensional unsaturated-saturated flow and transport equations*. Adv. Water Resour., 5, 47-55.
- Van Genuchten, M.Th., 1987. *A numerical model for water and solute movement in and below the root zone*. Res. Report, US Salinity Laboratory, Riverside, CA.
- Van Genuchten, M.Th., and R.J. Wagenet, 1989. *Two-site/two-region models for pesticide transport and degradation: Theoretical development and analytical solutions*. Soil Sci. Soc. Am. J., 53, 1303-1310.
- Van Genuchten, M.Th., F.J. Leij and S.R. Yates, 1991. *The RETC code for quantifying the hydraulic functions for unsaturated soils*. U.S. Salinity Laboratory, Riverside, California.
- Van Genuchten, M.Th., and F.J. Leij, 1992. *On estimating the hydraulic properties of unsaturated soils*. In 'Indirect methods for estimating hydraulic properties of unsaturated soils', M.Th. van Genuchten and F.J. Leij (eds.), Proc. Int. Workshop, Riverside, California, p. 1-14.
- Van Grinsven, J.J.M., C. Dirksen and W. Bouten, 1985. *Evaluation of hot air method for measuring soil water diffusivity*. Soil Sci. Soc. Am. J., 49, 1093-1099.
- Van Heemst, H.D.J., 1986a. *The distribution of dry matter during growth of a potato crop*. Potato Research 29, 55-66.
- Van Heemst, H.D.J., 1986b. *Crop phenology and dry matter distribution*. In: H. van Keulen and J. Wolf (Eds.). Modelling of agricultural production: soil, weather and crops. p. 13-60.
- Van Keulen, H., 1975. *Simulation of water use and herbage growth in arid regions*. Simulation Monographs. Pudoc, Wageningen, the Netherlands. 184 pp.
- Van Keulen, H., N.G. Seligman and R.W. Benjamin, 1981. *Simulation of water use and herbage growth in arid regions - A re-evaluation and further development of the model 'Arid Crop'*. Agricultural systems 6, 159-193.
- Van Keulen, H., and N.G. Seligman, 1987. *Simulation of water use, nitrogen nutrition and growth of a spring wheat crop*. Simulation Monographs. Pudoc, Wageningen, The Netherlands. 310 pp.

- Van Laar, H.H., J. Goudriaan and H. van Keulen (Eds.), 1992. *Simulation of crop growth for potential and water-limited production situations (as applied to spring wheat)*. Simulation reports CABO-TT 27. CABO-DLO, WAU-TPE, Wageningen. 72 pp.
- Van Ommen, H.C., M.Th. van Genuchten, W.H. van der Molen, R. Dijkema and J. Hulshof, 1989. *Experimental assessment of preferential flow paths in a field soil*. J. Hydrol., 105, 253-262.
- Van Stiphout, T.P.J., H.A.J. van Lanen, O.H. Boersma, and J. Bouma, 1987. *The effect of bypass flow and internal catchment of rain on the water regime in a clay loam grassland soil*. J. Hydrol. 95, 1-11.
- Van Wijk, W.R. (Ed.), 1966. *Physics of plant environment*. North Holland Publ. Comp., Amsterdam, The Netherlands, 2nd edition. 382 pp.
- Von Hoyningen-Hüne, J., 1983. *Die Interception des Niederschlags in landwirtschaftlichen Beständen*. Schriftenreihe des DVWK 57, 1-53.
- Walker, A., 1974. *A simulation model for prediction of herbicide persistence*. J. Environ. Qual., 3, 396-401.
- Warrick, A.W., 1991. *Numerical approximations of darcian flow through unsaturated soil*. Water Resour. Res., 27, 1215-1222.
- Weir, A.H., P.L. Bragg, J.R. Porter and J.H. Rayner, 1984. *A winter wheat crop simulation model without water and nutrient limitations*. Journal of Agricultural Science 102, 371-382.
- Wendroth, O., W. Ehlers, J.W. Hopmans, H. Kage, J. Halbertsma and J.H.M. Wösten, 1993. *Reevaluation of the evaporation method for determining hydraulic functions in unsaturated soils*. Soil Sci. Soc. Am. J., 57, 1436-1443.
- Wesseling, J.G., 1987. *Invloed van bodemsoort en vochtgehalte op de bodemtemperatuur. Een theoretische beschouwing*. Cultuurtechnisch tijdschrift, 27(2), 117-128.
- Wesseling, J.G., J.A. Elbers, P. Kabat and B.J. van den Broek, 1991. *SWATRE; instructions for input*. Internal note, Winand Staring Centre, Wageningen.
- Wesseling, J.G., J.G. Kroes, and K. Metselaar, 1998. *Global sensitivity analysis of the Soil-Water-Atmosphere-Plant (SWAP) model*. Report 160, Alterra, Wageningen, 67 p.
- Wolfe, N.L., U. Mingelgrin, G.C. Miller, 1990. *Abiotic transformations in water, sediments and soil*. In: H.H. Cheng (Ed.), *Pesticides in the soil environment: processes, impacts and modeling*. SSSA Book Series no. 2, Madison, Wisconsin, USA.
- Wösten, J.H.M., G.J. Veerman and J. Stolte, 1994. *Water retention and hydraulic conductivity functions of top- and subsoils in The Netherlands: The Staring series*. Technical Document 18, Winand Staring Centre, Wageningen, The Netherlands, 66 p. (in Dutch).
- Wösten, J.H.M., A. Lilly, A. Nemes and C. Le Bas, 1998. *Using existing soil data to derive hydraulic properties for simulation models in environmental studies and in land use planning*. Report 156, Winand Staring Centre, The Netherlands.
- Wösten, J.H.M., G.J. Veerman, W.J.M. de Groot, and J. Stolte, 2001. *Water retention and hydraulic conductivity functions of top- and subsoils in The Netherlands: The Staring series*. Alterra report 153, Wageningen, The Netherlands, 86 p. (in Dutch).
- Yates, S.R., M.Th. van Genuchten, A.W. Warrick and F.J. Leij, 1992. *Analysis of measured, predicted and estimated hydraulic conductivity using the RETC computer program*. Soil Sci. Soc. Am. J., 56, 347-354.
- Youngs, E.G., and R.I. Price, 1981. *Scaling of infiltration behaviour in dissimilar porous materials*. Water Resour. Res., 17, 1065-1070.
- Yule, D.F., and J.T. Ritchie, 1980a. *Soil shrinkage relationships of Texas Vertisols: I. Small cores*. Soil Sci. Soc. Am. J., 44: 1285-1291.
- Yule, D.F., and J.T. Ritchie, 1980b. *Soil shrinkage relationships of Texas Vertisols: II. Large cores*. Soil Sci. Soc. Am. J., 44: 1291-1295.

Zaidel, J., and D. Russo, 1992. *Estimation of finite difference interblock conductivities for simulation of infiltration into initially dry soils*. Water Resour. Res., 28, 2285-2295.

Appendix 1 Measurement methods to determine soil hydraulic functions

Laboratory and field methods may be applied to determine soil hydraulic functions, $\theta(h)$ and $K(\theta)$.

Commonly applied laboratory measurements of the retention function are the sandbox apparatus (Klute, 1986), pressure cell (Kool et al., 1985), pressure membrane (Klute, 1986) and vapour equilibration (Koorevaar et al., 1983). Commonly applied laboratory measurements of the hydraulic conductivity function are the suction cell (Klute and Dirksen, 1986), crust method (Bouma et al., 1983), drip infiltrometer (Dirksen, 1991), evaporation method (Wendroth et al., 1993), pressure cell (Van Dam et al., 1994) sorptivity method (Dirksen, 1979), hot air method (Van Grinsven et al., 1985), centrifuge method (Nimmo et al., 1987) and the spray method (Dirksen and Matula, 1994).

In the field, simultaneous measurement of θ and h directly provides the retention function. The $K(\theta)$ might be derived from these data by application of the instantaneous profile method (Hillel, 1980) or one of its modifications. In general irrigation-drainage events are used in order to achieve wet and dry conditions and a range of soil water fluxes (Kool et al., 1987). The h -range of the determined functions is limited to the actual drainage conditions (in general $-300 \text{ cm} < h < 0$).

Near saturation, $K(\theta)$ may change very rapidly. To determine K in the very wet range more accurately at field conditions, the suction infiltrometer has been developed (Elrick and Reynolds, 1992). In only a few years, this device has become widely used.

All these methods are so-called direct measurement methods. Also indirect and inverse methods can be used to determine the soil hydraulic functions. At indirect methods, $\theta(h)$ and $K(\theta)$ are derived from more easily obtained soil data as soil texture, bulk density and organic matter content (Van Genuchten and Leij, 1992). At inverse methods, non-linear parameter estimation is used to derive the soil hydraulic functions from a measured flow event, either in the laboratory or in the field (Carrera and Neuman, 1986; Kool et al., 1987; Russo et al., 1991; Feddes et al., 1993; Hopmans et al., 1994; Šimůnek et al., 1999).

An extensive overview of direct, indirect and inverse methods for laboratory and field has been provided by Dane and Topp (2002). In a review of $K(\theta)$ measurements, Dirksen (1991) provided criteria to select the appropriate measurement method for both field and laboratory. These criteria include the theoretical basis, control of initial and boundary conditions, error propagation in data analysis, range of application, equipment, operator skill and time, check on measurements and results obtained. Stolte et al. (1994) measured the hydraulic conductivity with six of these methods in case of a sand, a sandy loam and two silt loam soils. They compared the results and discussed the limitations of each method.

Data sets on soil hydraulic functions are reported by Mualem (1976), Carsel and Parrish (1988), Yates et al. (1992), Wösten et al. (1994), Leij et al. (1996) and Wösten et al. (1998). Appendix 2 lists model parameters derived from a data base of more than 800 soil samples in the Netherlands, known as the Staring series (Wösten et al., 2001). The Staring series correspond to the legend of the Dutch soil map 1:50 000. The data are meant to be applied

in regional studies. The units of the Staring series were obtained by recognizing a number of soil texture classes, with a separation between top- and sublayers. The average relationships per texture class are calculated by taking the geometric mean of every separate soil hydraulic function per unit. The geometric mean was used because of the log-normal distribution of the data. The Staring series may serve as a class-pedotransfer function, by which averaged soil hydraulic functions are assigned to a certain texture class. However, the user should be aware of the limitations of the Staring series:

- the definition of the units has been based on texture and organic matter content only, differences of geologic sediment or bulk density are not taken into account;
- geometric averaging may result in properties different from the real average;
- the units of the Staring series are developed for regional applications, for local applications measurements are indispensable;
- the Staring series apply to Dutch circumstances, in other countries different soil hydraulic functions may apply.

A large amount of soil hydraulic data in Europe has been stored in the HYPRESS database (Wösten et al., 1998). This database has been used to derive European pedotransfer functions. The input consists of soil texture, organic matter content, bulk density and position in soil profile. The output consists of Mualem-Van Genuchten parameters of the soil hydraulic functions.

Appendix 2 Parameters of soil hydraulic functions: Staring series (Wösten et al., 2001)

| TOP-SOILS | Dutch nomenclature | Clay-Silt (50µm) (%) | Clay (<2µm) (%) | Organic matter (%) | M50 (µm) | Dry bulk density (g cm ⁻³) |
|------------------|---|----------------------------|-----------------------|--------------------------|-------------|--|
| <i>Sand</i> | <i>Zand</i> | | | | | |
| B1 | Leemarm, zeer fijn tot matig fijn zand | 4-10 | | 1-4 | 140-170 | 1.4-1.7 |
| B2 | Sterk lemig, zeer fijn tot matig fijn zand | 11-18 | | 1-10 | 125-175 | 1.2-1.6 |
| B3 | Sterk lemig, zeer fijn tot matig fijn zand | 18-29 | | 3-13 | 105-165 | 1.1-1.5 |
| B4 | Zeer sterk lemig, zeer fijn tot matig fijn zand | 30-50 | | 2-5 | 118-160 | 1.1-1.5 |
| B5 | Grof zand | | | 1-3 | 350-500 | 1.3-1.6 |
| B6 | Keileem | 5-39 | | 1-8 | 150-400 | 1.1-1.6 |
| <i>Loam</i> | <i>Zavel</i> | | | | | |
| B7 | Zeer lichte zavel | | 10-12 | 1-6 | | 1.2-1.8 |
| B8 | Matig lichte zavel | | 12-16 | 0-4 | | 1.2-1.6 |
| B9 | Zware zavel | | 18-25 | 1-8 | | 1.2-1.6 |
| <i>Clay</i> | <i>Klei</i> | | | | | |
| B10 | Lichte klei | | 26-35 | 1-6 | | 1.1-1.6 |
| B11 | Matig zware klei | | 35-50 | 3-15 | | 0.9-1.7 |
| B12 | Zeer zware klei | | 51-77 | 3-5 | | 0.9-1.3 |
| <i>Silt</i> | <i>Leem</i> | | | | | |
| B13 | Zandige leem | 60-75 | | 1-8 | | 1.0-1.6 |
| B14 | Siltige leem | 85-95 | | 0-6 | | 1.1-1.6 |
| <i>Peat</i> | <i>Moerig</i> | | | | | |
| B15 | Venig zand | | 2-6 | 15-22 | | 1.0-1.3 |
| B16 | Zandig veen en veen | | 1-7 | 28-80 | | 0.2-1.0 |
| B17 | Venige klei | | 30-80 | 20-30 | | 0.9-1.2 |
| B18 | Kleiig veen | | 10-80 | 30-65 | | 0.4-0.8 |

| SUB-SOILS | Dutch nomenclature | Clay-Silt (50µm) (%) | Clay (<2µm) (%) | Organic matter (%) | M50 (µm) | Dry bulk density (g cm ⁻³) |
|------------------|---|----------------------------|-----------------------|--------------------------|-------------|--|
| <i>Sand</i> | <i>Zand</i> | | | | | |
| O1 | Leemarm, zeer fijn tot matig fijn zand | 1-10 | | 0-3 | 105-205 | 1.4-1.8 |
| O2 | Zwak lemig, zeer fijn tot matig fijn zand | 10-16 | | 1-3 | 105-175 | 1.4-1.7 |
| O3 | Sterk lemig, zeer fijn tot matig fijn zand | 20-32 | | 0-2 | 114-172 | 1.4-1.8 |
| O4 | Zeer sterk lemig, zeer fijn tot matig fijn zand | 36-47 | | 0-2 | 128-170 | 1.4-1.7 |
| O5 | Grof zand | | | 0-2 | 220-400 | 1.5-1.7 |
| O6 | Keileem | 5-40 | | 1-7 | 150-400 | 1.1-1.6 |
| O7 | Beekleem | 35-45 | | 1-3 | 100-140 | 1.0-1.7 |
| <i>Loam</i> | <i>Zavel</i> | | | | | |
| O8 | Zeer lichte zavel | | 8-11 | 0-2 | | 1.4-1.6 |
| O9 | Matig lichte zavel | | 12-17 | 0-2 | | 1.3-1.7 |
| O10 | Zware zavel | | 18-22 | 0-3 | | 1.3-1.5 |
| <i>Clay</i> | <i>Klei</i> | | | | | |
| O11 | Lichte klei | | 28-33 | 1-3 | | 1.3-1.6 |
| O12 | Matig zware klei | | 35-48 | 0-3 | | 1.0-1.5 |
| O13 | Zeer zware klei | | 50-77 | 0-3 | | 1.0-1.4 |
| <i>Silt</i> | <i>Leem</i> | | | | | |
| O14 | Zandige leem | 60-75 | | 0-2 | | 1.0-1.6 |
| O15 | Siltige leem | 85-92 | | 1-3 | | 1.1-1.6 |
| <i>Peat</i> | <i>Veen</i> | | | | | |
| O16 | Oligotroof veen | | | 40-96 | | 0.1-0.7 |
| O17 | Mesotroof en eutroof veen | | | 60-80 | | 0.1-0.6 |
| O18 | Moerige tussenlaag | | | 15-30 | | 0.8-1.4 |

| TOP-SOILS | | | | | | |
|------------------|---|---|------------------------------------|---------------------------------|------------------|------------------|
| | θ_{res} (cm ³ cm ⁻³) | θ_{sat} (cm ³ cm ⁻³) | K_{sat} (cm d ⁻¹) | α (cm ⁻¹) | λ (-) | $n^{(1)}$ (-) |
| <i>Sand</i> | | | | | | |
| B1 | 0.02 | 0.43 | 23.41 | 0.0234 | -0.000 | 1.801 |
| B2 | 0.02 | 0.42 | 12.52 | 0.0276 | -1.060 | 1.491 |
| B3 | 0.02 | 0.46 | 15.42 | 0.0144 | -0.215 | 1.534 |
| B4 | 0.02 | 0.46 | 29.22 | 0.0156 | 0.000 | 1.406 |
| B5 | 0.01 | 0.36 | 52.91 | 0.0452 | -0.359 | 1.933 |
| B6 | 0.01 | 0.38 | 100.69 | 0.0222 | -1.747 | 1.238 |
| <i>Loam</i> | | | | | | |
| B7 | 0.00 | 0.40 | 14.07 | 0.0194 | -0.802 | 1.250 |
| B8 | 0.01 | 0.43 | 2.36 | 0.0099 | -2.244 | 1.288 |
| B9 | 0.00 | 0.43 | 1.54 | 0.0065 | -2.161 | 1.325 |
| <i>Clay</i> | | | | | | |
| B10 | 0.01 | 0.43 | 1.70 | 0.0064 | -3.884 | 1.210 |
| B11 | 0.01 | 0.59 | 4.53 | 0.0195 | -5.901 | 1.109 |
| B12 | 0.01 | 0.54 | 5.37 | 0.0239 | -5.681 | 1.094 |
| <i>Silt</i> | | | | | | |
| B13 | 0.01 | 0.42 | 12.98 | 0.0084 | -1.497 | 1.441 |
| B14 | 0.01 | 0.42 | 0.80 | 0.0051 | 0.000 | 1.305 |
| <i>Peat</i> | | | | | | |
| B15 | 0.01 | 0.53 | 81.28 | 0.0242 | -1.476 | 1.280 |
| B16 | 0.01 | 0.80 | 6.79 | 0.0176 | -2.259 | 1.293 |
| B17 | 0.00 | 0.72 | 4.46 | 0.0180 | -0.350 | 1.140 |
| B18 | 0.00 | 0.77 | 6.67 | 0.0197 | -1.845 | 1.154 |
| SUB-SOILS | | | | | | |
| | θ_{res} (cm ³ cm ⁻³) | θ_{sat} (cm ³ cm ⁻³) | K_{sat} (cm d ⁻¹) | α (cm ⁻¹) | λ (-) | n (-) |
| <i>Sand</i> | | | | | | |
| O1 | 0.01 | 0.36 | 15.22 | 0.0224 | 0.000 | 2.286 |
| O2 | 0.02 | 0.38 | 12.68 | 0.0213 | 0.168 | 1.951 |
| O3 | 0.01 | 0.34 | 10.87 | 0.0170 | 0.000 | 1.717 |
| O4 | 0.01 | 0.35 | 9.86 | 0.0155 | 0.000 | 1.525 |
| O5 | 0.01 | 0.32 | 25.00 | 0.0521 | 0.000 | 2.374 |
| O6 | 0.01 | 0.33 | 33.92 | 0.0162 | -1.330 | 1.311 |
| O7 | 0.01 | 0.51 | 39.10 | 0.0123 | -2.023 | 1.152 |
| <i>Loam</i> | | | | | | |
| O8 | 0.00 | 0.47 | 9.08 | 0.0136 | -0.803 | 1.342 |
| O9 | 0.00 | 0.46 | 2.23 | 0.0094 | -1.382 | 1.400 |
| O10 | 0.01 | 0.48 | 2.12 | 0.0097 | -1.879 | 1.257 |
| <i>Clay</i> | | | | | | |
| O11 | 0.00 | 0.42 | 13.79 | 0.0191 | -1.384 | 1.152 |
| O12 | 0.00 | 0.56 | 1.02 | 0.0095 | -4.295 | 1.158 |
| O13 | 0.00 | 0.57 | 4.37 | 0.0194 | -5.955 | 1.089 |
| <i>Silt</i> | | | | | | |
| O14 | 0.01 | 0.38 | 1.51 | 0.0030 | -0.292 | 1.728 |
| O15 | 0.01 | 0.41 | 3.70 | 0.0071 | 0.912 | 1.298 |
| <i>Peat</i> | | | | | | |
| O16 | 0.00 | 0.89 | 1.07 | 0.0103 | -1.411 | 1.376 |
| O17 | 0.01 | 0.86 | 2.93 | 0.0123 | -1.592 | 1.276 |
| O18 | 0.01 | 0.57 | 43.45 | 0.0138 | -1.204 | 1.323 |

(1) The parameters of the Mualem - van Genuchten model are explained in Par. **Error! Reference source not found.**

Appendix 3 Critical pressure head values for root water extraction (Taylor and Ashcroft, 1972)

| Crop | h_{3h} | h_{3l} | Crop | h_{3h} | h_{3l} |
|--------------------------------|----------|----------|---------------------------|----------|----------|
| <i>Vegetative crops</i> | | | Deciduous fruit | -500 | -800 |
| Alfalfa | -1500 | -1500 | Avocadoes | -500 | -500 |
| Beans (snap and lima) | -750 | -2000 | Grapes | | |
| Cabbage | -600 | -700 | early season | -400 | -500 |
| Canning peas | -300 | -500 | during maturity | -1000 | -1000 |
| Celery | -200 | -300 | Strawberries | -200 | -300 |
| Grass | -300 | -1000 | Cantaloupe | -350 | -450 |
| Lettuce | -400 | -600 | Tomatoes | -800 | -1500 |
| Tobacco | -300 | -800 | Bananas | -300 | -1500 |
| Sugar cane | | | | | |
| tensiometer | -150 | -500 | <i>Grain crops</i> | | |
| blocks | -1000 | -2000 | Corn | | |
| Sweet corn | -500 | -1000 | vegetative period | -500 | -500 |
| Turfgrass | -240 | -360 | during ripening | -8000 | -12000 |
| | | | Small grains | | |
| <i>Root crops</i> | | | vegetative period | -400 | -500 |
| Onions | | | during ripening | -8000 | -12000 |
| early growth | -450 | -550 | | | |
| bulbing time | -550 | -650 | <i>Seed crops</i> | | |
| Sugar beets | -400 | -600 | Alfalfa | | |
| Potatoes | -300 | -500 | prior to bloom | -2000 | -2000 |
| Carrots | -550 | -650 | during bloom | -4000 | -8000 |
| Broccoli | | | during ripening | -8000 | -15000 |
| early | -450 | -550 | Carrots | | |
| after budding | -600 | -700 | at 60 cm depth | -4000 | -6000 |
| Cauliflower | -600 | -700 | Onions | | |
| | | | at 7 cm depth | -4000 | -6000 |
| <i>Fruit crops</i> | | | at 15 cm depth | -1500 | -1500 |
| Lemons | -400 | -400 | Lettuce | | |
| Oranges | -200 | -1000 | during productive phase | -3000 | -3000 |

Appendix 4 Salt tolerance data (Maas, 1990)^(a)

| Crop common name | Crop botanical name | $EC_{max}^{(b)}$ (dS m ⁻¹) | EC_{slope} (% per dS m ⁻¹) | Rating ^(c) | Ref. ^(d) |
|-----------------------------------|----------------------------|---|--|-----------------------|---------------------|
| Fiber and grain crops | | | | | |
| Barley ^(e) | Hordeum vulgare | 8.0 | 5.0 | T | 1 |
| Bean | Phaseolus vulgaris | 1.0 | 19.0 | S | 1 |
| Corn | Zea mays | 1.7 | 12.0 | MS | 1 |
| Cotton | Gossypium hirsutum | 7.7 | 5.2 | T | 1 |
| Peanut | Arachis hypogaea | 3.2 | 29.0 | MS | 1 |
| Rice (paddy) | Oryza sativa | 3.0 | 12.0 | S | 1 |
| Rye | Secale cereale | 11.4 | 10.8 | T | 2 |
| Sorghum | Sorghum bicolor | 6.8 | 16.0 | MT | 2 |
| Soybean | Glycine max | 5.0 | 20.0 | MT | 1 |
| Sugar beet ^(f) | Beta vulgaris | 7.0 | 5.9 | T | 1 |
| Sugar cane | Sacharum officinarum | 1.7 | 5.9 | MS | 1 |
| Wheat | Triticum aestivum | 6.0 | 7.1 | MT | 1 |
| Wheat, durum | Triticum turgidum | 5.9 | 3.8 | T | 2 |
| Grasses and forage crops | | | | | |
| Alfalfa | Medicago sativa | 2.0 | 7.3 | MS | 1 |
| Barley (forage) ^(e) | Hordeum vulgare | 6.0 | 7.1 | MT | 1 |
| Bermuda grass ^(g) | Cynodon dactylon | 6.9 | 6.4 | T | 1 |
| Clover, ladino | Trifolium repens | 1.5 | 12.0 | MS | 1 |
| Corn (forage) | Zea mays | 1.8 | 7.4 | MS | 1 |
| Cowpea (forage) | Vigna unguiculata | 2.5 | 11.0 | MS | 3 |
| Ryegrass, perennial | Lolium perenne | 5.6 | 7.6 | MT | 1 |
| Sundan grass | Sorghum sudanese | 2.8 | 4.3 | MT | 1 |
| Wheat (forage) ^(h) | Triticum aestivum | 4.5 | 2.6 | MT | 2 |
| Wheat, durum (forage) | Triticum turgidum | 2.1 | 2.5 | MT | 2 |
| Vegetables and fruit crops | | | | | |
| Bean | Phaseolus vulgaris | 1.0 | 19.0 | S | 1 |
| Beet, red ^(f) | Beta vulgaris | 4.0 | 9.0 | MT | 1 |
| Broccoli | Brassica oleracea botrytis | 2.8 | 9.2 | MS | 1 |
| Cabbage | Brassica oleracea capitata | 1.8 | 9.7 | MS | 1 |
| Carrot | Daucus carota | 1.0 | 14.0 | S | 1 |
| Corn, sweet | Zea mays | 1.7 | 12.0 | MS | 1 |
| Cucumber | Cucumis sativus | 2.5 | 13.0 | MS | 1 |
| Lettuce | Lactuca sativa | 1.3 | 13.0 | MS | 1 |
| Onion | Allium cepa | 1.2 | 16.0 | S | 1 |
| Potato | Solanum tuberosum | 1.7 | 12.0 | MS | 1 |
| Spinach | Spinacia oleracea | 2.0 | 7.6 | MS | 1 |
| Tomato | Lycopersicon lycopersicum | 2.5 | 9.9 | MS | 1 |

(a) These data serve only as a guideline to relative tolerances among crops. Absolute tolerances vary, depending on climate, soil conditions and cultural practices.

(b) In gypsiferous soils, plants will tolerate EC_e values about 2 dS/m higher than indicated.

(c) Ratings according to Maas (1990): S sensitive, MS moderately sensitive, MT moderately tolerant, and T tolerant.

(d) References: 1 Maas and Hoffman (1977), 2 Francois et al. (1986), 3 West and Francois (1982).

(e) Less tolerant during seedling stage, EC_e at this stage should not exceed 4 dS/m or 5 dS/m.

(f) Sensitive during germination and emergence, EC_e should not exceed 3 dS/m.

(g) Average of several varieties. Suwannee and Coastal are about 20% more tolerant, and common and Greenfield are about 20% less tolerant than the average.

(h) Data from one cultivar, 'Pobred'.

Appendix 5 Shrinkage characteristic data (Bronswijk and Vermeer, 1990)

| Place | Depth | Horizon | $\rho_s^{(2)}$ | Composition | | | | | | Shrinkage par. | | |
|----------------|--------|---------|--------------------|-------------------|------------------|---------------------------|------|-------|-------------------|----------------|-------|-------|
| | | | | weight % of soil | | weight % of mineral parts | | | | e_0 | v_1 | v_s |
| | | | | CaCO ₃ | H ⁽³⁾ | <2 | 2-16 | 16-50 | >50 μm | | | |
| ⁽¹⁾ | cm | - | g cm ⁻³ | | | | | | | | | |
| 1 | 0-22 | A11 | 2.52 | 0.0 | 10.3 | 39.9 | 20.9 | 33.4 | 5.8 | 0.45 | 1.0 | 0.0 |
| | 22-42 | ACg | 2.60 | 0.0 | 6.9 | 40.7 | 25.9 | 28.3 | 5.1 | 0.37 | 0.6 | 0.0 |
| | 42-78 | C1g | 2.66 | 2.5 | 4.5 | 58.1 | 24.7 | 16.2 | 1.1 | 0.43 | 0.7 | 0.0 |
| | 78-120 | C2g | 2.68 | 6.9 | 2.2 | 24.1 | 14.3 | 53.5 | 8.1 | 0.56 | 0.7 | 0.0 |
| 2 | 0-26 | Ap | 2.64 | 1.4 | 4.8 | 45.4 | 27.8 | 16.6 | 10.2 | 0.52 | 0.8 | 0.2 |
| | 26-34 | A12 | 2.61 | 0.8 | 3.9 | 45.9 | 27.4 | 18.9 | 6.8 | 0.46 | 0.9 | 0.0 |
| | 34-56 | C11g | 2.62 | 1.7 | 2.2 | 51.6 | 29.2 | 15.4 | 3.8 | 0.48 | 0.9 | 0.1 |
| | 56-75 | C12g | 2.68 | 3.3 | 1.9 | 39.1 | 24.1 | 32.8 | 4.0 | 0.50 | 0.9 | 0.1 |
| | 75-107 | C13g | 2.69 | 0.3 | 3.0 | 59.3 | 31.7 | 6.9 | 2.1 | 0.50 | 0.9 | 0.05 |
| 3 | 0-29 | Ap | 2.65 | 9.0 | 3.3 | 52.0 | 24.2 | 20.4 | 3.4 | 0.49 | 0.7 | 0.2 |
| | 29-40 | AC | 2.67 | 10.6 | 2.9 | 62.9 | 17.0 | 17.7 | 2.4 | 0.50 | 0.8 | 0.2 |
| | 40-63 | C21 | 2.69 | 11.3 | 2.7 | 52.4 | 25.3 | 18.3 | 4.0 | 0.55 | 0.8 | 0.1 |
| | 63-80 | C22g | 2.66 | 9.8 | 2.8 | 55.8 | 24.1 | 16.7 | 3.4 | 0.58 | 1.0 | 0.1 |
| | 80-100 | C23g | 2.69 | 11.6 | 2.2 | 59.6 | 26.4 | 12.2 | 1.8 | 0.57 | 1.0 | 0.1 |
| 4 | 0-21 | A11 | 2.59 | 11.7 | 5.9 | 34.8 | 17.9 | 27.9 | 19.5 | 0.52 | 1.0 | 0.0 |
| | 21-52 | A12 | 2.61 | 11.1 | 6.2 | 42.9 | 22.1 | 26.5 | 8.5 | 0.53 | 0.9 | 0.0 |
| | 52-77 | C21g | 2.62 | 17.6 | 3.7 | 32.1 | 20.4 | 33.2 | 14.2 | 0.82 | 1.2 | 0.0 |
| | 77-100 | C22g | 2.63 | 18.8 | 3.1 | 16.2 | 10.1 | 37.8 | 36.0 | 0.79 | 1.0 | 0.0 |
| 5 | 0-22 | Ap1 | 2.66 | 9.9 | 2.6 | 36.8 | 22.2 | 27.5 | 13.5 | 0.48 | 0.8 | 0.0 |
| | 22-38 | A12 | 2.66 | 8.1 | 2.2 | 45.6 | 27.2 | 22.9 | 4.3 | 0.56 | 0.8 | 0.0 |
| | 38-60 | C22g | 2.63 | 6.6 | 7.6 | 35.3 | 43.9 | 19.7 | 1.1 | 0.68 | 1.2 | 0.1 |
| | 60-90 | C23g | 2.59 | 5.8 | 7.0 | 15.9 | 23.9 | 58.2 | 2.0 | 1.10 | 2.0 | 0.0 |
| | 90-110 | C24g | 2.57 | 4.6 | 10.5 | 20.2 | 27.2 | 51.2 | 1.4 | 1.10 | 2.1 | 0.0 |
| 6 | 0-18 | A11 | 2.52 | 0.0 | 9.9 | 58.1 | 30.7 | 10.2 | 1.0 | 0.30 | 0.9 | 0.0 |
| | 18-30 | A12 | 2.60 | 0.0 | 7.5 | 55.8 | 35.5 | 8.1 | 0.6 | 0.34 | 0.9 | 0.0 |
| | 30-58 | C11g | 2.64 | 0.0 | 3.7 | 59.6 | 29.5 | 10.1 | 0.8 | 0.37 | 0.5 | 0.0 |
| | 58-85 | C12g | 2.59 | 0.0 | 3.8 | 51.7 | 37.0 | 9.6 | 1.7 | 0.40 | 0.8 | 0.05 |
| 7 | 0-35 | Ap | 2.67 | 10.2 | 2.1 | 30.8 | 15.7 | 30.2 | 23.3 | 0.43 | 1.0 | 0.0 |
| | 35-60 | C21g | 2.67 | 13.6 | 1.6 | 46.4 | 20.5 | 21.2 | 11.9 | 0.45 | 0.8 | 0.0 |
| | 60-80 | C22g | 2.70 | 15.7 | 1.3 | 41.9 | 18.3 | 23.3 | 15.5 | 0.40 | 1.3 | 0.0 |
| | 80-95 | C23g | 2.69 | 9.5 | 0.3 | 16.2 | 6.7 | 21.0 | 56.1 | 0.40 | 1.3 | 0.0 |

(1) Locations: 1-Oosterend, 2-Nieuw Beerta, 3-Nieuw Statenzijl, 4-Schermerhorn, 5-Dronen, 6-Bruchem and 7-Kats.

(2) Density of the solid phase

(3) Organic matter

Appendix 6 Summary of input data

Main input file (default name: Swap.swp) with the sections:

- *General section*
 - Environment
 - Timing of simulation period
 - Timing of boundary conditions
 - Processes which should be simulated
 - Optional output files
- *Meteorology section*
 - Name of file with meteorological data
 - Rainfall intensity
- *Crop section*
 - Crop rotation scheme (calendar and files)
 - Crop data input file
 - Calculated irrigation input file
 - Crop emergence and harvest
 - Fixed irrigation parameters (Amount and quality of prescribed irrigation applications)
- *Soil water section*
 - Initial moisture condition
 - Ponding
 - Soil evaporation
 - Vertical discretization of soil profile
 - Soil hydraulic functions
 - Hysteresis of soil water retention function
 - Maximum rooting depth
 - Similar media scaling of soil hydraulic functions
 - Preferential flow due to soil volumes with immobile water
 - Preferential flow due to macro pores
 - Snow and frost
 - Numerical solution of Richards' equation
- *Lateral drainage section*
 - (optional) name of file with drainage input data
 - (optional) name of file with runoff input data
- *Bottom boundary section*
 - (optional) name of file with bottom boundary conditions
 - selection out of 8 options
- *Heat flow section*
 - calculation method
- *Solute transport section*
 - Specify whether simulation includes solute transport or not
 - Top boundary and initial condition
 - Diffusion, dispersion, and solute uptake by roots
 - Adsorption
 - Decomposition
 - Transfer between mobile and immobile water volumes (if present)
 - Solute residence in the saturated zone

File with daily meteorological data (*.yyy)

Radiation, temperature, vapour pressure, wind speed, rainfall and/or reference evapotranspiration, rainfall intensities

File with Detailed crop growth (*.crp)

- *Crop section*
 - Crop height
 - Crop development
 - Initial values
 - Green surface area
 - Assimilation
 - Assimilates conversion into biomass
 - Maintenance respiration
 - Dry matter partitioning
 - Death rates
 - Crop water use
 - Salt stress
 - Interception
 - Root growth and density distribution
- *Calculated Irrigation section*
 - General
 - Irrigation time criteria
 - Irrigation depth criteria

File with Simple crop growth (*.crp)

- *Crop section*
 - Crop development
 - Light extinction
 - Leaf area index or soil cover fraction
 - crop factor or crop height
 - rooting depth
 - yield response
 - soil water extraction by plant roots
 - salt stress
 - interception
 - Root density distribution and root growth
- *Calculated Irrigation section*
 - General
 - Irrigation time criteria
 - Irrigation depth criteria

File with drainage data (*.dra)

- *Basic drainage section*
 - Table of drainage flux - groundwater level
 - Drainage formula of Hooghoudt or Ernst
 - Drainage and infiltration resistances
- *Extended drainage section*
 - Drainage characteristics
 - Surface water level of primary and/or secondary system
 - Simulation of surface water level
 - Weir characteristics

Appendix 7 Example main input file .SWP

```
*****
* Filename: Hupsel.swp
* Contents: SWAP 3 - Main input data
*****
* Comment area:
*
* Case: Water and solute transport in the Hupsel area,
*       a catchment in the eastern part of the Netherlands
*
*       This case is described as example in the User's Guide
*****

* The main input file .swp contains the following sections:
*   - General section
*   - Meteorology section
*   - Crop section
*   - Soil water section
*   - Lateral drainage section
*   - Bottom boundary section
*   - Heat flow section
*   - Solute transport section

*** GENERAL SECTION ***
*****
* Part 1: Environment
*****
PROJECT = 'Hupsel'           ! Project description, [A80]
PATHWORK = ' '              ! Path to work directory, [A80]
PATHATM = 'Data\Weather\'   ! Path to directory with weather files, [A80]
PATHCROP = 'Data\Crops\'    ! Path to directory with crop files, [A80]
PATHDRAIN = 'Data\Drainage\' ! Path to directory with drainage files, [A80]
SWSCRE   = 1                ! Switch, display progression of simulation run:
                        !   SWSCRE = 0: no display to screen
                        !   SWSCRE = 1: display waterbalance to screen
                        !   SWSCRE = 2: display daynumber to screen
SWERROR  = 1                ! Switch for printing errors to screen [Y=1, N=0]
*****

* Part 2: Simulation period
*
TSTART = 01-jan-1980 ! Start date of simulation run, give day-month-year, [dd-mmm-yyyy]
TEND   = 31-dec-1982 ! End   date of simulation run, give day-month-year, [dd-mmm-yyyy]
*****

* Part 3: Output dates
*****
* Output times for water and solute balances
SWYRVAR = 0                ! Switch, output at fixed or variable dates:
                        !   SWYRVAR = 0: each year output of balances at the same date
                        !   SWYRVAR = 1: output of balances at different dates

* If SWYRVAR = 0 specify fixed date:
DATEFIX = 31 12           ! Specify day and month for output of yearly balances, [dd mm]

* If SWYRVAR = 1 specify all output dates [dd-mmm-yyyy], maximum MAOUT dates:
OUTDAT =
31-dec-1981
31-dec-1982
* End of table

* Dates for intermediate output of state variables and fluxes
SWMONTH = 1               ! Switch, output each month, [Y=1, N=0]
PERIOD  = 0               ! Fixed output interval, ignore = 0, [0..366, I]
SWRES   = 0               ! Switch, reset output interval counter each year, [Y=1, N=0]
SWODAT  = 0               ! Switch, extra output dates are given in table, [Y=1, N=0]

* If SWODAT = 1, specify all intermediate output dates [dd-mmm-yyyy],
* maximum MAOUT dates:

OUTDATINT =
31-Jan-1980
29-Feb-1980
31-Mar-1980
.
.
31-Aug-1982
30-Sep-1982
31-Oct-1982
30-Nov-1982
31-Dec-1982
* End of table
*****

* Part 4: Output files
*****
OUTFIL = 'Result' ! Generic file name of output files, [A16]
SWHEADER = 0      ! Print header of each balance period, [Y=1, N=0]

* Optional output files for water quality models or other specific use

SWAFO = 0          ! Switch, output file with formatted hydrological data
                        !   SWAFO = 0: no output
                        !   SWAFO = 1: output to a file named *.AFO
                        !   SWAFO = 2: output to a file named *.BFO

SWAUN = 0          ! Switch, output file with unformatted hydrological data
                        !   SWAUN = 0: no output
                        !   SWAUN = 1: output to a file named *.AUN
```

```

! SWAUN = 2: output to a file named *.BUN
* if SWAFO = 1 or 2, or if SWAUN = 1 or 2 then specify SWDISCRVERT and CritDevMasBalAbs
SWDISCRVERT = 0 ! Switch to convert vertical discretization [Y=1, N=0]
! only when SWAUN=1 or SWAFO=1 the generated output
! files (*.afo,*.bfo,*.aun,*.bun) are influenced
! SWDISCRVERT = 0: no conversion
! SWDISCRVERT = 1: convert vertical discretization,
! numnodNew and dzNew are required
* Critical Absolute Deviation in water balance
* (when exceeded: simulation continues, but file with errors is created (file-extension *.DWB))
CritDevMasBalAbs = 0.1 ! Critical Absolute Deviation in water balance [1.0d-30..1.0 cm, R]
*
* Only If SWDISCRVERT = 1 then numnodNew and dzNew are required
* NUMNODNEW = 6 ! New number of nodes [1...macp,I,-]
* ! (boundaries of soil layers may not change, which implies
* ! that the sum of thicknesses within a soil layer must be
* ! equal to the thickness of the soil layer. See also:
* ! SoilWaterSection, Part4: Vertical discretization of soil profile)
* DZNEW = 10.0 10.0 10.0 20.0 30.0 50.0 ! thickness of compartments [1.0d-6...5.0d2, cm, R]
*
*
* SWVAP = 1 ! Switch, output profiles of moisture, solute and temperature, [Y=1, N=0]
* SWATE = 0 ! Switch, output file with soil temperature profiles, [Y=1, N=0]
* SWBLC = 1 ! Switch, output file with detailed yearly water balance, [Y=1, N=0]
*
* Required only when SWMACRO= 1 or 2 (see Soil Water section, Part 10: macropore flow)
* SWBMA = 0 ! Switch, output file with detailed yearly water balance Macropores, [Y=1, N=0]
*
* Required only when SWDRA=2 (see lateral section): input of SWDRF and SWSWB
* SWDRF = 1 ! Switch, output drainage fluxes, only for extended drainage, [Y=1, N=0]
* SWSWB = 1 ! Switch, output surface water reservoir, only for extended drainage, [Y=1, N=0]
*****

*** METEOROLOGY SECTION ***
*****
* General data
METFIL = 'Wageningen' ! File name of meteorological data without extension .YYY, [A16]
! Extension equals last 3 digits of year number, e.g. 2003 has extension .003
SWETR = 0 ! Switch, use reference ET values of meteo file [Y=1, N=0]
*
* If SWETR = 0, then LAT,ALT and ALTW must have realistic values
LAT = 52.0 ! Latitude of meteo station, [-60..60 degrees, R, North = +]
ALT = 10.0 ! Altitude of meteo station, [-400..3000 m, R]
ALTW = 2.0 ! Altitude of wind speed measurement (10 m is default) [0..99 m, R]
*
* SWRAIN = 0 ! Switch for use of actual rainfall intensity:
! SWRAIN = 0: Use daily rainfall amounts
! SWRAIN = 1: Use daily rainfall amounts + mean intensity
! SWRAIN = 2: Use daily rainfall amounts + duration
*
* If SWRAIN = 1, then specify mean rainfall intensity RAINFLUX [0.d0..1000.d0 cm/d, R]
* as function of time TIME [0..366 d, R], maximum 30 records
TIME RAINFLUX
1.0 2.0
360.0 2.0
* End of table
*****

*** CROP SECTION ***
*****
* Part 1: Crop rotation scheme during simulation period
*
* Specify information for each crop (maximum MACROP):
* CROPPSTART = date of crop emergence, [dd-mmm-yyyy]
* CROPPEND = date of crop harvest, [dd-mmm-yyyy]
* CROPPNAME = crop name, [A16]
* CROPPFIL = name of file with crop input parameters without extension .CRP, [A16]
* CROPPTYPE = type of crop model: simple = 1, detailed general = 2, detailed grass = 3
CROPPSTART CROPPEND CROPPNAME CROPPFIL CROPPTYPE
01-may-1980 15-oct-1980 'Maize' 'MaizeS' 1
10-may-1981 29-sep-1981 'Potato' 'PotatoD' 2
01-may-1982 15-oct-1982 'Maize' 'MaizeS' 1
* End of table
*****

* Part 2: Fixed irrigation applications
*
* SWIRFIX = 1 ! Switch for fixed irrigation applications
! SWIRFIX = 0: no irrigation applications are prescribed
! SWIRFIX = 1: irrigation applications are prescribed
*
* If SWIRFIX = 1:
*
* SWIRGFIL = 0 ! Switch for file with fixed irrigation applications:
! SWIRGFIL = 0: data are specified in the .swp file
! SWIRGFIL = 1: data are specified in a separate file
*
* If SWIRGFIL = 0 specify information for each fixed irrigation event (max. MAIRG):
* IRDATE = date of irrigation, [dd-mmm-yyyy]
* IRDEPTH = amount of water, [0.0..100.0 cm, R]
* IRCONC = concentration of irrigation water, [0.0..1000.0 mg/cm3, R]
* IRTYPE = type of irrigation: sprinkling = 0, surface = 1
IRDATE IRDEPTH IRCONC IRTYPE
05-jan-1980 0.5 1000.0 1
* --- end of table
*
* If SWIRGFIL = 1 specify name of file with data of fixed irrigation applications:
IRGFIL = 'testirri' ! File name without extension .IRG [A16]
*****

```

```

*** SOIL WATER SECTION ***
*****
* Part 1: Initial moisture condition

SWINCO = 2 ! Switch, type of initial moisture condition:
! 1 = pressure head as function of depth is input
! 2 = pressure head of each compartment is in hydrostatic equilibrium
! with initial groundwater level
! 3 = read final pressure heads from previous Swap simulation

* If SWINCO = 1, specify initial pressure head H [-1.d10..1.d4 cm, R] as function of
* soil depth ZI [-10000..0 cm, R], maximum MACP data pairs:
      ZI      H
      -0.5    -92.831
      -195.0  99.591
* End of table

* If SWINCO = 2, specify:
  GWLI = -75.0 ! Initial groundwater level, [-10000..100 cm, R]

* If SWINCO = 3, specify:
  INIFIL = 'result.end' ! name of final with extension .END [a200]
*****

*****
* Part 2: Ponding, Runoff and Runon
*
PONDIX = 0.2 ! Maximum thickness of ponding water layer, [0..1000 cm, R]
*
RSRO = 0.5 ! drainage Resistance of Surface RunOff [0.001..1.0 d, R]
RSROEXP = 1.0 ! exponent in relation of surface runoff [0.1...10.0, R]
*
* Specify whether runon from external source (fiel) should be included
*
SWRUNON = 0 ! Switch, input of runon:
! 0 = No input of runon
! 1 = runon as input
*
* If SWRUNON = 1 specify name of file with runon input data
* - this file may be an output-*.inc-file (with only 1 header) of previous Swap-simulation):
* - from this file 2 columns are read, with column-headers 'date' and 'Runoff'
* - the column 'date' must have dates that correpond to the current simulation period (dates are compared)
* RUFIL = 'runon.inc' ! File name (with extension) with input data, must have extension (e.g..INC) [A80]
*****

*****
* Part 3: Soil evaporation
*
SWCFBS = 0 ! Switch for use of coefficient CFBS for soil evaporation [Y=1, N=0]
! 0 = CFBS is not used
! 1 = CFBS used to calculate potential evaporation from potential
! evapotranspiration or reference evapotranspiration

* If SWCFBS = 1, specify coefficient CFBS:
  CFBS = 1.0 ! Coefficient for potential soil evaporation, [0.5..1.5 -, R]

  SWREDU = 1 ! Switch, method for reduction of potential soil evaporation:
! 0 = reduction to maximum Darcy flux
! 1 = reduction to maximum Darcy flux and to maximum Black (1969)
! 2 = reduction to maximum Darcy flux and to maximum Bo/Str. (1986)

  COFRED = 0.35 ! Soil evaporation coefficient of Black, [0..1 cm/dl/2, R],
! or Boesten/Stroosnijder, [0..1 cml/2, R]
  RSIGNI = 0.5 ! Minimum rainfall to reset models Black and Bo/Str., [0..1 cm/d, R]
*****

*****
* Part 4: Vertical discretization of soil profile
*
* Specify the following data (maximum MACP lines):
* ISOILLAY = number of soil layer, start with 1 at soil surface, [1..MAHO, I]
* ISUBLAY = number of sub layer, start with 1 at soil surface, [1..MACP, I]
* HSUBLAY = height of sub layer, [0.0..1000.0 cm, R]
* HCOMP = height of compartments in this layer, [0.0..1000.0 cm, R]
* NCOMP = number of compartments in this layer (= HSUBLAY/HCOMP), [1..MACP, I]

ISOILLAY ISUBLAY HSUBLAY HCOMP NCOMP
  1 1 10.0 1.0 10
  1 2 20.0 5.0 4
  2 3 30.0 5.0 6
  2 4 140.0 10.0 14
* --- end of table
*****

*****
* Part 5: Soil hydraulic functions
*
* Specify for each soil layer (maximum MAHO):
* ISOILLAY1 = number of soil layer, as defined in part 4 [1..MAHO, I]
* ORES = Residual water content, [0..0.4 cm3/cm3, R]
* OSAT = Saturated water content, [0..0.95 cm3/cm3, R]
* ALFA = Shape parameter alfa of main drying curve, [0.0001..1 /cm, R]
* NPAR = Shape parameter n, [1..4 -, R]
* KSAT = Saturated vertical hydraulic conductivity, [1.d-5..1000 cm/d, R]
* LEXP = Exponent in hydraulic conductivity function, [-25..25 -, R]
* ALFAW = Alfa parameter of main wetting curve in case of hysteresis, [0.0001..1 /cm, R]

ISOILLAY1 ORES OSAT ALFA NPAR KSAT LEXP ALPAW
  1 0.01 0.43 0.0227 1.548 9.65 -0.983 0.0454
  2 0.02 0.38 0.0214 2.075 15.56 0.039 0.0428
* --- end of table
*****

```

```

*****
* Part 6: Hysteresis of soil water retention function

SWHYST = 0 ! Switch for hysteresis:
! 0 = no hysteresis
! 1 = hysteresis, initial condition wetting
! 2 = hysteresis, initial condition drying

* If SWHYST = 1 or 2, specify:
TAU = 0.2 ! Minimum pressure head difference to change wetting-drying, [0..1 cm, R]
*****

* Part 7: Maximum rooting depth

RDS = 200.0 ! Maximum rooting depth allowed by the soil profile, [1..5000 cm, R]
*****

* Part 8: Similar media scaling of soil hydraulic functions

SWSCAL = 0 ! Switch for similar media scaling [Y=1, N=0]; no hysteresis is allowed
! in case of similar media scaling (SWHYST = 0)

* If SWSCAL = 1, specify:
NSCALE = 3 ! Number of simulation runs, [1..MASCALE, I]

* Supply the scaling factors for each simulation run and each soil layer:

RUN      SOIL1      SOIL2
  1       0.5       2.0
  2       1.0       1.0
  3       2.0       0.5
  4       1.0       1.0
  5       3.0       3.0
* End of table
*****

* Part 9: Preferential flow due to water repellency

SWMOBI = 0 ! Switch for preferential flow due to immobile water, [Y=1, N=0]; hysteresis
! or scaling are not allowed in case of preferential flow (SWHYST = 0; SWSCAL = 0)

* If SWMOBI = 1, specify mobile fraction as function of log -h for each soil layer:
*
* ISOILLY2 = number of soil layer, as defined in part 4 [1..MAHO, I]
* PF1 = first datapoint, log -h (cm), [0..5, R]
* FM1 = first datapoint, mobile fraction (1.0 = totally mobile), [0..1, R]
* PF2 = second datapoint, log -h (cm), [0..5, R]
* FM2 = second datapoint, mobile fraction (1.0 = totally mobile), [0..1, R]
* THETIM = specify volumetric water content in immobile soil volume, [0..0.3, R]

ISOILLY2  PF1  FM1  PF2  FM2  THETIM
  1       0.0  0.4  3.0  0.4  0.02
  2       0.0  1.0  3.0  1.0  0.02
* End of table
*****

* Part 10: Preferential flow due to macropores
SWMACRO = 0 ! Switch for macropore flow, [0..2, I]:
! 0 = no macropore flow
! 1 = simple macropore flow
! 2 = advanced macropore flow

* If SWMACRO = 1, specify parameters for simple macropore flow:
SHRINA = 0.53 ! Void ratio at zero water content, [0..2 cm3/cm3, R]
MOISR1 = 1.0 ! Moisture ratio at trans. residual --> normal shrinkage [0.5 cm3/cm3, R]
MOISR2 = 0.01 ! Amount of structural shrinkage, [0..1 cm3/cm3, R]
ZNCRACK = -5.0 ! Depth at which crack area of soil surface is calculated [-100..0 cm, R]
GEOMF = 3.0 ! Geometry factor (3 = isotropic shrinkage), [0..100, R]
DIAMPOL = 40.0 ! Diameter soil matrix polygon, [0..100 cm, R]
RAPCOEF = 10.1 ! Rate coef. bypass flow from cracks to surface water [0..10000 /d, R]
DIFDES = 0.2 ! Effective lateral solute diffusion coefficient, [0..10000 /cm, R]
* critical water content of each soil layer (max. MAHO), [0..1, R];
* if actual water becomes smaller than critical water content, cracks are formed
THETCR = 0.49 0.40 0.38 0.38 0.38 0.39 0.39

* End of input for simple macropore flow, advance to next part

* If SWMACRO = 2, specify parameters for advanced macropore flow:
Z_AH = -35.0 ! Depth bottom A-horizon [-1000..0 cm, R]
Z_IC = -70.0 ! Depth bottom Internal Catchment (IC) domain [-1000..0 cm, R]
Z_ST = -35.0 ! Depth bottom Static macropores [-1000..0 cm, R]
VLMPTSS = 0.05 ! Volume of Static Macropores at Soil Surface [0..1 cm3/cm3, R]
PPICSS = 0.5 ! Proportion of IC domain at Soil Surface [0..1 -, R]
NUMSBDM = 5 ! Number of Subdomains in IC domain [0..MaDm -, I]
POWM = 1.0 ! Power M for frequency distribut. curve IC domain (OPTIONAL, default 1.0) [0..100 -, R]
RZAH = 0.0 ! Fraction macropores ended at bottom A-horizon [OPTIONAL, default 0.0] [0..1 -, R]
SPOINT = 1.0 ! Symmetry Point for freq. distr. curve [OPTIONAL, default 1.0] [0..1 -, R]
SWPOWM = 0 ! Switch for double convex/concave freq. distr. curve (OPTIONAL, Y=1, N=0; default: 0) [0..1 -, I]
DIPOMI = 10.0 ! Minimal diameter soil polygons (shallow) [0.1..1000 cm, R]
DIPOMA = 50.0 ! Maximal diameter soil polygons (deep) [0.1..1000 cm, R]

*Start of Tabel with shrinkage characteristics
* ISOILLY3 = number of soil layer, as defined in part 4 [1..MAHO, I]
* SWSoilShr = Switch for kind of soil for determining shrinkage curve: 0 = rigid soil, 1 = clay, 2 peat [0..2 -, I]
* SWSoilShr = Switch for determining shrinkage curve [1..2 -, I]: 1 = parameters for curve are given;
* 2 = typical points of curve are given
*
* GeomFac = Geometry factor (3 = isotropic shrinkage), [0..100, R]
* ShrParA to ShrParE = parameters for describing shrinkage curves,
* depending on combination of SWSoilShr and SwShrInp [-1000..1000, R]:
* SWSoilShr = 0 : 0 variables required (all dummies)
* SWSoilShr = 1, SwShrInp 1 = : 3 variables required (ShrParA to ShrParC) (rest dummies)
* SWSoilShr = 1, SwShrInp 2 = : 2 variables required (ShrParA to ShrParB) (rest dummies)
* SWSoilShr = 2, SwShrInp 1 = : 4 variables required (ShrParA to ShrParD) (rest dummies)

```



```

*
      SWSoilShr = 2, SwShrInp 2 = : 5 variables required (ShrParA to ShrParE)
* ISOILLAY3  SWSoilShr  SwShrInp  ThetCrMP  GeomFac  ShrParA  ShrParB  ShrParC  ShrParD  ShrParE
  1          1          2          0.41     3.0     0.343  0.520  0.0     0.0     0.0
  2          1          2          0.40     3.0     0.343  0.520  0.0     0.0     0.0
  3          1          2          0.38     3.0     0.415  0.642  0.0     0.0     0.0
  4          1          2          0.38     3.0     0.400  0.659  0.0     0.0     0.0
  5          1          2          0.38     3.0     0.412  0.650  0.0     0.0     0.0
  6          1          2          0.39     3.0     0.406  0.700  0.0     0.0     0.0
  7          1          2          0.39     3.0     0.496  0.700  0.0     0.0     0.0
*End of Tabel with shrinkage characteristics

ZnCrAr = -5.0 ! Depth at which crack area of soil surface is calculated [-100..0 cm, R]

*Start of Tabel with sorptivity characteristics
* ISOILLAY4 = number of soil layer, as defined in part 4 [1..MAHO, I]
* SWSorp    = Switch for kind of sorptivity function [1..2 -, I]:
*           1 = calculated from hydraulic functions according to Parlange
*           2 = empirical function from measurements
* SorpFacPar1 = factor for modifying Parlange function (OPTIONAL, default 1.0) [0..100 -, R]
* SorpMax    = maximal sorptivity at theta residual [0..100 cm/d*0.5, R]
* SorpAlfa   = fitting parameter for empirical sorptivity curve [-10..10 -, R]
* ISOILLAY4  SWSorp  SorpFacPar1  SorpMax  SorpAlfa
  1          2          1.0         5.0     0.5
  2          2          1.0         5.0     0.5
  3          2          1.0         5.0     0.5
  4          2          1.0         5.0     0.5
  5          2          1.0         5.0     0.5
  6          2          1.0         5.0     0.5
  7          2          1.0         5.0     0.5
*End of Tabel with sorptivity characteristics

SwDrRap = 1 ! Switch for kind of drainage function TEMPORARY: TEST option [1..2 -, I]:
RapDraResRef = 1 * 0.1 ! Reference rapid drainage resistance [0..10000 /d, R]
                ! an array with a single element must be indicated using a multiplier asterix
                ! (see TUTTIL-manual, par. 5.2 Defining arrays)
RapDraReaCof = 2.0 ! reaction coefficient for rapid drainage [0..100 -, R]

*****

*****
* Part 11: Snow and frost
*
* SWSNOW = 0 ! Switch, calculate snow accumulation and melt. [Y=1, N=0]
*
* If SWSNOW = 1, then specify initial snow water equivalent and snowmelt factor
* SNOWINCO = 22.0 ! the initial SWE (Snow Water Equivalent), [0.0..1000.0 cm, R]
* SNOWCOEF = 0.3 ! calibration factor for snowmelt, [0.0..10.0 -, R]
*
* SWFROST = 0 ! Switch, in case of frost: stop soil water flow, [Y=1, N=0]
*****

*****
* Part 12 Numerical solution of Richards' equation
*
* DTMIN = 1.0d-7 ! Minimum timestep, [1.d-8..0.1 d, R]
* DTMAX = 0.2 ! Maximum timestep, [ 0.01..0.5 d, R]
* THETOL = 0.001 ! Maximum dif. water content between iterations, [1.d-5..0.01 cm3/cm3, R]
* GWLCONV = 100.0 ! Maximum dif. groundwater level between iterations, [1.d-5..1000 cm, R]
* CritDevMasBalDt = 0.01 ! Critical Deviation in water balance of timestep [1.0d-5..100.0 cm, R]
* MSTEPS = 100000 ! Maximum number of iteration steps to solve Richards', [ 2..100000 -, I]
* SWBALANCE = 0 ! Switch to allow compensation of water balance, [Y=1, N=0]
* (use of SWBALANCE=1 is not recommended in this version, not tested yet !)
*****

*** LATERAL DRAINAGE SECTION ***

*****
* Specify whether lateral drainage to surface water should be included
*
* SWDRA = 1 ! Switch, simulation of lateral drainage:
*         ! 0 = No simulation of drainage
*         ! 1 = Simulation with basic drainage routine
*         ! 2 = Simulation with extended drainage routine (includes surface water management)
*
* If SWDRA = 1 or SWDRA = 2 specify name of file with drainage input data:
* DRFIL = 'Hupsel' ! File name with drainage input data without extension .DRA, [A16]
*****

*** BOTTOM BOUNDARY SECTION ***

*****
* Bottom boundary condition

* SWBCCFILE = 0 ! Switch for file with bottom boundary conditions:
*             ! SWBCCFILE = 0: data are specified in the .swp file
*             ! SWBCCFILE = 1: data are specified in a separate file
*
* If SWBCCFILE = 1 specify name of file with bottom boundary conditions:
* BBCFIL = ' ' ! File name without extension .BBC [A16]
*
* If SWBCCFILE = 0, select one of the following options:
* 1 Prescribe groundwater level
* 2 Prescribe bottom flux
* 3 Calculate bottom flux from hydraulic head of deep aquifer
* 4 Calculate bottom flux as function of groundwater level
* 5 Prescribe soil water pressure head of bottom compartment
* 6 Bottom flux equals zero
* 7 Free drainage of soil profile
* 8 Free outflow at soil-air interface

* SWBOTB = 6 ! Switch for bottom boundary [1..8,-,I]

* Options 1,2,3,4,and 5 require additional data as specified below!
*****

```

```

*****
* SWBOTB = 1 Prescribe groundwater level
* specify DATE [dd-mmm-yyyy] and groundwater level [cm, -10000..1000, R]
      DATE1      GWLEVEL      ! (max. MABBC records)
01-jan-1981      -95.0
31-dec-1983      -95.0
* End of table
*****

*****
* SWBOTB = 2 Prescribe bottom flux
* Specify whether a sine or a table are used to prescribe the bottom flux:
SW2 = 2 ! Sine function = 1, table = 2
* In case of sine function (SW2 = 1), specify:
SINAVE = 0.1 ! Average value of bottom flux, [-10..10 cm/d, R, + = upwards]
SINAMP = 0.05 ! Amplitude of bottom flux sine function, [-10..10 cm/d, R]
SINMAX = 91.0 ! Time of the year with maximum bottom flux, [1..366 d, R]
* In case of table (SW2 = 2), specify date [dd-mmm-yyyy] and bottom flux QBOT2
* [-100..100 cm/d, R, positive = upwards]:
      DATE2      QBOT2      ! (maximum MABBC records)
01-jan-1980      0.1
30-jun-1980      0.2
23-dec-1980      0.15
* End of table
*****

*****
* SWBOTB = 3 Calculate bottom flux from hydraulic head in deep aquifer
* Specify:
SHAPE = 0.79 ! Shape factor to derive average groundwater level, [0..1 -, R]
HDRAIN = -110.0 ! Mean drain base to correct for average groundwater level, [-10000..0 cm, R]
RIMLAY = 500.0 ! Vertical resistance of aquitard, [0..10000 d, R]
* Specify whether a sine or a table are used to prescribe hydraulic head of deep aquifer:
SW3 = 1 ! 1 = Sine function, 2 = table
* In case of sine function (SW3 = 1), specify:
AQAVE = -140.0 ! Average hydraulic head in underlying aquifer, [-10000..1000 cm, R]
AQAMP = 20.0 ! Amplitude hydraulic head sinus wave, [0..1000 cm, R]
AQTMAX = 120.0 ! First time of the year with maximum hydraulic head, [1..366 d, R]
AQPER = 365.0 ! Period hydraulic head sinus wave, [1..366 d, I]
* In case of table (SW3 = 2), specify date [dd-mmm-yyyy] and average hydraulic head
* HAQUIF in underlying aquifer [-10000..1000 cm, R]:
      DATE3      HAQUIF      ! (maximum MABBC records)
01-jan-1980      -95.0
30-jun-1980      -110.0
23-dec-1980      -70.0
* End of table
* An extra groundwater flux can be specified which is added to above specified flux
SW4 = 1 ! 0 = no extra flux, 1 = include extra flux
* If SW4 = 1, specify date [dd-mmm-yyyy] and bottom flux QBOT4 [-100..100 cm/d, R,
* positive = upwards]:
      DATE4      QBOT4      ! (maximum MABBC records)
01-jan-1980      1.0
30-jun-1980      -0.15
23-dec-1980      1.2
* End of table
*****

*****
* SWBOTB = 4 Calculate bottom flux as function of groundwater level
* Specify coefficients of relation qbot = A exp (B*abs(groundwater level))
COFQHA = 0.1 ! Coefficient A, [-100..100 cm/d, R]
COFQHB = 0.5 ! Coefficient B [-1..1 /cm, R]
*****

*****
* SWBOTB = 5 Prescribe soil water pressure head of bottom compartment
* Specify DATE [dd-mmm-yyyy] and bottom compartment pressure head HBOT5
* [-1.d10..1000 cm, R]:
      DATE5      HBOT5      ! (maximum MABBC records)
01-jan-1980      -95.0
30-jun-1980      -110.0
23-dec-1980      -70.0
* End of table
*****

*** HEAT FLOW SECTION ***
*****
* Part 1: Specify whether simulation includes heat flow
SWHEA = 0 ! Switch for simulation of heat transport, [Y=1, N=0]
*****
* Part 2: Heat flow calculation method
SWCALT = 1 ! Switch for method: 1 = analytical method, 2 = numerical method
*****

```

```

*****
* Analytical method
* If SWCALT = 1 specify the following heat parameters:
TAMPLI = 10.0 ! Amplitude of annual temperature wave at soil surface, [0..50 C, R]
TMEAN = 15.0 ! Mean annual temperature at soil surface, [5..30 C, R]
TIMREF = 90.0 ! Time in the year with top of sine temperature wave [1..366 d, R]
DDAMP = 50.0 ! Damping depth of temperature wave in soil, [0..500 cm, R]
*****

*****
* Numerical method
* If SWCALT = 2 list initial temperature TSOIL [-20..40 C, R] as function of
* soil depth ZH [-1d5..0 cm, R]:
* When SWINCO = 3, dummy values can be present for ZH and TSOIL, because real values
* are read from file INIFIL (see this file: Soil Water section, Part 1)

      ZH      TSOIL      ! (maximum MACP records)
      -10.0   15.0
      -40.0   12.0
      -70.0   10.0
      -95.0    9.0
* End of table

* If SWCALT = 2 specify for each soil type the soil texture (g/g mineral parts)
* and the organic matter content (g/g dry soil):

      ISOILLY5  PSAND    PSILT    PCLAY    ORGMAT      ! (maximum MAHO records)
      1          0.80    0.15    0.05    0.100
      2          0.80    0.15    0.05    0.100
      3          0.78    0.14    0.08    0.012
* End of table
*****

*** SOLUTE SECTION ***
*****
* Part 1: Specify whether simulation includes solute transport
      SWSOLU = 1 ! Switch for simulation of solute transport, [Y=1, N=0]
*****

*****
* Part 2: Top boundary and initial condition
      CPRE = 0.0 ! Solute concentration in precipitation, [1..100 mg/cm3, R]
* List initial solute concentration CML [1..1000 mg/cm3, R] as function of soil depth ZC
* [-10000..0 cm, R], max. MACP records:
* When SWINCO=3, then dummy values must be present for ZC and CML, because real values
* are read from file INIFIL (See this file: SOIL WATER SECTION, part 1)
      ZC      CML
      -10.0   0.0
      -95.0   0.0
* End of table
*****

*****
* Part 3: Diffusion, dispersion, and solute uptake by roots
      DDIF = 0.0 ! Molecular diffusion coefficient, [0..10 cm2/day, R]
      LDIS = 5.0 ! Dispersion length, [0..100 cm, R]
      TSFC = 0.0 ! Relative uptake of solutes by roots, [0..10 -, R]
*****

*****
* Part 4: Adsorption
      SWSP = 0 ! Switch, consider solute adsorption, [Y=1, N=0]
* In case of adsorption (SWSP = 1), specify:
      KF = 1.0 ! Freundlich coefficient, [0..100 cm3/mg, R]
      FREXP = 0.9 ! Freundlich exponent, [0..10 -, R]
      CREF = 1.0 ! Reference solute concentration for adsorption, [0..1000 mg/cm3, R]
*****

*****
* Part 5: Decomposition
      SWDC = 0 ! Switch, consideration of solute decomposition, [Y=1, N=0]
* In case of solute decomposition (SWDC = 1), specify:
      DECPOT = 0.0 ! Potential decomposition rate, [0..10 /d, R]
      GAMPAR = 0.0 ! Factor reduction decomposition due to temperature, [0..0.5 /C, R]
      RTHETA = 0.3 ! Minimum water content for potential decomposition, [0..0.4 cm3/cm3, R]
      BEXP = 0.7 ! Exponent in reduction decomposition due to dryness, [0.2 -, R]
* List the reduction of pot. decomposition for each soil type, [0..1 -, R]:
      ISOILLY6  FDEPTH      ! (maximum MAHO records)
      1          1.00
      2          0.65
* End of table
*****

*****
* Part 6: Transfer between mobile and immobile water volumes
      SWPREF = 0 ! Switch, consider mobile-immobile water volumes, [Y=1, N=0]
* If SWPREF = 1, specify:
      KMOBIL = 0.3 ! Solute transfer coefficient between mobile-immobile parts, [0..100 /d, R]
*****

```

```
*****
* Part 7: Solute residence in the saturated zone
  SWBR = 0      ! Switch, consider mixed reservoir of saturated zone [Y=1, N=0]
* Without mixed reservoir (SWBR = 0), specify:
  CDRAIN = 0.1  ! solute concentration in groundwater, [0..100 mg/cm3, R]
* In case of mixed reservoir (SWBR = 1), specify:
  DAQUIF = 110.0 ! Thickness saturated part of aquifer, [0..10000 cm, R]
  POROS  = 0.4  ! Porosity of aquifer, [0..0.6, R]
  KFSAT  = 0.2  ! Linear adsorption coefficient in aquifer, [0..100 cm3/mg, R]
  DECSAT = 1.0  ! Decomposition rate in aquifer, [0..10 /d, R]
  CDRAINI = 0.2 ! Initial solute concentration in groundwater, [0..100 mg/cm3, R]
*****
* End of the main input file .SWP!
```

Appendix 8 Example weather input file .YYY

```

*****
* Filename: Wageningen.980
* Contents: SWAP 3.0 - Meteo data of Wageningen weather station
*****
* Comment area:
*
* Including rainfall duration
*****
* Station DD MM YYYY RAD Tmin Tmax HUM WIND RAIN ETref WET
  nr      nr      nr      kJ/m2   C   C   kPa  m/s   mm   mm   d
*****
'Wageningen' 1 1 1980 2540.0 -1.2 1.4 0.62 3.5 6.2 -99.9 0.1550
'Wageningen' 2 1 1980 3520.0 -6.5 1.4 0.53 1.7 0.0 -99.9 0.0000
'Wageningen' 3 1 1980 1510.0 -8.2 0.1 0.49 2.2 0.2 -99.9 0.0050
'Wageningen' 4 1 1980 740.0 -0.3 3.5 0.66 4.5 7.0 -99.9 0.1750
'Wageningen' 5 1 1980 990.0 2.8 5.1 0.78 3.0 2.2 -99.9 0.0550
'Wageningen' 6 1 1980 1090.0 3.8 6.0 0.82 3.7 8.7 -99.9 0.2175
'Wageningen' 7 1 1980 1720.0 1.4 5.5 0.76 1.5 0.3 -99.9 0.0075
'Wageningen' 8 1 1980 500.0 0.2 3.5 0.66 2.5 0.0 -99.9 0.0000
'Wageningen' 9 1 1980 1500.0 -0.1 1.3 0.59 2.2 0.0 -99.9 0.0000
'Wageningen' 10 1 1980 660.0 -1.6 0.5 0.49 2.5 0.0 -99.9 0.0000
'Wageningen' 11 1 1980 1080.0 -5.9 -1.2 0.39 2.7 0.0 -99.9 0.0000
\
\
\
\
\
\
\
\
\
'Wageningen' 30 11 1980 3870.0 -6.5 0.0 0.39 3.2 0.0 -99.9 0.0000
'Wageningen' 1 12 1980 4460.0 -8.2 1.6 0.41 1.2 0.0 -99.9 0.0000
'Wageningen' 2 12 1980 420.0 -1.5 2.6 0.59 2.4 1.1 -99.9 0.0275
'Wageningen' 3 12 1980 3090.0 -1.1 2.7 0.58 2.5 0.7 -99.9 0.0175
'Wageningen' 4 12 1980 2690.0 -2.3 3.3 0.60 2.4 2.3 -99.9 0.0575
'Wageningen' 5 12 1980 370.0 -1.4 6.7 0.69 3.1 8.4 -99.9 0.2100
'Wageningen' 6 12 1980 2780.0 -4.2 3.0 0.52 2.8 2.8 -99.9 0.0700
'Wageningen' 7 12 1980 1790.0 -6.3 -0.3 0.46 1.5 0.5 -99.9 0.0125
'Wageningen' 8 12 1980 2920.0 -7.7 1.2 0.50 1.6 0.0 -99.9 0.0000
'Wageningen' 9 12 1980 1710.0 -3.4 1.5 0.38 4.6 0.0 -99.9 0.0000
'Wageningen' 10 12 1980 1370.0 -1.8 5.9 0.53 4.7 0.0 -99.9 0.0000
'Wageningen' 11 12 1980 190.0 5.0 7.8 0.89 5.6 2.1 -99.9 0.0525
'Wageningen' 12 12 1980 520.0 4.7 7.6 0.91 3.4 0.0 -99.9 0.0000
'Wageningen' 13 12 1980 490.0 5.3 10.8 0.88 5.7 0.6 -99.9 0.0150
'Wageningen' 14 12 1980 720.0 6.8 12.2 1.04 5.4 2.7 -99.9 0.0675
'Wageningen' 15 12 1980 2880.0 3.8 8.8 0.81 4.7 2.0 -99.9 0.0500
'Wageningen' 16 12 1980 3230.0 0.8 7.5 0.69 2.5 2.2 -99.9 0.0550
'Wageningen' 17 12 1980 1980.0 0.8 5.1 0.63 5.3 10.4 -99.9 0.2600
'Wageningen' 18 12 1980 1960.0 0.7 5.6 0.70 2.9 5.9 -99.9 0.1475
'Wageningen' 19 12 1980 900.0 0.0 2.4 0.59 3.5 0.3 -99.9 0.0075
'Wageningen' 20 12 1980 510.0 -0.4 3.6 0.61 3.8 2.7 -99.9 0.0675
'Wageningen' 21 12 1980 650.0 0.1 4.0 0.69 2.6 2.5 -99.9 0.0625
'Wageningen' 22 12 1980 1060.0 0.3 8.0 0.80 2.9 0.0 -99.9 0.0000
'Wageningen' 23 12 1980 480.0 7.7 11.1 1.10 5.1 2.4 -99.9 0.0600
'Wageningen' 24 12 1980 1120.0 8.4 12.0 1.02 5.1 0.0 -99.9 0.0000
'Wageningen' 25 12 1980 1420.0 2.8 9.8 0.86 4.6 3.9 -99.9 0.0975
'Wageningen' 26 12 1980 2530.0 0.8 5.7 0.64 3.8 0.0 -99.9 0.0000
'Wageningen' 27 12 1980 3220.0 -3.3 4.3 0.60 1.1 0.7 -99.9 0.0175
'Wageningen' 28 12 1980 870.0 -2.7 3.4 0.62 2.8 0.0 -99.9 0.0000
'Wageningen' 29 12 1980 350.0 3.3 7.2 0.87 3.5 0.0 -99.9 0.0000
'Wageningen' 30 12 1980 320.0 6.4 8.2 0.92 4.3 0.0 -99.9 0.0000
'Wageningen' 31 12 1980 570.0 5.7 8.6 0.82 7.2 2.0 -99.9 0.0500

```

Appendix 9 Example simple crop input file .CRP

```
*****
* Filename: MaizeS.CRP
* Contents: SWAP 3.0 - Crop data of simple model
*****
* Comment area:
*****

*** PLANT GROWTH SECTION ***

*****
* Part 1: Crop development

  IDEV = 1          ! length of growth period: 1 = fixed, 2 = variable

* If fixed growth period (IDEV = 1), specify:
  LCC = 168        ! Length of the crop cycle [1..366 days, I]

* If variable growth period (IDEV = 2), specify:
  TSUMEA = 1050.0  ! Temperature sum from emergence to anthesis [0..10000 C, R]
  TSUMAM = 1000.0  ! Temperature sum from anthesis to maturity [0..10000 C, R]
  TBASE = 0.0      ! Start value of temperature sum [-10..30 C, R]
*****

* Part 2: Light extinction

  KDIF = 0.60      ! Extinction coefficient for diffuse visible light [0..2 -, R]
  KDIR = 0.75      ! Extinction coefficient for direct visible light [0..2 -, R]
*****

* Part 3: Leaf area index or soil cover fraction

  SWGC = 1 ! choice between LAI [=1] or soil cover fraction [=2]

* If SWGC = 1, list leaf area index [0..12 ha/ha, R], as function of dev. stage [0..2 -,R]:
* If SWGC = 2, list soil cover fraction [0..1 m2/m2, R], as function of dev. stage [0..2 -,R]:

*      DVS   LAI or SCF   ( maximum 36 records)
  GCTB =
    0.00  0.05
    0.30  0.14
    0.50  0.61
    0.70  4.10
    1.00  5.00
    1.40  5.80
    2.00  5.20
* End of table
*****

* Part 4: Crop factor or crop height

  SWCF = 2 ! choice between crop factor [=1] or crop height [=2]

* If SWCF = 1, list crop factor [0.5..1.5, R], as function of dev. stage [0..2 -,R]:
* If SWCF = 2, list crop height [0..1000 cm, R], as function of dev. stage [0..2 -,R]:

*      DVS   CF or CH   (maximum 36 records)
  CFTB =
    0.0    1.0
    0.3    15.0
    0.5    40.0
    0.7    140.0
    1.0    170.0
    1.4    180.0
    2.0    175.0
* End of table
*****

* Part 5: Rooting depth

* List rooting depth [0..1000 cm, R], as a function of development stage [0..2 -,R]:

*      DVS   RD   (maximum 36 records)
  RDTB =
    0.00  5.00
    0.30  20.00
    0.50  50.00
    0.70  80.00
    1.00  90.00
    2.00  100.00
* End of table
*****

* Part 6: Yield response

* List yield response factor [0..5 -,R], as function of development stage [0..2 -,R]:

*      DVS   KY   (maximum 36 records)
  KYTB =
    0.00  1.00
    2.00  1.00
* End of table
*****

* Part 7: Soil water extraction by plant roots

  HLM1L = -15.0 ! No water extraction at higher pressure heads, [-100..100 cm, R]
  HLM2U = -30.0 ! h below which optimum water uptake starts for top layer, [-1000..100 cm, R]
  HLM2L = -30.0 ! h below which optimum water uptake starts for sub layer, [-1000..100 cm, R]
  HLM3H = -325.0 ! h below which water uptake reduction starts at high Tpot, [-10000..100 cm, R]
```

```

HLIM3L = -600.0 ! h below which water uptake reduction starts at low Tpot, [-10000..100 cm, R]
HLIM4 = -8000.0 ! Wilting point, no water uptake at lower pressure heads, [-16000..100 cm, R]
RSC = 70.0 ! Minimum canopy resistance used for potential transpiration, [0..1000 s/m, R]
ADCRH = 0.5 ! Level of high atmospheric demand, [0..5 cm/d, R]
ADCRL = 0.1 ! Level of low atmospheric demand, [0..5 cm/d, R]
*****
* Part 8: Salt stress
*****
ECMAX = 2.0 ! ECsat level at which salt stress starts, [0..20 dS/m, R]
ECSLOP = 0.0 ! Decline of rootwater uptake above ECMAX [0..40 %/dS/m, R]
*****
* Part 9: Interception
*****
SWINTER = 1 ! Switch for rainfall interception method:
! 0 = No interception calculated
! 1 = Agricultural crops (Von Hoyningen-Hune and Braden)
! 2 = Trees and forests (Gash)
* In case of interception method for agricultural crops (SWINTER = 1) specify:
COFAB = 0.25 ! Interception coefficient Von Hoyningen-Hune and Braden, [0..1 cm, R]
* In case of interception method for trees and forests (SWINTER = 2) specify as function
* of time of the year T [0..366 d, R]:
* PFREE = free throughfall coefficient, [0.d0..1.d0 -, R]
* PSTEM = stem flow coefficient, [0.d0..1.d0 -, R]
* SCANOPY = storage capacity of canopy, [0.d0..10.d0 cm, R]
* AVPREC = average rainfall intensity, [0.d0..100.d0 cm, R]
* AVEVAP = average evaporation intensity during rainfall from a wet canopy, [0.d0..10.d0 cm, R]
      T      PFREE      PSTEM      SCANOPY      AVPREC      AVEVAP (maximum 36 records)
      0.0      0.9      0.05      0.4      6.0      1.5
      365.0    0.9      0.05      0.4      6.0      1.5
* End of table
*****
* Part 10: Root density distribution and root growth
*****
* List relative root density [0..1 -, R], as function of relative rooting depth [0..1 -, R]:
* Rdepth Rdensity (maximum 11 records)
RDCTB =
      0.00      1.00
      1.00      0.00
* End of table
*****
*** IRRIGATION SCHEDULING SECTION ***
*****
* Part 1: General
*****
SCHEDULE = 0 ! Switch for application irrigation scheduling [Y=1, N=0]
* If SCHEDULE = 0, no more information is required in this input file!
* If SCHEDULE = 1, continue ....
STARTIRR = 30 3 ! Specify day and month after which irrigation scheduling is allowed [dd mm]
CIRRS = 0.0 ! solute concentration of scheduled irrig. water, [0..100 mg/cm3, R]
ISUAS = 1 ! Switch for type of irrigation method:
! 0 = sprinkling irrigation
! 1 = surface irrigation
*****
* Part 2: Irrigation time criteria
*****
* Choose one or a combination of the following 5 time criteria:
*** Daily stress ***
TCS1 = 1 ! Switch, criterion Daily Stress, [Y=1, N=0]
* If TCS1 = 1, specify minimum of ratio actual/potential transpiration Trel [0..1, R],
* as function of development stage DVS_tc1 [0..2, R], maximum 7 records:
DVS_tc1 Trel
      0.0 0.95
      2.0 0.95
* End of table
*** Depletion of Readily Available Water ***
TCS2 = 0 ! Switch, criterion Depletion of Readily Available Water, [Y=1, N=0]
* If TCS2 = 1, specify minimal fraction of readily available water RAW [0..1, R],
* as function of development stage DVS_tc2 [0..2, R], maximum 7 records:
DVS_tc2 RAW
      0.0 0.95
      2.0 0.95
* End of table
*** Depletion of Totally Available Water ***
TCS3 = 0 ! Switch, criterion Depletion of Totally Available Water, [Y=1, N=0]
* If TCS3 = 1, specify minimal fraction of totally available water TAW [0..1, R],
* as function of development stage DVS_tc3 [0..2, R], maximum 7 records:
DVS_tc3 TAW
      0.0 0.50
      2.0 0.50
* End of table

```

```

*** Depletion Water Amount ***
TCS4 = 0      ! Switch, criterion Depletion Water Amount, [Y=1, N=0]
* If TCS4 = 1, specify maximum amount of water depleted below field cap. DWA [0..500 mm, R],
* as function of development stage DVS_tc4 [0..2, R], maximum 7 records:
DVS_tc4  DWA
0.0  40.0
2.0  40.0
* End of table

*** Pressure head or Moisture content ***
TCS5 = 0      ! Switch, criterion pressure head or moisture content, [Y=1, N=0]
* If TCS5 = 1, specify:
PHORMC = 0    ! Switch, use pressure head (PHORMC=0) or water content (PHORMC=1)
DCRIT = -30.0 ! Depth of the sensor [-100..0 cm, R]
* Also specify critical pressure head [-1.d6..-100 cm, R] or moisture content
* [0..1.0 cm3/cm3, R], as function of development stage DVS_tc5 [0..2, R]:
DVS_tc5  Value_tc5
0.0     -1000.0
2.0     -1000.0
* End of table
*****

*****
* Part 3: Irrigation depth criteria
* Choose one of the following 2 options:
*** Back to Field Capacity ***
DCS1 = 1      ! Switch, criterion Back to Field Capacity, [Y=1, N=0]
* If DCS1 = 1, specify amount of under (-) or over (+) irrigation dI [-100..100 mm, R],
* as function of development stage DVS_dc1 [0..2, R], maximum 7 records:
DVS_dc1  dI
0.0  10.0
2.0  10.0
* End of table

*** Fixed Irrigation Depth ***
DCS2 = 0      ! Switch, criterion Fixed Irrigation Depth, [Y=1, N=0]
* If DCS2 = 1, specify fixed irrigation depth FID [0..400 mm, R],
* as function of development stage DVS_dc2 [0..2, R], maximum 7 records:
DVS_dc2  FID
0.0  60.0
2.0  60.0
* End of table

End of simple crop input file .CRP

```

Appendix 10 Example detailed crop input file .CRP

```
*****
* Filename: PotatoD.CRP
* Contents: SWAP 3.0 - Data for detailed crop model
*****
* Potato (Solanum tuberosum L.)
*****

*** PLANT GROWTH SECTION ***

*****
* Part 1: Crop factor or crop height

  SWCF = 1 ! choice between crop factor [=1] or crop height [=2]
*
* If SWCF = 1, list crop factor [0.5..1.5, R], as function of dev. stage [0..2 -,R]:
* If SWCF = 2, list crop height [0..1000 cm, R], as function of dev. stage [0..2 -,R]:

*      DVS  CF or CH  (maximum 15 records)
CFTB =
      0.00  1.00
      1.00  1.10
      2.00  1.10
* End of Table
*****

* Part 2 : Crop development

  IDSL = 0 ! Switch for crop development:
          ! 0 = Crop development before anthesis depends on temperature only
          ! 1 = Crop development before anthesis depends on daylength only
          ! 2 = Crop development before anthesis depends on both

* If IDSL = 1 or 2, specify:
  DLO = 14.0 ! Minimum day length for optimum crop development [0..24 h, R]
  DLC = 8.0  ! Shortest day length for any development, [0..24 h, R]

* If IDSL = 0 or 2 specify:
  TSUMEA = 152.00 ! Temperature sum from emergence to anthesis, [0..10000 C, R]
  TSUMAM = 1209.00 ! Temperature sum from anthesis to maturity [0..10000 C, R]

* List increase in temperature sum [0..60 C, R] as function of daily average temp. [0..100 C, R]

*      TAV  DTSM  (maximum 15 records)
DTSMTB =
      0.00  0.00
      2.00  0.00
      13.00 11.00
      29.00 11.00
* End of Table

  DVSEND = 2.00 ! development stage at harvest [-]
*****

* Part 3: Initial values

  TDWI = 33.0 ! Initial total crop dry weight [0..10000 kg/ha, R]
  LAIEM = 0.0589 ! Leaf area index at emergence [0..10 m2/m2, R]
  RGRLAI = 0.01200 ! Maximum relative increase in LAI [0..1 m2/m2/d, R]
*****

* Part 4: Green surface area

  SPA = 0.0000 ! Specific pod area [0..1 ha/kg, R]
  SSA = 0.0000 ! Specific stem area [0..1 ha/kg, R]
  SPAN = 35.00 ! Life span under leaves under optimum conditions, [0..366 d, R]
  TBASE = 2.00 ! lower threshold temperature for ageing of leaves ,[-10..30 C, R]

* List specific leaf area [0..1 ha/kg, R] as function of devel. stage [0..2, R]

*      DVS  SLA  (maximum 15 records)
SLATB =
      0.00 0.0030
      1.10 0.0030
      2.00 0.0015
* End of Table
*****

* Part 5: Assimilation

  KDIF = 1.00 ! Extinction coefficient for diffuse visible light, [0..2 -, R]
  KDIR = 0.75 ! Extinction coefficient for direct visible light, [0..2 -, R]
  EPF = 0.45 ! Light use efficiency for real leaf [0..10 kg CO2 /J adsorbed), R]

* List max CO2 assimilation rate [0..100 kg/ha/hr, R] as function of development stage [0..2 -, R]

*      DVS  AMAX  (maximum 15 records)
AMAXTB =
      0.00 30.000
```

```

1.57 30.000
2.00 0.000
* End of table

* List reduction factor of AMAX [-, R] as function of average day temp. [-10..50 C, R]

*      TAVD   TMPF   (maximum 15 records)
TMPFTB =
    0.00  0.010
    3.00  0.010
   10.00  0.750
   15.00  1.000
   20.00  1.000
   26.00  0.750
   33.00  0.010
* End of table

* List reduction factor of AMAX [-, R] as function of minimum day temp. [-10..50 C, R]

*      TMNR   TMNF   (maximum 15 records)
TMNFTB =
    0.00  0.000
    3.00  1.000
* End of table
*****
*****
* Part 6: Conversion of assimilates into biomass

CVL  = 0.7200 ! Efficiency of conversion into leaves,      [0..1 kg/kg, R]
CVO  = 0.8500 ! Efficiency of conversion into storage organs, [0..1 kg/kg, R]
CVR  = 0.7200 ! Efficiency of conversion into roots,      [0..1 kg/kg, R]
CVS  = 0.6900 ! Efficiency of conversion into stems,      [0..1 kg/kg, R]
*****
*****
* Part 7: Maintenance respiration

Q10  = 2.0000 ! Rel. increase in respiration rate with temperature, [0..5 /10 C, R]
RML  = 0.0300 ! Rel. maintenance respiration rate of leaves, [0..1 kgCH2O/kg/d, R]
RMO  = 0.0045 ! Rel. maintenance respiration rate of st. org., [0..1 kgCH2O/kg/d, R]
RMR  = 0.0100 ! Rel. maintenance respiration rate of roots, [0..1 kgCH2O/kg/d, R]
RMS  = 0.0150 ! Rel. maintenance respiration rate of stems, [0..1 kgCH2O/kg/d, R]

* List reduction factor of senescence [-, R] as function of dev. stage [0..2 -, R]

*      DVS   RFSE   (maximum 15 records)
RFSETB =
    0.00  1.00
    2.00  1.00
* End of table
*****
*****
* Part 8: Partitioning

* List fraction of total dry matter increase partitioned to the roots [0..1 -, R]
* as function of development stage [0..2 -, R]

*      DVS   FR   (maximum 15 records)
FRTB  =
    0.00  0.20
    1.00  0.20
    1.36  0.00
    2.00  0.00
* End of table

* List fraction of total above ground dry matter incr. part. to the leaves [0..1 -, R]
* as function of development stage [0..2 -, R]

*      DVS   FL   (maximum 15 records)
FLTB  =
    0.00  0.75
    1.00  0.75
    1.27  0.00
    2.00  0.00
* End of table

* List fraction of total above ground dry matter incr. part. to the stems [0..1 -, R]
* as function of development stage [0..2 -, R]

*      DVS   FS   (maximum 15 records)
FSTB  =
    0.00  0.25
    1.27  0.25
    1.36  0.00
    2.00  0.00
* End of table

* List fraction of total above ground dry matter incr. part. to the st. organs [0..1 -, R]
* as function of development stage [0..2 -, R]

*      DVS   FO   (maximum 15 records)
FOTB  =
    0.00  0.00
    1.00  0.00
    1.27  0.75
    1.36  1.00

```

```

      2.00  1.00
* End of table
*****

*****
* Part 9: Death rates

PERDL = 0.030 ! Maximum rel. death rate of leaves due to water stress [0..3 /d, R]

* List relative death rates of roots [kg/kg/d] as function of dev. stage [0..2 -, R]

*      DVS   RDRR   (maximum 15 records)
RDRRTB =
      0.0000 0.0000
      1.5000 0.0000
      1.5001 0.0200
      2.0000 0.0200
* End of table

* List relative death rates of stems [kg/kg/d] as function of dev. stage [0..2 -, R]

*      DVS   RDRS   (maximum 15 records)
RDRSTB =
      0.0000 0.0000
      1.5000 0.0000
      1.5001 0.0200
      2.0000 0.0200
* End of table
*****

*****
* Part 10: Crop water use

HLIM1 = -10.0 ! No water extraction at higher pressure heads, [-100..100 cm, R]
HLIM2U = -25.0 ! h below which optimum water uptake starts for top layer, [-1000..100 cm, R]
HLIM2L = -25.0 ! h below which optimum water uptake starts for sub layer, [-1000..100 cm, R]
HLIM3H = -300.0 ! h below which water uptake reduction starts at high Tpot, [-10000..100 cm, R]
HLIM3L = -500.0 ! h below which water uptake reduction starts at low Tpot, [-10000..100 cm, R]
HLIM4 = -10000.0 ! Wilting point, no water extraction at lower pressure heads, [-16000..100 cm, R]
RSC = 70.0 ! Minimum canopy resistance used for potential transpiration, [0..1000 s/m, R]
ADCRH = 0.5 ! Level of high atmospheric demand, [0..5 cm/d, R]
ADCRL = 0.1 ! Level of low atmospheric demand, [0..5 cm/d, R]
*****

*****
* Part 11: Salt stress

ECMAX = 1.7 ! ECsat level at which salt stress starts, [0..20 dS/m, R]
ECSLOP = 12.0 ! Decline of rootwater uptake above ECMAX [0..40 %/dS/m, R]
*****

*****
* Part 12: Interception

COFAB = 0.25 ! Interception coefficient Von Hoyningen-Hune and Braden, [0..1 cm, R]
*****

*****
* Part 13: Root growth and root density profile

RDI = 10.00 ! Initial rooting depth, [0..1000 cm, R]
RRI = 1.20 ! Maximum daily increase in rooting depth, [0..100 cm/d, R]
RDC = 50.00 ! Maximum rooting depth crop/cultivar, [0..1000 cm, R]

* List relative root density [0..1 -, R], as function of rel. rooting depth [0..1 -, R]:
*      Rdepth Rdensity (maximum 11 records)
RDCTB =
      0.00 1.00
      1.00 1.00
* End of table
*****

*** IRRIGATION SCHEDULING SECTION ***

*****
* Part 1: General

SCHEDULE = 0 ! Switch for application irrigation scheduling [Y=1, N=0]

* If SCHEDULE = 0, no more information is required in this input file!
* If SCHEDULE = 1, continue ....

STARTIRR = 30 3 ! Specify day and month after which irrigation scheduling is allowed [dd mm]
CIRRS = 0.0 ! solute concentration of scheduled irrig. water, [0..100 mg/cm3, R]
ISUAS = 1 ! Switch for type of irrigation method:
          ! 0 = sprinkling irrigation
          ! 1 = surface irrigation
*****

*****
* Part 2: Irrigation time criteria

* Choose one or a combination of the following 5 time criteria:

*** Daily stress ***

```

```

TCS1 = 1      ! Switch, criterion Daily Stress, [Y=1, N=0]

* If TCS1 = 1, specify minimum of ratio actual/potential transpiration Trel [0..1, R],
* as function of development stage DVS_tc1 [0..2, R], maximum 7 records:

DVS_tc1  Trel
    0.0  0.95
    2.0  0.95
* End of table

*** Depletion of Readily Available Water ***

TCS2 = 0      ! Switch, criterion Depletion of Readily Available Water, [Y=1, N=0]

* If TCS2 = 1, specify minimal fraction of readily available water RAW [0..1, R],
* as function of development stage DVS_tc2 [0..2, R], maximum 7 records:

DVS_tc2  RAW
    0.0  0.95
    2.0  0.95
* End of table

*** Depletion of Totally Available Water ***

TCS3 = 0      ! Switch, criterion Depletion of Totally Available Water, [Y=1, N=0]

* If TCS3 = 1, specify minimal fraction of totally available water TAW [0..1, R],
* as function of development stage DVS_tc3 [0..2, R], maximum 7 records:

DVS_tc3  TAW
    0.0  0.50
    2.0  0.50
* End of table

*** Depletion Water Amount ***

TCS4 = 0      ! Switch, criterion Depletion Water Amount, [Y=1, N=0]

* If TCS4 = 1, specify maximum amount of water depleted below field cap. DWA [0..500 mm, R],
* as function of development stage DVS_tc4 [0..2, R], maximum 7 records:

DVS_tc4  DWA
    0.0  40.0
    2.0  40.0
* End of table

*** Pressure head or Moisture content ***

TCS5 = 0      ! Switch, criterion pressure head or moisture content, [Y=1, N=0]

* If TCS5 = 1, specify:
PHORMC = 0    ! Switch, use pressure head (PHORMC=0) or water content (PHORMC=1)
DCRIT = -30.0 ! Depth of the sensor [-100..0 cm, R]

* Also specify critical pressure head [-1.d6..-100 cm, R] or moisture content
* [0..1.0 cm3/cm3, R], as function of development stage DVS_tc5 [0..2, R]:

DVS_tc5  Value tc5
    0.0  -1000.0
    2.0  -1000.0
* End of table
*****

*****
* Part 3: Irrigation depth criteria
* Choose one of the following 2 options:

*** Back to Field Capacity ***

DCS1 = 1      ! Switch, criterion Back to Field Capacity, [Y=1, N=0]

* If DCS1 = 1, specify amount of under (-) or over (+) irrigation dI [-100..100 mm, R],
* as function of development stage DVS_dc1 [0..2, R], maximum 7 records:

DVS_dc1  dI
    0.0  10.0
    2.0  10.0
* End of table

*** Fixed Irrigation Depth ***

DCS2 = 0      ! Switch, criterion Fixed Irrigation Depth, [Y=1, N=0]

* If DCS2 = 1, specify fixed irrigation depth FID [0..400 mm, R],
* as function of development stage DVS_dc2 [0..2, R], maximum 7 records:

DVS_dc2  FID
    0.0  60.0
    2.0  60.0
* End of table

* End of detailed crop input file .CRP!

```

Appendix 11 Example lateral drainage input file .DRA

```
*****
* Filename: Hupsel.DRA
* Contents: SWAP 3.0 - Data for basic and extended drainage
*****
* Comment area:
*
*****

*** BASIC DRAINAGE SECTION ***

*****
* Part 0: General
*
* DRAMET = 2 ! Switch, method of lateral drainage calculation:
*   METHOD 1 = Use table of drainage flux - groundwater level relation
*   METHOD 2 = Use drainage formula of Hooghoudt or Ernst
*   METHOD 3 = Use drainage/infiltration resistance, multi-level if needed

* SWDIVD = 1 ! Calculate vertical distribution of drainage flux in groundwater [Y=1, N=0]

* If SWDIVD = 1, specify anisotropy factor COFANI (horizontal/vertical saturated hydraulic
* conductivity) for each soil layer (maximum MAHO), [0..1000 -, R] :
* COFANI = 1.0 1.0
*****

*****
* METHOD 1 - Part 1: Table of drainage flux - groundwater level relation (DRAMET = 1)
*
* If SWDIVD = 1, specify the drain spacing:
* LM1 = 30. ! Drain spacing, [1..1000 m, R]

* Specify drainage flux Qdrain [-100..1000 cm/d, R] as function of groundwater level
* GWL [-1000.0..10.0 cm, R, negative below soil surface]; maximum of 25 records
* start with highest groundwater level:

*   GWL      Qdrain
*   -20.0     0.5
*   -100.     0.1
* End of table
*****

*****
* METHOD 2 - Part 2: Drainage formula of Hooghoudt or Ernst (DRAMET = 2)
*
* Drain characteristics:
* LM2 = 11. ! Drain spacing, [1..1000 m, R]
* WETPER = 30.0 ! Wet perimeter of the drain, [0..1000 cm, R]
* ZBOTDR = -80.0 ! Level of drain bottom, [-1000..0 cm, R, neg. below soil surface]
* ENTRES = 20.0 ! Drain entry resistance, [0..1000 d, R]

* Soil profile characteristics:
*
* IPOS = 2 ! Position of drain:
*   1 = On top of an impervious layer in a homogeneous profile
*   2 = Above an impervious layer in a homogeneous profile
*   3 = At the interface of a fine upper and a coarse lower soil layer
*   4 = In the lower, more coarse soil layer
*   5 = In the upper, more fine soil layer

* For all positions specify:
* BASEGW = -200. ! Level of impervious layer, [-1d4..0 cm, R]
* KHTOP = 25. ! Horizontal hydraulic conductivity top layer, [0..1000 cm/d, R]

* In addition, in case IPOS = 3,4,5
* KHBOT = 10.0 ! horizontal hydraulic conductivity bottom layer, [0..1000 cm/d, R]
* ZINTF = -150. ! Level of interface of fine and coarse soil layer, [-1d4..0 cm, R]

* In addition, in case IPOS = 4,5
* KVTOP = 5.0 ! Vertical hydraulic conductivity top layer, [0..1000 cm/d, R]
* KVBOT = 10.0 ! Vertical hydraulic conductivity bottom layer, [0..1000 cm/d, R]

* In addition, in case IPOS = 5
* GEOFAC = 4.8 ! Geometry factor of Ernst, [0..100 -, R]
*****

*****
* METHOD 3 - Part 3: Drainage and infiltration resistance (DRAMET = 3)
*
*
* NRLEVS = 2 ! Number of drainage levels, [1..5, I]
*
* Option for interflow in highest drainage level (shallow system with short residence time)
* SWINTFL = 0 ! Switch for interflow [0,1, I]
* If SWINTFL = 1, then specify COFINTFLB and EXPINTFLB
* COFINTFLB = 0.5 ! Coefficient for interflow relation [0.01..10.0 d, R]
```

```

EXPINTFLB = 1.0 ! Exponent for interflow relation [0.1..1.0 -, R]
*****

*****
* Part 3a: Drainage to level 1
*
DRARES1 = 100 ! Drainage resistance, [10..1d5 d, R]
INFRES1 = 100 ! Infiltration resistance, [0..1d5 d, R]
SWALLO1 = 1 ! Switch, for allowance drainage/infiltration:
! 1 = Drainage and infiltration are both allowed
! 2 = Drainage is not allowed
! 3 = Infiltration is not allowed

* If SWDIVD = 1 (drainage flux vertically distributed), specify the drain spacing:
L1 = 20. ! Drain spacing, [1..1000 m, R]

ZBOTDR1 = -90.0 ! Level of drainage medium bottom, [-1000..0 cm, R]
SWDTYP1 = 2 ! Type of drainage medium: 1 = drain tube, 2 = open channel

* In case of open channel (SWDTYP1 = 2), specify date DATOWL1 [dd-mmm-yy] and channel
* water level LEVEL1 [cm, negative if below soil surface], maximum MAOWL records:

    DATOWL1  LEVEL1
12-jan-1981  -90.0
14-dec-1981  -90.0
* End of table
*****

*****
* Part 3b: Drainage to level 2
*
DRARES2 = 100 ! Drainage resistance, [10..1E5 d, R]
INFRES2 = 100 ! Infiltration resistance, [0..1E5 d, R]
SWALLO2 = 1 ! Switch, for allowance drainage/infiltration:
! 1 = Drainage and infiltration are both allowed
! 2 = Drainage is not allowed
! 3 = Infiltration is not allowed

* If SWDIVD = 1 (drainage flux vertically distributed), specify the drain spacing:
L2 = 20. ! Drain spacing, [1..1000 m, R]

ZBOTDR2 = -90.0 ! Level of drainage medium bottom, [-1000..0 cm, R]
SWDTYP2 = 2 ! Type of drainage medium: 1 = drain tube, 2 = open channel

* In case of open channel (SWDTYP2 = 2), specify date DATOWL2 [dd-mmm-yy] and channel
* water level LEVEL2 [cm, negative if below soil surface], maximum MAOWL records:

    DATOWL2  LEVEL2
12-jan-1981  -90.0
14-dec-1981  -90.0
* End of table
*****

*****
* Part 3c: Drainage to level 3
*
DRARES3 = 100 ! Drainage resistance, [10..1E5 d, R]
INFRES3 = 100 ! Infiltration resistance, [0..1E5 d, R]
SWALLO3 = 1 ! Switch, for allowance drainage/infiltration:
! 1 = Drainage and infiltration are both allowed
! 2 = Drainage is not allowed
! 3 = Infiltration is not allowed

* If SWDIVD = 1 (drainage flux vertically distributed), specify the drain spacing:
L3 = 20. ! Drain spacing, [1..1000 m, R]

ZBOTDR3 = -90.0 ! Level of drainage medium bottom, [-1000..0 cm, R]
SWDTYP3 = 2 ! Type of drainage medium: 1 = drain tube, 2 = open channel

* In case of open channel (SWDTYP3 = 2), specify date DATOWL3 [dd-mmm-yy] and channel
* water level LEVEL3 [cm, negative if below soil surface], maximum MAOWL records:

    DATOWL3  LEVEL3
12-jan-1981  -90.0
14-dec-1981  -90.0
* End of table
*****

*****
* Part 3d: Drainage to level 4
*
DRARES4 = 100 ! Drainage resistance, [10..1E5 d, R]
INFRES4 = 100 ! Infiltration resistance, [0..1E5 d, R]
SWALLO4 = 1 ! Switch, for allowance drainage/infiltration:
! 1 = Drainage and infiltration are both allowed
! 2 = Drainage is not allowed
! 3 = Infiltration is not allowed

* If SWDIVD = 1 (drainage flux vertically distributed), specify the drain spacing:
L4 = 20. ! Drain spacing, [1..1000 m, R]

ZBOTDR4 = -90.0 ! Level of drainage medium bottom, [-1000..0 cm, R]
SWDTYP4 = 2 ! Type of drainage medium: 1 = drain tube, 2 = open channel

```

```

* In case of open channel (SWDTYP4 = 2), specify date DATOWL4 [dd-mmm-yy] and channel
* water level LEVEL4 [cm, negative if below soil surface], maximum MAOWL records:
      DATOWL4  LEVEL4
      12-jan-1981  -90.0
      14-dec-1981  -90.0
* End of table
*****

*****
* Part 3e: Drainage to level 5
*
DRARES5 = 100  ! Drainage resistance, [10..1E5 d, R]
INFRES5 = 100  ! Infiltration resistance, [0..1E5 d, R]
SWALLO5 = 1    ! Switch, for allowance drainage/infiltration:
                ! 1 = Drainage and infiltration are both allowed
                ! 2 = Drainage is not allowed
                ! 3 = Infiltration is not allowed

* If SWDIVD = 1 (drainage flux vertically distributed), specify the drain spacing:
L5 = 20.      ! Drain spacing, [1..1000 m, R]

ZBOTDR5 = -90.0 ! Level of drainage medium bottom, [-1000..0 cm, R]
SWDTYP5 = 2    ! Type of drainage medium: 1 = drain tube, 2 = open channel

* In case of open channel (SWDTYP5 = 2), specify date DATOWL5 [dd-mmm-yy] and channel
* water level LEVEL5 [cm, negative if below soil surface], maximum MAOWL records:
      DATOWL5  LEVEL5
      12-jan-1981  -90.0
      14-dec-1981  -90.0
* End of table
*****

*** EXTENDED DRAINAGE SECTION ***

*****
* Part 0: Reference level

ALTCU = 0.0 ! Altitude of the Control Unit relative to reference level
*           AltCu = 0.0 means reference level coincides with
*           surface level [-300000..300000 cm, R]

*****
* Part 1: drainage characteristics
*
NRSRF = 2    ! number of subsurface drainage levels [1..5, I]

*** Table with physical characteristics of each subsurface drainage level:
*
* LEVEL ! drainage level number [1..NRSRF, I]
* SWDTYP ! type of drainage medium [open=0, closed=1]
* L      ! spacing between channels/drains [1..1000 m, R]
* ZBOTDRE ! altitude of bottom of channel or drain [ALTCU-1000..ALTCU-0.01 cm,R]
* GWLINF ! groundw. level for max. infiltr. [-1000..0 cm rel. to soil surf., R]
* RDRAIN ! drainage resistance [1..100000 d, R]
* RINFI  ! infiltration resistance [1..100000 d, R]
* Variables RENTRY, REXIT, WIDTHR and TALUDR must have realistic values when the
* type of drainage medium is open (second column of this table:SWDTYP=0)
* For closed pipe drains (SWDTYP=1) dummy values may be entered
* RENTRY ! entry resistance [1..100 d, R]
* REXIT  ! exit resistance  [1..100 d, R]
* WIDTHR ! bottom width of channel [0..100 cm, R]
* TALUDR ! side-slope (dh/dw) of channel [0.01..5, R]
*
LEV SWDTYP  L  ZBOTDRE  GWLINF  RDRAIN  RINFI  RENTRY  REXIT  WIDTHR  TALUDR
1   0       250.0  1093.0 -350.0  150.0  4000.0  0.8   0.8   100.0  0.66
2   0       200.0  1150.0 -300.0  150.0  1500.0  0.8   0.8   100.0  0.66
* End of table
*****

*****
SWNRSRF = 0    ! Switch to introduce rapid subsurface drainage [0..2, I]
*           0 = no rapid drainage
*           1 = rapid drainage in the highest drainage system (=NRSRF)
*             (implies adjustment of RDRAIN of highest drainage system)
*           2 = rapid drainage as interflow according to a power relation
*             (implies adjustment of RDRAIN of highest drainage system)
* When SWNRSRF = 1, then enter realistic values for rapid drainage
RSURFDEEP = 30.0 ! maximum resistance of rapid subsurface Drainage [0.001..1000.0 d, R]
RSURFSHALLOW = 10.0 ! minimum resistance of Rapid subsurface Drainage [0.001..1000.0 d, R]
*
* When SWNRSRF = 2, then enter coefficients of power function
COFINTFL = 0.1  ! coefficient of interflow relation [0.01..10.0 d-1, R]
EXPINTFL = 0.5  ! exponent of interflow relation [0.1..1.0 -, R]

*****
* Part 2a: Specification and control of surface water system
*
SWSRF = 2 ! option for interaction with surface water system [1..3, I]
*       1 = no interaction with surface water system
*       2 = surf. water system is simulated with no separate primary system
*       3 = surf. water system is simulated with separate primary system
*****

```

```

*****
* Part 2b: Surface water level of primary system
*
* Only if SWSRF = 3 then the following table must be entered
* Table with Water Levels in the Primary system [max. = 52]:
* no levels above soil surface for primary system
*
* Water level in primary water course WLP [ALTCU-1000..ALTCU-0.01 cm, R] as function of
* DATE1 [dd-mmm-yyyy]
      DATE1      WLP
02-jan-1980    -100.
14-jun-1980     -80.
24-oct-1980    -120.
*End_of_table
*****
*
*****
* Part 2c: Surface water level of secondary system
*
* If SWSRF = 2 or 3 then the variable SWSEC must be entered
      SWSEC = 2 ! option for surface water level of secondary system [1..2, I]
*          1 = surface water level is input
*          2 = surface water level is simulated
*****
*****
* Part 3: surface water level in secondary water course is input
*
* Table with Water Levels in the Secondary system [max. = 52]:
*
* Water level in secondary water course WLS [ALTCU-1000..ALTCU-0.01 cm, R] as function of
* DATE2 [dd-mmm-yyyy]
      DATE2      WLS
02-jan-1980    -100.
14-jun-1980     -80.
24-oct-1980    -120.
*End_of_table
*****
*****
* Part 4: surface water level is simulated
*
*****
* Part 4a: Miscellaneous parameters
*
WLACT = 1123.0 ! initial surface water level [ALTCU-1000..ALTCU cm,R]
OSSWLM = 2.5 ! criterium for warning about oscillation [0..10 cm, R]
*****
*****
* Part 4b: management of surface water levels
*
NMPER = 4 ! number of management periods [1..10, I]
*
* For each management period specify:
* IMPER index of management period [1..NMPER, I]
* IMPEND date that period ends [dd-mm-yyyy]
* SWMAN type of water management [1..2, I]
*          1 = fixed weir crest
*          2 = automatic weir
* WSCAP surface water supply capacity [0..100 cm/d, R]
* WLDIP allowed dip of surf. water level, before starting supply [0..100 cm, R]
* INTWL length of water-level adjustment period (SWMAN=2 only) [1..31 d, R]

      IMPER_4b      IMPEND      SWMAN      WSCAP      WLDIP      INTWL
1          31-jan-1980          1          0.00          0.0          1
2          01-apr-1980          2          0.00          5.0          1
3          01-nov-1980          2          0.00          5.0          1
4          31-dec-1980          1          0.00          0.0          1
*End_of_table
*
* SWQHR = 1 ! option for type of discharge relationship [1..2, I]
*          1 = exponential relationship
*          2 = table
*****
*****
* Part 4c: exponential discharge relation (weir characteristics)
*
* If SWQHR=1 and for ALL periods specify:
*
SOFUCU = 100.0 ! Size of the control unit [0.1..100000.0 ha, R]
*
* IMPER index of management period [1..NMPER, I]
* HBWEIR weir crest; levels above soil surface are allowed, but simulated
* surface water levels should remain below 100 cm above soil surface;
* the crest must be higher than the deepest channel bottom of the
* secondary system (ZBOTDR(1 or 2), [ALTCU-ZBOTDR..ALTCU+100 cm,R]).
* If SWMAN = 2: HBWEIR represents the lowest possible weir position.
* ALPHAW alpha-coefficient of discharge formula [0.1..50.0, R]
* BETAW beta-coefficient of discharge formula [0.5..3.0, R]

      IMPER_4c      HBWEIR      ALPHAW      BETAW
1          1114.0          3.0          1.4765
2          1110.0          3.0          1.4765

```



```

      3  1110.0  3.0  1.4765
      4  1114.0  3.0  1.4765
*End_of_table
*****
*
*****
* Part 4d: table discharge relation
*
LABEL4d = 1 ! Do not modify
*
* If SWQHR=2 and for ALL periods specify:
*
* IMPER index of management period [1..NMPER, I]
* ITAB index per management period [1..10, I]
* HTAB surface water level [ALTCU-1000..ALTCU+100 cm, R]
      (first value for each period = ALTCU + 100 cm)
* QTAB discharge [0..500 cm/d, R]
      (should go down to a value of zero at a level that is higher than
      the deepest channel bottom of secondary surface water system)
*
IMPER_4d IMPTAB HTAB QTAB
  1      1      -75.0  2.0
*End_of_table
*****
* Part 4e: automatic weir control
*
LABEL4e = 1 ! Do not modify
*
* For the periods when SWMAN=2 specify next two tables:
*
*** Table #1
*
* IMPER index of management period [1..NMPER, I]
* DROPR maximum drop rate of surface water level [0..100 cm/d, positive, R]
      if the value is set to zero, the parameter does not play
      any role at all
* HDEPTH depth in soil profile for comparing with HCRIT
      [-100..0 cm below soil surface, R]
*
IMPER_4E1 DROPR HDEPTH
  2      0.0  -15.0
  3      0.0  -15.0
*End_of_table
*
*** Table #2
*
* IMPER index of management period [1..NMPER, I]
* IPHASE index per management period [1..10, I]
* WLSMAN surface water level of phase IPHASE [ALTCU-500.0..ALTCU cm,R]
* GWLCRIT groundwater level of phase IPHASE, max. value
      [-500..0 cm below soil surface, R]
* HCRIT critical pressure head, max. value, (at HDEPTH, see above)
      for allowing surface water level [-1000..0 cm, neg., R]
* VCRIT critical unsaturated volume (min. value) for all
      surface water level [0..20 cm, R]
*
* Notes: 1) The zero's for the criteria on the first record are in fact
*          dummy's, because under all circumstances the scheme will set
*          the surface water level at least to wlsman(imper,1)
*          2) The lowest level of the scheme must still be above the
*          deepest channel bottom of the secondary surface water system
*
IMPER_4E2 IMPPHASE WLSMAN GWLCRIT HCRIT VCRIT
  2      1  1114.0  0.0  0.0  0.0
  2      2  1124.0 -80.0  0.0  0.0
  2      3  1124.0 -90.0  0.0  0.0
  2      4  1154.0 -100.0  0.0  0.0
  3      1  1114.0  0.0  0.0  0.0
  3      2  1124.0 -80.0  0.0  0.0
  3      3  1124.0 -90.0  0.0  0.0
  3      4  1154.0 -100.0  0.0  0.0
*End_of_table
*****
* End of .dra file!

```

Appendix 12 Summary of output data

Short water and solute balance (*.bal)

Final and initial water and solute storage
Water balance components
Solute balance components

Extended water balance (*.blc)

Final and initial water storage
Water balance components of sub systems

Incremental water balance (*.inc)

Gross rainfall and irrigation
Interception
Runon and runoff
Potential and actual transpiration
Potential and actual evaporation
Net drainage and bottom flux

Cumulative water balance (*.wba)

Gross and net rainfall
Runon and runoff
Potential and actual transpiration
Potential and actual evaporation
Net lateral flux (drainage)
Net bottom flux
Change water storage in profile
Groundwater level
Water balance error

Cumulative solute balance (*.sba)

Flux at soil surface
Amount decomposed
Amount taken up by plant roots
Amount in soil profile
Amount in cracks
Flux at soil profile bottom
Drainage flux
Bypass flux from cracks
Amount in defined saturated aquifer
Flux from defined saturated aquifer

Soil temperatures (*.ate)

Soil temperature of all nodes

Soil profiles (*.vap)

Profiles of water content, pressure head, solute concentration, temperature, water flux and solute flux

Irrigation (*.irg)

Calculated irrigation applications

Detailed crop growth (*.crp)

Development stage
Leaf area index
Crop height
Rooting dept
Cumulative relative transpiration during 0-2 DVS

Cumulative relative transpiration during 1-2 DVS
Cumulative potential and actual weight of dry matter
Cumulative potential and actual weight of storage

Simple crop growth (*.crp)

Development stage
Leaf area index
Crop height
Rooting depth
Cumulative relative transpiration
Cumulative relative crop yield

Extended drainage components (*.drf)

Drainage fluxes of each level
Total drainage flux
Net runoff
Rapid drainage

Surface water management 1 (*.swb)

Groundwater level
Weir target level
Surface water level
Storage in surface water reservoir
Sum of drainage, runoff and rapid drainage
External supply to surface water reservoir
Outflow from surface water reservoir

Surface water management 2 (*.man)

Weir type
Groundwater level
Pressure head for target level
Total air volume in soil profile
Weir target level
Surface water level and outflow
Number of target level adjustments
Indicator weir overflow
Weir crest level

Snowpack water balance (*.snw)

Final and initial water storage
Water balance components

Detailed waterbalance Macropores (*.bma)

Final and initial water storage
Water balance components

Log file (SWAP.log)

Echo of input (*.swp-file)
Errors and warnings

Final values of state variables (*.end)

Snow and ponding layer
Soil water pressure heads
Solute concentrations
Soil temperatures

Appendix 13 Example short water and solute balance output file *.bal

```
* Project:      Hupsel
* File content: overview of actual water and solute balance components
* File name:    Result.bal
* Model version: swap_3_0_3
* Generated at: 12-Dec-2003 00:24:55
```

```
Period          : 01-Jan-1980 until 31-Dec-1980
Depth soil profile : 200.00 cm
```

| | Water storage | Solute storage |
|-----------|---------------|-------------------|
| Final : | 71.66 cm | 0.4604E+03 mg/cm2 |
| Initial : | 72.07 cm | 0.0000E+00 mg/cm2 |
| Change | -0.41 cm | 0.4604E+03 mg/cm2 |

Water balance components (cm)

| In | | Out | |
|-------------|---------|------------------|---------|
| Rain | : 66.01 | Interception | : 4.52 |
| Runon | : 0.00 | Runoff | : 0.00 |
| Irrigation | : 0.50 | Transpiration | : 26.56 |
| Bottom flux | : 0.00 | Soil evaporation | : 14.42 |
| | | Crack flux | : 0.00 |
| | | Drainage level 1 | : 21.42 |
| Sum | : 66.51 | Sum | : 66.93 |

Solute balance components (mg/cm2)

| In | | Out | |
|-------------|--------------|---------------|--------------|
| Rain | : 0.0000E+00 | Decomposition | : 0.0000E+00 |
| Irrigation | : 0.5000E+03 | Root uptake | : 0.0000E+00 |
| Bottom flux | : 0.0000E+00 | Cracks | : 0.0000E+00 |
| | | Drainage | : 0.3964E+02 |
| Sum | : 0.5000E+03 | Sum | : 0.3964E+02 |

```
Period          : 01-Jan-1981 until 31-Dec-1981
Depth soil profile : 200.00 cm
```

| | Water storage | Solute storage |
|-----------|---------------|--------------------|
| Final : | 73.38 cm | 0.2397E+03 mg/cm2 |
| Initial : | 71.66 cm | 0.4604E+03 mg/cm2 |
| Change | 1.72 cm | -0.2207E+03 mg/cm2 |

Water balance components (cm)

| In | | Out | |
|-------------|---------|------------------|---------|
| Rain | : 79.89 | Interception | : 1.41 |
| Runon | : 0.00 | Runoff | : 0.29 |
| Irrigation | : 0.00 | Transpiration | : 21.56 |
| Bottom flux | : 0.00 | Soil evaporation | : 17.57 |
| | | Crack flux | : 0.00 |
| | | Drainage level 1 | : 37.34 |
| Sum | : 79.89 | Sum | : 78.17 |

Solute balance components (mg/cm2)

| In | | Out | |
|-------------|--------------|---------------|--------------|
| Rain | : 0.0000E+00 | Decomposition | : 0.0000E+00 |
| Irrigation | : 0.0000E+00 | Root uptake | : 0.0000E+00 |
| Bottom flux | : 0.0000E+00 | Cracks | : 0.0000E+00 |
| | | Drainage | : 0.2207E+03 |
| Sum | : 0.0000E+00 | Sum | : 0.2207E+03 |

Appendix 14 Example extended water balance output file *.blc

* Project: Hupsel
 * File content: overview of actual water balance components (cm)
 * File name: Result.blc
 * Model version: swap_3_0_3
 * Generated at: 12-Dec-2003 00:24:55

Period : 01-Jan-1980 until 31-Dec-1980
 Depth soil profile : 200.00 cm

| INPUT | | | | | OUTPUT | | | | |
|---------------------|-------|------|-------|--------|---------------------|-------|------|-------|--------|
| | PLANT | SNOW | POND | SOIL | | PLANT | SNOW | POND | SOIL |
| Initially Present | | 0.00 | 0.00 | 72.07 | Finally present | | 0.00 | 0.00 | 71.66 |
| Gross Rainfall | 66.01 | | | | Nett Rainfall | 61.49 | | | |
| Nett Rainfall | | 0.00 | 61.49 | | Nett Irrigation | 0.50 | | | |
| Gross Irrigation | 0.50 | | | | Interception | 4.52 | | | |
| Nett Irrigation | | | 0.50 | | Snowmelt | | 0.00 | | |
| Snowfall | | 0.00 | | | Sublimation | | 0.00 | | |
| Snowmelt | | | 0.00 | | Plant Evaporation | | | | 26.56 |
| | | | | | Soil Evaporation | | | 14.42 | |
| Runon | | | 0.00 | | Runoff | | | 0.00 | |
| Inundation | | | 0.00 | | Infiltr. Soil Surf. | | | 55.14 | |
| Infiltr. Soil Surf. | | | | 55.14 | Exfiltr. Soil Surf. | | | | 7.57 |
| Exfiltr. Soil Surf. | | | 7.57 | | Drainage | | | | |
| Infiltr. subsurf. | | | | | - system 1 | | | | 21.42 |
| - system 1 | | | | 0.00 | Downward seepage | | | | 0.00 |
| Upward seepage | | | | 0.00 | | | | | |
| Sum | 66.51 | 0.00 | 69.56 | 127.21 | Sum | 66.51 | 0.00 | 69.56 | 127.21 |
| Storage Change | | 0.00 | 0.00 | -0.41 | | | | | |
| Balance Deviation | 0.00 | 0.00 | 0.00 | 0.00 | | | | | |

Period : 01-Jan-1981 until 31-Dec-1981
 Depth soil profile : 200.00 cm

| INPUT | | | | | OUTPUT | | | | |
|---------------------|-------|------|-------|--------|---------------------|-------|------|-------|--------|
| | PLANT | SNOW | POND | SOIL | | PLANT | SNOW | POND | SOIL |
| Initially Present | | 0.00 | 0.00 | 71.66 | Finally present | | 0.00 | 0.00 | 73.38 |
| Gross Rainfall | 79.89 | | | | Nett Rainfall | 78.48 | | | |
| Nett Rainfall | | 0.00 | 78.48 | | Nett Irrigation | 0.00 | | | |
| Gross Irrigation | 0.00 | | | | Interception | 1.41 | | | |
| Nett Irrigation | | | 0.00 | | Snowmelt | | 0.00 | | |
| Snowfall | | 0.00 | | | Sublimation | | 0.00 | | |
| Snowmelt | | | 0.00 | | Plant Evaporation | | | | 21.56 |
| | | | | | Soil Evaporation | | | 17.57 | |
| Runon | | | 0.00 | | Runoff | | | 0.29 | |
| Inundation | | | 0.00 | | Infiltr. Soil Surf. | | | 68.99 | |
| Infiltr. Soil Surf. | | | | 68.99 | Exfiltr. Soil Surf. | | | | 8.37 |
| Exfiltr. Soil Surf. | | | 8.37 | | Drainage | | | | |
| Infiltr. subsurf. | | | | | - system 1 | | | | 37.34 |
| - system 1 | | | | 0.00 | Downward seepage | | | | 0.00 |
| Upward seepage | | | | 0.00 | | | | | |
| Sum | 79.89 | 0.00 | 86.85 | 140.65 | Sum | 79.89 | 0.00 | 86.86 | 140.65 |
| Storage Change | | 0.00 | 0.00 | 1.72 | | | | | |
| Balance Deviation | 0.00 | 0.00 | 0.00 | 0.00 | | | | | |

Appendix 15 Description of the output files *.afo and *.aun

This annex describes the content of the output files with extension *.afo and *.aun. The content of both files is identical; they only differ in format: one file is binary and unformatted (*.aun) and the other file is formatted (*.afo). The description given in this annex uses the following symbols:

- Unit = units as applied in these output files; units differ from those applied in Swap !
- R = data are written to a new record;
- DT = data type; R means Real*4, I means Integer*2;
- Mnemonic = the name of the variable as applied in the source code of Swap

| Description of variable | Unit | Range | R | DT | Mnemonic |
|--|--------------------------------|---------------|---|----|-----------------|
| Time domain | | | | | |
| Year when hydrological simulation started | - | [1..∞> | * | I | bruny |
| Year when hydrological simulation ended | - | [bruny..∞> | - | I | eruny |
| Time (Julian daynumber) when hydrological simulation started (Minimum); will be 0.0 when simulation started at 1st of January, 00.00 hour. | - | [0.0..366] | - | R | brund-1 |
| Time (Julian daynumber) when hydrological simulation ended (Maximum) | - | [0.0..366] | - | R | erund |
| Stepsize of time-interval for dynamic hydrological data | d | [1.0..30.0] | - | R | period |
| Geometry of model system | | | | | |
| Number of model compartments | - | [1..numnod] | * | I | numnod |
| Number of horizons | - | [1 ..numlay | - | I | numlay |
| Number of drainage systems (value must be 0, 1, 2, 3, 4 or 5) | - | [0,1,2,3,4,5] | - | I | nrlevs |
| <i>The following 4 variables (botcom – thetawp) are given for the horizons 1 – numlay:</i> | | | | | |
| Compartment number of the deepest compartment (bottom) of each horizon/layer | - | [1..numnod] | * | I | botcom(numlay) |
| Volume fraction moisture at Saturation | m ³ m ⁻³ | [0.0 .. 1.0] | * | R | thetas (numlay) |
| Volume fraction moisture at Field Capacity | m ³ m ⁻³ | [0.0 .. 1.0] | * | R | thetafc(numlay) |
| Volume fraction moisture at Wilting point | m ³ m ⁻³ | [0.0 .. 1.0] | * | R | thetawp(numlay) |
| <i>The following variable dz is given for the compartments 1 – numnod</i> | | | | | |
| Thickness of compartments | m | [0.001..100] | * | R | dz(numnod) |

| Description of variable | Unit | Range | R | DT | Mnemonic |
|---|--------------------------------|--------------|---|----|------------------|
| Initial conditions | | | | | |
| <i>The following variable theta is given for the compartments 1 – numnod</i> | | | | | |
| Volume fraction moisture initially present in compartments 1 – NUMNOD | m ³ m ⁻³ | [0.0 .. 1.0] | * | R | theta(numnod) |
| Initial groundWATERlevel | m- surface | [0.0..∞> | * | R | gwl |
| Storage by initial ponding (m+surface) | m+ surface | [0.0..∞> | - | R | pond |
| Dynamic part | | | | | |
| Time (Julian daynumber) in hydrological model | - | [0.0..∞> | * | R | tcum |
| Precipitation (<i>incl. irrigation</i>) water flux | m d ⁻¹ | [0.0..∞> | - | R | iprec |
| Evaporation flux by interception | m d ⁻¹ | [0.0..∞> | - | R | iintc |
| Actual evaporation flux by bare soil | m d ⁻¹ | [0.0..∞> | - | R | ievap |
| Evaporation flux by ponding | m d ⁻¹ | [0.0] | - | R | 0.0 |
| Potential evaporation flux by soil | m d ⁻¹ | [0.0..∞> | - | R | ipeva |
| Potential transpiration flux | m d ⁻¹ | [0.0..∞> | - | R | iptra |
| Flux of surface RUNoff | m d ⁻¹ | [0.0..∞> | - | R | iruno |
| GroundwATER level at end of time-interval | m- surface | [0.0..∞> | - | R | gwl |
| Storage by ponding at soil surface at end of time-interval | m+ surface | [0.0..∞> | - | R | pond |
| <i>The variables h - inqdra are given for the compartments 1 - numnod, with one exception for inq, which is given for the compartments 1 – numnod+1</i> | | | | | |
| Suction (pressure head) of soil moisture (negative when unsaturated) | cm | <-∞..+∞> | * | R | h(numnod) |
| Volume fraction of moisture at end of time-interval | m ³ m ⁻³ | [0.0 .. 1.0] | * | R | theta(numnod) |
| Actual transpiration flux | m d ⁻¹ | [0.0..∞> | * | R | inqrot(numnod) |
| Flux incoming from above (compartments 1 – numnod+1, downward=positive) | m d ⁻¹ | [0.0..∞> | * | R | inq(numnod+1) |
| <i>The presence of values for variables inqdra1-inqdra5 is determined by the variable nrlevs. The value of nrlevs determines the number of drainage systems for which flux densities must be given.</i> | | | | | |
| Flux of drainage system of 1st order (e.g. canal) | m d ⁻¹ | [0.0..∞> | * | R | inqdra(1,numnod) |
| Flux of drainage system of 2nd order (e.g. ditch) | m d ⁻¹ | [0.0..∞> | * | R | inqdra(2,numnod) |
| Flux of drainage system of 3rd order (e.g. trench) | m d ⁻¹ | [0.0..∞> | * | R | inqdra(3,numnod) |
| Flux of drainage system of 4th order (e.g. tube drain) | m d ⁻¹ | [0.0..∞> | * | R | inqdra(4,numnod) |
| Flux of drainage system of 5th order (e.g. rapid drainage) | m d ⁻¹ | [0.0..∞> | * | R | inqdra(5,numnod) |

Appendix 16 Description of the output files *.bfo and *.bun

This annex describes the content of the output files with extension *.bfo and *.bun. The content of both files is identical; they only differ in format: one file is binary and unformatted (*.bun) and the other file is ASCII and formatted (*.bfo). Differences between the (*.bfo, *.bun) and (*.aun, *.afo, Appendix 15) are indicated with a vertical line next to the text.

Part of the content of this file is optional and indicated with grey shading of the corresponding rows. The optional content is indicated with the switch SWOP (see section File Options).

The temperature parameter (Tsoil) has a value of “-99.9” when temperature processes were not simulated. The snow-parameters (Ssnow, Igsnow, Isubl) have a value of “0”, when snow processes were not simulated. This 0-value instead of -99.9-value is applied to facilitate uniformity of water balance calculations.

The description given in these pages uses the following symbols:

- Unit = units as applied in these output files; units mostly differ from those applied in Swap
- Range = upper and lower boundary of given data
- R = an asterisk (*) indicates that data are written to a new record;
- DT = data type; R means Real*4, I means Integer*2, C means CharacterString;
- Mnemonic = the name of the variable as applied in the source code of Swap

| Description of variable | Unit | Range | R | DT | Mnemonic |
|--|------|-----------------|---|-----|----------|
| Header of 5 records, each records with a fixed length of 80 characters | | | | | |
| Project Name (example: * Project: CranGras) | - | ... | * | C80 | Project |
| File Content (example: * File content: formatted hydrological data) | - | ... | * | C80 | FileText |
| File Name (example: * File name: Result.bfo) | - | ... | * | C80 | FileNam |
| Model Version (example: * Model version: SWAP3.0.0) | - | ... | * | C80 | Model_ID |
| Date and time of file creation (example: * Generated at: 28-Mar-2003 13:59:31) | - | ... | * | C80 | DTString |
| File Options | | | | | |
| SWitch for OPTions of content of this file (shaded parts in this table) SwOp = 1 : no data of macro pore flow SwOp = 2 : data of macro pore flow (in this table: shaded and red) | - | [1 ... 2] | * | I | swop |
| Time domain | | | | | |
| Year when hydrological simulation started | - | [1 ...] | * | I | bruny |
| Year when hydrological simulation ended | - | [bruny ...] | - | I | eruny |
| Time (Julian daynumber) when hydrological simulation started (Minimum); will be 0.0 when simulation started at 1st of January, 00.00 hour. | - | [0.0 ... 366.0] | - | R | brund-1 |
| Time (Julian daynumber) when hydrological simulation ended (Maximum) | - | [0.0 ... 366.0] | - | R | erund |

Geometry of model system

| | | | | | |
|--|---|----------------|---|---|--------|
| Number of model compartments | - | [1 ... numnod] | * | I | numnod |
| Number of horizons | - | [1 ... numlay] | - | I | numlay |
| Number of drainage systems (value must be 0, 1, 2, 3, 4 or 5) | - | [0 ... 5] | - | I | nrlevs |

The following 4 variables (*botcom* ... *thetawp*) are given for the horizons 1 ... *numlay*:

| | | | | | |
|--|--------------|----------------|---|---|-----------------|
| Compartment number of the deepest compartment (bottom) of each horizon/layer | - | [1 ... numnod] | * | I | botcom(numlay) |
| Volume fraction moisture at Saturation | $m^3 m^{-3}$ | [0.0 ... 1.0] | * | R | thetas(numlay) |
| Volume fraction moisture at Field Capacity | $m^3 m^{-3}$ | [0.0 ... 1.0] | * | R | thetafc(numlay) |
| Volume fraction moisture at Wilting point | $m^3 m^{-3}$ | [0.0 ... 1.0] | * | R | thetawp(numlay) |

The following variable *dz* is given for the compartments 1 ... *numnod*

| | | | | | |
|---------------------------|---|-------------------|---|---|------------|
| Thickness of compartments | m | [0.001 ... 100.0] | * | R | dz(numnod) |
|---------------------------|---|-------------------|---|---|------------|

Geometry of macropore system

| | | | | | |
|--|--------------|------------------|---|---|-------------------|
| Areic volume of static macropores in domain 1 (Main Bypass Flow domain) per compartment 1 ... NUMNOD | $m^3 m^{-2}$ | [0.0 ...] | * | R | VIMpStDm1(numnod) |
| Areic volume of static macropores in domain 2 (Internal Catchment domain) per compartment 1 ... NUMNOD | $m^3 m^{-2}$ | [0.0 ...] | * | R | VIMpStDm2(numnod) |
| Diameter of soil matrix polygones per compartment 1 ... NUMNOD | m | [0.001 ... 10.0] | * | R | DiPoCp(numnod) |

Initial conditions

The following variable *theta* and *tempi* are given for the compartments 1 ... *numnod*

| | | | | | |
|---|--------------|------------------|---|---|---------------|
| Volume fraction moisture initially present in compartments 1 ... NUMNOD | $m^3 m^{-3}$ | [0.0 ... 1.0] | * | R | Theta(numnod) |
| Initial groundwaterlevel (negative below soil surface, when positive use Pond) | m-surf. | [0.0 ...] | * | R | Gwl |
| Storage by initial ponding | m | [0.0 ...] | - | R | Pond |
| Storage by snow | m | [0.0 ...] | * | R | Ssnow |
| Soil temperature of compartments 1 ... NUMNOD | °C | [-50.0 ... 50.0] | * | R | Tsoil(numnod) |

Initial conditions for macropores, domain 1 (Main Bypass Flow domain)

| | | | | | |
|--|--------------|------------|---|---|----------|
| Water level | m-surf. | [0.0 ...] | * | R | WaLevDm1 |
| Areic volume | $m^3 m^{-2}$ | [0.0 ...] | - | R | VIMpDm1 |
| Areic volume of water stored | $m^3 m^{-2}$ | [0.0 ...] | - | R | WaSrDm1 |
| <i>Initial conditions for macropores, domain 2 (Internal Catchment domain)</i> | | | | | |
| Areic volume | $m^3 m^{-2}$ | [0.0 ...] | - | R | VIMpDm2 |
| Areic volume of water stored | $m^3 m^{-2}$ | [0.0 ...] | - | R | WaSrDm2 |

| Description of variable | Unit | Range | R | DT | Mnemonic |
|---|--------------------------------|------------------|---|----|------------------|
| Dynamic part | | | | | |
| Time (Julian daynumber) in hydrological model. (1.0 means: 1st of January, 24.00 hour) | - | [0.0 ...] | * | R | Daycum |
| Stepsize of time-interval for dynamic hydrological data | d | [1.0 ... 30.0] | - | R | period |
| Rainfall water flux | m d ⁻¹ | [0.0 ...] | - | R | lgrai |
| Snowfall water flux | m d ⁻¹ | [0.0 ...] | - | R | lgsnow |
| Irrigation flux | m d ⁻¹ | [0.0 ...] | - | R | lgrid |
| Evaporation flux by interception of precipitation water | m d ⁻¹ | [0.0 ...] | - | R | lgrai-inrai |
| Evaporation flux by interception of irrigation water | m d ⁻¹ | [0.0 ...] | - | R | lgrid-inird |
| Sublimation of snow (Evaporation flux) | m d ⁻¹ | [0.0 ...] | - | R | ISubl |
| Actual evaporation flux by bare soil | m d ⁻¹ | [0.0 ...] | - | R | levap |
| Evaporation flux by ponding | m d ⁻¹ | [0.0] | - | R | 0.0 |
| Potential evaporation flux by soil | m d ⁻¹ | [0.0 ...] | - | R | lpeva |
| Potential transpiration flux | m d ⁻¹ | [0.0 ...] | - | R | lptra |
| Flux of surface Runon (originates from other source/field) | m d ⁻¹ | [0.0 ...] | - | R | lrunon |
| Flux of surface Runoff (negative value means inundation) | m d ⁻¹ | [...] | - | R | lruno |
| Groundwater level at end of time-interval (negative below soil surface, when positive use Pond) | m-surf. | [0.0 ...] | - | R | Gwl |
| Storage by ponding at soil surface at end of time-interval | m | [0.0 ...] | - | R | Pond |
| Storage by snow at end of time-interval | m | [0.0 ...] | - | R | SSnow |
| Error in Water Balance | m | [...] | - | R | Wbalance |
| <i>The variables h ... inqdra are given for the compartments 1 ... numnod, with one exception for inq, which is given for the compartments 1 ... numnod+1</i> | | | | | |
| Suction (pressure head) of soil moisture (negative = unsaturated) | cm | [...] | * | R | h(numnod) |
| Volume fraction of moisture at end of time-interval | m ³ m ⁻³ | [0.0 ... 1.0] | * | R | theta(numnod) |
| Actual transpiration flux | m d ⁻¹ | [0.0 ...] | * | R | inqrot(numnod) |
| Flux incoming from above (compartments 1 ... numnod+1, positive = downward) | m d ⁻¹ | [...] | * | R | inq(numnod+1) |
| <i>The presence of values for variables inqdra1...inqdra5 is determined by the variable nrlevs. The value of nrlevs determines the number of drainage systems for which flux densities must be given (positive: from soil to drainage system)</i> | | | | | |
| Flux of drainage system of 1st order (e.g. canal) | m d ⁻¹ | [...] | * | R | inqdra(1,numnod) |
| Flux of drainage system of 2nd order (e.g. ditch) | m d ⁻¹ | [...] | * | R | inqdra(2,numnod) |
| Flux of drainage system of 3rd order (e.g. trench) | m d ⁻¹ | [...] | * | R | inqdra(3,numnod) |
| Flux of drainage system of 4th order (e.g. tube drain) | m d ⁻¹ | [...] | * | R | inqdra(4,numnod) |
| Flux of drainage system of 5th order (e.g. rapid drainage) | m d ⁻¹ | [...] | * | R | inqdra(5,numnod) |
| Soil cover | m ² m ⁻² | [0.0 ... 1.0] | * | R | soco |
| LAI | m ² m ⁻² | [0.0 ... 10.0] | - | R | lai |
| Rooting Depth | m | [0.0...numnod] | - | R | drz |
| Crop Factor (or crop height) | - or cm | [0.0 ...] | - | R | cf |
| Average daily air temperature | °C | [-50.0 ... 50.0] | * | R | tav |
| Average daily soil temperature of compartments 1... NUMNOD | °C | [-50.0 ... 50.0] | * | R | tsoil(numnod) |

Dynamic part for macropores, domain 1 (Main Bypass Flow domain)

| | | | | | |
|---|--------------------------------|------------|---|---|------------------------|
| Water level at end of time-interval | m-surf. | [0.0 ...] | * | R | WaLevDm1 |
| Areic volume at end of time-interval | m ³ m ⁻² | [0.0 ...] | - | R | VIMpDm1 |
| Areic volume of water stored at end of time-interval | m ³ m ⁻² | [0.0 ...] | - | R | WaSrDm1 |
| Infiltration flux at soil surface directly by precipitation | m d ⁻¹ | [0.0 ...] | - | R | IQInTopPreDm1 |
| Infiltration flux at soil surface indirectly by lateral overland flow (runoff) | m d ⁻¹ | [0.0 ...] | - | R | IQInTopLatDm1 |
| Exchange flux with soil matrix per compartment 1-numnod (positive: from macropores into matrix) | m d ⁻¹ | [...] | * | R | InQExcMtxDm1Cp(numnod) |
| Rapid drainage flux towards drain tube per compartment 1-numnod | m d ⁻¹ | [0.0 ...] | * | R | InQOutDrRapCp(numnod) |
| Average fraction of macropore wall in contact with macropore water during timestep per comp. 1-numnod | m d ⁻¹ | [0.0 ...] | * | R | FrMpWalWetDm1(numnod) |

Dynamic part for macropores, domain 2 (Internal Catchment domain)

| | | | | | |
|---|--------------------------------|-------------|---|---|------------------------|
| Areic volume at end of time-interval | m ³ m ⁻² | [0. 0 ...] | * | R | VIMpDm2 |
| Areic volume of water stored at end of time-interval | m ³ m ⁻² | [0. 0 ...] | - | R | WaSrDm2 |
| Infiltration flux at soil surface directly by precipitation | m d ⁻¹ | [0. 0 ...] | - | R | IQInTopPreDm2 |
| Infiltration flux at soil surface indirectly by lateral overland flow (runoff) | m d ⁻¹ | [0. 0 ...] | - | R | IQInTopLatDm2 |
| Exchange flux with soil matrix per compartment 1-numnod (positive: from macropores into matrix) | m d ⁻¹ | [...] | * | R | InQExcMtxDm2Cp(numnod) |
| Average fraction of macropore wall in contact with macropore water during timestep per comp. 1-numnod | m d ⁻¹ | [0.0 ...] | * | R | FrMpWalWetDm2(numnod) |

Appendix 17 Ranges of values of input parameters

| Code | Minimum | Maximum | Array | Type |
|------------------|---------|---------|--------|-----------|
| adcrh | 0 | 5 | | real |
| adcll | 0 | 5 | | real |
| alfa | 0.0001 | 1 | maho | real |
| alfaw | 0.0001 | 1 | maho | real |
| alphaw | 0.1 | 50 | mamp | real |
| alt | -400 | 3000 | | real |
| altcu | -300000 | 300000 | | real |
| altw | 0 | 99 | | real |
| amaxtb | 0 | 100 | 30 | real |
| amaxtb | 0 | 366 | 30 | real |
| aqamp | 0 | 1000 | | real |
| aqave | -10000 | 1000 | | real |
| aqper | 0 | 366 | | real |
| aqtmax | 0 | 366 | | real |
| avevap | 0 | 10 | 36 | real |
| avprec | 0 | 100 | 36 | real |
| basegw | -10000 | 0 | | real |
| bbefil | | | | character |
| betaw | 0.5 | 3 | mamp | real |
| bexp | 0 | 2 | | real |
| cdrain | 0 | 100 | | real |
| cdraini | 0 | 100 | | real |
| cfbs | 0.5 | 1.5 | | real |
| cftb | 0 | 5000 | 30 | real |
| cftb | 0 | 100000 | 72 | real |
| cirrs | 0 | 100 | | real |
| Cml | 0 | 1000 | macp | real |
| cofab | 0 | 1 | | real |
| cofani | 0 | 1000 | maho | real |
| CofAniMp | 0 | 100 | | real |
| cofintfl | 0.01 | 10 | | real |
| cofintflb | 0.01 | 10 | | real |
| cofqha | -100 | 100 | | real |
| cofqhb | -1 | 1 | | real |
| cofred | 0 | 1 | | real |
| cpre | 0 | 100 | | real |
| cref | 0 | 1000 | | real |
| CritDevMasBalAbs | 1.0d-30 | 1 | | real |
| CritDevMasBalDt | -100000 | 100 | | real |
| cropfil | | | macrop | character |
| cropname | | | macrop | character |
| cropstart | | | macrop | date |
| croptype | 1 | 3 | macrop | integer |
| cvl | 0 | 1 | | real |
| cvl | 0 | 1 | | real |
| cvo | 0 | 1 | | real |
| cvr | 0 | 1 | | real |
| cvr | 0 | 1 | | real |
| cvs | 0 | 1 | | real |
| cvs | 0 | 1 | | real |
| daqui | 0 | 10000 | | real |
| date | | | maxdat | date |
| date1 | | | mawlp | date |
| date1 | | | mabbc | date |
| date2 | | | mawlp | date |
| date2 | | | mabbc | date |

| Code | Minimum | Maximum | Array | Type |
|-----------|---------|---------|-------|-----------|
| date3 | | | mabbc | date |
| date4 | | | mabbc | date |
| date5 | | | mabbc | date |
| datefix | 1 | 31 | 2 | integer |
| datowl1 | | | maowl | date |
| datowl2 | | | maowl | date |
| datowl3 | | | maowl | date |
| datowl4 | | | maowl | date |
| dcrit | -100 | 0 | | real |
| dcs1 | 0 | 1 | | integer |
| dcs2 | 0 | 1 | | integer |
| dd | 1 | 31 | 366 | integer |
| ddamp | 0 | 500 | | real |
| ddif | 0 | 10 | | real |
| decpot | 0 | 10 | | real |
| decsat | 0 | 10 | | real |
| di | -100 | 100 | 7 | real |
| diampol | 0 | 100 | | real |
| difdes | 0 | 10000 | | real |
| DiPoMa | 0.1 | 1000 | | real |
| DiPoMi | 0.1 | 1000 | | real |
| dlc | 0 | 24 | | real |
| dlo | 0 | 24 | | real |
| dramet | 1 | 3 | | integer |
| drares1 | 10 | 100000 | | real |
| drares2 | 10 | 100000 | | real |
| drares3 | 10 | 100000 | | real |
| drares4 | 10 | 100000 | | real |
| drares5 | 10 | 100000 | | real |
| drfil | | | | character |
| dropr | 0 | 100 | mamp | real |
| dtmax | 0.01 | 0.5 | | real |
| dtmin | 1.0d-10 | 0.1 | | real |
| dtsmtb | 0 | 100 | 30 | real |
| dvs_dc1 | 0 | 2 | 7 | real |
| dvs_dc2 | 0 | 2 | 7 | real |
| dvs_tc1 | 0 | 2 | 7 | real |
| dvs_tc2 | 0 | 2 | 7 | real |
| dvs_tc3 | 0 | 2 | 7 | real |
| dvs_tc4 | 0 | 2 | 7 | real |
| dvs_tc5 | 0 | 2 | 7 | real |
| dvsend | 0 | 3 | | real |
| dwa | 0 | 500 | 7 | real |
| dzNew | 1.0d-6 | 500 | macp | real |
| ecmax | 0 | 20 | | real |
| ecslop | 0 | 40 | | real |
| eff | 0 | 10 | | real |
| eff | 0 | 10 | | real |
| entres | 0 | 1000 | | real |
| etref | etrminn | etrmax | 366 | real |
| expintfl | 0.1 | 1 | | real |
| expintflb | 0.01 | 1 | | real |
| fdepth | 0 | 1 | maho | real |
| fid | 0 | 400 | 7 | real |
| fltb | 0 | 3 | 30 | real |
| fltb | 0 | 366 | 30 | real |
| fm1 | 0 | 1 | maho | real |
| fm2 | 0 | 1 | maho | real |
| fotb | 0 | 3 | 30 | real |
| | | | | |

| Code | Minimum | Maximum | Array | Type |
|-----------|------------|-----------|-------|-----------|
| frexp | 0 | 10 | | real |
| frtb | 0 | 3 | 30 | real |
| frtb | 0 | 366 | 30 | real |
| fstb | 0 | 3 | 30 | real |
| fstb | 0 | 366 | 30 | real |
| gampar | 0 | 0.5 | | real |
| gctb | 0 | 12 | 72 | real |
| gctb | 0 | 2 | 72 | real |
| geofac | 0 | 100 | | real |
| geomf | 0 | 100 | | real |
| GeomFac | 0 | 10 | maho | real |
| gwl | -10000 | 0 | 25 | real |
| gwlconv | -100000 | 1000 | | real |
| gwlcrit | -500 | 0 | mamp | real |
| gwlevel | -10000 | 1000 | mabbc | real |
| gwli | -10000 | 100 | | real |
| gwlinf | -10000 | 0 | 5 | real |
| h | -1.d10 | 10000 | macp | real |
| haquif | -10000 | 1000 | mabbc | real |
| hbot5 | -1.0d10 | 1000 | mabbc | real |
| hbweir | altcu+zb | altcu+100 | mamp | real |
| hcomp | 0 | 1000 | macp | real |
| hcrit | -1000 | 0 | mamp | real |
| hdepth | -100 | 0 | mamp | real |
| hdrain | -10000 | 0 | | real |
| hlim1 | -100 | 100 | | real |
| hlim2l | -1000 | 100 | | real |
| hlim2u | -1000 | 100 | | real |
| hlim3h | -10000 | 100 | | real |
| hlim3l | -10000 | 100 | | real |
| hlim4 | -16000 | 100 | | real |
| hsublay | 0 | 1000 | macp | real |
| htab | altcu-1000 | altcu+10 | mamp | real |
| hum | hummin | hummax | 366 | real |
| idev | 1 | 2 | | integer |
| idsl | 0 | 2 | | integer |
| imper_4b | 1 | nmper | mamp | integer |
| imper_4c | 1 | nmper | mamp | integer |
| imper_4d | 1 | nmper | mamp | integer |
| imper_4e1 | 1 | nmper | mamp | integer |
| imper_4e2 | 1 | nmper | mamp | integer |
| impphase | 1 | nmper | mamp | integer |
| imptab | 1 | nmper | mamp | integer |
| infres1 | 10 | 100000 | | real |
| infres2 | 10 | 100000 | | real |
| infres3 | 0 | 100000 | | real |
| infres4 | 0 | 100000 | | real |
| infres5 | 0 | 100000 | | real |
| inifil | | | | character |
| intwl | 1 | 31 | mamp | integer |
| ipos | 1 | 5 | | integer |
| irconc | 0 | 1000 | mairg | real |
| irdate | | | mairg | date |
| irdepth | 0 | 100 | mairg | real |
| irdepth | 0 | 1000 | mairg | real |
| irgfil | | | | character |
| irtype | 0 | 1 | mairg | integer |
| isoillay | 1 | maho | macp | integer |
| isuas | 0 | 1 | | integer |
| isublay | 1 | macp | macp | integer |

| Code | Minimum | Maximum | Array | Type |
|-----------|---------|-----------|---------|-----------|
| kdif | 0 | 2 | | real |
| kdif | 0 | 2 | | real |
| kdif | 0 | 2 | | real |
| kdir | 0 | 2 | | real |
| kdir | 0 | 2 | | real |
| kf | 0 | 100 | | real |
| kfsat | 0 | 100 | | real |
| khbot | 0 | 1000 | | real |
| khtop | 0 | 1000 | | real |
| kmobil | 0 | 100 | | real |
| ksat | 1.d-5 | 1000 | maho | real |
| kvbot | 0 | 1000 | | real |
| kvtop | 0 | 1000 | | real |
| kytb | 0 | 5 | 72 | real |
| l | 1 | 100000 | 5 | real |
| l1 | 1 | 100000 | | real |
| l2 | 1 | 100000 | | real |
| l3 | 1 | 100000 | | real |
| l4 | 1 | 100000 | | real |
| l5 | 1 | 100000 | | real |
| laiem | 0 | 10 | | real |
| laiem | 0 | 10 | | real |
| lat | -60 | 60 | | real |
| lcc | 1 | 366 | | integer |
| ldis | 0 | 100 | | real |
| lev | 1 | 5 | 5 | integer |
| level1 | -1000 | 10 | maowl | real |
| level2 | -1000 | 10 | maowl | real |
| level3 | -1000 | 10 | maowl | real |
| level4 | -1000 | 10 | maowl | real |
| lexp | -25 | 25 | maho | real |
| lm1 | 1 | 1000 | | real |
| lm2 | 1 | 1000 | | real |
| metfil | | | | character |
| mm | 1 | 12 | 366 | integer |
| moisr1 | 0 | 5 | | real |
| moisrd | 0 | 1 | | real |
| msteps | 2 | 100000000 | | integer |
| name | 0 | 100 | mascale | real |
| ncomp | 0 | macp | macp | integer |
| nmper | 1 | mamp | | integer |
| npar | 1 | 4 | maho | real |
| nrlevs | 1 | 5 | | integer |
| nrsrf | 1 | 5 | | integer |
| nummodNew | 1 | macp | | integer |
| NumSbDm | 0 | MaDm-2 | | integer |
| ores | 0 | 1 | maho | real |
| orgmat | 0 | 1 | maho | real |
| osat | 0 | 1 | maho | real |
| osswlm | 0 | 10 | | real |
| outdat | | | maout | date |
| outdatint | | | maout | date |
| outfil | | | | character |
| pathatm | | | | character |
| pathcrop | | | | character |
| pathdrain | | | | character |
| pathdrain | | | | character |
| pathwork | | | | character |
| pclay | 0 | 1 | maho | real |
| perdl | 0 | 3 | | real |

| Code | Minimum | Maximum | Array | Type |
|--------------|---------|---------|-------|-----------|
| perdl | 0 | 3 | | real |
| period | 0 | 366 | | integer |
| pfl | 0 | 5 | maho | real |
| pf2 | 0 | 5 | maho | real |
| pfree | 0 | 1 | 36 | real |
| phormc | 0 | 1 | | integer |
| pond | 0 | 100 | | real |
| pondmx | 0 | 1000 | | real |
| poros | 0 | 0.6 | | real |
| PowM | 0 | 100 | | real |
| PpIcSs | 0 | 0.99 | | real |
| project | | | | character |
| psand | 0 | 1 | maho | real |
| psilt | 0 | 1 | maho | real |
| pstem | 0 | 1 | 36 | real |
| q10 | 0 | 5 | | real |
| q10 | 0 | 5 | | real |
| qbot2 | -100 | 100 | mabbc | real |
| qbot4 | -100 | 100 | mabbc | real |
| qdrain | -100 | 1000 | 25 | real |
| qtab | 0 | 500 | mamp | real |
| rad | radmin | radmax | 366 | real |
| rain | rainmin | rainmax | 366 | real |
| rainflux | 0 | 1000 | 30 | real |
| rapcoef | 0 | 10000 | | real |
| RapDrareaCof | 0 | 100 | | real |
| RapDraResRef | 0 | 10000 | 5 | real |
| raw | 0 | 1 | 7 | real |
| rdc | 0 | 1000 | | real |
| rdctb | 0 | 100 | 22 | real |
| rdctb | 0 | 100 | 22 | real |
| rdi | 0 | 1000 | | real |
| rdrain | 1 | 100000 | 5 | real |
| rdrrtb | 0 | 3 | 30 | real |
| rdrrtb | 0 | 366 | 30 | real |
| rdrstb | 0 | 3 | 30 | real |
| rdrstb | 0 | 366 | 30 | real |
| rds | 1 | 5000 | | real |
| rdtb | 0 | 1000 | 72 | real |
| rentry | 0 | 10 | 5 | real |
| rexit | 0 | 10 | 5 | real |
| rfsetb | 0 | 3 | 30 | real |
| rfsetb | 0 | 366 | 30 | real |
| rgrlai | 0 | 1 | | real |
| rgrlai | 0 | 10 | | real |
| rimlay | 0 | 100000 | | real |
| rinfi | 1 | 100000 | 5 | real |
| rml | 0 | 1 | | real |
| rml | 0 | 1 | | real |
| rmo | 0 | 1 | | real |
| rmr | 0 | 1 | | real |
| rmr | 0 | 1 | | real |
| rms | 0 | 1 | | real |
| rms | 0 | 1 | | real |
| rri | 0 | 100 | | real |
| rsc | 0 | 1000 | | real |
| rsigni | 0 | 1 | | real |
| rsro | 0.001 | 1 | | real |
| rsroexp | 0.01 | 10 | | real |
| rsurfdeep | 0.001 | 1000 | | real |

| Code | Minimum | Maximum | Array | Type |
|--------------|---------|---------|---------|-----------|
| rsurfshallow | 0.001 | 1000 | | real |
| rtheta | 0 | 0.4 | | real |
| rufil | | | | character |
| run | 1 | mascale | mascale | integer |
| runoff | 0 | 1000 | maxdat | real |
| Rzah | 0 | 1 | | real |
| scanopy | 0 | 10 | 36 | real |
| schedule | 0 | 1 | | integer |
| shape | 0 | 1 | | real |
| shrina | 0 | 2 | | real |
| ShrParA | -1000 | 1000 | maho | real |
| ShrParB | -1000 | 1000 | maho | real |
| ShrParC | -1000 | 1000 | maho | real |
| ShrParD | -1000 | 1000 | maho | real |
| ShrParE | -1000 | 1000 | maho | real |
| sinamp | -10 | 10 | | real |
| sinave | -10 | 10 | | real |
| sinmax | 0 | 366 | | real |
| slatb | 0 | 2 | 30 | real |
| slatb | 0 | 366 | 30 | real |
| snowcoef | 0 | 10 | | real |
| snowinco | 0 | 1000 | | real |
| sofcu | 0.1 | 100000 | | real |
| SorpAlfa | -10 | 10 | maho | real |
| SorpFacParl | 0 | 100 | maho | real |
| SorpMax | 0 | 100 | maho | real |
| spa | 0 | 1 | | real |
| span | 0 | 366 | | real |
| span | 0 | 366 | | real |
| Spoint | 0 | 1 | | real |
| ssa | 0 | 1 | | real |
| ssa | 0 | 1 | | real |
| ssnow | 0 | 1000 | | real |
| startirr | 1 | 31 | 2 | integer |
| station | | | 366 | character |
| sw2 | 1 | 2 | | integer |
| sw3 | 1 | 2 | | integer |
| sw4 | 0 | 1 | | integer |
| swafo | 0 | 2 | | integer |
| swallo1 | 1 | 3 | | integer |
| swallo2 | 1 | 3 | | integer |
| swallo3 | 1 | 3 | | integer |
| swallo4 | 1 | 3 | | integer |
| swallo5 | 1 | 3 | | integer |
| swate | 0 | 1 | | integer |
| swaun | 0 | 2 | | integer |
| swbalance | 0 | 0 | | integer |
| swbbcfile | 0 | 1 | | integer |
| swble | 0 | 1 | | integer |
| swbma | 0 | 1 | | integer |
| swbotb | 1 | 8 | | integer |
| swbr | 0 | 1 | | integer |
| swcalt | 1 | 2 | | integer |
| swcf | 1 | 2 | | integer |
| swcf | 1 | 2 | | integer |
| swcfbs | 0 | 1 | | integer |
| swdc | 0 | 1 | | integer |
| swdisrvert | 0 | 1 | | integer |
| swdivd | 0 | 1 | | integer |
| swdivd | 0 | 1 | | integer |

| Code | Minimum | Maximum | Array | Type |
|-----------|---------|---------|-------|---------|
| swdra | 0 | 2 | | integer |
| swdrf | 0 | 1 | | integer |
| SwDrRap | 1 | 2 | | integer |
| swdtyp | 0 | 1 | 5 | integer |
| swdtyp1 | 1 | 2 | | integer |
| swdtyp2 | 1 | 2 | | integer |
| swdtyp3 | 1 | 2 | | integer |
| swdtyp4 | 1 | 2 | | integer |
| swdtyp5 | 1 | 2 | | integer |
| swerror | 0 | 1 | | integer |
| swetr | 0 | 1 | | integer |
| swfrost | 0 | 1 | | integer |
| swgc | 1 | 2 | | integer |
| swhea | 0 | 1 | | integer |
| swheader | 0 | 1 | | integer |
| swhyst | 0 | 2 | | integer |
| swinco | 1 | 3 | | integer |
| swinter | 0 | 2 | | integer |
| swintfl | 0 | 1 | | integer |
| swirfix | 0 | 1 | | integer |
| swirgfil | 0 | 1 | | integer |
| swmacro | 0 | 2 | | integer |
| swman | 1 | 2 | mamp | integer |
| swmobi | 0 | 1 | | integer |
| swmonth | 0 | 1 | | integer |
| swnrstf | 0 | 2 | | integer |
| swodat | 0 | 1 | | integer |
| SwPowM | 0 | 1 | | integer |
| swpref | 0 | 1 | | integer |
| swqhr | 1 | 2 | | integer |
| swrain | 0 | 2 | | integer |
| swredu | 0 | 2 | | integer |
| swres | 0 | 1 | | integer |
| swrunon | 0 | 1 | | integer |
| swscal | 0 | 1 | | integer |
| swscre | 0 | 2 | | integer |
| swsec | 1 | 2 | | integer |
| SwShrInp | 1 | 2 | maho | integer |
| swsnow | 0 | 1 | | integer |
| SwSoilShr | 0 | 2 | maho | integer |
| swsolu | 0 | 1 | | integer |
| SwSorp | 1 | 2 | maho | integer |
| swsp | 0 | 1 | | integer |
| swsrf | 1 | 3 | | integer |
| swswb | 0 | 1 | | integer |
| swvap | 0 | 1 | | integer |
| swyrvar | 0 | 1 | | integer |
| t | 0 | 366 | 36 | real |
| taludr | 0.01 | 5 | 5 | real |
| tampli | 0 | 50 | | real |
| tau | 0 | 1 | | real |
| taw | 0 | 1 | 7 | real |
| tbase | -10 | 30 | | real |
| tbase | -10 | 30 | | real |
| tbase | -10 | 30 | | real |
| tcs1 | 0 | 1 | | integer |
| tcs2 | 0 | 1 | | integer |
| tcs3 | 0 | 1 | | integer |
| tcs4 | 0 | 1 | | integer |
| tcs5 | 0 | 1 | | integer |

| Code | Minimum | Maximum | Array | Type |
|-----------|-----------------------|------------|-------|---------|
| tdwi | 0 | 10000 | | real |
| tdwi | 0 | 10000 | | real |
| tend | | | | date |
| theter | 0 | 1 | maho | real |
| ThetCrMP | 0 | 1 | maho | real |
| thetim | 0 | 1 | maho | real |
| thetol | -100000 | 0.01 | | real |
| time | 0 | 366 | 30 | real |
| timref | 0 | 366 | | real |
| tmax | tmxmin | tmxmax | 366 | real |
| tmean | 5 | 30 | | real |
| tmin | tminmin | tminmax | 366 | real |
| tmnfb | -10 | 50 | 30 | real |
| tmnfb | -10 | 50 | 30 | real |
| tmpfb | -10 | 50 | 30 | real |
| tmpfb | -10 | 50 | 30 | real |
| trel | 0 | 1 | 7 | real |
| tscf | 0 | 10 | | real |
| tsoil | -50 | 50 | maho | real |
| Tsoil | -50 | 50 | macp | real |
| tstart | | | | date |
| tsumam | 0 | 10000 | | real |
| tsumam | 0 | 10000 | | real |
| tsumea | 0 | 10000 | | real |
| tsumea | 0 | 10000 | | real |
| value_tc5 | -1000000 | -100 | 7 | real |
| value_tc5 | 0 | 1 | 7 | real |
| vcrit | 0 | 20 | mamp | real |
| VIMpStSs | 0 | 0.5 | | real |
| wet | 0 | 1 | 366 | real |
| wetper | 0 | 1000 | | real |
| widthr | 0 | 10000 | 5 | real |
| wind | winmin | winmax | 366 | real |
| wlact | zbotdr(1+nrpri)+altcu | altcu | | real |
| wldip | 0 | 100 | mamp | real |
| wlp | altcu-1000 | altcu-0.01 | mawlp | real |
| wls | altcu-1000 | altcu-0.01 | mawlp | real |
| wlsman | altcu-500 | altcu | mamp | real |
| wscap | 0 | 10 | mamp | real |
| yyyy | iyear | iyear | 366 | integer |
| Z_Ah | maxdepth | 0 | | real |
| z_Cml | -100000 | 0 | macp | real |
| z_h | -100000 | 0 | macp | real |
| Z_ic | maxdepth | 0 | | real |
| Z_St | maxdepth | 0 | | real |
| z_Tsoil | -100000 | 0 | macp | real |
| zbotdr | -1000 | 0 | | real |
| zbotdr1 | -1000 | 0 | | real |
| zbotdr2 | -1000 | 0 | | real |
| zbotdr3 | -1000 | 0 | | real |
| zbotdr4 | -1000 | 0 | | real |
| zbotdr5 | -1000 | 0 | | real |
| zbotdre | altcu-1000 | altcu-0.01 | 5 | real |
| zc | -100000 | 0 | macp | real |
| ZDrLv | -1000 | 0 | | real |
| zh | -100000 | 0 | macp | real |
| zi | -100000 | 0 | macp | real |
| zintf | -10000 | 0 | | real |
| zncrack | -100 | 0 | | real |
| ZnCrAr | Z_Ah | 0 | | real |

